

Investigating the anti-apoptotic role of EBV
in endemic Burkitt lymphoma

by

LEAH FITZSIMMONS

A thesis submitted to
The University of Birmingham
for the degree of
DOCTOR OF PHILOSOPHY

School of Cancer Sciences
College of Medical and Dental Sciences
The University of Birmingham
September 2014

UNIVERSITY OF
BIRMINGHAM

University of Birmingham Research Archive

e-theses repository

This unpublished thesis/dissertation is copyright of the author and/or third parties. The intellectual property rights of the author or third parties in respect of this work are as defined by The Copyright Designs and Patents Act 1988 or as modified by any successor legislation.

Any use made of information contained in this thesis/dissertation must be in accordance with that legislation and must be properly acknowledged. Further distribution or reproduction in any format is prohibited without the permission of the copyright holder.

Abstract

Epstein-Barr virus (EBV) has been etiologically associated with Burkitt lymphoma (BL) since its discovery 50 years ago, but despite this long-standing association the precise role of the virus in the pathogenesis of BL remains enigmatic.

EBV can be lost spontaneously from EBV-positive BL cell lines, and these EBV-loss clones have been reported to exhibit increased sensitivity to apoptosis. We have confirmed and extended those observations and report that sporadic loss of EBV from BL cells is consistently associated with enhanced sensitivity to apoptosis-inducing agents and conversely, reduced tumorigenicity *in vivo*. Importantly, reinfection of EBV-loss clones with EBV can restore apoptosis protection, although surprisingly, individual Latency I genes cannot.

We also used inducible pro-apoptotic BH3 ligands to investigate Bcl-2-family dependence in BL clones as well as profiling gene expression changes in response to apoptosis induction in EBV-positive versus EBV-loss clones. We found that EBV-loss was consistently associated with enhanced sensitivity to BH3-ligand-induced death and increased activation of apoptosis signalling pathways, although no individual apoptosis-related gene was responsible. Instead we find that Latency I EBV genes co-operate to co-ordinately repress the BH3-only proteins Bim, Puma and Noxa to inhibit apoptosis in BL.

Acknowledgements

This PhD would not have been possible without the support and guidance of my supervisors, Martin Rowe and Gemma Kelly, to whom I am very grateful. I also owe special thanks to Dr Rosemary Tierney for discussion and guidance, as well as technical, intellectual and emotional support. I would like to thank the members of the Rowe and Strasser research groups who contributed their time, expertise, patience and advice to me particularly; Andreas Strasser, Marco Herold, Nikki Smith, Andrew Bell, and Claire Shannon-Lowe. I would also like to thank Alan Rickinson for all the helpful advice and discussion. I am grateful to several members of other research groups, who kindly contributed reagents and advice to this project, which rescued several sets of experiments when they ground to a halt. Additionally, I could not have undertaken this degree without financial support from the Kay Kendall Leukaemia Fund and Cancer Research UK.

I owe enormous thanks to my friends and family who have all been forced to endure endless tirades about viruses, cancer, immunology and non-coding RNAs. I am particularly grateful to Holly Joynes, Kathryn Warder, Tommy Morrison and Kipp Jones who have borne the worst of the brunt and will probably spend the rest of their lives avoiding scientists in order to recover. Most of all, I would like to thank Andrew Holland for keeping me together and forgiving me denying us a holiday for the last two years as well as putting up with me constantly organising our lives around my cell culture commitments. I promise we can go on holiday now, although I can't promise that you're not going to end up in tissue culture on New Year's Eve again.

Contents

1. Introduction.....	1
1.1 The early history of EBV research	1
1.1.1 'More than a curiosity'	1
1.1.2 'A cell filled with herpesvirus!'	2
1.1.3 A 'stalking horse'	2
1.2 EBV	3
1.2.1 Taxonomy	3
1.2.2 Structure.....	3
1.2.3 Viral genome	4
1.2.4 Strain variation	4
1.2.5 EBV infection and growth transformation <i>in vitro</i>	6
1.2.6 EBV infection and persistence <i>in vivo</i>	9
1.2.7 Reactivation and lytic cycle	10
1.2.8 Tissue tropism	12
1.2.9 Viral latency.....	12
1.2.10 Disease associations	16
1.3 Burkitt lymphoma.....	19
1.3.1 Incidence and clinical characteristics	19
1.3.2 The role of cofactors in BL pathogenesis	22
1.3.3 Genetic factors	24
1.3.4 Treatment and prognosis	26
1.3.5 The role of EBV in BL	27
EBNA1.....	29
EBER RNAs.....	30
BART microRNAs	31
1.4 Apoptosis.....	33
1.4.1 Overview of apoptosis.....	33
1.4.2 The Bcl-2 family	38
1.4.3 Regulation of the Bcl-2 family	43
1.4.4 The Bcl-2 family and lymphomagenesis.....	44
1.4.5 Targeting the Bcl-2 family in human disease	45
1.5 Aims and Objectives	46
2. Materials and Methods	47
2.1 Cell culture	47
2.1.1 Cell lines used in this study	47
2.1.2 Cell line maintenance	48
2.1.3 Single cell cloning of BL cell lines	49
2.1.4 Preparation of lentivirus stocks.....	49
2.1.5 Generation of stable lentivirus-transduced cell lines	50

2.1.6	Preparation of infectious stocks of recombinant EBV	51
2.1.7	Reinfection of EBV-loss clones with recombinant EBV	52
2.2	Cell death, cell growth and cell survival assays.....	53
2.2.1	Cell viability assays	53
2.2.2	Proliferation assays	53
2.2.3	Apoptosis assays.....	54
2.2.4	Data analysis for apoptosis assays	56
2.3	DNA analysis.....	58
2.3.1	DNA preparation	58
2.3.2	PCR quantitation of EBV genome load.....	58
2.4	PCR amplification of DNA.....	59
2.4.1	PCR amplification of viral and cellular genes	59
2.4.2	Agarose gel electrophoresis and purification of PCR products.....	59
2.4.3	Sequencing PCR.....	60
2.5	Bacteriology.....	60
2.5.1	Transformation of Stbl3 <i>E. Coli</i>	60
2.5.2	Isolation of plasmid DNA from bacterial cultures	61
2.5.3	Restriction digestion and DNA ligation	61
2.6	Molecular Cloning	62
2.6.1	Generation of EBNA1 lentivirus	62
2.6.2	Generation of FH1t-EBER-UTG lentiviruses.....	63
2.6.3	The pEKS10 EBER plasmid	63
2.6.4	Generation of BART lentiviruses	63
2.6.5	Bim ₅ lentiviruses.....	66
2.6.6	FTrex-BHRF1-UTG lentivirus.....	67
2.6.7	Akata-GFP2 recombinant EBV BAC	67
2.6.8	CpWp-KO recombinant EBV BAC.....	67
2.7	RNA analysis	68
2.7.1	Preparation of purified RNA.....	68
2.7.2	Synthesis of randomly-primed cDNA	68
2.7.3	Synthesis of stem loop-primed cDNA for the detection of miRNAs	68
2.7.4	TaqMan q-PCR for EBV and cellular genes.....	69
2.7.5	TaqMan q-PCR for miRNAs.....	71
2.7.6	TaqMan human apoptosis low density q-PCR arrays.....	72
2.7.7	Fluidigm viral gene expression q-PCR Arrays	73
2.7.8	Northern blotting	73
2.7.9	EBER in-situ hybridisation (ISH).....	74
2.8	Protein analysis	74
2.8.1	Protein preparation.....	74
2.8.2	SDS-PAGE / Western Blotting.....	75
2.8.3	Immunofluorescence (IF) staining.....	77

2.8.4	CD19 FACS Staining	78
2.8.5	Cell sorting.....	78
2.9	Reporter assays	79
2.10	Animal Work.....	79
2.10.1	Xenografts	79
2.10.2	Histology.....	80
2.10.3	<i>Ex vivo</i> cell culture	80
3. Results Part I		
ISOLATING AND CHARACTERISING EBV-LOSS CLONES		81
3.1	Introduction	81
3.2	Single cell cloning of EBV-positive BL cell lines	83
3.2.1	Generating EBV-loss clones from EBV-positive BL cell lines	83
3.2.2	Viral transcription in BL clones.....	85
3.2.3	Viral protein expression in BL clones	90
3.2.4	Viral RNA expression in single cells	91
3.3	Investigating the response of BL clones to apoptosis inducers	93
3.3.1	Etoposide and α -IgM: DNA damage response versus BCR crosslinking.....	93
3.3.2	Ionomycin: a second calcium-dependent intrinsic apoptosis inducer.....	96
3.3.3	Roscovitine and Staurosporine	98
3.3.4	Cell death inhibitors	98
3.3.5	ABT-737	102
3.4	Screening for cellular genes involved in the EBV-loss phenotype	104
3.4.1	Microarrays	104
3.4.2	Protein expression studies	104
3.4.3	<i>MYC</i>	105
3.5	Investigating the effect of pro-survival signals on EBV-loss.....	108
3.5.1	Mechanism of EBV-loss	108
3.5.2	Expressing BHRF1 in Latency I BLs.....	109
3.5.3	Single cell cloning of BHRF1-expressing BLs.....	111
3.5.4	Apoptosis phenotype of BHRF1-expressing BL clones	113
3.6	Investigating the tumorigenicity of BL clones <i>in vivo</i>	114
3.6.1	Design of <i>in vivo</i> studies	114
3.7	Features of BL xenograft tumours in NSG Mice	116
3.7.1	Sites of tumour formation.....	116
3.7.2	Histology – H&E stains	116
3.7.3	Human CD19 FACS.....	119
3.8	Survival of BL xenotransplant mice	120
3.9	Analysis of EBV in xenotransplants	122
3.10	Akata-BL xenotransplants	122

Conclusions I.....	124
4. Results Part II	
INVESTIGATING THE ROLE OF LATENCY I EBV-ENCODED GENES IN APOPTOSIS	127
4.1 Outline of Latency I gene re-expression studies	127
4.2 EBNA1.....	129
4.2.1 Expressing EBNA1 in EBV-loss BL clones	129
4.2.2 EBNA1 Reporter Assays.....	131
4.2.3 The apoptosis phenotype of EBNA1-expressing EBV-loss clones	133
4.3 EBERs.....	136
4.3.1 Expressing the EBER RNAs in EBV-loss BL clones	136
4.3.2 The apoptosis phenotype of EBER-expressing EBV-loss clones	141
4.3.3 Expression and function of human IL-10 in EBV-loss clones.....	141
4.3.4 Further investigations into EBER function in BL cells.....	145
4.4 BART microRNAs	147
4.4.1 Expressing the BART mRNAs in EBV-loss clones	147
4.4.2 Expressing the BART microRNAs in EBV-loss clones	150
4.4.3 The apoptosis phenotype of miR BART-expressing BL clones	153
4.4.4 Regulation of pro-apoptotic BH3-only proteins by miR BARTs.....	156
4.5 Reinfected EBV-loss clones: the Akata virus	158
4.5.1 Generating Latency I EBV-loss reinfected cells with Akata strain rEBV	158
4.5.2 Viral protein expression in Akata virus EBV-loss reinfected cells.....	160
4.5.3 Viral transcription in Akata virus EBV-loss reinfected cells.....	162
4.5.4 Expression of viral microRNAs in Akata virus EBV-loss reinfected cells.....	164
4.5.5 The apoptosis phenotype of Akata virus EBV-loss reinfected cells.....	165
4.6 Reinfected EBV-loss clones: the B95.8 rEBV	168
4.6.1 Generating Latency I EBV-loss reinfected cells with CpWp-KO strain rEBV.....	168
4.6.2 Viral protein expression in CpWp-KO virus reinfected cells.....	168
4.6.3 EBER <i>in situ</i> hybridisation in CpWp-KO virus reinfected cells	170
4.6.4 Viral transcription in CpWp-KO virus EBV-loss reinfected cells	171
4.6.5 Expression of viral microRNAs in CpWp-KO EBV-loss reinfected cells.....	173
4.6.6 Phenotype of EBV-loss clones reinfected with CpWp-KO virus	174
4.6.7 Comparison of apoptosis in CpWp-KO and Akata rEBV reinfected cells.....	178
4.7 Loss of Akata rEBV from Akata clone n5 reinfected cells.....	180
4.8 Further investigation of viral transcription in Latency I BLs.....	182
Conclusions II.....	185
5. Results Part III	
THE ROLE OF CELLULAR GENES IN THE APOPTOSIS-PHENOTYPE OF EBV-LOSS CLONES.....	190
5.1 Apoptosis-response of EBV-loss clones to BH3 ligands	190

5.1.1	Expressing Bim _S -derived BH3 ligands in EBV-loss clones	191
5.1.2	Generating Bim _S variant-expressing cell lines	193
5.1.3	The apoptosis phenotype of Bim _S variant expressing cell lines	197
5.1.4	Summary of BH3 variant re-expression studies	199
5.2	The cellular apoptosis response in BL clones: preliminary data	201
5.2.1	Assay design and validation	201
5.2.2	Bcl-2 family expression in drug-treated EBV-loss clones	204
5.3	The cellular apoptosis response in BL clones: q-PCR arrays	207
5.3.1	Experimental set-up	207
5.3.2	Apoptosis response of Kem-BL clones in scaled-up assays	209
5.3.3	Analysis of similarity between clones of Kem-BL in q-PCR arrays.....	212
5.3.4	Grouped pairwise analyses	214
5.3.5	Pairwise analyses of individual clones	220
5.3.6	Relative quantitation.....	223
5.4	Apoptosis-related changes in clones of Kem-BL at the protein level	227
5.4.1	Western blotting experimental set up	227
5.4.2	Caspases	228
5.4.3	Targets from q-PCR arrays.....	230
5.4.4	The IAP family.....	233
5.4.5	The Bcl-2 family	235
5.4.6	Summary of Western blotting for apoptosis related proteins.....	237
5.5	FACS analysis of protein expression changes in Kem-BL clones	240
5.5.1	Bim.....	241
5.5.2	Noxa	242
5.5.3	Puma.....	244
5.5.4	Summary of FACS data	246
	Conclusions III.....	248
	6. Discussion and future work.....	252
	References.....	257

Figures and Illustrations

1. Introduction

1.1 Schematic of EBV genome and position of transcripts	5
1.2 Viral Latency programmes found in EBV infected cells	14
1.3 Position of BART transcripts and microRNAs within the EBV genome	32
1.4 Overview of the intrinsic and extrinsic apoptosis pathways	36
1.5 Schematic of functional domains in Bcl-2 family proteins	39
1.6 Binding specificities of Bcl-2 family members	41

2. Materials and Methods

2.1 Apoptosis assay gating strategies	57
2.2 Schematics of plasmids used in this thesis	65

3. Results I

3.1 Workflow of experiments carried out to isolate and characterise BL clones	82
3.2 Example of average viral loads in single cell clones of Kem-BL	84
3.3 Transcription of viral gene products in EBV-positive BL clones	89
3.4 BZLF1 transcription in EBV-positive BL clones	90
3.5 Viral protein expression in BL clones	91
3.6 EBER FACS in BL clones	92
3.7 Sensitivity of BL clones to α -IgM and Etoposide	95
3.8 Sensitivity of BL clones to ionomycin	97
3.9 Sensitivity of BL clones to Roscovitine and Staurosporine	99
3.10 Ability of cell death inhibitors to block ionomycin-induced killing	101
3.11 Sensitivity of BL clones to ABT-737	103
3.12 Screening BL clones for gene expression changes associated with EBV-loss	107
3.13 Expression of BHRF1 in Latency I BLs	110
3.14 Average viral loads in clones of BHRF1-expressing Akata-BL cells	111
3.15 Survival of BHRF1-expressing BL cells versus control cell lines	113
3.16 Experimental workflow of <i>in vivo</i> experiments	115
3.17 Appearance of BL xenograft tumours in NSG mice	118
3.18 Example of CD19 staining of <i>ex vivo</i> xenograft cells compared to controls	119
3.19 Survival analysis of NSG mice injected with BL clones	121
3.20 Quantitative PCR on xenotransplanted BL cells <i>ex vivo</i>	123

4. Results II

4.1 Workflow for EBNA1 re-expression experiments	128
4.2 EBNA1 expression in FTrex-EBNA1-UTG transduced BL clones	130
4.3 Schematic of EBNA1 FR-tk-reporter system	131
4.4 Luciferase reporter activation by EBNA1 in EBV-loss Akata cells	132
4.5 Apoptosis phenotype of FTrex-EBNA1-UTG transduced BL clones	135
4.6 Expression of EBER RNAs in FH1-EBER1/2-UTG transduced cells	137
4.7 PolyT tracts in EBV and CELO virus compared to lentivirus constructs	139
4.8 EBER RNA expression in EKS10 transfected BL clones	140
4.9 Apoptosis phenotype of EKS10 transfected BL clones	142

4.10	IL-10 mRNA expression in EBV-positive and negative BL cell lines	143
4.11	IL-10 function in BL clones	144
4.12	EBER FACS in EKS10 transfectants	145
4.13	Proliferation in EBV-expressing EBV-loss clones	146
4.14	Schematic of organisation of BART miRNAs in EBV genome	147
4.15	BARTs primary transcripts in FTREx-BARTs-UTG transduced BL cells	148
4.16	Expression of GFP in BARTs-FT-UTG transduced cells	149
4.17	Expression of mature BART miRs in transduced BL cells	151
4.18	Expression of miR BARTs in lentivirus-transduced 293 cells	152
4.19	Effect of miR BARTs on the apoptosis phenotype of EBV-loss clones	155
4.20	Regulation of pro-apoptotic BH3-only proteins by miR BARTs	157
4.21	Experimental workflow used for reinfection of EBV-loss clones	159
4.22	Viral protein expression in Akata virus EBV-loss reinfected cells	161
4.23	Transcription of viral genes in Akata virus EBV-loss reinfected cells	163
4.24	Expression of BART miRNAs in Akata virus EBV-loss reinfected cells	164
4.25	Apoptosis phenotype of Akata virus EBV-loss reinfected cells	167
4.26	Protein expression in CpWp-KO reinfected cells	169
4.27	Representative EBV FACS in CpWp-KO reinfected cells	170
4.28	Viral transcript expression in CpWp-KO reinfected cells	172
4.29	Expression of BART miRNAs in CpWp-KO EBV-loss reinfected cells	173
4.30	Apoptosis data from CpWp-KO reinfected EBV-loss clones	177
4.31	Apoptosis phenotypes of CpWp-KO and Akata virus reinfected cells	179
4.32	Effect of a second EBV-loss event on cell death in Akata n5 subclones	181
4.33	Position of LF genes in EBV genome	183
4.34	Transcription of Latency I-associated and LF genes in BL cell lines	184

5. Results III

5.1	Binding specificity and affinity of BH3 proteins and mimetic ligands	192
5.2	Bim ₅ -variant expression in BL clones	194
5.3	GFP intensity in BL clones after successive rounds of GFP sorting	195
5.4	The apoptosis phenotype of Bim ₅ -variant expressing BL clones	198
5.5	Summary of BH3 variant expression studies in BL clones	200
5.6	Cell death in Kem-BL and loss clone n1 after apoptosis induction	202
5.7	Lytic gene expression in Kem-BL after apoptosis induction	204
5.8	Time course of Puma- α and Mcl-1 protein expression in Kem-BL cells	205
5.9	Time course of Puma, Mcl-1 and Noxa transcription in Kem-BL cells	206
5.10	Experiments to investigate cellular gene changes in response to apoptotic stimulus.	208
5.11	Viability of EBV-positive and loss clones of Kem-BL in scaled-up apoptosis assays	209
5.12	Western blots of PARP expression and cleavage in Kem-BL clones	211
5.13	Global gene expression comparisons from q-PCR arrays	212
5.14	Summary of similarity between pairs of EBV-positive and EBV-loss clones	213
5.15	Gene expression changes in EBV-loss clones after apoptosis induction	215
5.16	Gene expression changes in EBV-positive clones after apoptosis induction	216
5.17	Gene expression changes in EBV-positive and loss clones after apoptosis induction	217
5.18	Gene expression changes of 2-fold or more in individual clones	222
5.19	Relative quantitation of CASP7, c-IAP1 and CFLAR	224

5.20	Relative quantitation of Puma expression	225
5.21	Relative quantitation of DEDD2 and FLASH	226
5.22	Caspase-3, -7 and -9 Western blots	229
5.23	Protein expression of targets identified by q-PCR array	231
5.24	Expression of IAP family member proteins in Kem-BL clones	234
5.25	Expression of pro-survival Bcl-2 proteins in Kem-BL clones	235
5.26	Expression of pro-apoptotic Bcl-2 homologues in Kem-BL clones	236
5.27	Bim protein expression in Kem-BL clones	241
5.28	Noxa protein expression in Kem-BL clones	243
5.29	Puma protein expression in Kem-BL clones	245
5.30	Summary of Noxa, Bim and Puma expression in Kem-BL clones	247

Tables

1.1	Features of EBV-associated diseases	18
1.2	Features of BL that are known to vary by sub-type	19
2.1	Details of cell lines used in this thesis	48
2.2	Details of drugs used in apoptosis assays and length of assays	55
2.3	Details of Bim _s variant constructs	66
2.4	Details of inventoried q-PCR assays	69
2.5	Details of unpublished, custom made q-PCR assays	70
2.6	Details of commercially available EBV miR q-PCR assays used in this study	71
2.7	Details of primary antibodies used for Western blotting	76
3.1	Compiled data from all BL single cell cloning	86
3.2	Compiled data from BHRF1 single cell cloning experiments	112
3.3	Summary of sites of BL xenografts tumour formation in NSG mice	117
5.1	Summary of gene expression changes from grouped pairwise analyses	219
5.2	Summary of apoptosis-related protein expression in Western blots	238

Definitions and abbreviations

α -IgM	Anti-immunoglobulin M	DOX	Doxycycline
β 2M	β -2-microglobulin	EBER	EBV-encoded RNA
ADP	Adenosine diphosphate	eBL	Endemic Burkitt lymphoma
AID	Activation induced (cytidine) deaminase	EBNA	EBV nuclear antigen
AIDS	Acquired immune deficiency syndrome	EBV	Epstein-Barr virus
ACV	Acyclovir	EBV-GC	EBV-associated gastric carcinoma
BAC	Bacterial artificial chromosome	EDTA	Ethylenediaminetetraacetic acid
BARTs	BamHI A rightward transcripts	ENKTL	Extranodal NK/T cell lymphoma
BCR	B cell receptor	FACS	Fluorescence-activated cell sorting
BH	Bcl-2 homology	FCS	Foetal calf serum
BL	Burkitt lymphoma	F-ISH	Fluorescence in situ hybridisation
BSA	Bovine serum albumin	FITC	Fluorescein isothiocyanate
CAD	Caspase activated DNase	FR	Family of repeats
CAEBV	Chronic active EBV	GC	Germinal centre
CARD	Caspase recruitment domain	GCOS	GeneChip Operating Software
CDK	Cyclin-dependent kinase	GFP	Green fluorescent protein
cDNA	Complementary deoxyribonucleic acid	HAART	Highly active anti-retroviral therapy
CELO	Chicken embryonic lethal orphan virus	HINGS	Heat-inactivated goat serum
CpWp-KO	C promoter/W promoter knock out rEBV	HIV	Human immune deficiency virus
Ct	Threshold cycle	HIV-BL	HIV-associated Burkitt lymphoma
CTL	Cytotoxic lymphocyte	HL	Hodgkin lymphoma
DABCO	1,4-diazabicyclo[2.2.2]octane	HLA	Human leukocyte antigen
dCTP	Deoxycytidine triphosphate	HLH	Haemophagocytic lymphohistiocytosis
ddH ₂ O	Double distilled water	HRS	Hodgkin and Reed-Sternberg
DED	Death effector domain	HYG	Hygromycin
DEPC	Dethylpyrocarbonate	IAP	Inhibitor of apoptosis protein
DISC	Death induced signalling complex	IF	Immunofluorescence
DLBCL	Diffuse large B cell lymphoma	Ig	Immunoglobulin
DMSO	Dimethyl sulphoxide	IL-10	Interleukin 10
DNA	Deoxyribonucleic acid	IL2R γ KO	Interleukin 2 receptor gamma knock out
dnEBNA1	Dominant negative EBNA1	IM	Infectious mononucleosis
dNTPs	Deoxynucleotide triphosphates		

IFN- γ	Interferon gamma	PNA	Peptide nucleic acid
IP	Intra peritoneal	Pol II	Polymerase II
ISH	In situ hybridisation	Pol III	Polymerase III
kb	Kilobase(s)	pri-miR	Primary microRNA transcript
Kbp	Kilobase pairs	PS	Phosphatidylserine
kDa	kilo-Daltons	PTLD	Post-transplant lymphoproliferative disease
KSHV	Karposi's sarcoma associated herpesvirus	PTM	Post-translational modification
LCL	Lymphoblastoid cell line	q-PCR	Quantitative PCR
LCV	lymphocryptovirus	QVD	Q-VD.OPh
LMP	Latent membrane protein	Q-VD.Oph	Quinoline-Val-Asp-difluorophenoxymethylketone
MES	Morpholinoethanesulfonic acid	rEBV	Recombinant Epstein-Barr virus
miR	microRNA (also miRNA)	RNA	Ribonucleic acid
MMLV	Moloney murine leukaemia virus	RNP	Ribonucleoprotein
MOI	Multiplicity of infection	RT	Reverse transcriptase
MOMP	Mitochondrial outer membrane permeabilisation	sBL	Sporadic Burkitt lymphoma
MS	Multiple sclerosis	SC	Subcutaneous
MuHV-4	Murid herpesvirus 4	SCID	Severe combined immunodeficiency
MuLV	Murine leukaemia virus	SD	Standard deviation
NGS	Next generation sequencing	SHM	Somatic hypermutation
NHL	Non-Hodgkin lymphoma	TBE	Tris/Borate/EDTA
NK	Natural killer	TLDA	TaqMan Low Density Array
NOD	Non-obese diabetic	T _m	Melting temperature
NPC	Nasopharyngeal carcinoma	TNF-R	Tumour necrosis factor receptor
NSG	NOD/SCID/IL2gRKO	TPA	12-O-tetradecanoyl phorbol-13-acetate
ORF	Open reading frame	TR	Terminal repeats
P.I.	Post induction	U-GSB	Urea gel sample buffer
PARP	Poly ADP-ribose polymerase	UV	Ultraviolet
PBMC	Peripheral blood mononuclear cell	v-Bcl-2	Viral Bcl-2 homologue
PBS	Phosphate-buffered saline	WEHI	Walter and Eliza Hall Institute
PBS-T	Phosphate-buffered saline with Tween-20	Wp-BL	Wp-restricted Burkitt lymphoma
PCR	Polymerase chain reaction	XLA	X-linked agammaglobulinaemia
PI	Propidium iodide	XLP	X-linked lymphoproliferative syndrome
PI3K	Phosphoinositide 3-kinase	ZRE	BZLF1 response element
PKR	RNA-dependent protein kinase		

1. Introduction

1.1 The early history of EBV research

The discovery of the Epstein-Barr virus (EBV), in an unusual yet common paediatric cancer in sub-Saharan Africa, has become something of legend within the cancer research community. Not only because it is a remarkable story, but also because it was in the research fields of EBV and Burkitt lymphoma (BL), as the African cancer came to be called, in which many of the paradigms of cancer biology were first demonstrated [1, 2].

1.1.1 'More than a curiosity'

In 1958, Denis Parsons Burkitt, a missionary bush surgeon working in Uganda, published the first detailed clinical study of 38 children with tumours of the jaw, in a paper that is now a citation classic [3]. Although the disease had been described before, Burkitt was the first to realise that the additional swellings in the abdomen and elsewhere, which were seen in almost every patient, were part of the same disease, and that these related tumours, which could arise at the same time or even before those in the jaw, were not simply metastases [4, 5].

Burkitt, with the help of several colleagues, went on to show that the all of the tumour cells were lymphocytes, regardless of the site of the tumour, and that these often rapidly fatal lymphomas accounted for up to 50% of all malignancies of African children [6-8]. This careful cataloguing of the incidence of the 'lymphoma syndrome' alerted Burkitt to another peculiarity; its occurrence appeared to be geographically restricted. BL was only ever recorded in low-lying tropical areas with high rainfall, distributed across a swathe of Africa he referred to as the 'lymphoma belt'; a distribution exactly coincident with that of holoendemic malaria and other arthropod-borne infections [9-11].

1.1.2 'A cell filled with herpesvirus!'

During visits back to the UK, Burkitt would give lectures about the 'African lymphoma syndrome' and it was after one such lecture, at Middlesex Hospital in 1961, that Burkitt first met Anthony Epstein. Epstein, who was working on animal viruses, was enthralled by the prospect of searching for a virus that might be relevant to human cancer. Burkitt agreed to send biopsies to Epstein and eventually, after three disheartening years of failure, during which Epstein and his colleagues, Bert Achong and Yvonne Barr, tried all of the then known methods to propagate malignant cells and prove the presence of any virus therein, there was a breakthrough. The EB1 cell line, which grew out from the 26th biopsy sample, was one of the first human lymphoid cell lines to be grown in culture [12, 13]. Soon after the technique of culturing the cells was mastered came the remarkable images of the previously undescribed virus contained within them, and so EBV became the first virus to be identified by electron microscopy alone, without experimental demonstration of viral activity [14].

1.1.3 A 'stalking horse'

In the decades that followed, discoveries about this seemingly rather inert virus and the disease in which it was discovered came thick and fast. Respected virologists, Gertrude and Werner Henle confirmed the presence, experimental inertness, and therefore uniqueness of the virus in the EB1 cell line [15], and showed that EBV is widespread in all populations, with over 90% of all adults and all African Burkitt lymphoma patients being seropositive [16].

Soon afterwards, two groups showed that human lymphocytes could be transformed into continuously growing lymphoblastoid cell lines (LCLs) using BL cell lines as a source of virus [17, 18]. This provided the first evidence of EBV's growth transforming capabilities. Furthermore, epidemiological studies and detailed analysis of virus load in children living in areas where BL is

endemic showed that the disease tended to arise in individuals who were infected very young and had high levels of circulating virus, directly implicating EBV as the causative agent [19].

Apart from the virological discoveries, Burkitt lymphoma was also the first cancer shown to respond effectively to chemotherapy [20-22], and was one of the first cancers shown to carry a characteristic chromosomal translocation in every cell [23, 24]. This genomic aberration, which turned out to be the critical cellular determinant of BL, causes constitutive expression of the potent oncogene *MYC*, a transcription factor capable of reprogramming the cell for maximum proliferative capacity [25-28]. Oncogenes were initially discovered in RNA viruses and so the demonstration that these growth transforming viral factors had cellular homologues, of which *MYC* was one of the first identified, was a landmark in cancer research [29-31].

1.2 EBV

1.2.1 Taxonomy

Due to a recent restructure of virus taxonomy, Human herpesvirus 4 (EBV), now resides in the order *Herpesvirales* which encompasses 3 families, 3 sub-families, 17 genera and more than 90 species and has been reviewed in detail by Davison [32]. EBV is a gammaherpesvirus of the genus lymphocryptovirus (LCV) and is the only known human virus of this genus; the remaining members of the LCV genus infect Old World and New World primates [33]. The use of primate models of herpesvirus infection using LCVs has provided important insights into the behaviour of the virus *in vivo* [34].

1.2.2 Structure

Characteristic of *Herpesvirillae*, EBV has a complex structure comprised of multiple layers enveloped by a host-derived lipid-bilayer [35]. The envelope is studded with viral glycoproteins which mediate plasma membrane binding, fusion, and entry of the virus into the cytoplasm

[36, 37]. Beneath the viral envelope lies the tegument layer, components of which are likely to direct virus trafficking to the nucleus and egress of newly formed virus particles, although this is not well understood [38, 39]. Recently it has been reported that EBV virions also contain viral RNAs which may function immediately following host cell entry to enhance infection [40]. Inside the tegument layer the viral DNA is contained within a nucleocapsid comprised of 162 capsomer proteins arranged in a T=16 icosahedral lattice [41], inside which the EBV genome is encoded within approximately 170-180 kilobase pairs (kbp) of double-stranded DNA; the exact size varying by strain.

1.2.3 Viral genome

The EBV genome is often described in terms of BamHI regions, a reference to the molecular cloning studies which used libraries of restriction fragments to obtain the first complete EBV genome sequence [42-46]. When linearised, the viral genome is flanked by a variable number of terminal repeat (TR) regions which mediate circular episome formation. The number of terminal repeats in a given virus isolate can also be used to give an indication of the clonality of EBV in cells [47, 48]. A schematic of the viral genome is shown in Figure 1.1, which is adapted from Kalla and Hammerschmidt [49]. The majority of the approximately 85 open reading frames (ORFs) of EBV are only expressed during the productive lytic cycle and are not shown, apart from the lytic cycle initiator, BZLF1. The highly spliced latent genes of EBV that are expressed in LCLs and confer the growth transforming abilities of the virus are shown, as are the promoters that drive their expression. The non-coding RNAs; the EBERs, the BART microRNAs and the BHRF1 microRNAs are also indicated.

1.2.4 Strain variation

EBV genomes are classified as either type 1 or type 2 (previously type A and B) and then further sub-divided into a number of strains [50, 51]. Since variability is most common within

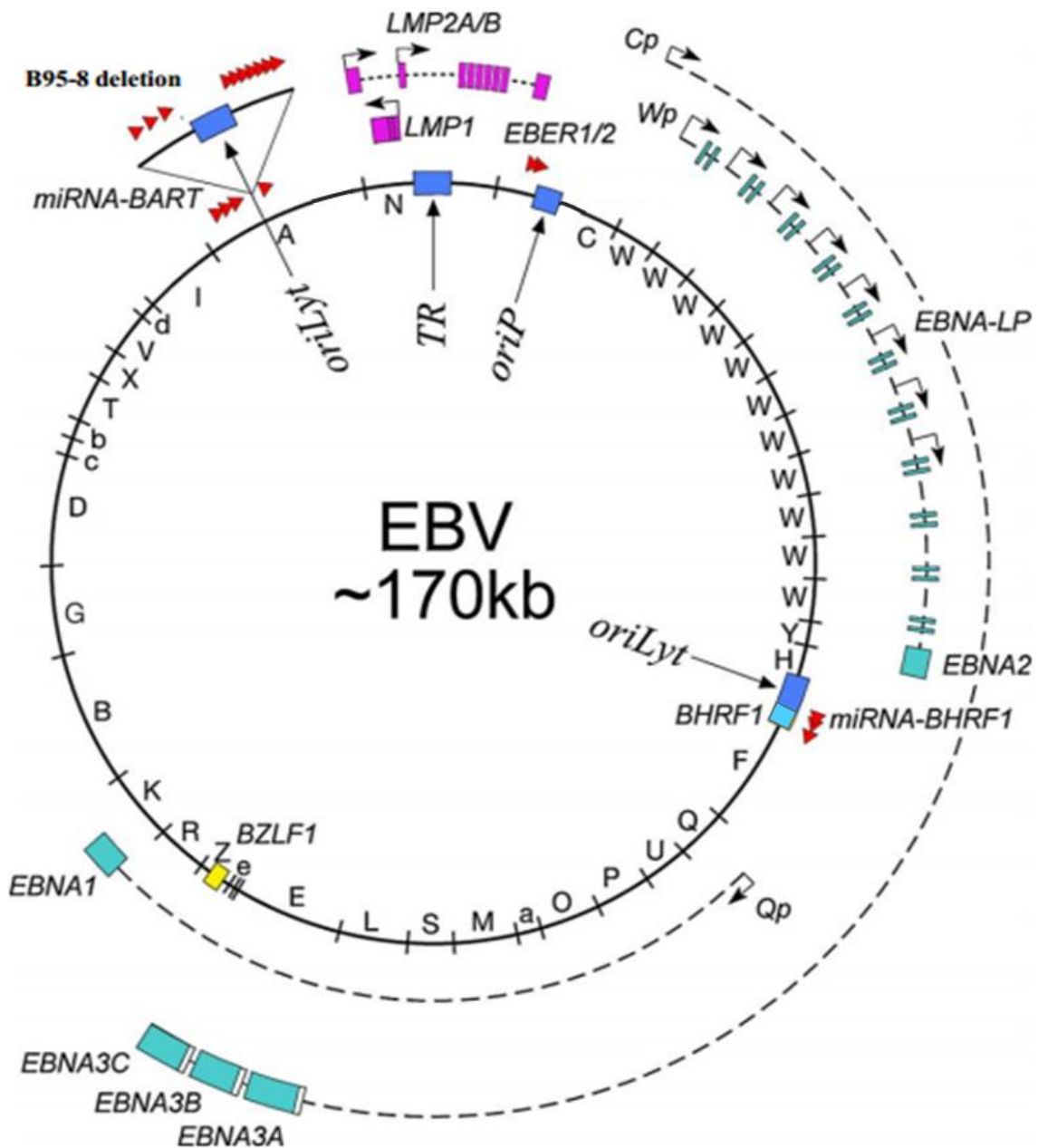


Figure 1.1 Schematic of EBV genome and position of transcripts

BamHI A regions indicated by single letter code around circular genome

Latent transcripts: EBNA-LP, EBNA2, BHRF1, EBNA3A, B and C, EBNA1. Driven from promoters; Cp, Wp and Qp

Latent membrane proteins: LMP1 and LMP2A/B driven from terminal repeats (TR)

Non-coding RNAs: BART microRNAs, BHRF1 microRNAs and EBERs 1 and 2

Lytic cycle initiator: BZLF1

oriLyt: origin of lytic replication, **oriP:** origin of plasmid replication, the characteristic 12kb deletion harboured by the prototype B95.8 strain is also indicated

Adapted from Kalla and Hammerschmidt, 2012 [49].

the latent genes which govern cellular transformation, it is possible that strain type may affect the pathogenicity of EBV [52-55]. Interestingly, type 2 EBV is less efficient at transforming lymphocytes [56], a feature that was recently found to be conferred by a single amino acid polymorphism of EBNA2 [57]. Type 2 EBV is more prevalent in regions where BL is endemic [58], although it has been suggested that this association may reflect altered immune recognition of EBV between different populations [59, 60].

Many attempts have been made to correlate disease risk and prevalence with virus strain, particularly where risk varies geographically as in BL and Nasopharyngeal carcinoma (NPC) [61, 62], or where an aetiological role for EBV is not proven or poorly understood, for example; in multiple sclerosis (MS) or rheumatoid arthritis [63, 64]. The revolution in Next Generation Sequencing (NGS) has allowed whole virus genomes to be sequenced, annotated and analysed, more quickly, cheaply and accurately than previously possible [65-67], and large scale efforts to sequence dozens of complete virus isolates are now underway (Paul Farrell, Oral Presentation, Oxford, March 2014. Alan Chiang, Oral Presentation, Brisbane, July 2014). If these projects are able to conclusively show correlations between viral strains and disease prevalence or outcome there may be significant implications for immunotherapy and vaccine development.

1.2.5 EBV infection and growth transformation *in vitro*

The ability of EBV to cause growth transformation of B cells was first reported in 1967, when Henle et al. demonstrated that co-cultivation of peripheral leukocytes with lethally irradiated BL cells leads to the outgrowth of a continuously proliferating cell line [17]. The establishment of EBV-transformed lymphoblastoid cell lines or LCLs has since provided a useful model of EBV infection and latency away from host immune responses. The efficiency of B cell infection *in vitro* is dependent on the multiplicity of infection (MOI) as this dictates the number of virus particles that are likely to bind at the B cell surface [68]. EBV binding to B cells is mediated by

the viral envelope glycoproteins, gp350 and gp42, interacting with the cellular CD21 complement receptor (alternatively called CR2) and human leukocyte antigen (HLA) class II molecules, respectively [69-71]. Once bound, the virus undergoes membrane fusion and endocytosis of the viral capsid into the cytoplasm [72, 73], followed by tegument-mediated delivery of the virus to the nucleus [74]. Once in the nucleus, the viral DNA particle becomes circularised and is maintained as an episome by 'piggy backing' onto the host replication machinery during mitosis [75] although, in rare instances, viral DNA may become integrated into the host chromosomal DNA [76, 77].

Viral gene expression during transformation of B cells

The first detectable *de novo* transcripts are driven rightwards from the Wp promoter, which is present in multiple copies within the BamHI W region. These long transcripts are differentially spliced to encode the Epstein-Barr Nuclear Antigens; Leader Protein (EBNA-LP), and EBNA-2 [78], which then go on to transactivate the Cp and LMP1 promoters [79-81]. Transcription from the activated Cp promoter gives rise to heavily spliced mRNAs from which EBNA3A, 3B, 3C and EBNA1 are generated in addition to EBNA-2 and EBNA-LP [82-84]. EBNA2 also induces expression of the three Latent Membrane Proteins; LMP1, LMP2A and LMP2B [85, 86] and these, along with the 6 previously mentioned viral antigens make up the so called 'growth', or Latency III programme of gene expression that is evident in all LCLs [87].

More recently, BHRF1, a viral Bcl-2 homologue (v-Bcl-2), previously thought to be expressed exclusively in lytic phase has also been shown to be important in growth transformation, although it is only essential for transformation when BALF1, which may be a functional homologue of BHRF1, is also deleted [88]. In primary infection *in vitro*, BHRF1 is initially expressed from the Wp promoter and like other Wp-transcribed genes, reaches maximal expression at around 12 hours post infection. In LCLs BHRF1 is expressed continuously at low levels [89].

Viral non-coding RNAs in transformation

Viral non-coding RNAs are also expressed during early infection, although their role(s) in transformation are less well understood. The non-coding EBER RNAs are abundantly expressed in LCLs but are not-detectable until around 72 hours after infection [90], and there have been conflicting reports about the effect their deletion from the viral genome has on the transformation of B cells [91-93].

The EBV-encoded microRNAs (miRs/miRNAs) are divided into two families, according to their location within the viral genome. The BHRF1 miRNAs, which reside either side of the BHRF1 ORF, are detectable within 24 hours of infection, peaking at 72-120 hours [94] and have been found to enhance transformation *in vitro* [95-97], although they did not affect tumorigenicity in a humanised mouse model [98]. The second family of EBV miRNAs are derived from the BamHI A rightward transcripts (BARTs). Despite abundant primary BART transcript expression at early time points, the BART miRNAs are not detectable until at least 72 hours post infection [94], and their role in transformation is unclear. One group found that a recombinant EBV lacking both BART and BHRF1 miRs was equally as efficient in transformation assays as a virus lacking only BHRF1 miRs, indirectly suggesting that BART miRs are not necessary for this function [95]. Whilst a second group showed more efficient outgrowth of B cells infected with recombinant viruses expressing all known BART miRs compared to the 2089 recombinant, which is deleted for the majority of the miR-BARTs. Interestingly however, there was greater variation between two different miR-BART repaired recombinant virus strains than between the B95.8 strain and the less efficient repaired strain [99].

Morphological consequences of transformation

Transformation was first described in terms of the striking changes that occur in the morphology and antigenic properties of the B cells and is synonymous to antigenic or mitogenic B cell stimulation during normal B cell maturation and differentiation. Within 24-48

hours of infection, cells enlarge and become blast-like in their appearance before rapid DNA synthesis and EBV-driven proliferation begin [100]. Blasts upregulate HLA and adhesion molecules, secrete immunoglobulin and are able to efficiently process antigen [101-103]. By 5 days post infection the cells have adhered to one another and become part of tightly packed clumps which are visible to the naked eye.

Once transformed, Latency III LCLs proliferate in culture for up to approximately 200 population doublings, at which point the cells appear to reach a crisis. The number of doublings the cells can undergo before crisis is dictated by telomere length in progenitor cells. If cells within an LCL culture mutate to acquire a permanently activated telomerase this crisis can be overcome leading to the outgrowth of a truly immortalised cell line [104, 105].

1.2.6 EBV infection and persistence *in vivo*

In the developing world, primary infection with EBV occurs early in childhood; >90% of infants seroconvert by 3 years of age, and infection is usually asymptomatic. Conversely, in developed countries, infection is delayed; around 50% of children are still seronegative at ten years of age [106]. Half to three quarters of those who are infected during late childhood or adolescence develop the self-limiting lymphoproliferative disease infectious mononucleosis (IM). Despite the age of seroconversion tending to be delayed in Western countries, by adulthood, infection is ubiquitous worldwide, although interestingly, around 5% of adults remain uninfected long term [107].

EBV is transmitted in the saliva [108], though it may also be transmissible via other bodily fluids [109]. In one widely accepted model of *in vivo* infection, the virus infects naïve B cells in the tonsillar crypts after passing through the oropharyngeal epithelium [110-112]. Although it is not yet known whether passage of the virus through the oropharynx involves infection of the epithelium or whether the epithelial cells play a strictly passive role. Once infected, naïve B cells are thought to be activated into growth and proliferation by Latency III EBV gene

expression mimicking normal B cell activation and differentiation caused by cognate antigen stimulation. EBV-activated B cells, which may or may not have undergone clonal expansion, then pass into germinal centres where they are subjected to selection and maturation [110].

In the germinal centre, B cells undergo affinity maturation during which somatic hypermutation (SHM) and selection leads to the retention of only those B cells with receptors which display a high affinity for antigen [113]. Once all low-affinity antigen-presenting B cells have been eliminated, the remaining cells are subject to isotype switching and differentiate into either antibody-secreting plasma cells, or resting memory B cells [114]. By subversion of this normal maturation pathway, EBV is thought to enter and persist benignly within the circulating memory B cell population at a frequency of <50 cells per million lymphocytes [115, 116]. It has been noted however, that X-linked agammaglobulinaemia (XLA) patients, who lack naïve B cells, show no evidence of EBV infection or immunity, suggesting that the lack of mature B lymphocytes renders them refractory to infection [117]. Additionally, that patients suffering from X-link proliferative disease (XLP) who lack functional germinal centres are still persistently infected with EBV, implying that EBV can exploit additional mechanisms in order to persist [118].

In healthy carriers EBV resides as a latent infection in resting memory B cells, where the virus remains largely quiescent, although detection of non-coding RNAs, LMP2A and periodic expression of EBNA1 to maintain the viral genome has been reported [119-122]. This immunologically silent gene expression pattern is referred to as Latency 0 [1].

1.2.7 Reactivation and lytic cycle

In vitro, a large number of stimuli have been reported to induce latently-infected B cells to reactivate into lytic cycle and produce infectious virus. Many studies have investigated chemical means of inducing reactivation including; 12-O-tetradecanoyl phorbol-13-acetate (TPA), sodium butyrate, phorbol ester, calcium ionophore and chemotherapeutic agents [123-

127], although more physiologically relevant inducers such as TGF- β , interaction with CD4⁺ T cells and immunoglobulin (Ig) crosslinking have also been reported [128-131].

In vivo, reactivation is thought to be induced when infected cells undergo differentiation. When infected memory B cells bind antigen causing crosslinking of the B cell receptor (BCR), the cells differentiate into antibody-producing plasma cells, whilst simultaneously homing to mucosa [132, 133]. Therefore, when the viral lytic cycle is completed and the cell lyses, the infectious virions that are released are able to easily access body fluids from which they can be transmitted to other individuals. It seems likely that EBV infects epithelial cells when entering and/or leaving the body, although finding such infected epithelial cells in healthy individuals has proved difficult. Interestingly, there is some evidence that infection of epithelial cells is directional; EBV can only infect polarised epithelium via the basolateral surface, implying that infection occurs when the virus is leaving the body [134]. Additionally, since differentiated epithelial cells can support high levels of lytic viral replication, they may also release infectious virus if they become infected by EBV as it transits out of the body [135].

Lytic cycle is initiated by expression of the immediate early lytic genes, BZLF1 and BRLF1, and then proceeds in phases of early gene expression followed by late gene expression. BZLF1 binds and activates promoters containing Z-response elements (ZREs) [136, 137], and seems to preferentially bind ZREs that are highly methylated [138, 139]. BRLF1 can enhance transcription directly, by binding DNA at GC-rich promoter sequences to activate transcription [140], or indirectly, where DNA-binding is not necessary [141, 142]. These transcription factors then go on to stimulate the expression of a second wave of lytic-associated viral genes, known as the early lytic genes. Early genes include; those required for viral DNA synthesis, inhibitors of apoptosis and immune evasion genes. Together these viral genes function to replicate the viral DNA whilst ensuring the survival of the reactivated cell long enough for the complete virions to be assembled. Once the DNA has replicated, the late lytic genes are expressed, many of which are structural or packaging elements of the virus. A single EBV-infected cell may

produce as many as a thousand virions before the cell lyses, releasing the newly synthesised infectious virus [143].

1.2.8 Tissue tropism

In vitro, EBV readily infects B cells derived from a number of sources, including peripheral blood, lymphoid tissues and cord blood, and at different stages of maturation (naïve, switched memory and non-switched memory) [144-147]. In contrast to B cells, epithelial cells are relatively refractory to infection with EBV using cell-free virus *in vitro* however, the virus can infect epithelial cells when transferred from a B cell, via the formation of a virological synapse [134]. Some NK and T cell tumours are known to carry EBV, yet there is little reliable evidence that primary T and NK cells can be infected *in vitro* [148-151]. It is possible that the conditions required for NK and T cell infection only occur in rare circumstances, such as during chronic inflammation and thus entry into these cell types represents an unusual biological accident [152]. Or it may be that EBV entry into these cell types is restricted by surface receptors that are transiently expressed, and may require a sequential and directional passage through other cell types. This scenario appears to be the case for the murine Kaposi's sarcoma-associated herpes virus (KSHV) homologue, MuHV-4, which must first pass through neuroepithelium and myeloid cells before gaining entry to the B cell compartment [153, 154]. There has also been suggestion that viral strain may influence the tropism of EBV, as was recently reported by Delecluse and colleagues who isolated a previously undescribed virus strain, M-81, which appears to show enhanced tropism for epithelial cells compared to the prototype B95.8 strain [66].

1.2.9 Viral latency

The majority of the genes encoded by EBV function during the viral lytic cycle and so are generally not expressed in EBV-associated malignancies, where most, if not all, of the tumour

cells necessarily support a non-productive infection. Several different programmes of latent infection have been described, known as Latency I, Latency II, Latency III, Latency 0 and Wp-restricted Latency, which vary by cell type and disease setting. A schematic of the known Latency patterns is shown in Figure 1.2. Since many of the EBV latent genes are immunogenic, generally fewer viral antigens are expressed in malignancies where patients tend to be more immunocompetent, whereas a greater repertoire of viral genes may be expressed in the immunocompromised.

Latency III

In Latency III, the profile of gene expression characteristic of LCLs, all of the essential growth transforming proteins; EBNA1, EBNA2, EBNA-LP, EBNA3A, 3B, 3C, and LMP1 are expressed as well as LMP2A, 2B, and low levels of BHRF1 [89, 107]. Additionally, a number of non-coding RNAs are present including; the EBER RNAs, all three BHRF1 miRNAs and the BART microRNAs [94, 155, 156]. LCLs created by infecting B cells *in vitro* express Latency III, but this gene expression pattern is also found in lymphoproliferations and lymphomas of the T-cell immunocompromised, such as transplant patients receiving immunosuppression, or in late stage AIDS [157-159].

Latency II

EBV exhibits a Latency II pattern of gene expression in which the EBER RNAs, EBNA1, LMP-1, -2A, and -2B proteins and high levels of BART microRNAs are expressed in several types of malignancy including; Nasopharyngeal carcinoma (NPC), Hodgkin lymphoma (HL), and extranodal NK/T cell lymphoma [160-163]. In these diseases the immunodominant EBNA2 and

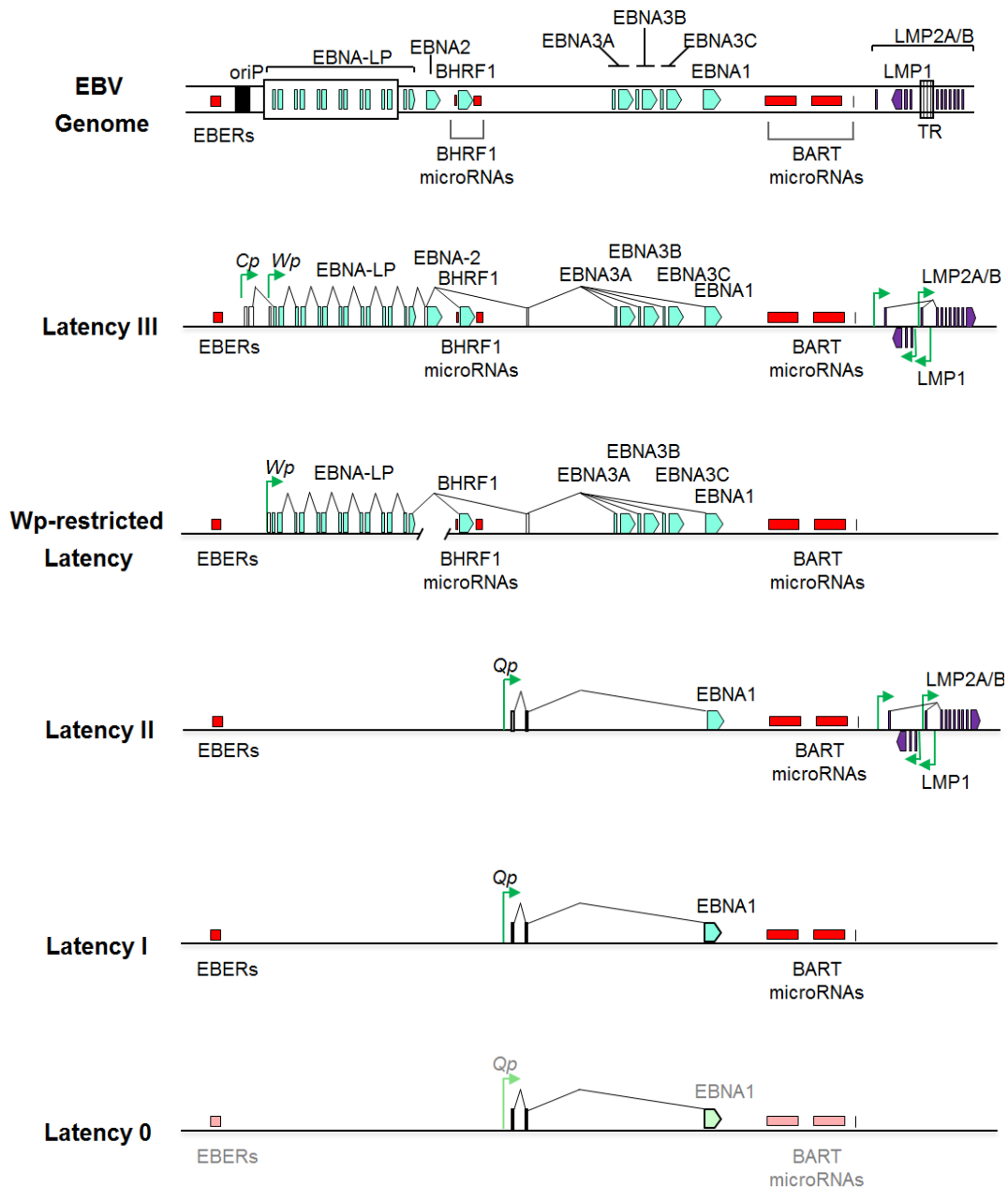


Figure 1.2 Viral Latency programmes found in EBV infected cells

EBV Genome - shows the relative positions of relevant genes

Latency III - also called the growth transforming programme, found in LCLs and PTLDs

Wp-restricted Latency - found in a subset of 15% of BLs, gene expression imposed by deletion in viral genome

Latency II - also called the default programme, found in a number of epithelial and lymphoid malignancies (see Section 1.2.10)

Latency I - found in 85% of EBV-positive BLs

Latency 0 - in resting B cells EBV has been reported to express Latency I genes, possibly periodically and at very low levels as there are no reports of finding all Latency I-associated genes in a single healthy donor

Adapted from Rowe, Fitzsimmons, and Bell, 2014 [280]

EBNA3 proteins are not expressed, although the latent membrane proteins, which can also be recognised by cytotoxic CD8⁺ lymphocytes (CTLs) are present [164, 165]. The LMP proteins are thought to modulate NF-κB signalling and inhibit apoptosis [166, 167], whilst the high level of BART miRNAs may contribute to immune evasion [168, 169].

Latency I

Latency I is the most restricted form of viral gene expression found in EBV-associated diseases, where only the EBNA1 protein, the EBER RNAs and the BART miRNAs are expressed. The virus exhibits Latency I in around 85% of all EBV-positive BL as well as in EBV-associated cases of gastric carcinoma [170-173]. Recent studies have also suggested that additional transcripts may be present in Latency I BL cell lines however; it is currently unclear whether these transcripts are present in every cell or what function they may have [174, 175].

Wp-restricted Latency

In a small sub-set of BLs, comprising around 15% of the biopsies we have had the opportunity to examine, the pattern of EBV gene expression is more extensive than that seen in the Latency I tumours and includes EBNA3A, B, and C, a truncated form of EBNA-LP (t-EBNA-LP) and the BHRF1 protein, in addition to EBNA1, EBERs and BARTs [89, 176]. More recently we have also found that two of the three BHRF1 miRNAs are also expressed in these tumours [94]. This pattern of gene expression, known as Wp-restricted Latency (Wp-BL) appears to occur uniquely in BL, and is imposed by a large deletion within the transcriptionally active viral genome in the cell. The exact size of the deletion varies between tumour samples, but always encompasses the coding region of the EBNA2 gene, placing BHRF1 adjacent to the promoter-encoding Wp repeat region [176]. This promoter, which is silent in Latency I BL, drives high levels of BHRF1 expression and also transcribes the EBNA proteins [89]. Interestingly, wild-type genomes can also be isolated from cells expressing Wp-restricted

Latency, but they appear to be transcriptionally silent [176]. Presumably, the deletion of EBNA2 arises as a rare, random event however; the observation that EBNA2 expression is incompatible with c-myc [177], suggests that Wp-BLs may arise from a Latency III lymphoblast that has acquired an Ig/MYC translocation, which then selects against expression of EBNA2. Once the deletion has occurred it is likely to be strongly selected for as BHRF1, t-EBNA-LP, EBNA3s all confer apoptosis resistance to BL cells [178-181].

In addition to several examples of Wp-BL where every cell exhibits this pattern of viral gene expression, we also identified a tumour in which multiple forms of Latency were evident. From this single biopsy we were able to isolate single cell clones exhibiting Latency I, a novel form of EBNA2⁺/LMP1⁻ Latency or Wp-restricted Latency as well as cells that had apparently lost the viral genome entirely. Compellingly, these viral gene expression programmes were also shown to confer varying degrees of apoptosis resistance, with the EBV-loss cells exhibiting the most sensitive phenotype [178, 182].

Latency 0

As mentioned in Section 1.2.5, EBV is found to be almost entirely quiescent in circulating memory B cells, in a state known as Latency 0. No viral proteins are expressed in Latency 0, but EBER RNAs and BART miRNAs have been detected in blood from healthy donors [119, 121, 183, 184]. Additionally, EBNA1 transcripts driven from the Qp promoter have been detected in replicating cells and LMP2A transcripts have also been reported [119, 122].

1.2.10 Disease associations

Outside of its long-held association with Burkitt lymphoma, EBV has also long been associated with a variety of other malignant and non-malignant diseases. Previous estimates suggested

that EBV contributes to around 2% of the global cancer burden [185, 186], and a recent evaluation of current data has calculated that annually, there are around 200,000 cases of EBV-associated cancer globally and 120,000 cases of infectious mononucleosis in the US alone [187]. Therefore, despite the fact that a relatively small percentage of carriers will go on to develop an EBV-associated disease, the vast number of individuals that are infected worldwide means that the virus poses a significant challenge to global health. A detailed discussion of EBV-associated disease is outside of the scope of this review; however Table 1.1 contains a summary of the principle features of several cancers and diseases that are commonly associated with the virus. In addition to those listed, it has been suggested that EBV may also play an aetiological role in a number of other cancers including; certain epithelial tumours of the salivary gland, lung, oesophagus, cervix and breast [188]. Although since case reports of EBV-positive tumours of almost every type can be found in the literature, further investigation is required to determine whether the virus genuinely contributes to the pathogenesis of these cancers. EBV has also long been implicated in a range of autoimmune diseases including; multiple sclerosis (MS), Sjögrens syndrome, rheumatoid arthritis and systemic lupus erythematosus. It is difficult to prove a role for EBV in inflammatory diseases, as EBV is recruited in infected B cells to sites of inflammation. However, recent meta analyses have shown that the association of EBV with MS is extremely robust [189, 190] .

Disease	Features
Infectious mononucleosis (IM)	Most commonly occurs when primary infection with EBV is delayed until adolescence. Self-limiting lymphoproliferative disease. Symptoms include; sore throat, fever, malaise and lymphadenopathy, but can be life-threatening. Causes vast expansion of EBV-specific CD8 ⁺ T cells.
Post-transplant lymphoproliferative disease (PTLD)	Occurs as a result of EBV reactivation in the immunosuppressed. Neoplastic cells can be poly-or mono-clonal and EBV gene expression can be Latency III or more restricted. The more rapidly after transplant the PTLD occurs, the more likely it will be polyclonal and expressing all Latency III-associated genes.
Nasopharyngeal carcinoma (NPC)	Incidence geographically restricted, always EBV-positive. In high incidence areas prevalence can be >20/100,000. Latency II viral genes expressed. Exposure to N-nitrosamines is a known risk factor.
Hodgkin lymphoma (HL)	Malignant cells account for only 1-2% of tumour. Mixed cellularity sub-type is highly associated with EBV (<90%), but there is a much lesser degree of association with other sub-types. EBV-infected tumour cells express the Latency II gene expression programme.
EBV-associated gastric carcinoma (EBV-GC)	Around 9% of gastric carcinomas EBV-positive, accounting for over 80,000 cases per year. EBV gene expression restricted to Latency I.
Extranodal NK/T cell lymphoma (ENKTL)	Relatively rare, but accounts for up to 5% of non-Hodgkin lymphoma in East Asia. Tumour cells exhibit the Latency II programme of viral gene expression.
Chronic active EBV (CAEBV) and HLH	Premalignant diseases. CAEBV resembles chronic IM clinically and can last several years. HLH is typified by phagocytosis of erythrocytes in the bone marrow. In both cases EBV may be found in either the NK or T cells and both predispose to later occurrence of EBV-driven lymphomas.

Table 1.1 Features of EBV-associated diseases.

All characteristics as described in Rickinson and Kieff, 2007 [107].

HLH – haemophagocytic lymphohistiocytosis

1.3 Burkitt lymphoma

1.3.1 Incidence and clinical characteristics

BL tends to be referred to as three sub-types; endemic (eBL), sporadic (sBL) and HIV-associated (HIV-BL), defined on the basis of epidemiology, as outlined in Table 1.2 [191]. It has also been reported that subtypes of BL differ in terms of their primary site of tumour presentation, with endemic BL tending to occur as a tumour of the jaw, and other subtypes tending to present as an abdominal swelling. However, there have recently been reports of a shift in primary tumour site in endemic regions which raises the possibility that earlier data may have been misleading

Feature	Burkitt lymphoma subtypes		
	Endemic	Sporadic	HIV-associated
Geographic location	Central Africa and New Guinea	Worldwide	
Peak age of incidence	5-9 years	11 years	10-19 years
Annual incidence (per 100,000)	5-10	10-100-fold less than eBL (varies geographically)	10-100-fold more than eBL (in untreated HIV+ individuals)
EBV associated cases (%)	100%	10-85%	<40%
Known co-factors	Holoendemic malaria	None yet known	Untreated HIV infection
MYC translocation	Immunoglobulin heavy chain, VDJ region, 5' to MYC	Immunoglobulin heavy or light chain, class switch region, within MYC ORF	

Table 1.2 Features of BL that are known to vary by sub-type

Adapted from Kelly and Rickinson, 2007 [190], with additional data from sources as cited within the main text

[192, 193]. After all, in rural Africa abdominal swelling may be misdiagnosed, and it can be hard to tell from hospital records whether abdominal swellings may have been attributable to BL. Interestingly, although the differences between the BL subtypes may suggest differences in the route to pathogenesis, there is little evidence for histologic or molecular differences between the subtypes [194, 195].

Histology

Histologically, BL appears as rapidly growing (>95% Ki67 positive), small to medium sized, regular-shaped B cells with prominent nucleoli, as a diffuse infiltrate interspersed with macrophages giving the tumours a characteristic 'starry sky' appearance. Immunohistochemically, BL cells are defined by their expression of centroblastic or germinal centre markers CD10, CD77, CD38 and Bcl-6 and the absence of Bcl-2 expression [196, 197]. In-keeping with a germinal centre or post-germinal centre cell phenotype, BL cells also harbour Ig V rearrangements; this phenotype has also been confirmed by transcriptional microarrays [198]. Ig rearrangements are monoclonal within individual tumours and most BLs express surface IgM, although other phenotypes have also been reported.

Endemic BL

In endemic regions of sub-Saharan Africa and New Guinea BL is common, probably accounting for 30-50% of all childhood lymphomas [199]. Incidence of eBL peaks in children aged 5-9 and tends to occur earlier in life and more commonly in boys than girls, although estimates vary. Furthermore, recent studies have brought attention to misdiagnosis of BL leading both to under-reporting and over-reporting in different centres [200, 201]. Malaria is likely to be a cofactor in the pathogenesis of eBL, although this is poorly understood (see Section 1.3.2). Intriguingly, eBL patients appear to be immunocompetent and yet this is the only subtype with which EBV is 100% associated. Additionally, there are areas, such as Northern Brazil, where BL

incidence is described as intermediate, as it is less common than eBL, but >50 times more common than sBL and 75-90% of cases are EBV-positive [202-204], which implicates a role for other geographically-restricted cofactors in these areas.

Sporadic BL

Outside of 'intermediate' areas, the sporadic form of BL (sBL) is rare at around 1-3 cases per million as a worldwide average [199]. The peak age of incidence is also slightly delayed in comparison to eBL and tumour cells are EBV-positive in only 15-30% of cases [205, 206]. Patients diagnosed with sBL appear to be immunocompetent and as yet no other contributory cofactors have been identified, although there may be some differences in cellular mutations or miRNA expression between eBL and sBL [207, 208].

HIV-associated BL

HIV-associated BL (HIV-BL) became of clinical importance in the early 1980's when there was an 'outbreak' of BL in the US, predominantly presenting in homosexual males [209, 210]. It was soon realised that these patients were also infected with HIV, although at the time of BL diagnosis, T cell counts were not depleted and there was no other suggestion of immune deficiency; in fact BL was often the first indication of their HIV status. BL remains a common early complication of HIV infection, accounting for <40% of AIDS-associated non-Hodgkin lymphoma (NHL) and EBV is found in the tumour cells of 30-40% of HIV-BL cases [211]. The peak age of HIV-BL is reported as 10-19, although the data that was gained during the HIV epidemic in the US, on which this statistic is based, actually shows that the actual number of HIV-BL cases within this age group was very small (14 cases versus 496 in those aged 19-50 and 80 cases in those aged over 50) [212].

1.3.2 The role of cofactors in BL pathogenesis

The reasons for variation in EBV-association between different forms may well be explainable in terms of the cofactors associated with each subtype. Malaria and HIV are known cofactors for developing BL, yet the interactions of these infections with EBV are not well described.

Malaria

BL is endemic in Africa and Papua New Guinea where malaria is holoendemic, meaning that the population is chronically exposed to the *Plasmodium* parasite from birth [213]. Since children with greater exposure to malaria exposure tend to have higher EBV viral loads [214, 215], it was hypothesised that malaria might cause polyclonal B cell expansion [216]. However, it has also been proposed that malaria may instead inhibit T cell function and therefore lead to poor control of primary EBV infection, which may also result in elevated viral loads [217].

The T-cell hypothesis was given early support by findings that PBMCs from malaria-infected children could not inhibit the growth of autologous LCLs [218, 219], unlike those from healthy donors [220]. There is now a good deal more data concerning how T cells might control EBV, although we still have little idea of exactly what dictates the balance in otherwise healthy individuals *in vivo*. Recent publications have found that CD8⁺ T cells from children in holoendemic malaria regions are deficient in IFN- γ production and that EBV latent gene specific T cells exhibit a more differentiated phenotype than those specific for lytic genes, and than the T cells of non-malarial individuals [221-223]. Additionally, it has recently been hypothesised that EBV may alternatively induce SHM in infected B cells, leading to a greater risk of *MYC*-translocation occurring [224].

Co-infection with HIV

HIV vastly increases the risk of an individual developing NHL, although the risk of developing several subtypes that are also associated with non-HIV immune deficiencies, such as PTLN,

DLBCL and Kaposi's sarcoma, has decreased significantly since the introduction of highly active anti-retroviral therapy (HAART). Surprisingly, there has been no such decrease in the incidence of HIV-BL [225, 226], and diagnosis of the infection and the malignancy are still often coincident (800 of 1,100 HIV-BLs in one recent study). Curiously, this study also showed that those with impaired CD4⁺ T cell counts due to AIDS were at a significantly decreased risk of developing BL [227]. It may be that CD8⁺ T cell activation status may explain the predisposition of immunocompetent HIV-positive individuals to develop BL; one study recently showed that CD8⁺ cell activation was significantly increased in 13 HIV-BLs versus controls, but more data is needed to support this finding [228].

Another hypothesis, and one that has also been posited to be a consequence of malaria infection, is that the presence of HIV increases expression of activation-induced (cytidine) deaminase (AID) in the B cell compartment and that the concomitant increase in SHM increases the risk of a *MYC* translocation [224]. However, although increased AID expression has been described in HIV-positive individuals [229], a different study found that detection of *MYC* translocations in the blood was not predictive of HIV-BL [230]. It is noteworthy that many HIV-infected individuals in the US are undiagnosed and also that some cancer registry entries fail to record patients' HIV-status, meaning that comparisons of HIV-BL to non HIV-BL may be skewed [231].

Other cofactors

There have also been a number of studies investigating the role of other possible environmental cofactors in the pathogenesis of BL. Ever since the 'lymphoma belt' was first mapped out there has been suspicion that infections other than malaria may play a role in BL. However, despite several studies, there is still little evidence to implicate those suggested which include; Chikungunya virus, O'Nyong-nyong virus, and sexually transmitted infections [227, 232, 233]. Lifestyle factors such as selenium deficiency, gum damage, use of some

traditional or Western medicines and exposure to known carcinogens have been the focus of other studies, but these are mainly stand-alone publications which often rely on retrospective self-reporting [234-240]. There is evidence to suggest that additional cofactors may play a role in BL; BL 'outbreaks' do not always correlate with malaria exposure [234, 241] and age-distribution curves of BL in the US indicates non-cumulative risk factors [242]. However, larger and more detailed studies are needed to fully understand and interpret these observations.

1.3.3 Genetic factors

***MYC* translocation**

Common to all cases of BL is the hallmark reciprocal translocation between the *MYC* oncogene, which lies on the long arm of chromosome 8 (8q24), and one of the immunoglobulin (Ig) loci positioned on chromosomes 2, 14 and 22. In the majority of cases (80%), *MYC* is expressed from the Ig heavy chain locus 14q32, whereas the variant translocations; to either the kappa (2p12) or lambda (22q11) light chain locus, each occur at a frequency of around 10% [2, 243-245]. Interestingly, several papers have described differences in the position of the breakpoint, with respect to both the Ig gene and *MYC*, which vary between endemic and sporadic BL. In endemic cases the Ig breakpoint tends to occur in the VDJ region of the heavy chain, juxtaposing *MYC* at the 5' end, proximal to its start site. Whilst in sporadic cases the light chain switch region is more frequently the site of translocation and intersects *MYC* within its ORF [206, 246, 247]. These findings may reflect different routes of pathogenesis for the different BL subtypes.

***MYC* function**

Regardless of the breakpoint, *MYC* translocation leads to constitutive overexpression of c-myc, a global transcription factor capable of binding and regulating around 15% of cellular genes in BL cells [248]. In normal cells, *MYC* is expressed transiently in order to stimulate proliferation

in resting cells and its expression is strictly regulated. Unsurprisingly, unchecked expression of c-myc has a dramatic effect on the cellular phenotype and has been shown to deregulate many genes and pathways (reviewed in [249]). For some time the mechanisms behind these pleiotropic effects were not understood, but recently, two groups reported that c-myc binds to, and enhances expression from, only those loci that are already transcriptionally active [250, 251]. Thus, *MYC* acts as a 'megaphone' for whatever signalling pathways and processes are already active in a particular cell [252]. In immature B cells, which are poised to undergo clonal expansion, this leads to rapid proliferation through upregulation of cyclin D and derepression of cyclin E, whilst concomitantly reinforcing a centroblastic differentiation state by inhibiting NF- κ B and interferon signalling [253-257].

***MYC* and apoptosis**

In many cell types, c-myc over-expression is a double-edged sword as it also amplifies apoptosis-regulating genes, which serve to protect against inappropriate cell growth and are normally restrained in healthy cells [258]. Therefore, overcoming apoptosis is a prerequisite step in *MYC*-driven lymphomagenesis. One well-characterised pro-apoptotic pathway activated by c-myc is the p53-ARF-MDM2 axis and around 30% of BL biopsies [259], and around 70% of BL cell lines have mutated p53 sequences [260-262]. Furthermore, in BLs where p53 has a wild type sequence, p14^{ARF}, p16^{INK4} or MDM2 are altered in their expression or function in order to circumvent p53-dependent cell death [263, 264]. It appears that suppression of p53 signalling is necessary, yet insufficient to overcome c-myc [265, 266].

Accordingly, several members of a second important family of apoptosis regulators; the Bcl-2 homologues, are also commonly deregulated in *MYC*-driven lymphomas [267-273]. Additionally, deletion of the pro-apoptotic Bcl-2 family members Bim, Puma and Noxa have been found to synergistically contribute to lymphomagenesis in the E μ -myc mouse model, where *MYC* is constitutively expressed from the IgM heavy chain enhancer [266, 274].

Interestingly, *MYC* itself is frequently found to be mutated in BL [275], and this is also thought to reflect a need to avoid apoptosis activation whilst retaining or enhancing its proliferative capability [276, 277]. Indeed, one common *MYC* mutation abolishes upregulation of Bim [269]. Outside of the p53 and Bcl-2 pathways, mutations in other signalling pathways may also play a role in BL. Recent genome-wide studies have identified *ID3*, the transcription factor E2A and cyclin D3 as frequently mutated in BL biopsies and cell lines [277-279]. Interestingly, these targets all contribute to a third survival axis, which is ultimately co-ordinated by PI3K; hence several different diversion mechanisms may contribute to apoptosis escape in BL [280].

1.3.4 Treatment and prognosis

Early chemotherapeutics showed great promise in treating BL, with Burkitt himself reporting that even one dose of methotrexate can cause tumours to completely regress [281, 282]. Indeed, the current recommended treatment in Europe, known as COPAD, where only two cycles of cyclophosphamide, vincristine, prednisolone and doxorubicin are given, achieves 99% 5 year survival in children and adolescents with NHL (40% of the cohort had BL) [283]. Additionally, even 90% of those with central nervous system or significant bone marrow involvement have been shown to survive at least 5 years when treated with COPAD plus the anti-CD20 antibody, rituximab [284], but sadly, these impressive survival rates are not achieved in all BL patient cohorts.

In the developing world, where intensive patient support is not available and chemotherapeutic options are limited, survival is greatly reduced. One study evaluated a 28-day treatment with cyclophosphamide, methotrexate and hydrocortisone, which cost just \$50 per patient to administer. Whilst the treatment was affordable and well tolerated, only 48% of patients survived more than 5 years [285]. There is also poor survival worldwide in elderly patients; two recent studies carried out in the US report 5-year survival rates of only 29-33% in patients over 60, this is a remarkable contrast to the almost complete cure rate in

younger patients [242, 286]. Additionally, patients who respond poorly, relapse, or have refractory disease have an extremely poor prognosis and very few of these patients respond to further treatment [287].

1.3.5 The role of EBV in BL

EBV infection is known to induce cellular genomic instability in a number of settings [288-290], possibly via upregulation of AID and SHM [147, 291], which direct hypermutation and class switching in B cells. Therefore it has been hypothesised that the major role for EBV in BL occurs prior to tumour formation by increasing the likelihood of the c-myc translocation however, there are several lines of evidence which suggest that the virus makes an ongoing contribution to the tumour cells [292, 293].

In EBV-positive BLs, the virus is present in every tumour cell at around 20-100 episomal copies per cell [294], and in contrast to cell lines derived from other EBV-positive lymphomas, is efficiently maintained in cultured BL cells long term. Yet, virus episome replication and segregation to daughter cells is imperfect; around 16% of plasmids are not replicated per cycle and, despite episomal pairing at sister chromatids, they are unevenly distributed during mitosis [295-297]. Therefore, it appears that there is strong selection against loss of the virus. Additionally, treating BL cells with a dominant negative EBNA1 (dnEBNA1), which enforces the loss of viral genomes, also induces apoptosis, suggesting that EBV is essential to these cells [298, 299]. Interestingly, there are differences between the number of somatic mutations and in the frequency of chromosomal copy number changes in EBV-positive versus EBV-negative tumours [208, 300]. This suggests that EBV-negative BLs appear to arise via a slightly different pathogenic route, independently of EBV.

Given that subversion of apoptosis is an essential step in MYC-driven lymphomagenesis, and that inactivation of p53 alone is insufficient in this regard [265, 301, 302], it has long been suggested that EBV may provide additional protection against apoptosis in the established

tumour. In the 15% of eBLs that exhibit Wp-restricted Latency the evidence for this is clear; BHRF1 provides a strong survival advantage via binding to pro-apoptotic members of the intrinsic apoptosis pathway [89, 303-305], whilst the EBNA3 proteins have been shown to epigenetically silence expression of a protein from the same family [181, 306]. In fact, the anti-apoptotic phenotype of Wp-restricted BL cells is so pronounced in comparison to Latency I counterparts that we suspect that these tumours may be resistant to chemotherapy, although this has yet to be fully investigated.

In classical Latency I BL, the nature of the ongoing contribution of EBV has been much discussed, but remains controversial (reviewed in [1, 307, 308]). In 1994, a report that spontaneous loss of EBV from a sporadic BL cell line increased the sensitivity of the cells to apoptosis, impaired their growth and rendered them non-tumorigenic in a mouse model provided compelling evidence and for the first time, demonstrated a system in which isogenic cells that contained or had 'lost' the virus could be directly compared [309]. This group later showed that the 'EBV-loss' phenotype could be reversed by restoring the virus genome; a key result which directly implicated the virus as a protective agent in BL [310]. However, since the Akata-BL cell line used in these studies had been passaged over 200 times before it gave rise to EBV loss cells and because eBL cell lines often retain EBV indefinitely in culture, several studies were initiated to determine the generality of these findings.

The Sixbey group used hydroxyurea to eliminate the viral genome from Mutu-BL as well as Akata-BL, but found that only Akata-BL-derived EBV-loss cells showed an increase in apoptosis sensitivity [311]. An alternative strategy was used by the Sugden group, who treated BL cells with dnEBNA1 to evict EBV and found that loss of EBV genomes consistently induces apoptosis in both Latency I and Wp-restricted BL cells [99, 182, 298, 299, 312]. Although this approach convincingly demonstrates the addiction of BL cells to the presence of EBV, due to the toxicity of this treatment, it is difficult to isolate EBV-loss clones to allow for comparison to EBV-positive cells in the same manner as the spontaneous loss method. Interestingly, the Awia-BL

cell line that was generated by our group from an endemic BL yielded spontaneous EBV-loss clones during early passage and also exhibited increased sensitivity to apoptosis compared to isogenic EBV-positive clones [178]. Since our group had amassed a collection of early passage eBL tumour cell lines, we therefore initiated a project to investigate the frequency and consequence of EBV-loss on a large panel of eBLs; the findings of which form the basis of this thesis.

There has also been a significant amount of debate about the mechanisms by which EBV might subvert the cell death machinery. Since EBNA3s can epigenetically silence the tumour suppressor protein, Bim, it has been suggested that the viral gene(s) responsible might themselves be silenced after carrying out this modification and therefore, be absent from the resulting tumour. However, whilst Bim is irreversibly downregulated by EBV during primary infection [313], it is highly expressed in our panel of Latency I BLs [301]. Ectopic expression of LMP2A has also been shown to protect some BL cell lines from apoptosis [167, 314], and can enhance tumorigenicity in a mouse model [315, 316], but we find no evidence that LMP2A protein is expressed in our Latency I cell lines [317]. Therefore we have focussed our attention on the EBNA1 protein, EBER RNAs and BART microRNAs that are consistently present in Latency I BLs.

EBNA1

The critical function of EBNA1 in viral genome maintenance through tethering of the viral genome to sister chromatids and directing viral replication has been well characterised, but it has also been ascribed several other important functions [297, 318, 319]. Apart from its status as the only viral protein known to be expressed in BL, the first suggestion that EBNA1 might contribute to survival in BL was the finding that EBV-positive cells undergo apoptosis when treated with dnEBNA1, whereas EBV-negative cells are unaffected [298]. Whilst this does support an essential role for EBV in BL, since dnEBNA1 causes the virus to be rapidly lost from

the cells, it does not necessarily implicate EBNA1 as the protective factor. There are several other mechanisms by which EBNA1 has been suggested to inhibit apoptosis including modulation of p53 signalling and upregulation of Survivin [320-322]. However, no direct evidence exists to support these findings in a BL model. EBNA1 has also been reported to exhibit tumorigenic properties in mice [323, 324], but this finding could not be repeated in a different model, which implied that the increased tumorigenicity was an experimental artefact of transgene integration [325, 326]. Importantly, two groups who ectopically expressed EBNA1 in EBV-loss clones could not demonstrate any effect on cell survival [310, 327].

EBER RNAs

The highly abundant small non-coding EBER RNAs are also expressed in all recognised forms of EBV latency [78, 328] and several functions have been attributed to them. Principally, they are thought to be involved in the evasion of innate immunity and inhibition of apoptosis, although a varying number of differing, and sometimes conflicting, mechanisms have been proposed to govern these functions. The EBER RNAs share several features with the two small adenovirus RNAs, VAI and VAI1, which suggested that these RNAs might also be functionally homologous. The VAs bind the host-protein shut-off regulator, RNA-dependent protein kinase (PKR), in order to maintain protein translation, which is critical to allow replication of adenovirus when the interferon signalling pathway is activated due to the presence of the viral genome [329, 330]. Although EBERs can partially rescue the replication of an adenovirus lacking VAs [331, 332], there are several lines of evidence that suggest it is unlikely that they inhibit PKR function during EBV infection. The location of the EBERs appears to be strictly nuclear, and they cannot shuttle to the cytoplasm unlike VAs [333, 334]. Additionally, the presence or absence of EBERs neither alter the activity of PKR as measured by interferon sensitivity in LCLs, nor do they affect the phosphorylation of PKR and its substrate eIF2 in EBV-loss Akata-BL clones or LCLs [335-337], although this second point is disputed [338].

EBERs have been shown to confer apoptosis protection to EBV-loss cells [339], although other studies found that this protection was only partial when compared to EBV-positive cells [327, 340], which was attributed to upregulation of Bcl-2 and IL-10 as well as PKR signalling [339-342]. Importantly, all of these studies addressing a possible pro-survival role for EBERs in BL were carried out in EBV-loss clones of Akata-BL and, therefore, further studies are needed in other tumour backgrounds in order to reconcile these data and establish their generality.

The EBERs have also been subject to a number of detailed biochemical analyses, which have demonstrated that EBERs are able to bind the ribonucleoproteins (RNPs), La and L22 [343-346], but the functional consequences of this binding have remained doggedly enigmatic. Although one group has proposed that EBERs are able to provide a growth advantage to L22-positive cells, but not in its absence [347].

BART microRNAs

Although the BamHI A region, which is transcriptionally active in several malignancies, has long been known to give rise to a complex variety of transcripts driven from 2 promoters (known as P1 and P2) [348-351], it took until 2004 to discover that these transcripts give rise to tiny non-coding RNAs, known as microRNAs [352]. A schematic of the primary transcripts and the microRNAs is shown in Figure 1.3. It had previously been proposed that these transcripts encoded proteins [353-355], but whilst they could be transcribed and investigated *in vitro*, there was little evidence for the existence of BamHI A-derived proteins in EBV-positive cell lines [356, 357].

The class of short (22-24nt), regulatory RNAs known as microRNAs (miRs) function as part of the RISC complex, which selectively binds to mRNAs causing them either to become unstable and be degraded, or inhibiting their translation, although the exact mechanisms governing this are unclear. Like many other miRs, the BARTs are encoded within introns and are initially transcribed as long primary transcripts (pri-miRNAs) which are then processed by Drosha and

Dicer and transported to the cytoplasm where the mature miR becomes incorporated into the RISC complex. This complex then goes on to bind its target transcript to which the miR confers

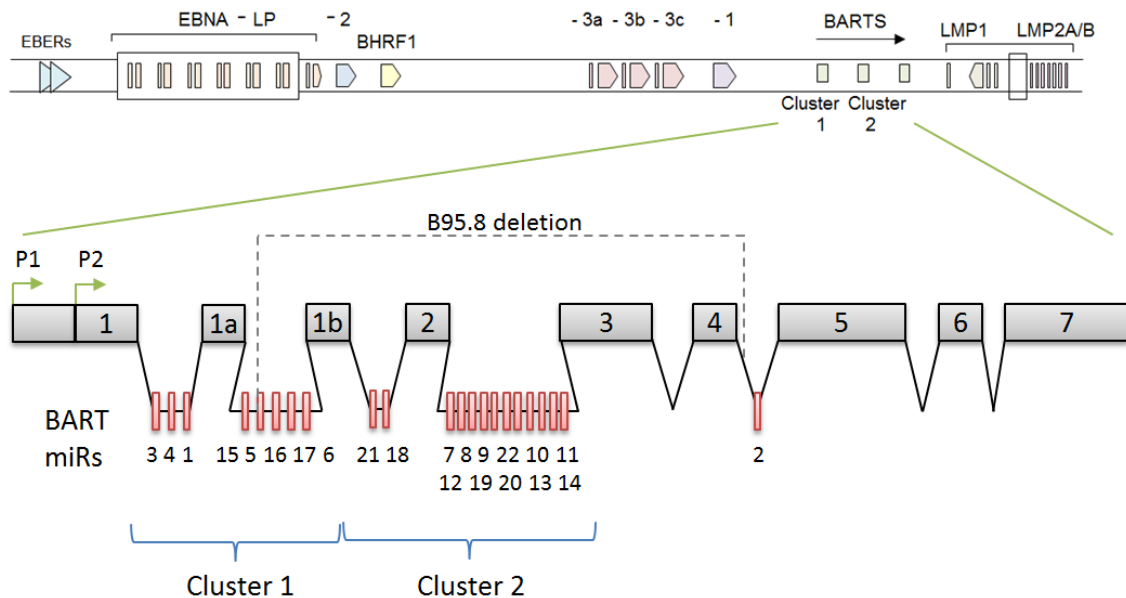


Figure 1.3 Position of BART transcripts and microRNAs within the EBV genome
Transcripts are driven from promoters, P1 and P2. Coding exons (grey) and microRNAs (red) are shown against a schematic of the linearised viral genome. The position of the deletion in the prototypic EBV strain, B95.8 is also indicated.

specificity by virtue of its short (6nt) ‘seed sequence’, which recognises a region or regions within the 3’ UTR of the mRNA with perfect or near perfect complementarity (reviewed in [358, 359]).

The BART miRNAs are reported to play a role in the regulation of many processes including; virus replication and lytic cycle regulation, apoptosis (inhibition and activation), NF- κ B signalling and cell growth via targeting of a number of cellular and EBV-encoded transcripts [360-371]. However, the majority of these studies were carried out in epithelial cells where the BART miRNAs are very highly expressed [156, 372, 373] and so may not be relevant to BL. The BART miRNAs are expressed at lower levels in B cells compared to epithelial cells, although

they still number thousands of copies per cell in total [168], and are consistently detected in all types of Latency [94, 171].

A number of *in silico* and *in vitro* methods have been used to identify possible targets of the miR-BARTs in B cells which include; *CASP3*, *CLEC2D*, *LY75*, *SP100* (miR-BART 1), *DAZAP2*, *IPO7*, *PDE7A*, *PELI1* (miR-BART 3), *MICB*, *TOM22*, *DICER*, *CAPRN2* and *C1orf109* (miR-BARTs 2, 16, 6, and 13, respectively) [99, 168, 368, 371, 374]. Although several have been shown to interact with miR-BARTs in reporter assays, there is still notable variation between studies, cell lines, and different identification methods even within a single study [375]. Interestingly, one recent study from the Sugden group found that ectopic expression of miR BARTs in Latency I BL clones can inhibit apoptosis when the cells are treated with dnEBNA1 [99]. RISC complexes precipitated from the miR BART-supplemented cells were found to be enriched for Caspase-3 after treatment with dnEBNA1. Therefore, inhibition of pro-apoptotic Caspase-3 is the proposed mechanism by which miR BARTs inhibit apoptosis in this model however, miR BARTs were not shown to directly target Caspase-3 in Sav-BL; reporter assays were instead carried out in miR BART-transfected 293 cells or EBV-positive and loss cells isolated from a Wp-restricted BL.

1.4 Apoptosis

1.4.1 Overview of apoptosis

Although the peculiar morphological changes associated with programmed cell death were first described over 170 years ago by Carl Vogt, it took until 1972 for apoptosis to be christened and properly recognised for its essential role in normal development and organism homeostasis as well as being a crucial method of clearing faulty or damaged cells [376]. In common with other essential cellular processes, loss of control or subversion of apoptosis can

have disastrous consequences and as such, evasion of apoptosis is recognised as one of the hallmarks of cancer [377]. Apoptosis is now an enormous area of research, which has grown almost exponentially in recent decades, and it is now known that the commitment to programmed cell death is governed by extremely complex and interweaving signalling pathways that are delicately and subtly maintained. This introduction therefore, will only provide a brief overview of some of the most critical and well understood processes; specific details about particular components will be discussed alongside the relevant data in the following chapters.

The extrinsic pathway

Apoptosis is divided into the intrinsic and the extrinsic pathways (see Figure 1.4), based on the nature of the initial stimulus and the ensuing signalling events [378]. The extrinsic, or death receptor pathway, is triggered by the ligation of death receptors at the plasma membrane. The death receptors are members of the Tumour Necrosis Factor Receptor superfamily (TNF-R) that contain death domains, and they include; TNFR-1, Fas/CD95, DR4 and DR5. Different TNF-Rs each recognise specific ligands which, in the case of those receptors previously mentioned are; TNF α , FasL, and TRAIL, respectively (reviewed in [379]). Following stimulation, the TNF-Rs are able to recruit the adaptor proteins, FADD and TRADD via their death domains, which initiate the formation of the death inducing signalling complex (DISC) and resulting in the activation of Caspase-8 and -10 [380].

Caspases

Regardless of the pathway by which cell death is initiated, the caspase family of proteins are responsible for the ultimate demolition of the cell. Caspases are a family of cysteine-dependent aspartate-specific proteases that lie dormant in the cell in the form of inactive zymogens until they are required. They are divided into two types by their structure and

function (reviewed in [381]). The initiators; Caspase-2, -8, -9 and -10, instigate the caspase cascade and contain binding domains such as CARDs (caspase activation and recruitment domains) or DEDs (death effector domains), which recruit downstream apoptosis regulators known as scaffold proteins [382]. Whereas the effector, or executioner, Caspases (-3, -6 and -7) orchestrate the destruction of the cellular contents. Initiator caspases are activated when they are cleaved by members of the extrinsic or intrinsic pathway, and then the cleaved fragments of the caspase assemble into functional multimers which go on to activate scaffold proteins such as, FADD and Apaf-1, as well as the executioner caspases [383]. The executioner caspases then begin to cleave their hundreds of substrates [384]; destroying the majority, but also activating other destructive enzymes like Caspase-Activated DNase (CAD) [385], which then co-operate in disintegrating the remaining components of the cell. Interestingly, caspase cleavage does not always necessarily induce cell death; both initiator and executioner caspases have been reported to play important non-apoptotic roles in immune function, cell proliferation, differentiation and migration and neurodegeneration [386]. For example, Caspase-1 is known to process IL-1 β , IL-18 and IL-33 to their mature forms and is able to activate lipid metabolism and can thereby regulate pro-inflammatory, anti-inflammatory and innate immune responses as well as apoptosis [387-390].

The intrinsic apoptosis pathway

The intrinsic apoptosis pathway is principally governed by the Bcl-2 family of apoptosis mediators, which consists of at least 15 members in humans. Unlike the extrinsic pathway, the intrinsic pathway is triggered by a wide variety of intra- and extracellular stimuli including; DNA damage, oxidative stress, growth factor starvation and cytotoxic agents, all of which can be detected by the Bcl-2 family [391, 392]. Although Bcl-2 family members may be pro- or anti-apoptotic, they all share homology in their BH3 binding domain, which allows them to interact and agonise or antagonise one another's function. Therefore, when the intrinsic pathway is

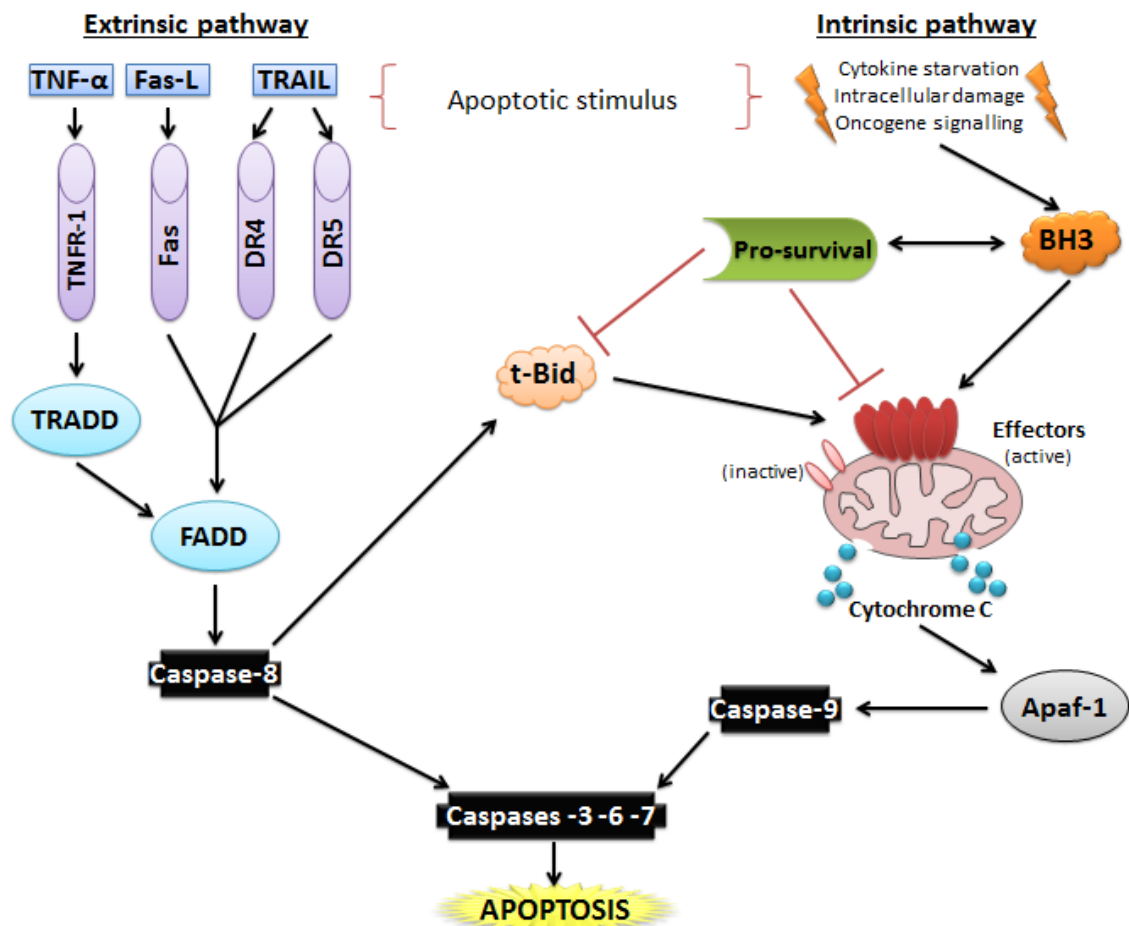


Figure 1.4 Overview of the intrinsic and extrinsic apoptosis pathways

Typical stimuli are shown for each pathway followed by generalised signal transduction pathways. For each pathway an example initiator caspase is shown (Caspase-8 and Caspase-9, respectively), rather than extensive list. Similarly, only a generalised BH3-only and pro-survival Bcl-2 protein is depicted.

Extrinsic pathway – TNF receptors (purple) are engaged by their ligands (pale blue). Adaptors (bright blue) are then recruited to TNF receptor death domains, initiating formation of the DISC. The DISC then activates initiator caspases (black), which feed forward to executioner caspases (black).

Intrinsic pathway – the Bcl-2 family BH3-only sensor proteins (orange) sense pro-apoptotic stimuli however, not all pro-apoptotic stimuli are disastrous for the cell (e.g., repairable DNA damage), so the pro-survival proteins (green) keep the BH3-only proteins in check, by inhibiting both them and their downstream effectors (red). If this inhibition is overcome, the effectors oligomerise and permeabilise the mitochondria, releasing cytochrome C (cyan). Cytochrome C then activates scaffold proteins (grey), initiating formation of the apoptosome. The apoptosome then activates initiator caspases (black), which feed forward to executioner caspases (black).

engaged, the fate of the cell is decided by the overall balance of pro-survival versus pro-apoptotic (BH3-only sensors and effectors) interactions. The cell is committed to undergoing apoptosis via the intrinsic pathway when the mitochondrial outer membrane becomes permeabilised (MOMP), which occurs when the balance of Bcl-2 family signalling is tipped in favour of the Bcl-2 effector proteins. Once the mitochondrial membrane is breached, cytochrome C is able to leak out and further potentiate the pro-apoptotic signal. Cytochrome C goes on to activate the scaffold protein Apaf-1 which, as mentioned earlier, is able to activate and complex with cleaved initiator caspases, forming the apoptosome. Once the mitochondrial pores (from which cytochrome C escapes) are formed, they continue to enlarge, releasing additional mitochondrial contents into the cytoplasm, which further drive the caspase cascade or alleviate downstream apoptosis inhibition. For example, Smac/DIABLO and Omi/HtrA2 promote apoptosis by binding and antagonising or causing cleavage of the IAP family of apoptosis inhibitors upon release into the cytoplasm [393-395], whereas AIF and Endonuclease G translocate to the nucleus where they are involved in DNA fragmentation and degradation [396, 397].

Finally, the executioner caspases are activated and the cell is dismantled (reviewed in [398, 399]). The careful orchestration of apoptosis leads to the maintenance of the plasma membrane until the majority of the cellular contents are destroyed [400] and *in vivo*, the cellular corpse is then rapidly engulfed by phagocytes [401]. This avoids the release of pro-inflammatory molecules from the dying cell; rendering this form of cell death 'immunologically silent' [402]. Since oncogenes trigger the intrinsic apoptosis pathway and this study is concerned with the possibility that EBV might counteract c-myc in BL, a more detailed exploration of the precise interactions of the Bcl-2 family of intrinsic apoptosis regulators is warranted.

1.4.2 The Bcl-2 family

The first Bcl-2 family member identified was Bcl-2 itself, in the context of a common **B Cell Lymphoma** mutation cloned from a tumour in 1984 [403]. Its function was discovered by David Vaux, along with Suzanne Cory and Jerry Adams at the Walter and Eliza Hall Institute (WEHI) [404], who found that it could rescue rat fibroblasts from c-myc-induced cell death, thus allowing c-myc to growth transform the cells. As previously mentioned, Bcl-2 family members are divided into three types, depending on their structure and function (see Figure 1.5). Bcl-2 and the other pro-survival family members generally contain four helical **Bcl-2** **h**omology domains (BH1-4) as well as a C-terminal transmembrane domain and their overall structure is that of an 8 α -helical bundle. The pro-apoptotic effector proteins, Bak and Bax, contain three BH domains (BH1-3) and the transmembrane domain, but are composed of 9 α -helices in total [405]. In contrast, the pro-apoptotic sensor proteins generally contain only the BH3 domain (although Bim, Bik and Hrk also have a transmembrane domain); hence they are also referred to as the BH3-only proteins and, apart from Bid, which is also an α -helical bundle [406, 407], they are largely unstructured when not bound [408]. The BH3 domain is around 26 amino acids long and confers the specificity and affinity with which different Bcl-2 family members bind one another.

Evading apoptosis

Bcl-2 has a number of cellular anti-apoptotic homologues, most notably; Bcl-XL, Mcl-1, Bcl-w and A1 (or Bcl-2-A1). These Bcl-2-homologues interact with their pro-apoptotic counterparts via their hydrophobic BH3-binding groove [409] and their primary function appears to be to sequester the BH3 only sensor proteins, thus preventing them from activating the effector proteins. The pro-survival proteins also bind the activated forms of the effector proteins directly, which stops them from binding to one another and therefore initiating MOMP.

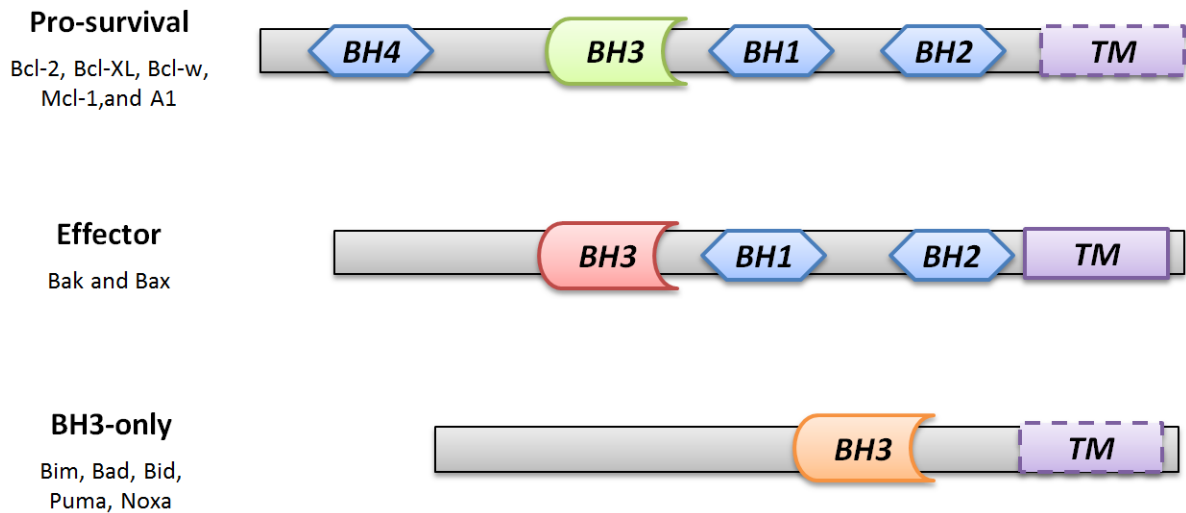


Figure 1.5 Schematic of functional domains in Bcl-2 family proteins

The **pro-survival** proteins range in size from 20-37kDa, with Bcl-w and A1 being the smallest and Mcl-1 the largest. All contain the transmembrane TM domain except A1.

The **effector** proteins lack the N-terminal BH4 domain compared to their pro-survival counterparts and both contain the transmembrane domain which allows them to insert into and form pores in the mitochondrial outer membrane (MOM). Bax is 21kDa and Bak is 24kDa.

The **BH3-only** proteins range from 11-22kDa in size, with Noxa being the smallest and Bim and Bid being the largest. Only Bim, Bik and Hrk contain the transmembrane domain.

Sizes quoted are based on most commonly expressed isoforms.

Transmembrane domains insert into endoplasmic reticulum (ER) or MOM where the proteins may be permanently tethered (Bak/Bax) or only insert into membrane upon stimulus [380].

A number of viruses, including EBV, are known to encode homologues of cellular Bcl-2 in order to evade apoptosis triggered as part of the anti-viral response. Viral Bcl-2 proteins vary in their similarity to their cellular counterparts in sequence, structure and function and there are examples of v-Bcl-2s, such as some of those encoded by certain pox viruses, which only resemble their cellular counterparts in their three-dimensional fold and have no known anti-apoptotic activity (reviewed in [410]).

EBV encodes two v-Bcl-2s, BHRF1 and BALF1, which are thought to exhibit functional redundancy by inhibiting apoptosis during primary infection, since a virus deleted for both is

unable to transform resting B cells, yet viruses lacking either v-Bcl-2 transform B cells with the same efficiency as a wild-type virus [88]. BHRF1 is relatively well-characterised; it exhibits 38% C-terminus sequence similarity to Bcl-2 and structurally closely resembles Bcl-XL, binding BH3 ligands in a hydrophobic groove formed by α -helices 2-5 of its 7-helix bundle [411, 412]. BHRF1 has been shown to be potently anti-apoptotic *in vitro* and in an animal model and can confer protection to a wide variety of stimuli [89, 303-305, 411, 413-420]. Whilst it has long been thought to contribute primary infection and lytic cycle, it is now known that BHRF1 is also constitutively expressed in LCLs and highly over-expressed in the Wp-restricted subset of BLs, as previously mentioned [89]. The mechanism by which BHRF1 protects BL cells is thought to largely be via binding and sequestration of Bim and to a lesser extent Bak, Puma and Bid [304, 305, 411]. In contrast to BHRF1, little is known about BALF1 which was identified as a v-Bcl-2 on the basis of structural similarity to Bcl-2 and Bcl-XL, and though it has been shown to modulate apoptosis, it remains controversial as to whether it promotes or inhibits cell death [421, 422].

Sensing apoptosis

The pro-apoptotic BH3-only proteins vary greatly in their affinity and specificity for anti-apoptotic Bcl-2 proteins due to differences in the sequence and structure of their amphipathic BH3 domain (see Figure 1.6). Bim, Puma and the truncated form of Bid (tBid) exhibit the least specificity and are able to bind all of the well-characterised Bcl-2 homologues (Bcl-2, Bcl-XL, Mcl-1, Bcl-w and A1) with varying affinities, whereas other BH3-only proteins are more selective. For example, Noxa is able to bind to Mcl-1 and A1, but not Bcl-2, Bcl-XL or Bcl-w, which are specifically engaged by Bad, Bmf and Hrk, as depicted in Figure 1.6 [423, 424]. Accordingly, Bim, Puma and tBid are all potent inducers of cell death, whereas the other BH3-only proteins must act in combination. For instance, Noxa and Bad can efficiently induce apoptosis as together they are able to bind all pro-survival Bcl-2 proteins.

BH3-only proteins act as 'sensors' for cellular threats, damage, and stress and as such, are activated by a diverse range of stimuli. The precise mechanisms by which the balance between the Bcl-2 family proteins dictates the fate of the cell have not been fully elucidated however, two, not mutually exclusive models have been proposed [425, 426]. In the direct activation model, the promiscuous binders; Bim, Puma and tBid, directly activate Bak and Bax when they are not bound by pro-survival proteins [424, 427, 428]. In contrast, the other BH3-only proteins act as 'sensitisers', by displacing Bim, tBid and Puma from pro-survivals, leading to activation of Bak and Bax. In the indirect activation model [425], Bak and Bax become activated spontaneously and therefore, the BH3-only proteins simply need to bind to and inactivate all of the pro-survival proteins, stopping them from blocking the oligomerisation of Bak and Bax. *In vivo*, it is clear that both of these models can occur [429] and so the physiological situation is likely to be a hybrid of these two models [399].

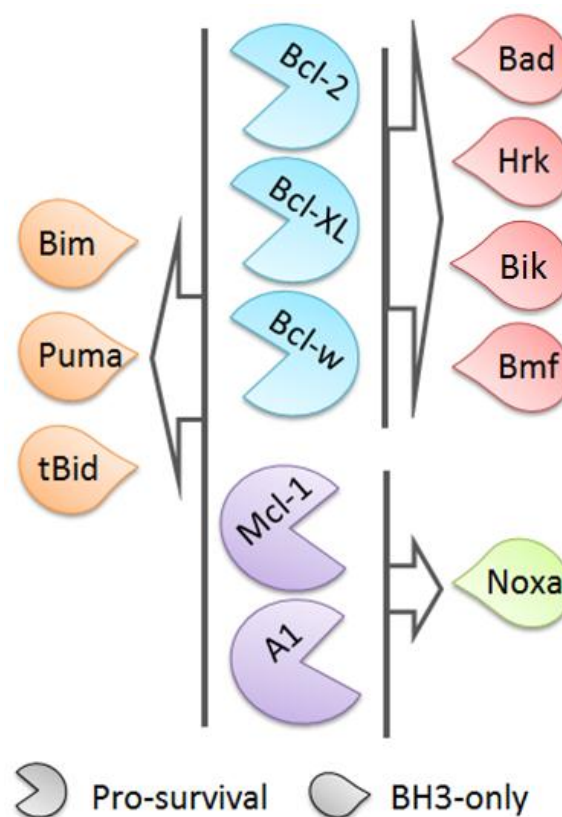


Figure 1.6 Binding specificities of Bcl-2 family members

Executing apoptosis

The primary function of the Bak and Bax effector proteins is to form pores in the mitochondrial membrane, allowing the release of cytochrome C and other proteins into the cytosol. The effector proteins exhibit functional redundancy, with either being sufficient for normal development in mice, whereas Bak^{-/-}/Bax^{-/-} mice exhibit gross abnormalities and Bak^{-/-}/Bax^{-/-} cell lines fail to undergo apoptosis [430, 431]. To carry out their function, Bak and Bax must be activated, which causes them to undergo a substantial conformational change and thereby exposing the BH3 domain as well as other functional domains [428, 432]. Pro-survival Bcl-2 proteins bind to effector proteins in order to block this activation, with Bcl-XL, Mcl-1 and A1 being able to restrain both Bak and Bax, but Bcl-2 and Bcl-w only able to bind Bax [425, 433]. Interestingly, whilst Bak is permanently associated with the mitochondrial membrane, Bax may be only loosely associated with the membrane or free within the cytoplasm [434]. There is also a third effector protein homologue, Bok, which may reside in the ER rather than mitochondrial membrane. Despite being widely expressed, the function of Bok remains poorly understood [435].

Once activated the effector proteins can oligomerise by linking together in a daisy-chain fashion (i.e., front-to-back) [436], or by reciprocal interactions of the BH3 domain (face-to-face) to form dimers [437-439]. In the latter mechanism, pairs of dimers link to one another by a second reciprocal interaction (back-to-back). Bak and Bax then congregate in large numbers in homo- or hetero-oligomers to form proteinaceous pores that allow the escape of molecules of at least several hundred kilo-Daltons [440, 441]. The conformational change that occurs during effector activation also releases two α -helices across the inner leaflet of the mitochondrial membrane, which may also be critical to pore formation [442].

1.4.3 Regulation of the Bcl-2 family

The varying specificities and affinities with which the Bcl-2 family bind to one another allow for a dynamic and intricate web of different interactions to be possible, reflecting the careful and complex regulation of apoptosis. However, many of the Bcl-2 family are also subject to regulation by a number of mechanisms other than binding and neutralisation by their counterparts.

Puma and Noxa were first identified as transcriptional targets of p53 [443, 444], although both can also be transcriptionally regulated in p53^{-/-} cells [445, 446]. Other Bcl-2 family members are also known to be transcriptionally activated, for example; the potent pro-apoptotic inducer, Bim, which is known to be upregulated by FoxO transcription factors in response to glucocorticoids [447-449]. Many of the Bcl-2 family may also exist as a number of functionally different isoforms, which may agonise or antagonise the function of any other isoforms present, providing a second level of transcriptional regulation. For instance, there are three well characterised protein-coding isoforms of Bim; Bim_{EL}, Bim_L and Bim_S, which vary in their potency, but there are also many other splice variants whose physiological function remains enigmatic [450, 451]. The pro-survival Bcl-2 homologues, Mcl-1 and Bcl-XL, can also exist in different isoforms, some of which have opposing functions to the common isoform [452, 453]. The Bcl-2 family are also subject to complex post translational modifications (PTMs), which are known to affect their activity, availability, binding affinity, and cause inactivation by sequestration or degradation. Bad can be phosphorylated at serines 112 and 136, causing it to be sequestered to the cytoskeleton [454], as well as at serine 155, which confers lower binding affinity for pro-survival proteins [455]. In contrast, ubiquitination of Mcl-1 causes it be rapidly degraded by proteasome-dependent and independent mechanisms [456, 457]. Bim also undergoes PTM and can be phosphorylated by ERK1/2 to undergo ubiquitin-independent degradation [458-460]. Interestingly, Bim is also sequestered to microtubules through

interaction with LC8, although this is not thought to be regulated by PTM [461]. Recently, even more mechanisms of Bcl-2 family regulation have been described, including modulation by miRNAs and steric regulation by membrane lipids. For example, the miR-17-92 cluster of microRNAs is able to decrease Bim expression [462] and the interaction of sphingolipids in the mitochondrial membrane with Bak and Bax is able to regulate MOMP directly [463]. The extremely complex and incompletely understood mechanisms of Bcl-2 family regulation protect the fidelity of this critical pathway however; it also makes it difficult to comprehensively study and therefore interpret the workings of the pathway as a whole.

1.4.4 The Bcl-2 family and lymphomagenesis

Following the finding that overexpression of Bcl-2 can rescue *MYC*-driven apoptosis *in vitro* [404], Bcl-2 has also been shown to accelerate lymphomagenesis in the E μ -myc mouse model [464]. However, since Bcl-2 protein is usually undetectable in BLs, alternative mechanisms of c-myc rescue must occur in this setting. More recently, Bcl-2, Bcl-XL, Bcl-w, Bcl-B, Mcl-1 and Bfl-1 have all been shown to be able to individually co-operate with c-myc to cause leukaemia in mice [465]. Additionally, Bcl-XL and Mcl-1 can significantly accelerate lymphomagenesis in E μ -myc mice [466, 467]. Concordantly, deletion of the pro-apoptotic Bcl-2 family members can also contribute to murine tumorigenesis; Bax, Bim, Puma and Bmf can all act as tumour suppressors *in vivo* [267, 268, 270, 468]. Furthermore, and consistent with human BL, Bax^{-/-} E μ -myc tumours often exhibit p53 inactivation via modulation of MDM2 or p14^{ARF} [270]. Additionally, mice knocked out for both Bim and Puma can spontaneously develop lymphoma [469] and myc-driven tumours require the activity of Bim as well as Puma and Noxa to be efficiently induced to undergo apoptosis [274].

In human cancers, there is also evidence that the Bcl-2 family are frequently knocked out, mutated, or selected against. Pro-survival proteins have been found to be overexpressed or have their loci amplified in many lymphoid tumours [465, 470], which may be due to mutation

or activation of the gene, but in other cases they may be indirectly activated. For instance, deletion of E3 ligase components can enhance lymphomagenesis by stabilising Mcl-1 [471, 472], whilst Puma and Bim are often absent in BL through both deletion and epigenetic silencing [267, 473]. Given the dependence of so many lymphoid tumours on the Bcl-2 family *in vivo*, there is currently optimism that specific targeting of the Bcl-2 family will prove a successful strategy for therapeutic intervention.

1.4.5 Targeting the Bcl-2 family in human disease

Since the BH3 domain confers binding specificity to Bcl-2 family proteins, small molecule inhibitors, known as BH3 mimetics, have been developed that can bind and inactivate pro-survival Bcl-2 proteins. ABT-737 and ABT-199 are *bone fide* BH3 mimetics; specifically binding Bcl-2, Bcl-XL and Bcl-w (ABT-737) or Bcl-2 alone (ABT-199) with high affinity and are non-functional in the absence of effector proteins [474, 475]. Both ABT-199 and the orally-available analogue of ABT-737, ABT-263, are currently included in clinical trials [476-478]. There is also a considerable work underway to develop BH3 mimetics that can bind and inactivate other pro-survival Bcl-2 proteins, such as Mcl-1 [301, 479].

1.5 Aims and Objectives

This project aimed to expand previous findings, regarding the role of EBV in maintaining BL tumours by isolating a panel of EBV-loss clones from a range of endemic BL cell lines; thereby allowing them to be compared phenotypically to isogenic clones that do contain the virus. We aimed to compare human BL cells that contain or have lost EBV, to profile their response to apoptosis-inducing agents and determine their tumorigenicity *in vivo*, in order to fully characterise the EBV-loss phenotype and assess the generality of previous findings. We also wanted to map any modulation of apoptosis by the virus by re-expressing viral genes both individually and in combination. Finally, we profiled cellular changes associated with apoptosis induction in EBV-positive and EBV-loss BL clones. Overall, we hoped to gain insights into the regulation of apoptosis by EBV in endemic Burkitt lymphoma in order to better understand viral modulation of apoptosis and therefore, to identify potential therapeutic targets for this aggressive disease.

2. Materials and Methods

2.1 Cell culture

2.1.1 Cell lines used in this study

The basis of this work is the comparison of single cell clones of several BL cell lines which either contain EBV expressing the Latency I gene expression pattern, or have lost the virus. All cell lines used are described in Table 2.1. Akata-BL was obtained from the Takada group [480], Martin Rowe developed the AKBM GFP-reporter cell line [481], and all other BL cell lines were established by Alan Rickinson and colleagues [178, 179, 482]. Jurkat clone E6.1 was from the European Collection of Cell Cultures, HEK 293 cells we obtained from the American Tissue Culture Collection (product number: ATCC CRL-1573) and the 293FT cell line used for high titre lentivirus production were from Life Technologies (R700-07).

In the results sections EBV positive clones are denoted by the prefix 'P', whereas EBV-loss clones are denoted by the prefix 'n'. Clones are differentiated from one another numerically, so for example; Kem n1 always refers to a particular loss clone of Kem-BL, whilst Kem n2 refers to a different EBV-loss clone also derived from the Kem-BL tumour background.

Cell line	Viral gene expression	Description
Akata-BL	Latency I and EBV-loss	Sporadic BL established from a mesenteric tumour; 4-year old Japanese female
Awia-BL	Latency I and EBV-loss (also other Latency types)	Endemic BL established from a retroperitoneal tumour; 12-year old Ugandan female. <i>MYC</i> translocation 8:14
Elijah-BL	Latency I and EBV-loss	Endemic BL established from a 3-year old Kenyan patient. Site of tumour unknown
Kem-BL	Latency I and EBV-loss	Endemic BL; Ugandan patient, age sex and site of tumour unknown. <i>MYC</i> translocation 8:14
Mutu-BL	Latency I and EBV-loss clones (also Latency III)	Endemic BL established from a thigh tumour; 8-year old Kenyan male
X50-7	Latency III	LCL derived from cord blood
Oku-BL	Wp-restricted	Endemic BL established from a maxillofacial tumour; 2-year old Ugandan male
AKBM	Supports high levels of EBV lytic replication	Derivative of Akata-BL transduced with the pHEBO-BMRF1-CD2-GFP reporter construct. Lytic cells express GFP
HEK 293/293FT	EBV-negative. 293 clones infected with EBV BACs support lytic replication	Parental human embryonic kidney (HEK) 293 used to produce recombinant EBV. 293T line used for packaging lentivirus carries polyoma large T antigen
Jurkat	EBV-negative	T cell lymphoma cell line

Table 2.1 Details of cell lines used in this thesis

2.1.2 Cell line maintenance

Cell lines were maintained in RPMI 1640 supplemented with 10% foetal calf serum (FCS) (Gibco), 6mM glutamine, 1mM pyruvate, 50µM α-thioglycerol, 20nM bathocupronine disulphonic acid and 8µg/ml gentamycin (all Sigma). Lymphoid cultures were passaged every 48-72 hours by resuspension in fresh medium to approximately 3×10^5 cells/ml. Adherent cells were seeded at $\sim 10 \times 10^3$ /cm² and were passaged twice weekly when the cells reached 80-90% confluence; cells were dissociated from tissue culture dishes using Gibco TrypLE at 37°C for 5 minutes before resuspension in fresh FCS-containing medium to inactivate the trypsin.

All cell lines have been cryopreserved in liquid nitrogen. Briefly, this involved pelleting $5-10 \times 10^6$ cells by centrifugation at 1,400rpm ($\sim 450g$) for 5 minutes in a BIOliner™ Swinging Bucket Rotor (Thermo Scientific) before resuspending the cells in freezing medium, which comprised: 50% v/v RPMI 1640, 40% v/v FCS and 10% v/v dimethylsulphoxide (DMSO) (Sigma), in Nunc 1ml cryovials. Cryovials were then transferred to a Mr Frosty™ container (Nalgene) filled with isopropanol and transferred to -80°C overnight. Samples were then stored in the gas phase of a liquid nitrogen freezer. Cell lines were recovered from nitrogen by rapidly thawing vials in a 37°C water bath, followed by the drop-wise addition of the appropriate pre-warmed medium. Cells were then pelleted as previously described before being resuspended in fresh media and then cultured as described.

All cells were routinely grown at 37°C in a humidified atmosphere containing 5% CO_2 , in 25cm^2 flasks (suspension cells) or 10cm culture dishes (adherent cells).

2.1.3 Single cell cloning of BL cell lines

Subclones of BL tumour lines were isolated using a standard limiting dilution technique whereby cultures were diluted to 10 cells/ml and seeded at $100\mu\text{l}$ /well in round-bottomed 96-well plates. Several hours after seeding wells were checked by eye to ascertain the number of cells on average per well. Plates were then fed weekly with fresh medium until cells were numerous enough to be harvested for genome load analysis (at least 1000 cells per well). In these experiments maintenance medium used was as described in 2.1.2, with the addition of $200\mu\text{M}$ acycloguanosine (ACV), a nucleoside analogue which inhibits lytic virus genome replication.

2.1.4 Preparation of lentivirus stocks

Lentivirus stocks were produced using the 293FT packaging cell line (Life Technologies, R700-07) using liposome-mediated delivery of lentiviral plasmid DNA and second generation

packaging vectors. On day 1 of the protocol, confluent, early passage (<20) 293FT cells were plated at $\sim 5 \times 10^4$ /ml in fresh media. The following day the cells were transfected with the vector containing the gene of interest, the modified HIV-derived packaging plasmid psPax2, and the VSV-G envelope glycoprotein-encoding pMD2.G, premixed with Lipofectamine 2000 (Life Technologies) as a DNA delivery agent in serum-free Optimem medium (Life Technologies). The prepared transfection mix was added directly to the medium on the 293FTs and consisted of 3ml Optimem, 36 μ l Lipofectamine 2000, 6 μ g psPax2, 4 μ g lentivirus plasmid DNA and 2 μ g pMD2.G per 10cm plate. Plates were then returned to the incubator overnight. The following day (~ 16 hours post-transfection) the transfection medium was removed and replaced with fresh medium supplemented with 0.1mM pyruvate. On day 5 the lentivirus-containing supernatant was harvested, briefly centrifuged and filtered at 0.45 μ m. Before use the lentiviral supernatant was concentrated ≥ 50 -fold by ultracentrifugation in an SW40 Ti rotor at 19,000rpm ($\sim 64,000g$) for 2 hours at 16°C.

2.1.5 Generation of stable lentivirus-transduced cell lines

For transduction of BL cells, 1×10^5 cells were placed in a 10ml centrifuge tube with concentrated lentivirus harvested from 1 x 10cm dish and supplemented with 10 μ g/ml Polybrene (Sigma) in a total volume of 400 μ l. Efficient transduction of the cells was achieved using a 'spin-infection' protocol, whereby tubes were transferred to an incubator at 37°C for 30 minutes to allow the lentiviral particles to bind to the cells and then spun at 2,200rpm ($\sim 1,100g$) in a BIOliner™ Swinging Bucket Rotor (Thermo Scientific) at 32°C for 2 hours. The supernatant was then discarded and the cells washed in fresh, warmed medium twice before transferring to 24-well plates. For transduction of the 293 cell line, 1×10^5 cells were plated in 6-well plates 24 hours before infection to allow them to adhere to the culture dish and then the plates were incubated and spun as above. Following centrifugation the supernatant was discarded and fresh medium gently applied.

All of the lentivirus constructs used in this thesis were derivatives of FTGW [483], which contains a constitutively-expressed enhanced GFP (eGFP) driven from a ubiquitin promoter, allowing lentivirus-transduced cells to be selected for on the basis of GFP expression. At 7-10 days following transduction cells were sorted on a MoFlo cell sorter (Becton Dickinson) and GFP-positive cells were collected and put back into culture. Cells were sorted for a second time 7-10 days later and selected for high GFP expression, with the top 5-10% of GFP-positive cells of the gene-of-interest-transduced cells being collected. Identical gates were used for all lines within a set, including controls. Two rounds of sorting were carried out to normalise gene expression between constructs as we and others have found that GFP-expression correlates with both the number of integrated lentiviral genomes and expression of the gene of interest [484].

All genes-of-interest were placed under the control of tet-inducible promoters and expression was induced by addition of doxycycline (DOX) to a final concentration of 1 μ g/ml (Sigma) to the cell culture medium. Cells were used for functional assays or gene expression experiments 24-48 hours after induction, unless otherwise stated. In the case of the Bim_S variant constructs cells were supplemented with 25 μ M Q-VD-OPh (Quinoline-Val-Asp-difluorophenoxymethylketone) (MP Biomedicals) to inhibit caspase activation and cell death during gene expression assays.

2.1.6 Preparation of infectious stocks of recombinant EBV

Infectious virus of the CpWp-KO strain [485], was produced from 293 cells stably transfected with recombinant EBV bacterial artificial chromosomes (BACs) which were induced into lytic cycle by transfection with BZLF1 and BALF4. Briefly, BAC-containing 293 cells were seeded in 6-well plates and when ~70% confluent were co-transfected with 0.5 μ g each of plasmids p509 (BZLF1) and p2670 (BALF4) [486, 487] using Lipofectamine reagent (Life Technologies) in Optimem reduced-serum medium (Gibco). Transfection medium was replaced with fresh

target cell medium 16 hours after transfection and the virus-containing supernatant collected 72 hours later, spun down to remove any cells and filtered using a 0.45µm filter to remove cell debris and ensure sterility. Virus stocks were stored at -80°C until use.

Stocks of infectious Akata-BAC-GFP2 virus [488] were produced from a stable EBV-loss Akata cell line which had been reinfected with the Akata virus BAC. Unusually for a BL cell line Akata-BL is induced into lytic replication by crosslinking of surface IgG [130]. Therefore, the stably reinfected line containing the Akata BAC was stimulated with 0.5%v/v Fab₂ α-IgG (1mg/ml, from Cappel) for two hours with gentle shaking and then transferred to fresh medium and returned to a 37°C incubator. Virus-containing supernatant was collected 72 hours later, sterilised using a 0.45µm filter and stored in aliquots at -80°C.

2.1.7 Reinfection of EBV-loss clones with recombinant EBV

The critical cellular receptor for EBV binding and entry of B cells is CD21 [489] however, many BL cell lines are found to express only low levels of CD21 on the outer membrane [490]. EBV-loss BL cells were transduced with CD21 lentivirus according to the spin-infection method as described in Section 2.1.5, then seeded into 6-well plates at 2×10^6 EBV-loss cells/well with EBV-containing medium at >100 MOI (multiplicity of infection), in a total volume of 5mls. The cells were then infected according to the spin-infection method as described in Section 2.1.4, except that the cells were not washed following infection. Instead, the majority of the supernatant was gently removed and fresh medium added. After infection the cells were left to recover for 48 hours before selection of EBV-positive cells was begun by the addition of antibiotics to the cell culture medium. Cells infected with the Akata recombinant EBV (rEBV) were selected for G418 (Sigma) resistance (using 400, 700 or 1000µg/ml for clones of Kem, Akata or Mutu-BL, respectively), whereas reinfected cells carrying the CpWp-KO virus were selected on the basis of hygromycin-B (Sigma) resistance (500µg/ml for all EBV-loss clones).

We and others has previously shown that reinfection of EBV-loss or EBV negative cell lines often results in a Latency III-pattern of viral gene expression [491, 492]. However, a 2011 publication by the Sample group described Latency I reinfection being achieved only after an extended period in culture [493] and so, after subsequent correspondence with Professor Sample, we decided to screen our re-infected cells after a minimum of 8-weeks in culture in selection medium. Unlike in previous experiments, we found that we were now able to generate stable cell lines expressing only Latency I-associated genes. Some reinfected bulk cultures were found to express EBNA2 in a subpopulation of cells; such cultures were subjected to single cell cloning, as described in Section 2.1.3 in order to isolate Latency I expressing cells.

2.2 Cell death, cell growth and cell survival assays

2.2.1 Cell viability assays

Routine cell viability assays were carried out prior to setting up all apoptosis assays by adding 20 μ l of trypan blue (0.4% solution, from Sigma) to 20 μ l of thoroughly mixed cell suspension. This was then mixed by pipetting and 10 μ l applied to a cell counting slide and the percentage of viable cells was quantified using a TC-10 cell counter (Bio-Rad). A minimum of two separate counting chambers was measured per sample and the viability taken to be the mean of the recorded values. This method was also used to quantify cell viability during apoptosis time course experiments where cells were subsequently harvested for gene expression analysis.

2.2.2 Proliferation assays

Cells were initially plated at $9 \times 10^4/\text{cm}^2$ in 10cm dishes in standard BL cell media, and thoroughly resuspended every 24 hours at which time 3 x 75 μ l aliquots were removed for counting. Each 75 μ l aliquot was then passed through the Accuri C6 Flow Cytometer (BD

Bioscience) to obtain absolute cell counts per unit volume. Counts were recorded and expressed relative to measurements taken immediately after seeding. The mean and standard deviation (SD) of triplicate measurements was calculated and plotted to compare the growth of different cell lines over time.

2.2.3 Apoptosis assays

For all assays, actively dividing cells (passaged 24 hours before apoptosis induction) were seeded at $9 \times 10^4 / \text{cm}^2$ and treated with various apoptosis-inducing stimuli or DMSO as a vehicle-only control as listed in Table 2.2. For small scale assays, cells were seeded in 96-well plates with triplicate wells being set up for each treatment or control and each experiment being carried out on at least three occasions. For apoptosis assays where cells were harvested for gene expression studies, 10cm dishes were used and triplicate data were taken from three independent experiments.

Sensitivity to apoptosis-inducing stimuli was determined using flow cytometry to differentiate between live, apoptotic and dead cells. The translocation of phosphatidylserine (PS), from the inner to the outer leaflet of the plasma membrane, is a well-defined marker of entry to apoptosis and so fluorescent conjugates of Annexin-V, which has a high affinity for PS, are widely used to detect cells in the early stages of cell death [494, 495]. Propidium iodide (PI) is excluded from live cells and cells in the early stages of apoptosis and is only able to enter cells which have lost outer membrane integrity when the cells are dead or in the late stages of apoptosis. The response of EBV-loss clones to different stimuli, compared to their EBV-positive counterparts, was characterised by dual staining of cells with Annexin-V and PI at 24-72 hours, depending on the stimulus used (see Table 2.2). In assays where cell lines were GFP-positive, Annexin-V was conjugated to Alexa-Fluor 647 (Life Technologies), and in other assays a FITC-Annexin V conjugate was used (eBiosciences). In all assays a 2x mix of Annexin-V and PI was made up in 2x Annexin binding buffer (eBioscience), then 100 μ l of cell suspension from each

Reagent	Manufacturer	Product code	Concentration	Assay length
α -IgM	Cappel	56960	10-20 μ g/ml	72 hours
Etoposide	Sigma	E1383	25-50 μ M	24 hours
Ionomycin	Sigma	I0634	0.5-2 μ g/ml	48 hours
Roscovitine	CST	#9885	25-50 μ M	48 hours
Staurosporine	CST	#9953	250nM	24 hours
QVD-OPh	MP Biomedicals	03OPH109	25 μ M	24-72 hours
Necrostatin-1	Selleck Chemicals	S8037	30 μ M	48 hours
ABT-737	Selleck Chemicals	S1002	1 μ g/ml	24 hours
Human IL-10	Peprotech	200-10	50-500ng/ml	48 hours
Interferon- α	Peprotech	300-02A	500-10,000 U/ml	<7 days

Table 2.2 Details of drugs used in apoptosis assays and length of assays. Where a range of concentrations has been used the exact concentration of drug used in individual experiments is stated in the Results text or Figure legend.

assay well was harvested and 100 μ l of the 2x Annexin V/PI mixture was added. The final concentration of both Annexin V and PI was 2.5 μ g/ml. Each tube was briefly mixed and then analysed immediately on an Accuri C6 or LSR I flow cytometer (both Becton Dickinson).

Cells were first gated according to forward and side scatter profiles to eliminate debris (events with very low forward and side scatter) from the analysis, the selected events were then analysed on two-dimensional dot plots of Annexin-V vs PI to quantify the percentage of live, apoptotic and dead cells, respectively, as shown in Figure 2.1-A and 2.1-B. At the time-points chosen for our phenotypic assays we found that we rarely detected Annexin-positive/PI-negative cells; all of the non-viable cells also stained for PI and so on some occasions PI staining alone was used to quantify cell death, as shown in Figure 2.1-C. As with the dual-

staining assays, a 2x dilution of PI was mixed with harvested cells 1:1 and samples were analysed on the Accuri C6 cytometer.

2.2.4 Data analysis for apoptosis assays

For each sample a minimum of 10,000 events was recorded and data were analysed using FlowJo software (Treestar) or Accuri C6 software (Becton Dickinson), depending on which instrument was used to process samples. Induced cell death was calculated as: $(\% \text{ total death in drug treated cells} - \text{mean } \% \text{ cell death in matched untreated cells}) / \text{mean } \% \text{ viable cells in untreated sample}$. Mean and standard deviation were calculated and the significance of any differences between cell lines was determined using a two-tailed Student's T-test. Values of $p < 0.05$ were considered significant.

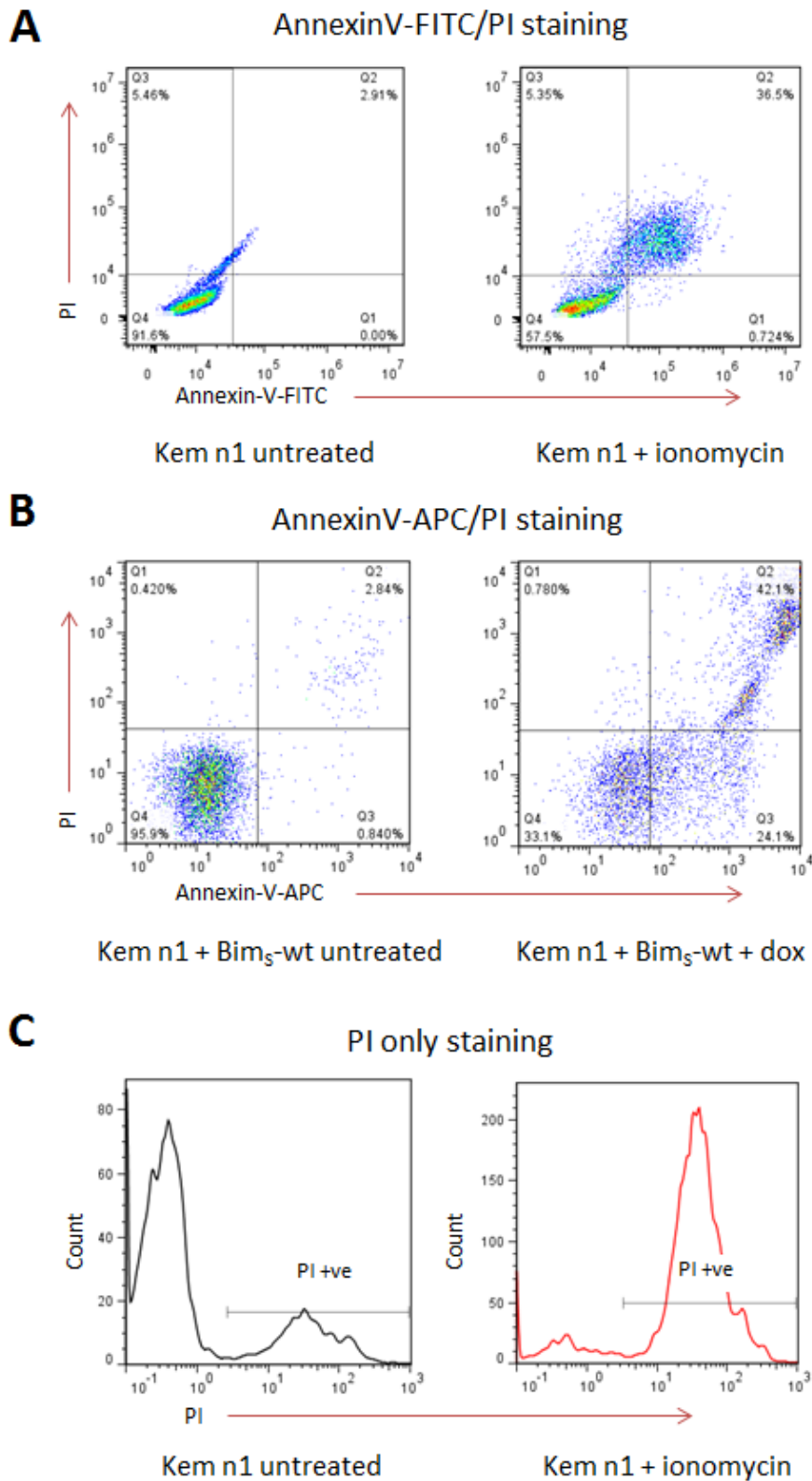


Figure 2.1 Apoptosis assay gating strategies

A Annexin-V-FITC/PI staining on untreated and ionomycin-treated Kem n1 EBV-loss cells

B Example of Annexin-V-APC/PI staining on GFP-positive untreated and doxycycline-induced Bim₅-wt-transduced Kem n1 EBV-loss cells

C PI-only viability staining on untreated and ionomycin-treated Kem n1 EBV-loss cells

2.3 DNA analysis

2.3.1 DNA preparation

For analysis of viral genome load in single cell clones in preliminary screening assays, a small aliquot of cells was resuspended in 100µl lysis buffer comprised of; 1.5mM MgCl₂, 50mM KCl 10mM Tris-HCl, 1% Tween-20, and 40µg/ml Proteinase K (all Sigma), then incubated at 55°C for 1 hour to lyse the cells, followed by 10 minutes at 95°C to inactivate the Proteinase K.

For more accurate genome load or other DNA analysis, such as sequencing or for use in cloning, purified DNA was extracted from 5-10x10⁶ cells using the GenElute Genomic DNA Kit (Sigma), according to the manufacturer's instructions and eluted in 50µl diethylpyrocarbonate (DEPC) treated water. DNA concentration and purity was measured using a Nanodrop 1000 spectrophotometer (Thermo Scientific).

2.3.2 PCR quantitation of EBV genome load

The copy number of EBV genomes per cell was determined using quantitative DNA-PCR for the EBV polymerase gene, BALF5, and normalised to the cellular gene, β-2-microglobulin (β2M) as previously described [496]. Briefly, assays were carried out in a total volume of 25µl in 96-well PCR plates (Geneflow). The reaction mix contained 1x Taqman Universal Master Mix II (Life Technologies) and BALF5 and β2M Taqman assays and samples consisted of 5µl of lysed cells, 5µl lysed virus-containing supernatant (to measure the concentration of purified virus stocks), or 5µl of 2ng/µl purified DNA. Threshold values (Cts) were quantitated by comparison to a standard curve of DNA extracted from the Namalwa-BL cell line, which contains 2 integrated copies of the EBV genome per cell. Clones were deemed to be EBV negative where a well was found to be negative for BALF5, but positive for β2M. The EBV-positive clones selected for comparison were chosen for having a similar average viral genome to the parental BL cell line.

2.4 PCR amplification of DNA

2.4.1 PCR amplification of viral and cellular genes

Portions of cellular and viral genomic DNA were amplified for molecular cloning by end-point PCR. Primers consisted of 15-20 bases of complementary sequence to the 5' end or reverse complement of the 3' end of the target sequence with the addition of necessary restriction sites or spacers. G+C content, melting temperatures (T_m) were calculated and sequence specificity checked using Primer3 (NCBI). Details of genes and genomic fragments amplified can be found in Section 2.6.

Typically, reactions were carried out in a total volume of 50 μ l containing; 300nM primers, 1x MgCl₂-containing PCR buffer (Roche), 200-500ng of template DNA (EBV-positive Raji-BL), and 200 μ M dNTPs (Roche). Tubes were heated to 96°C for 4 minutes and then the reaction was started by addition of 1 μ l of high fidelity DNA polymerase (Roche). Thermal cycling was carried out in a Techne TC-512 for 40 cycles comprised of: 15 seconds at 96°C, 15 seconds at 50-65°C (depending on T_m) and 30 seconds at 72°C per kb of sequence to amplify, followed by a 10 minute final extension at 72°C.

2.4.2 Agarose gel electrophoresis and purification of PCR products

Following PCR amplification DNA fragments were separated by electrophoresis at 90V in 1x TBE buffer (90mM Tris-borate, 2mM EDTA) according to size on 1-2% agarose gels containing 0.5 μ g/ml ethidium bromide. DNA samples and 1kb Plus DNA Ladder (Life Technologies) were mixed with FastDigest gel sample buffer (Thermo Scientific) prior to loading and once the yellow dye (corresponding to 10bp) had migrated the full length of the gel, electrophoresis was stopped and gels examined on a UV transilluminator.

Bands containing the desired PCR products were excised from gels using a scalpel blade and then purified using the Qiaquick Gel Extraction kit (Qiagen) according to the manufacturer's

instructions. DNA was then precipitated by the addition of 0.1 volumes of 0.3M sodium acetate, followed by 2 volumes of 100% ethanol. After overnight storage at -80°C DNA was pelleted, washed in 70% ethanol and resuspended in DEPC-treated water.

2.4.3 Sequencing PCR

DNA sequencing analysis of amplified DNA fragments, ligation products and plasmid DNA was carried out on an Applied Biosystems 3700 DNA Analyser operated by the University of Birmingham Functional Genomics department. Each reaction comprised of 200-500ng DNA and 3.2pmol of sequencing primer.

2.5 Bacteriology

Chemically competent Stb13 *E. coli* cells were used for the preparation of concentrated plasmid DNA as these cells are able tolerate lentivirus constructs, which contain repeat regions that may be unstable in other strains [497]. Stocks of competent Stb13s were made using the Inoue method [498].

Bacterial cell suspension cultures were grown in Lennox LB medium and bacterial colonies were propagated on LB-agar plates. Both agar and Lennox LB were from Sigma and were used as directed by the manufacturer. Bacterial work was carried out under sterile conditions and equipment and solutions were autoclaved before use if not pre-packed sterile. LB media and LB agar were supplemented with antibiotics before use where constructs contained selection cassettes for simplified screening.

2.5.1 Transformation of Stb13 *E. Coli*

Aliquots (<100µl) of Stb13 were thawed on ice and 10ng of plasmid DNA or <10µl of ligation mix was added and the mixture incubated on ice for 30 minutes. Tubes were then heat

shocked at 42°C for 90 seconds and then briefly returned to ice before adding 1ml LB medium and leaving to recover at 37°C in a shaking heat block for 1 hour. Cells were then spun for 1 minute at 6500rpm (~4,000g) in a microcentrifuge and the pelleted cells spread onto agar plates and incubated at 37°C overnight.

2.5.2 Isolation of plasmid DNA from bacterial cultures

Single colonies were picked from plates following overnight incubation and used to inoculate 3mls of LB medium. If the bacteria were transformed with the products of a ligation reaction multiple colonies (usually 12) were chosen for screening. Cultures were placed in a benchtop shaking incubator at 225rpm, 37°C, until confluent (around 8 hours) and then plasmid DNA was extracted using the QIAPrep Spin Miniprep kit (Qiagen) according to the manufacturer's instructions.

Where larger amounts or higher concentrations of pure plasmid DNA were required a 3ml culture was used to inoculate 200-400ml LB medium overnight and plasmid DNA was extracted using the Qiagen Plasmid Maxi kit as per the supplied protocol. DNA purity and concentration was measured using the Nanodrop 1000 (Thermo Scientific) and plasmids were checked by restriction digest before use in cells.

2.5.3 Restriction digestion and DNA ligation

Restriction digests were carried out using FastDigest system (Thermo Scientific) according to the manufacturer's instructions. Briefly, the products of a PCR reaction or <5µg DNA were digested in a 50µl volume containing 1x FastDigest Buffer and 1-2µl of the required enzyme(s) (up to 5µl total). Digests were incubated at 37°C for 15-30 minutes and a small amount of the reaction mix was checked on a gel to confirm complete cutting. Before use in cloning, digested DNA was purified using a HighPure PCR Purification kit (Roche).

Ligations were generally set up using 10-20ng of vector DNA and a vector:insert molar ratio of 1:3 and 1:10 using the Rapid DNA Ligation kit (Roche) according to the manufacturer's instructions. Reaction mixtures were incubated at 16°C overnight then transformed into competent bacteria.

2.6 Molecular Cloning

Lentivirus constructs were used to express EBV genes in this thesis in order to overcome limitations we have found with other systems such as; poor transfection efficiencies and poor maintenance of episomal vectors. Episomal vectors also rely on constitutive expression of EBNA1 to maintain them in cells, which complicates EBNA1 functional studies. All of our lentiviral constructs were derived from the FTUG vector [483], which can be used to express Pol II driven genes by cloning the gene of interest into the original FTUG vector immediately downstream of the tet-on Trex promoter and then the whole expression cassette subcloned into the FH1t-UTG vector in place of the PacI-flanked H1t-shINSR expression cassette (see Figure 2.2). Alternatively Pol III transcribed genes can be cloned into an intermediate vector downstream of the human H1 promoter and then the whole expression cassette subcloned into the FH1t-UTG vector in place of the PacI-flanked H1t-shINSR expression cassette. All constructs were sequence verified before use.

2.6.1 Generation of EBNA1 lentivirus

FTrex-EBNA1-FLAG-UTG, a gift from Dr Graham Taylor, which contained the full length EBNA1 sequence subcloned from pRTS-CD2-EBNA1-FLAG [499], was modified to include an optimised Kozac sequence and a 3' polyA signal as protein expression from the unmodified vector was found to be poor (Tracey Haigh, unpublished). A schematic is shown in Figure 2.2-A.

2.6.2 Generation of FH1t-EBER-UTG lentiviruses

Each EBER was amplified from B95.8 genomic DNA using primers to generate fragments of 167 and 172 nucleotides corresponding to positions 6629-6796 and 6956-7128 of the prototypic EBV genome sequence (Genbank record AJ507799), respectively. These fragments were then cloned into a small plasmid downstream of a tet-on human H1 promoter and the expression cassette consisting of the EBER sequence and the H1 promoter was then cloned into the F-UTG lentiviral vector backbone (see Figure 2.2-B), which also expresses a tet-repressor and eGFP separated by a T2A sequence from a constitutively active ubiquitin promoter.

2.6.3 The pEKS10 EBER plasmid

The pEKS10 plasmid was generated by the Takada laboratory [310] in the following manner. A fragment of the pcDNA3 vector (Life Technologies) containing the neomycin (G418) resistance cassette was ligated to the SacI-EcoRI subfragment of the EcoRI K fragment of the Akata strain of EBV (Genbank reference KC207813.1) to give rise to pEK, which contains one copy of each EBER. Linker sequences containing a BglII or BamHI restriction site were then added to both ends of the SacI-EcoRI subfragment to allow successive additions of SacI-EcoRI subfragments by concatenation in a directional fashion to generate pEKS10 which contains 10 tandem repeats of the EBERs and surrounding sequence (6,297-7,325bp of KC207813.1). A schematic of pEKS10 is shown in Figure 2.2-C.

2.6.4 Generation of BART lentiviruses

Genomic fragments encoding the two clusters of miR BARTs were amplified from Raji genomic DNA, cloned into the FUTG vector and then subcloned along with the Trex promoter into the FH1t-UTG vector (Figure 2.2-D). Cluster 1 consisted of nucleotides 138997 to 140144 whilst Cluster 2 was comprised of nucleotides 145770 to 149022 of the EBV reference genome (AJ507799) using an identical strategy to that used by Pratt et al. [171].

Figure 2.2 Schematics of plasmids used in this thesis

A FTrex-EBNA1-FLAG-UTG

B FH1t-EBER1-UTG, identical to the construct used to express EBER2 except for the gene of interest

C pEKS10 plasmid

D FTrex-BARTs cluster 1-UTG, identical to the construct used to express BARTs cluster 2 except for the gene of interest

E FH1t-miR BART 5-UTG

The control vector for all lentivirus experiments contained all backbone elements of the FUTG lentivirus but containing no gene of interest expression cassette which was generated by excising the PacI-PacI fragment of FH1t-shINSR-UTG and re-ligating the vector.

The control vector for pEKS10 experiments was pcDNA3 containing a neomycin resistance cassette but no EBV DNA.

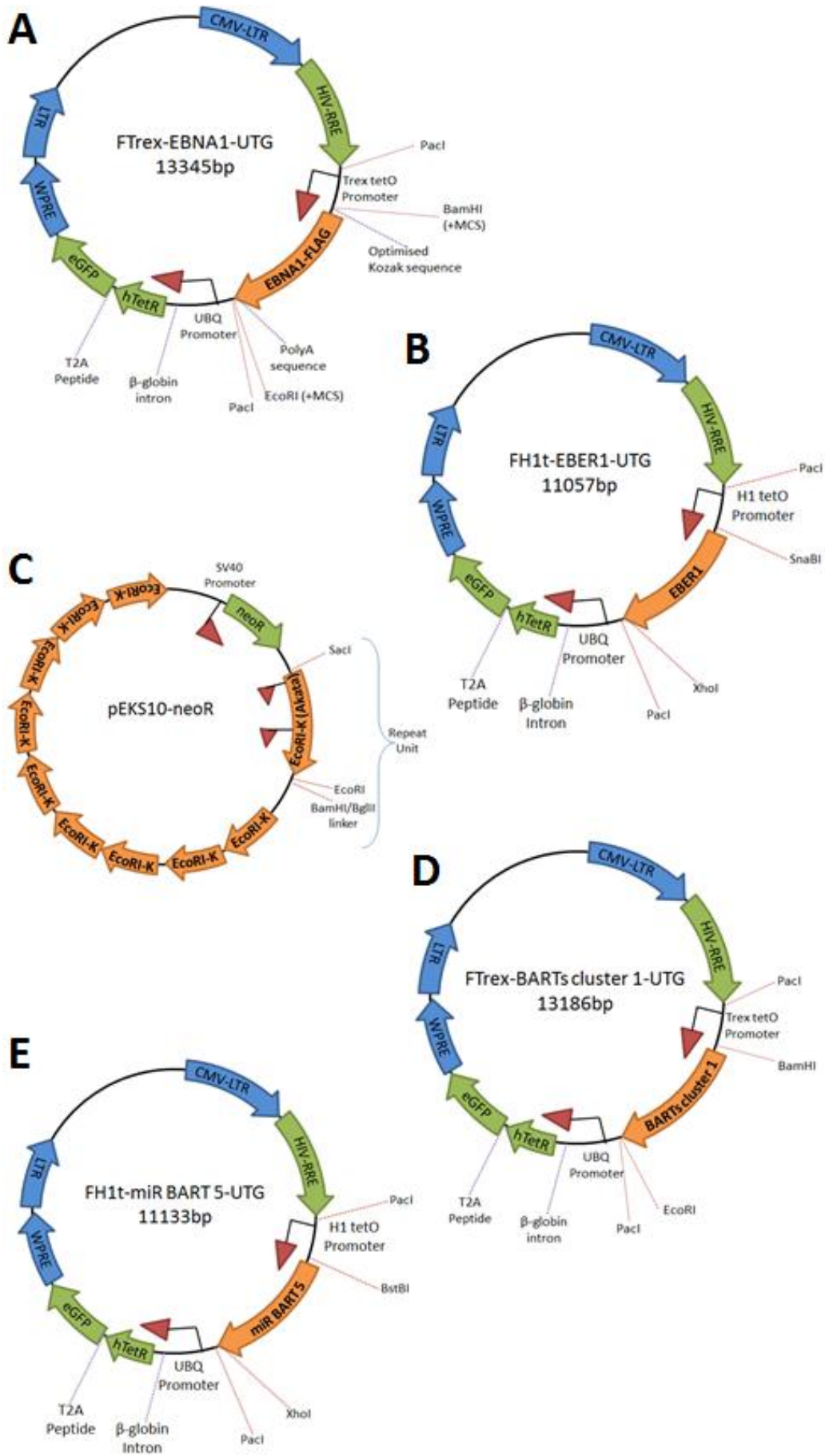


Figure 2.2

An EBV genome fragment encoding pre-miR BART 5 was amplified from Raji DNA using identical primers to those published by Choy et al. [365], which amplify a fragment corresponding to nucleotides 946-1196 of the BamHI A region of C666.1 (Accession no. EF102892) and introduce a termination sequence (AAAAAA) at the 3' end. This fragment was cloned downstream of a tet-regulated version of the human H1 promoter and then subcloned along with the promoter into the FH1t-UTG vector (see Figure 2.2-E).

2.6.5 Bim_S lentiviruses

The human Bim_S-derived BH3 variant-expressing lentiviruses were a kind gift from Dr Toru Okamoto who cloned the Bim_S variants into the FTrex-UTG system. The Bim_S variants themselves are described in Table 2.3 and were generated by Lin Chen (Bim_S-wt, -Noxa, -Bad and -4e) and Erinna Lee (Bim_S-2a) and colleagues at the Walter and Eliza Hall Institute (WEHI) [423, 500].

BH3 Variant	Description
Bim _S - wt	Full length human Bim _S protein. Accession number NP_001191035.1
Bim _S - 2a	Bim _S -wt with 2 single amino acid mutations, L62A and F69A. Confers specificity to Mcl-1 ,abolishes binding to Bcl-2, Bcl-XL and Bcl-w, reduces binding to A1.
Bim _S -Noxa	Bim _S -wt with amino acids 51-76 replaced with amino acids 20-43 of human Noxa. Confers Noxa-like binding to prosurvival Bcl-2 homologues (Mcl-1 and A1)
Bim _S -Bad	Bim _S -wt with amino acids 51-76 replaced with amino acids 103-126 of human Bad. Confers Bad-like binding to prosurvival Bcl-2 homologues (Bcl-2, Bcl-XL and Bcl-w)
Bim _S - 4e	Bim _S -wt with 4 single amino acid mutations, I58E, L62E, I65E and F69E. Abolishes binding to all pro-survival Bcl-2 homologues

Table 2.3 Details of Bim_S variant constructs cloned into the FTrex-UTG lentivirus system for functional BH3-induced cell death assays.

2.6.6 FTrex-BHRF1-UTG lentivirus

The FTrex-BHRF1-UTG lentivirus was a kind gift from Rachael Cartlidge. It contains the coding region of BHRF1 amplified from the pRTS-CD2-BHRF1 vector [89], cloned into FUTG lentiviral backbone downstream of the Trex promoter and subcloned along with the promoter to create FTrex-BHRF1-UTG

2.6.7 Akata-GFP2 recombinant EBV BAC

The Akata virus genome was isolated from the Akata-BL cell line by Takada and colleagues as described by Kanda et al. [488]. The wt virus genome was engineered to contain an F-plasmid for replication and maintenance within *E. coli*. The BAC then had GFP and a G418 selection marker inserted into the genome at the BamHI X locus to give rise to the Akata-GFP2 BAC plasmid.

2.6.8 CpWp-KO recombinant EBV BAC

The CpWp-KO virus is derived from the 2089 EBV BAC [486], but contains deletions to disrupt viral gene expression driven from the Wp and Cp promoters. The virus construct was made from the 0W BAC [493], which completely lacks the BamHI-W repeats where Wp resides, by Dr Rosemary Tierney for use in an unrelated project [485]. In addition to lacking Wp, the CpWp-KO BAC also contains a deletion spanning the entire Cp promoter (coordinates 10799 to 12190 of Genbank reference genome NC-007605). All constructs were checked by BamHI restriction digest analysis before being cloned into 293 virus producer cells.

2.7 RNA analysis

2.7.1 Preparation of purified RNA

For total RNA purification, including small RNAs, $1-5 \times 10^6$ cells were harvested during exponential growth phase (24 hours after last subculture) and processed according to manufacturer's instructions using the miRVANA RNA Extraction Kit (Ambion). Samples were eluted in DEPC-treated water and purity and concentration then measured using the Nanodrop 1000 (Thermo Scientific). RNA was stored at -80°C and kept on ice during use to prevent sample degradation. Where downstream applications required the use of DNA-free RNA (low density array cards or q-PCR to detect unspliced/single exon transcripts) purified RNA was treated with recombinant DNaseI (Ambion) according to the manufacturer's instructions.

2.7.2 Synthesis of randomly-primed cDNA

RNA was reverse transcribed using the qScript cDNA SuperMix (Quanta Biosciences) which is a 5x master mix containing qScript MMLV-derived reverse transcriptase, dNTPs, MgCl_2 , an RNase inhibitor, and oligonucleotide primers. Each $20\mu\text{l}$ reaction contained $4\mu\text{l}$ SuperMix cDNA synthesis mastermix and $0.5-1\mu\text{g}$ RNA template. Reaction tubes were then incubated at 25°C for 5 minutes, followed by 42°C for 30 mins and 5 minutes at 85°C as per the manufacturer's instructions. For q-PCR cDNA was diluted in DEPC water to a concentration equivalent to 5ng template RNA per microliter. For Low Density TaqMan Array cards 500ng of RNA template was used for cDNA synthesis in a $20\mu\text{l}$ reaction and diluted to $300\mu\text{l}$.

2.7.3 Synthesis of stem loop-primed cDNA for the detection of miRNAs

Reverse transcription of miRNAs was carried out using the TaqMan microRNA Reverse Transcription Kit according to the manufacturer's instructions. Briefly, for each miRNA to be

amplified, a master mix was prepared containing 0.15µl dNTPs, 1µl Multiscribe MuLV-derived reverse transcriptase, 1.5µl buffer 0.19µl RNase inhibitor, 4.16µl DEPC water and 3µl miR-specific RT primer per sample (allowing for error). Primers specific for each microRNA were supplied with TaqMan miRNA q-PCR assays, all other reagents were included in the kit. For each sample 5µl of template RNA diluted to 2ng/µl (a total of 10ng) added to 10µl of master mix and transcription was performed by incubating samples at 16°C followed by 42°C for 30 minutes each, then at 85°C for 5 minutes.

2.7.4 TaqMan q-PCR for EBV and cellular genes

Quantitative PCR assays were carried out using an Applied Biosystems 7500 real-time PCR system (Life Technologies) in 96-well optical plates (Geneflow). Each reaction well contained 1x TaqMan q-PCR master mix (Life Technologies), gene-specific primers and probes, endogenous control primers and probes and 5µl diluted cDNA in a 25µl total volume. All samples were plated out in duplicate or triplicate and mean and standard deviation calculated for each sample. All data were analysed using the $\Delta\Delta C_t$ method relative to a reference sample that was known to express the gene of interest [501].

Assay Name	Assay Number	Assay Name	Assay Number
Bim	Hs00197982_m1	MYC	Hs00905030_m1
CXCR3	Hs00171041_m1	PMAIP1/Noxa	Hs00560402_m1
GAPDH	4310884E	Puma (total)	Hs00248075_m1
IL10	Hs00961622_m1	Puma-β	Hs01080223_m1
Mcl-1	Hs00172036_m1	SASH1	Hs00323932_m1

Table 2.4 Details of inventoried q-PCR assays

Cellular q-PCR assays were purchased from Applied Biosystems, details of which can be found in Table 2.4. EBV gene assays were designed by Dr A Bell and are published elsewhere [90, 317], except for the BZLF1, BHRF1 total mRNA, BARTs cluster 1 mRNA, BARTs cluster 2 mRNA LF1, LF2 and LF3 gene assays which were developed for this study and are described in Table 2.5. Primer and probe sequences were designed using the Applied Biosystems custom assay tool and validated in-house according to published guidelines [502]. For quality control the R² value was checked over a serial dilution, where a value of >0.98 was deemed acceptable and no template, no RT, and no DNase controls were also included for all assays. Validation of all EBV assays for both mRNAs and microRNAs has been published (Bell 2006, Pol paper, Amoroso 2011). All probes were labelled with FAM with a TAMRA quencher except for the GAPDH probe which was labelled with VIC to allow it to be multiplexed with FAM-labelled probes.

Assay Name	Forward Primer	Reverse Primer	Probe
BARTs cluster 1	GCCGCTGTTACCTA AAGTGA	TCCACACCTGAAAG CCTGGTA	AAGGTCTGTCAGCCG CCA
BARTs cluster 2	CACCTGGAGCCCTGA TCATT	ACTAGCGCACCAAAC TGTCTGA	CGGCTTTTACTGCCA CCTGGCTTCTG
BHRF1	CGAACATGTGGATCT GGATTTAACTC	AACGCGCGCCCAAG	TCACCGTGGAGACCC
BZLF1	CCCAAACCTCGACTTCTGA AGATGTA	TGATAGACTCTGGTAGCT TGGTCAA	CCCATACCAGGTGCCTTT
LF1	GACTGACTCAGGGCCACA TC	AGAAAGCGGGCCCATGA AGG	ACGCCGCTCGCCAG
LF2	CCGGACCGTCAGCTTGAG	CAACCCGGTCTTCTACGT CTAC	CCGGCTTCCACTCCTG
LF3	AGGGCTGGGTCTGAGA	ACACGTGATGTAAGTTTA GCCAGTT	GACTTTCGGGGCATT

Table 2.5 Details of unpublished, custom made q-PCR assays. Used to detect EBV-encoded transcripts as indicated, all sequences are in the 5'-3' orientation

2.7.5 TaqMan q-PCR for miRNAs

Quantitative PCR assays for microRNAs were also carried out using an Applied Biosystems 7500 real-time PCR system (Life Technologies) in 96-well optical plates (Geneflow). Each reaction well contained 1x TaqMan q-PCR master mix (Life Technologies), Taqman micro-RNA specific stem-loop primers and probes or endogenous control primers and probes and 1.33µl undiluted miR-specific cDNA in 20µl total volume. All samples were plated out in duplicate or triplicate and mean and standard deviation calculated for each sample. All data were analysed using the $\Delta\Delta C_t$ method relative to a reference sample that was known to express the miRNA of interest [503]. Assays for miRNAs were purchased from Applied Biosystems, details of which can be found in Table 2.6. All probes, including the RNU48 endogenous control probe, were labelled with FAM as these assays were not multiplexed.

Assay Name	Assay Number	Assay Name	Assay Number
miR-BART 1-5p	TM:197199	miR-BART 5	TM: 197237_mat
miR-BART 13	TM: 005446	miR-BART 7	TM: 197206_mat
miR-BART 15	TM 5699	miR-BART 22	TM: 6609
miR-BART 3	MIMAT0003411 ::CCOH8C8	RNU48	TM:1006
miR-BART 4	TM: 5623		

Table 2.6 Details of commercially available EBV miR q-PCR assays used in this study

2.7.6 TaqMan human apoptosis low density q-PCR arrays

Low-density q-PCR arrays for apoptosis-related human genes were carried out using TaqMan Low Density Array (TLDA) cards which are pre-loaded with 93 q-PCR assays to detect a panel of genes that are known to be important in controlling apoptosis and are reported to be transcriptionally regulated, together with 3 endogenous control genes (Life Technologies, part number 4378701). TLDA work on the same principle as standard q-PCR but using far smaller volumes of samples and allowing transcription of 96 genes in 4 samples to be assayed on a single card, increasing the efficiency and cost effectiveness of the workflow. Each cDNA sample was generated as described in Section 2.7.2 and checked for quality using conventional q-PCR; comparing DNA-free cDNA to cDNA made from untreated RNA and a no RT control. Once verified, 2 x 100µl aliquots of the cDNA were pipetted into 2 adjacent loading ports (each port fills 48 wells and so supplies sample to only half of the 96 genes) and a total of 200ng template RNA was used per sample. Samples were evenly distributed into wells by centrifugation as per the manufacturer's guidelines, checked for even filling and sealed, before running on the Applied Biosystems 7900HT real time PCR system (Life Technologies). All apoptosis gene arrays were carried out on three EBV-positive and 3 EBV-loss clones and samples from all six clones in all three independent experiments were run in duplicate.

Data were collected using SDS software v2.4.1 (Life Technologies) and analysed with DataAssist software v3.01 (Life Technologies) using the $\Delta\Delta C_t$ relative quantitation method [501]. Gene expression data were normalised to the mean of GAPDH and ACTB, (the third endogenous control, 18S, was not used as it was expressed at levels far in excess of any other transcript in our samples) and the calibrator sample was untreated EBV-positive Kem clone P1 cells or the mean of the three untreated EBV-positive clones, depending on whether a grouped or individual analysis was being carried out. The fold-change cut off used for classifying a gene as

differentially regulated between two samples or groups was 2 and the significance cut off was $p=0.05$.

2.7.7 Fluidigm viral gene expression q-PCR Arrays

Rather than running a large number of individual assays for EBV gene expression in xenograft tumour samples and some cell lines, 48 EBV transcript-specific assays and endogenous controls were loaded onto Fluidigm Dynamic Array microfluidic chips. These chips can be used to quantitate expression of all 48 transcripts of interest in up to 48 samples simultaneously. In addition, we used a plasmid containing DNA amplicons complementary to all 48 assays to allow us to absolutely quantitate the number of each of the 48 transcripts present in each sample. The use of this method for high throughput analysis of EBV gene expression in a range of samples is described in detail elsewhere [175], but is essentially similar to conventional q-PCR except that cDNA undergoes 14 rounds of pre-amplification in the presence of primers specific to each of the 48 assays loaded onto the card. Pre-amplification is necessary due to the very small amounts of template RNA used per sample. For each assay, linearity of control DNA over a range of dilutions was confirmed.

2.7.8 Northern blotting

RNA was isolated using Trizol reagent (Life Technologies) according to the manufacturer's instructions and separated on 6% TBE-Urea pre-cast gels in TBE buffer (Life Technologies) followed by semi-dry blotting onto nylon membranes (Amersham). RNA loading was checked by UV-visualisation of ethidium bromide stained gels. Radiolabelled DNA probes were generated by PCR amplification of the EcoRI-J fragment of the EBV genome using forward primer 5'-TGCTAGGGAGGAGACGTGTGT and reverse primer 3'-GAATCCTGACTTGCAAATGCTCTA in the presence of ^{32}P labelled dCTP (Hartmann Analytic), followed by column purification and nick translation (Roche). Probe hybridisation and washes

were carried out using the XpressHyb system, (Clontech) according to the manufacturer's instructions. Exposures were carried out at -80°C for 1-14 days.

2.7.9 EBER in-situ hybridisation (ISH)

EBER expression at the single cell level cells were analysed using a FITC-conjugated EBER probe which was hybridised to permeabilised cells in solution and then analysed by flow cytometry. For each assay, 1×10^6 PFA-fixed cells were permeabilised by 15 minute incubation in 50µl of 0.5% Tween 20 in phosphate-buffered saline (PBS), and then washed in 200µl formamide buffer (75µl formamide, 10mM NaCl, 5mM Na₂EDTA and 50mM Tris-HCl, pH7.5) to maximise probe binding. Cells were then resuspended in 50µl EBER-PNA probe solution (Dako) and hybridised at 56°C for 1 hour. Following hybridisation, cells were washed twice for 10 minutes at 56°C in 1ml 0.5% Tween 20 in PBS to remove any unbound probe and then resuspended in 1ml PBS supplemented with 2% FCS and 1mM EDTA, placed on ice and analysed immediately on an Accuri C6 flow cytometer (Becton Dickinson).

For each sample a minimum of 5,000 events were recorded and analysis carried out using Accuri C6 software. Gating was set to exclude dead cells, debris and doublets and remaining events were plotted on a histogram compared to negative control samples (both control probe stained EBV-positive and EBV negative cells) to determine the percentage of EBER-expressing cells.

2.8 Protein analysis

2.8.1 Protein preparation

For Western blot analysis, $5-10 \times 10^6$ cells were harvested, washed in PBS and then lysed in 9M urea buffered with 50mM Tris pH 7.5 on ice. Samples were then homogenised for 30 seconds each by sonication (QSonica, model CL-18) to shear DNA and cell debris. Samples were titrated

against bovine serum albumin (BSA) standards of known concentration and quantitated using a BioRad DC colorimetric assay kit according to the manufacturer's instructions. Cell lysates were diluted to 0.5-2mg/ml in urea gel sample buffer (U-GSB) (5M Urea, 10% glycerol, 5% β -mercaptoethanol, 4% SDS, 62.5mM Tris pH6.8 and 0.01% bromophenol blue), denatured for 5 minutes at 100°C, and stored at -20°C until needed.

2.8.2 SDS-PAGE / Western Blotting

Proteins were separated on pre-cast 4-12% Bis-Tris gels (Life Technologies) in MES buffer (comprising 50mM 2-[N-morpholino]-ethanesulphonic acid (MES), 50mM Tris base, 1mM EDTA and 0.1% (w/v) SDS, pH 7.3) at 100 volts until the dye front had migrated almost the whole length of the gel (around 100 minutes). Wells were loaded with 20 μ g of protein or 10 μ l of prestained size markers (SeeBlue 2.0 Plus, Life Technologies). Proteins were blotted onto methanol-activated PVDF membranes in an XCell blotting module (Life Technologies) filled with blotting buffer (25mM Tris base, 192mM glycine and 20% v/v methanol). The reservoir around the blotting module was filled with water to keep the apparatus cool during blotting, which was carried out for 100 minutes at 30 volts.

After blotting, non-specific protein binding was blocked by incubating membranes in 5% non-fat milk diluted in PBS containing 0.1% Tween-20 (PBS-T) for 1 hour at room temperature. Primary antibodies were diluted in blocking buffer and bound overnight at 4°C, except for the loading controls, β -actin and calregulin, which were incubated at room temperature for 1 hour. All primary antibodies are described in Table 2.7, those specific to EBV proteins are described in the following publications; BHRF1 [504], EBNA1 and 2 [505], LMP1 [506]. Membranes were thoroughly washed (6 PBS-T washes over 1 hour) in PBS-T and then incubated with horseradish peroxidase-conjugated secondary antibodies, (all from Sigma) diluted 1/1000 in blocking buffer, for 1-2 hours at room temperature, and finally thoroughly washed again.

Target	Antibody	Origin	Dilution
β -actin	Clone AC-15, Sigma	Mouse	1/10,000
Bad	Clone C-7, Santa Cruz	Mouse	1/200
Bak	Clone N-20, Santa Cruz	Goat	1/200
Bax	Clone N-20, Santa Cruz	Rabbit	1/200
Bcl-2	Clone C-2, Santa Cruz	Mouse	1/200
Bcl-XL	H-5, Santa Cruz	Mouse	1/200
Bid/t-Bid	#2002, Cell Signalling	Rabbit	1/1000
Bim	#2819, Cell Signalling	Rabbit	1/1000
Calregulin	Clone N-19, Santa Cruz	Rabbit	1/1000
Calregulin	Clone N-19, Santa Cruz	Goat	1/1000
CARD6	18029-1-AP, Proteintech	Rabbit	1/500
Caspase-3	#9662, Cell Signalling	Rabbit	1/1000
Caspase-7	#9492, Cell Signalling	Rabbit	1/1000
Caspase-9	#9502, Cell Signalling	Rabbit	1/1000
CFLAR/FLIP	10394-1-AP, Proteintech	Rabbit	1/500
c-IAP1 (BIRC2)	#4952, Cell Signalling	Rabbit	1/1000
DEDD2	14574-1-AP, Proteintech	Rabbit	1/200
FLASH	M-300, Santa Cruz	Rabbit	1/100
Livin	D61D1, Cell Signalling	Rabbit	1/1000
Mcl-1	Clone S-19, Santa Cruz	Mouse	1/200
Noxa	114C307, Abcam	Mouse	1/250
PARP	#9542, Cell Signalling	Rabbit	1/1000
Puma	Clone G-3, Santa Cruz	Mouse	1/100
Survivin	71G4B7, Cell Signalling	Rabbit	1/1000
XIAP	3B6, Cell Signalling	Rabbit	1/1000
BHRF1	5B11	Mouse hybridoma	*
EBNA1	A. Mo	Human serum	*
EBNA2	PE2.2	Mouse hybridoma	*
LMP1	CS1-4	Mouse hybridoma	*

Table 2.7 Details of primary antibodies used for Western blotting

*All determined empirically as antibody concentrations vary between preparations

Chemiluminescence was detected by applying Enhanced ECL solution (GE Healthcare) and exposing membranes to autoradiography film for 1-20 minutes or using the BioRad ChemiDoc MP imaging system, which was also used to carry out densitometry calculations. Since traditional films can also be imaged and processed on the ChemiDoc MP, it was also used to determine band sizes as details of the ladder being used can be programmed in and then protein sizes calculated using point-to-point (semi-log) regression.

For total protein analysis gels were stained in 0.1% Coomassie Blue R250 in 50% methanol, 40% ddH₂O and 10% acetic acid for 60 minutes and then destained in 50% methanol, 40% ddH₂O and 10% acetic acid over 3 hours with 3 changes of the solvent solution and then gels were photographed.

2.8.3 Immunofluorescence (IF) staining

Cells were harvested during log growth phase, washed in PBS, resuspended at 10×10^6 /ml and spotted onto slides (SM011, Hendley-Essex). Slides were air dried, fixed in pre-cooled 1:1 methanol:acetone for 10 minutes at -20°C, and then dried again before adding BZLF1 primary mouse monoclonal antibody [135], diluted to 0.2µg/ml in PBS containing 10% heat-inactivated goat serum (HINGGS). Both primary and secondary incubations were carried out in a sealed, humidified atmosphere at 37°C for 1 hour. After primary antibody binding, cells were washed twice in PBS, air dried, and then Alexa Fluor 488-conjugated α-mouse secondary antibody (Life Technologies) was applied at 1/1000 in 10% HINGGS PBS. Slides were incubated for a further hour, washed in PBS twice and air dried. Finally, a drop of 1,4-diazabicyclo[2.2.2]octane (DABCO) mounting medium was applied to each dot, and a cover slip placed over the stained cells. Slides were viewed and photographed using a Nikon E600 fluorescence microscope and each experiment included positive and negative control cells, including a positive control cell line incubated with secondary antibody only.

2.8.4 CD19 FACS Staining

To detect the proportion of human cells in single cell suspensions of murine xenograft tumours, cells were stained for human CD19 and analysed by fluorescence-activated cell sorting (FACS). Most samples were analysed immediately after harvesting, but a small number had previously been cultured for up to 24 hours. There was no detectable difference in the proportion of cells which stained positive for CD19 regardless of whether they were freshly isolated or previously cultured. Briefly, 1×10^6 cells were washed twice in PBS and resuspended at 10×10^6 /ml in Fc block (BD Pharmingen) diluted 1/100 in FACS buffer (1xPBS, 2% FCS, 1mM EDTA) and incubated for 20 minutes on ice. Cells were then spun down for 5 minutes at 1500rpm, then resuspended in FITC-conjugated CD19 antibody (clone HIB19, BD Pharmingen) diluted 1/20 in ice cold FACS buffer. Staining was carried out at room temperature for 30 minutes in the dark. Finally, cells were washed twice in ice cold FACS buffer and resuspended in 100 μ l FACS buffer containing 1 μ g/ml PI and analysed immediately on an LSRI flow cytometer (Becton Dickinson). Cells were gated to exclude dead cells and debris (PI positive) and then the percentage of FITC-CD19 positive cells was determined on a histogram compared to unstained control cells. As an additional control murine B lymphoma cells were confirmed to be negative for human CD19 staining using this protocol. We recorded a minimum of 5,000 events per sample and data analysis was carried out using FlowJo software (Treestar).

2.8.5 Cell sorting

In order to generate cell lines in which every cell carries a vector or recombinant virus of interest cultures were sorted for GFP, which was constitutively expressed in the majority of the constructs used in this thesis (see Section 2.1.4). Cells were washed in PBS, resuspended at 25×10^6 /ml in sorting medium (2% FCS, 16 μ g/ml gentamycin in PBS) and passed through a 50 μ m cell filter before being placed on ice and taken for processing to the cell sorting facility at

either the University of Birmingham or WEHI, depending on where the experiments were carried out. Cells transduced with lentiviruses required at least two rounds of sorting several days apart to enrich for cells expressing the highest possible levels of GFP, and related samples (i.e. empty control and gene of interest in the same background) had identical gates applied to them. The purity of the collected cells was generally found to be around 98% (+/-2%).

2.9 Reporter assays

For each assay, 1×10^7 EBNA1-transduced or control cells were transfected by electroporation at 270V, 950 μ F in 4mm cuvettes (Geneflow) with 10 μ g FR-*tk*-luciferase and 1 μ g *Renilla* vector in order to normalise for transfection efficiency in the presence of 1 μ g/ml DOX or DMSO as a control. *Renilla*-only controls were also included. At 24 hours after transfection cells were harvested, lysed and analysed for luciferase and *Renilla* expression using the Dual-Luciferase Reporter Assay System (Promega) according to the manufacturer's instructions. Briefly, 1×10^6 cells per experimental condition were lysed in passive lysis buffer for 15 minutes at room temperature with vigorous shaking before being transferred to 96 well plates. Stop and Glow reagents (50 μ l of each) were added to wells at 1 minute intervals by automated injectors and read on an Orion-L luminometer (Berthold). All transfections were carried out in triplicate.

2.10 Animal Work

2.10.1 Xenografts

Mice used for xenografts were of the NOD.Cg-*Prkdc*^{scid}*il2rg*^{tm1Wjl}/SzJ strain (more commonly referred to as NOD/SCID/IL2R γ KO or NSG) originally developed by the Jackson Lab [507, 508]. Single cell suspensions of 5×10^4 - 1×10^7 BL cells in a 200 μ l volume of PBS were injected into the

peritoneum of 8 week-old recipient NSG mice by trained animal technicians. Mice were then palpated to determine tumour growth 3-4 times weekly and were sacrificed when total tumour burden reached approximately 1cm³ in accordance with Walter and Eliza Hall Institute (WEHI) Animal Ethics Committee Guidelines. Monitoring continued for up to 250 days at which point any remaining mice were discarded.

One animal developed lameness that was unrelated to the xenograft and so was sacrificed and excluded from the study and in an additional animal we found that viral gene expression had changed *in vivo* from Latency I to Latency III and therefore this animal was also excluded. Kaplan-Meier plots and log-rank tests to compare the survival of mice injected with different clones were carried out using Graphpad Prism™ 5.0 software.

2.10.2 Histology

Tumours, sternum, spine, heart, pancreas, kidneys, liver, lungs, spleen, and lymph nodes (if enlarged) were removed post-mortem and fixed in 10% Formalin. Preserved material was then sectioned, mounted on slides and H&E stained by the WEHI Histology Department. Analysis of H&E stained sections was carried out by haematologist Dr Brandon Aubrey at WEHI. Ki67 staining was carried out by Dr Claudia Roberts in the Department of Cellular Pathology, Queen Elizabeth Hospital, Birmingham.

2.10.3 *Ex vivo* cell culture

Tumour samples were also harvested from mice for *ex vivo* characterisation; tissue was harvested into a small volume of ice cold medium, passed through a 100µm cell strainer (Falcon) and then filtered through a sterile cotton wool plug to create a single cell suspension. Several aliquots of these cells were immediately frozen and the remaining cells were washed in PBS, resuspended in fresh, warmed medium and placed into culture. Routine cell culture and cell freezing was carried out as described in Section 2.1.1.

3. Results Part I

ISOLATING AND CHARACTERISING EBV-LOSS CLONES

3.1 Introduction

In the 50 years since EBV was first associated with BL there have been many investigations into the role of the virus within the tumour cells. However, it is still not clear exactly how the virus contributes [509]. In 1994, the Takada group reported the spontaneous loss of EBV from EBV-positive Akata-BL [309], allowing for comparison of isogenic tumour cells which either contain or have lost the virus. This model offers significant advantages over comparisons of EBV-negative BLs to their EBV-infected counterparts because EBV-negative tumours may have cellular mutations that substitute for the presence of EBV compared to EBV-positive tumours. It is surprising then, that this phenomenon has only been reported in two additional BL cell lines, Mutu-BL and Awia-BL, to date [178, 341]. The Awia-BL cell line and its clones were generated from a panel of BL biopsies collected here in Birmingham during the 1980's and 1990's from which a number of well-characterised BL cell lines have been generated (see Section 2.1.1). Therefore the Birmingham group initiated a project seeking to generate spontaneous EBV-loss clones from a panel of 12 EBV positive BL cell lines derived from our collection of biopsies.

We also considered other approaches; treatment with hydroxyurea or a dominant negative EBNA1 (dnEBNA1) can expel the viral genome from EBV-positive BL cells [299, 311]. However, hydroxyurea is known to inhibit DNA synthesis and DNA damage repair [510], causing the accumulation of double strand breaks [511], and treating cells with dnEBNA1 or drugs to inhibit EBNA1 is highly toxic to BL cells [99, 182]. Therefore we were concerned that it would be difficult to isolate EBV-positive and EBV-loss clones from cultures undergoing high rates of apoptosis and that clones that were recovered might be phenotypically different to the parental BL. Consequently we chose to isolate EBV-loss clones by single cell cloning.

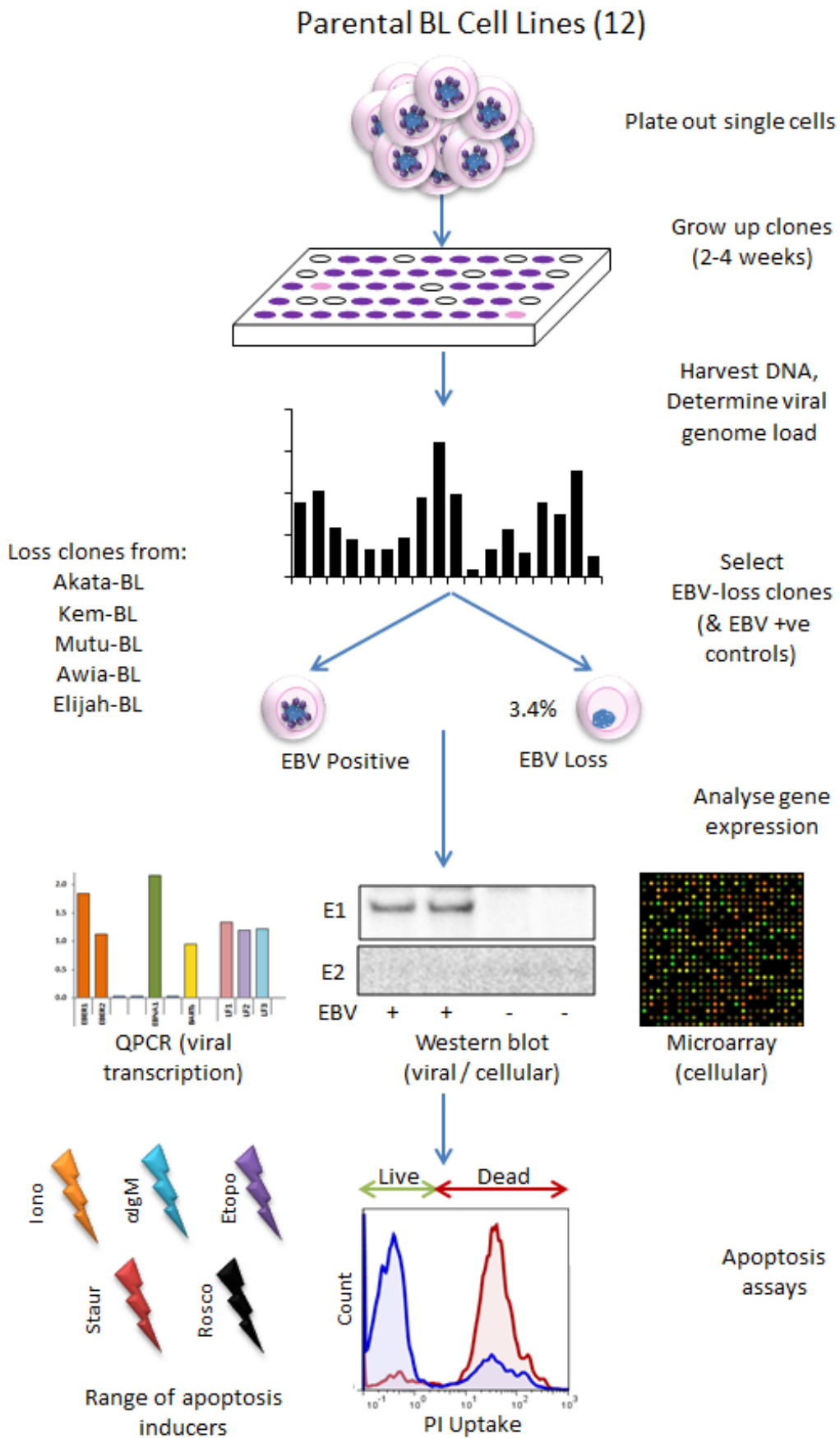


Figure 3.1 Workflow of experiments carried out to isolate and characterise BL clones

By comparing a panel of EBV-loss cells to their EBV-positive counterparts from the same patient we aimed to resolve conflicting reports in the literature about the possible anti-apoptotic role(s) of EBV in BL and the mechanisms by which the virus may act [99, 323, 326, 341, 512]. We were also interested to determine how widely the phenomenon of EBV-loss occurs, as this may provide insights into the pathogenesis and maintenance of BL tumours *in vivo*. The single cell cloning protocol used is detailed in Section 2.1.2 and the workflow of these experiments is depicted in Figure 3.1. Briefly, single cells from each BL cell line were expanded in 96-well plates and then a sample taken to analyse by q-PCR once cells from each clone had become numerous enough to determine the average viral genome load. Clones found to have no detectable EBV DNA were then selected for further expansion and analysis, as were a selection of EBV-positive clones which contained a similar viral load to the parental EBV-positive line. In this study we have generated several hundred BL clones in addition to those generated by previous members of this research group, screened for EBV-loss and then characterised the viral gene expression and apoptosis phenotype of selected clones. In order to gain a more detailed insight into the role of EBV in BL we have also studied the role of pro-survival signals in the mechanism of EBV-loss from BL cells and compared the tumorigenicity of EBV-positive and loss clones *in vivo*.

3.2 Single cell cloning of EBV-positive BL cell lines

3.2.1 Generating EBV-loss clones from EBV-positive BL cell lines

Our single cell cloning experiments showed that the average EBV genome load in single cell clones can vary greatly from zero to hundreds of copies per cell. Figure 3.2 shows the genome loads determined for clones of Kem-BL that were generated and tested as part of a single experiment. Interestingly, for the cell lines analysed in this study, the mean viral load of clones

generated in a single experiment was similar to the viral load of the parental cell line from which the clones were derived. For instance, in the example shown, the average viral load of the parental cell line, Kem-BL, is around 37 genomes per cell – shown as a blue dashed line on Figure 3.2-A, whilst the mean of all of the clones in this experiment was found to be 54, shown as an orange dashed line. This variation in viral load supports the theory that EBNA1 is not totally efficient at tethering viral genomes to sister chromatids evenly. Data to support this was first published by the Sugden group [295] and corroborated by a previous member of this group who found unequal numbers of genomes in sister cells undergoing mitosis by *in situ* hybridisation (Regina Feederle, unpublished).

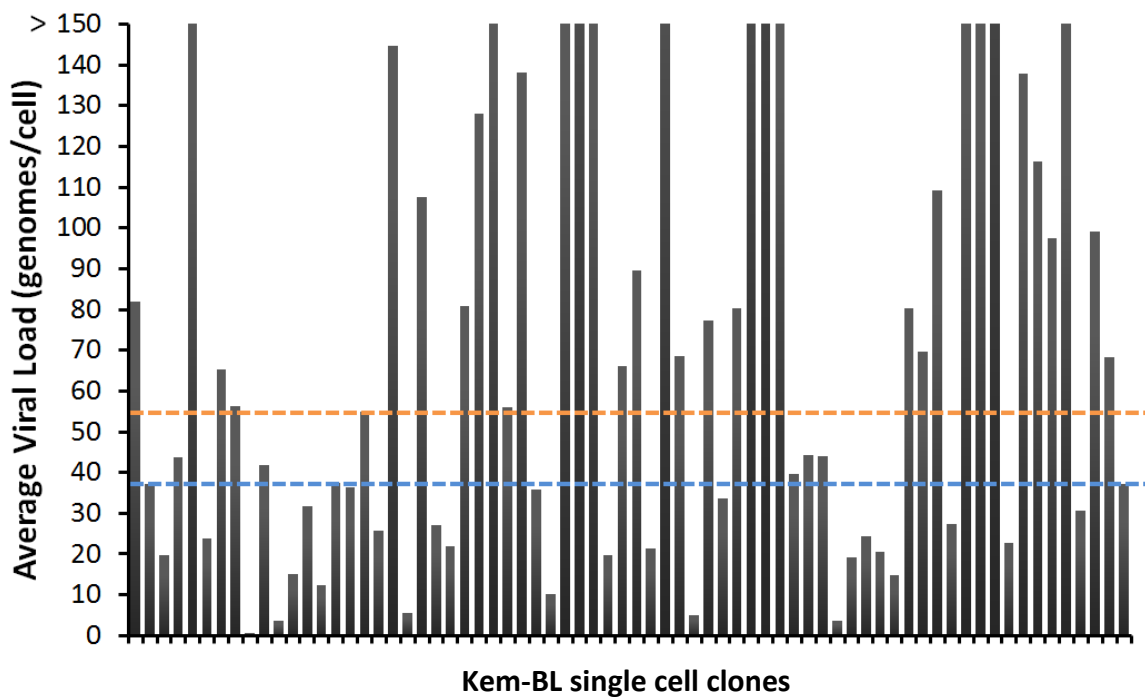


Figure 3.2 Example of average viral loads in single cell clones of Kem-BL

Whole cell lysates from single cell clones generated in a single experiment were subjected to DNA q-PCR as described in Section 2.3.2

Blue dashed line – average viral load of parental cell line

Orange dashed line – average viral load of clones in this experiment

In total we have screened 1,820 single cell clones as part of this project, around 500 of which were generated as part of my thesis; a summary of all the single cell cloning experiments performed by myself and by previous members of the group (Drs Andrew Boyce and Gemma Kelly) is shown in Table 3.1. Overall, we found that EBV-loss was rare, only 3.4% of clones screened had lost the virus, and the vast majority of these were isolated from a single tumour background, Elijah-BL (Eli-BL). Although there was substantial variation in the rate of EBV-loss between individual cell lines, we did find that Akata-BL gave rise to EBV-loss clones at a similar rate to that reported by Takada et al. [310].

Three of the BL cell lines cloned (Avako-BL, Salina-BL and Oku-BL) exhibit Wp-restricted Latency, in which high levels of the anti-apoptotic viral Bcl-2 homologue, BHRF1, are expressed [89]. Of 365 Wp-restricted clones screened only a single clone of Avako-BL, which later died before a cell line could be established, had lost the virus, which may indicate that these BL cells are unable to tolerate EBV-loss. This may be due to addiction to BHRF1, similar to the addiction to cellular pro-survival oncogenes that has been described in a number of other tumours [513, 514]. The parental Awia-BL cell line is also predominantly comprised of cells expressing Wp-restricted Latency, but is unique in that the biopsy appeared to be heterogeneous for EBV antigen expression at the single cell level. Awia-BL gave rise to rare Latency I and EBNA2+ve/LMP1-ve clones in early passage in addition to 2 EBV-loss clones [178]. Of the remaining BLs, only Mutu-BL, which was cloned at passage 4, gave rise to EBV-loss clones during early or intermediate passage (<40 passages); Akata-BL, Kem-BL and Elijah-BL only yielded loss clones at very late passage (120-200 passages). These data suggest that retention of the virus is also highly selected for in Latency I BLs in the absence of a viral Bcl-2 homologue.

3.2.2 Viral transcription in BL clones

It is well documented that viral gene expression in EBV-positive Latency I BL cells can 'drift' to the growth transforming Latency III programme in culture [505] therefore, we screened our

Cell line	EBV-loss frequency		Viral load range
Avako-BL	1 / 158	0.6%	0-68
Awia-BL	2 / 190	1.1%	0-35
Oku-BL	0 / 135		5-37
Salina-BL	0 / 72		6-30
Akata-BL	15 / 272	5.5%	0-200
Chep-BL	0 / 149		2-60
Dante-BL	0 / 95		11-68
Elijah-BL	38 / 103	36.9%	0-68
Kem-BL	3 / 185	1.6%	0-300
Mutu-BL	3 / 195	1.5%	0-150
Rael-BL	0 / 91		7-300
Sav-BL	0 / 175		30-500

Table 3.1 Compiled data from all BL single cell cloning carried out by this group

Cell lines in shaded section express a Wp-restricted pattern of Latency
EBV-loss frequencies are highlighted in red, except for the single loss clone of Avako-BL which was excluded because it did not survive

single cell clones for expression levels of a number of viral transcripts by q-PCR. All EBV-positive clones were profiled before further use and representative results from these experiments are shown in Figures 3.3 and 3.4. For each individual viral gene ΔC_t values were normalised to the housekeeping gene GAPDH to control for variation in the amount of cDNA in the sample and then expressed relative to a reference cell line that is known to express the viral gene of interest. This means that if the gene is 'on' it will have a relative quantity close to or in excess of 1 and genes that are 'off' will have a relative quantity of close to zero. We wanted to determine how Latency I-like our EBV-positive clones were and so Qp-driven EBNA1 transcripts were expressed relative to Kem-BL; a stable uncloned Latency I Burkitt, whilst

Latency III-associated genes (EBNA2, BHRF1 and LMP1) were expressed relative to X50-7, an LCL.

EBERs are highly expressed in all BLs so they were also normalised to Kem-BL, but were not used to discriminate between Latency types. Whilst there was some variation in absolute expression levels between BL backgrounds and clones, the majority of EBV-positive clones derived from Latency I parental cell lines clearly expressed a Latency I genotype (Figure 3.3). The same was true of lytic transcripts; levels of BZLF1 in EBV-positive clones were compared to Kem-BL and 100% BZLF1-positive AKBM cells (Figure 3.4), showing that EBV-positive clones exhibited similar low levels of lytic activity to parental Latency I cells. Occasionally clones of Mutu-BL did drift to Latency III, as shown in Figure 3.3-D, and these clones were removed from further analysis. As might be expected, the change in gene expression was accompanied by a change in phenotype, with the cells becoming lymphoblast-like in their size, shape and adherence to one another, so these clones were easy to detect. EBV-loss clones were also assayed for the presence of viral transcripts, both immediately after isolation and consistently showed no evidence of viral gene expression.

Figure 3.3 Transcription of viral gene products in EBV-positive BL clones

All values were calculated using the $\Delta\Delta C_t$ method, normalised to the housekeeping gene GAPDH, and the expressed relative to either Kem-BL (EBER1, EBER2, EBNA1 (Qp-driven)) or X50-7 (EBNA2, BHRF1, LMP1). Using this system, a value of ~ 1 for **EBNA1** with very low or undetectable levels of **EBNA2**, **BHRF1** and **LMP1** would suggest the cells being analysed express a 'typical' Latency I gene expression pattern. **EBERs** are highly expressed in all BLs, but levels vary between cell lines so their expression is not an indicator of Latency type. All q-PCR assays were carried out in duplicate.

A EBV-positive clone of Akata-BL (Latency I)

B EBV-positive clone of Kem-BL (Latency I)

C EBV-positive clone of Mutu-BL (Latency I)

D EBV-positive clone of Mutu-BL that has drifted and is expressing the Latency III-associated genes, EBNA2, BHRF1 and LMP1

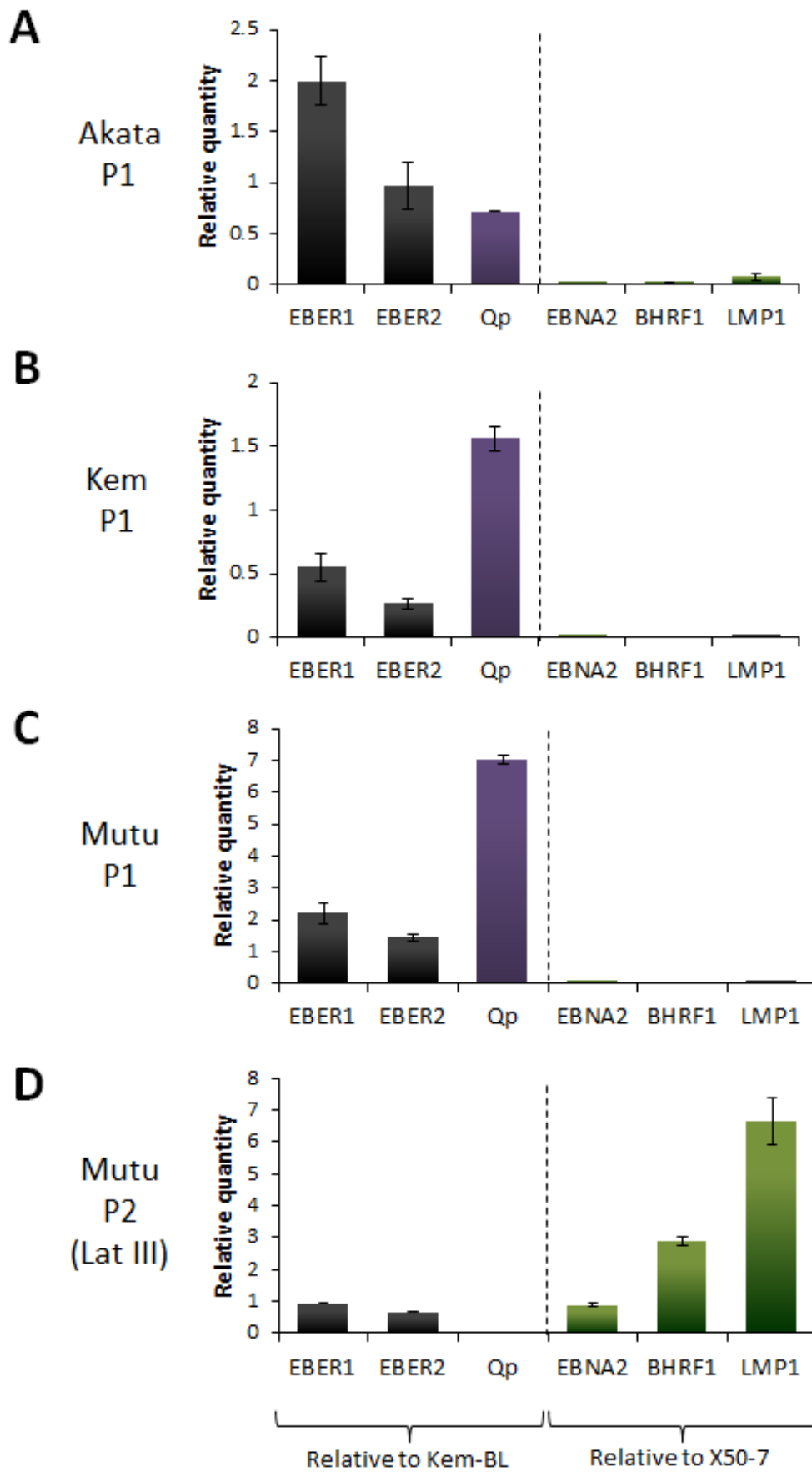


Figure 3.3

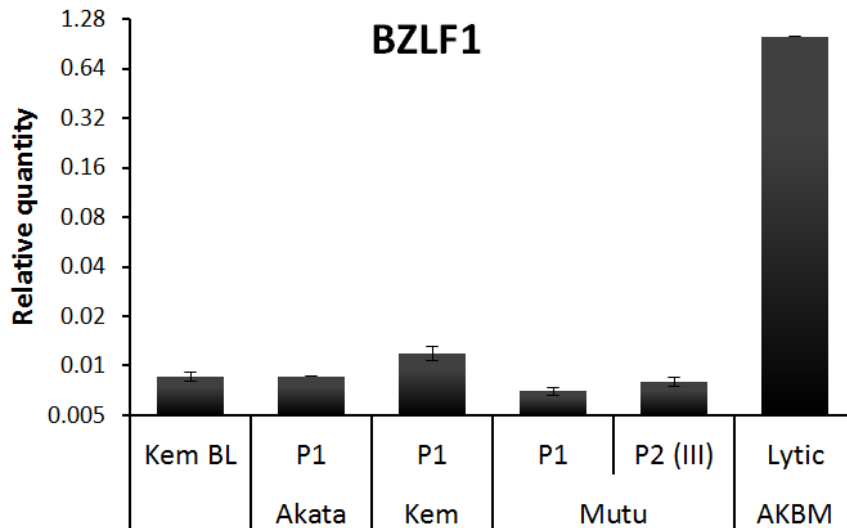


Figure 3.4 BZLF1 transcription in EBV-positive BL clones

Due to the magnitude of difference in BZLF1 expression between lytic and latent cells relative expression values are shown on a \log_2 scale relative to lytic AKBM cells that have been sorted for BZLF1 protein positivity and therefore are presumably 100% positive for BZLF1 transcript.

3.2.3 Viral protein expression in BL clones

Although q-PCR provides a quick, convenient and quantifiable method to determine the expression of a wide range of viral transcripts it can be difficult to interpret results where transcription of a gene is low but not absent, as the consequence of this for coding genes also depends upon how efficiently the message is translated and the half-life of the protein. Therefore we also characterised viral gene expression at the protein level in our EBV-positive clones. A Western blot of EBNA1 expression in EBV-positive and loss clones of 4 of the 5 BLs that yielded loss clones is shown in Figure 3.5-A, confirming that all cells found to be EBV negative by DNA q-PCR also contained no viral protein. To verify our q-PCR data we also blotted for EBNA2 and LMP1 proteins and found that both were undetectable in EBV-positive clones that exhibited a Latency I transcriptional profile. Example blots carried out on clones of Awia-BL are shown in Figure 3.5-B.

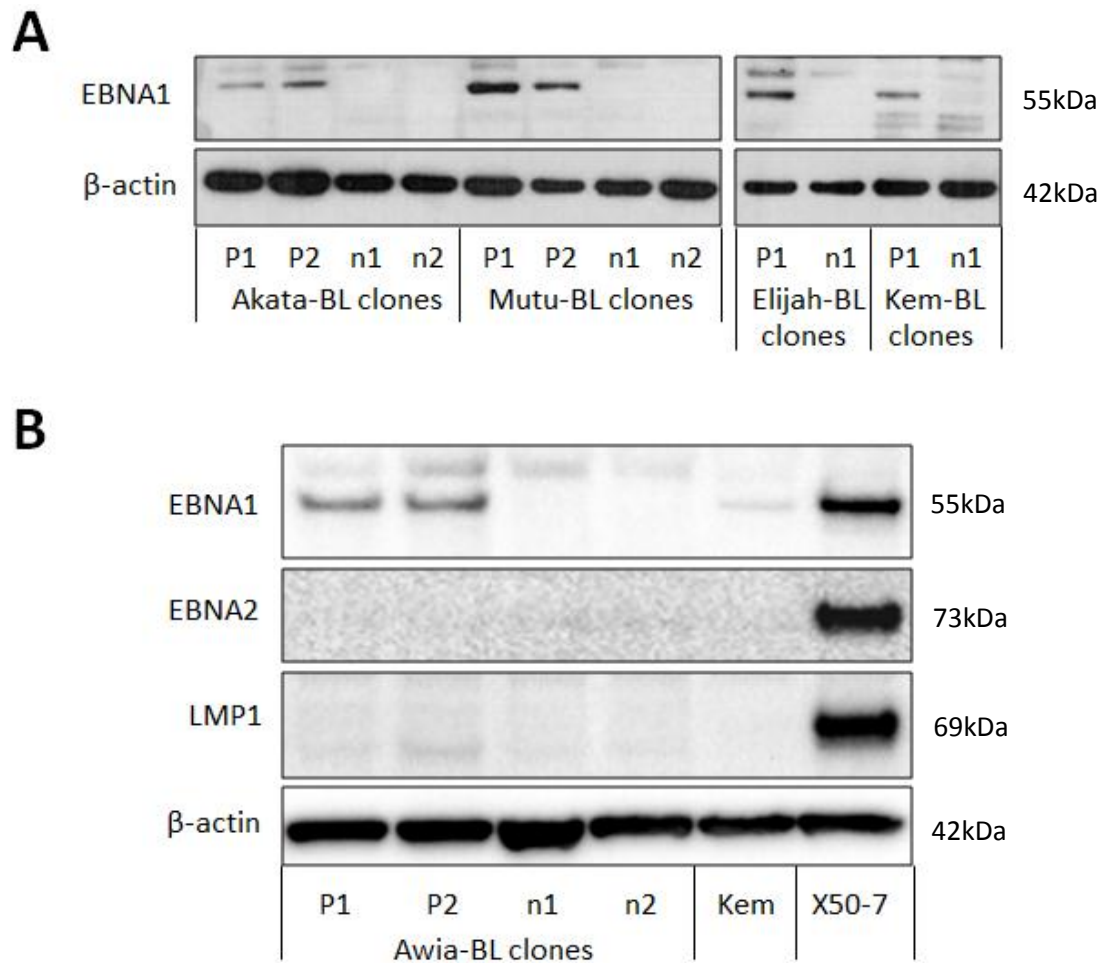


Figure 3.5 Viral protein expression in BL clones

A EBNA1 blot confirming EBV-positive clones (P1-P2) of Akata-BL, Mutu-BL, Elijah-BL and Kem-BL express the viral maintenance protein EBNA1, whilst loss clones (n1-n2) are EBNA1 negative. EBNA1 Western blots were carried out on all clones used in this study

B Western blot of EBV protein expression in clones of Awia-BL confirming that EBV-positive clones express a Latency I phenotype; i.e., EBNA1 in the absence of EBNA2 and LMP1

3.2.4 Viral RNA expression in single cells

As we were interested in whether there was a difference in apoptosis protection between EBV-positive and loss cells we needed to be certain that all of our EBV-positive cell lines contained virus in every cell and were not a mixture of EBV-positive and loss cells, as this may

mask any EBV-associated phenotype. Therefore, we carried out fluorescence *in situ* hybridisation (F-ISH) on our BL cell lines using an EBER-specific synthetic peptide nucleic acid (PNA) probe to check for EBER expression at the single cell level.

We found that EBV-positive clones of Akata-BL, Awia-BL, Elijah-BL, Kem-BL and Mutu-BL were >99% positive for EBER expression by FACS whilst EBV-loss clones were completely negative compared to cells that had never contained virus (Figure 3.6).

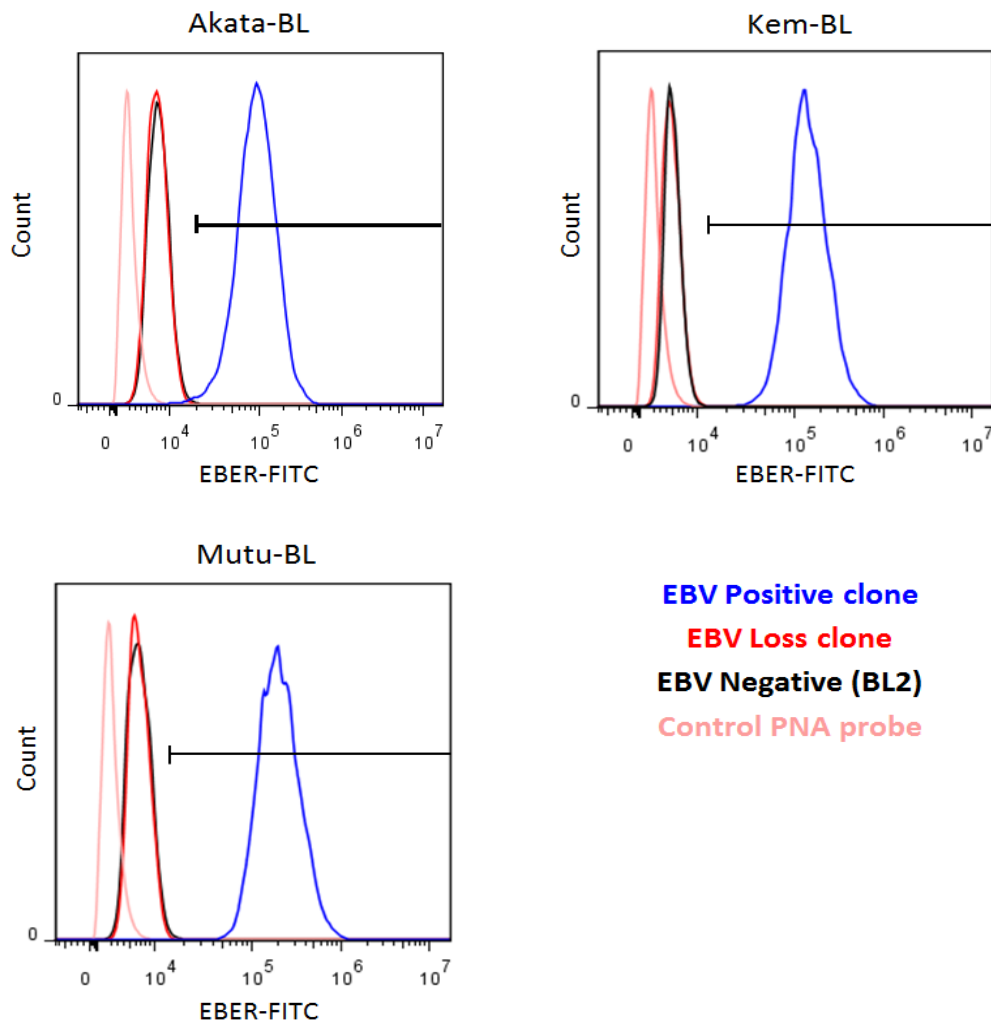


Figure 3.6 EBER FACS in BL clones

Examples of EBV-positive and loss clones of Akata-BL, Kem-BL and Mutu-BL stained with a FITC-conjugated EBER-PNA probe. BL cells that have never contained EBV (BL2 cell line) and EBV-positive cells stained with a negative control probe (control PNA probe) are shown as negative controls.

3.3 Investigating the response of BL clones to apoptosis inducers

3.3.1 Etoposide and α -IgM: DNA damage response versus BCR crosslinking

EBV has previously been shown to confer protection against α -IgM-induced apoptosis in Latency I clones of Awia-BL compared to EBV-loss clones [178] and so we wanted to investigate whether this finding held true for EBV-loss clones derived from other tumours. Since Akata-BL is surface IgM negative [130] we carried out apoptosis assays on α -IgM-treated clones of Kem-BL and Mutu-BL as well as Awia-BL (Figure 3.7-A). We found that EBV consistently provided protection to Latency I BL clones compared to their EBV-loss counterparts in all three tumour backgrounds. Although there was some variability between experiments, tumour backgrounds and clones in the precise amount of apoptosis induced, α -IgM was generally found to cause around twice as much cell death in EBV-loss clones versus EBV-positive clones.

Etoposide causes apoptosis by disrupting DNA replication leading to the accumulation of single and double strand breaks, leading to induction of the DNA-damage response [515]. It is also a commonly used chemotherapeutic agent which can be effective in treating non-Hodgkin's lymphomas [516]. Therefore we were interested to determine whether EBV can protect Latency I BL clones from Etoposide-induced apoptosis. In Akata-BL clones Etoposide induced a similar amount of cell killing in all clones tested, whereas the amount of cell death induced varied between clones of Kem-BL and Mutu-BL (Figure 3.7-B). In all cases there was no discernible protection conferred by the presence of the virus, and in fact, EBV-loss clones of Kem-BL were less susceptible to cell death than were their EBV-positive counterparts.

Crosslinking of surface IgM on resting B cells and lymphoma cell lines induces apoptosis via the hydrolysis of phosphoinositide and subsequent release of calcium from intracellular stores, leading to activation of Caspase-2 and -9, followed by the executioner protein Caspase-3 [517]. Anti-IgM treatment therefore induces apoptosis via the intrinsic apoptosis pathway.

Figure 3.7 Sensitivity of BL clones to α -IgM and Etoposide

A Example data of EBV-positive and loss clones of Awia-BL, Kem-BL and Mutu-BL treated with 10ng/ml α -IgM for 72 hours

B Example data of EBV-positive and loss clones of Awia-BL, Kem-BL and Mutu-BL treated with Etoposide at two concentrations (25 or 50nM, as indicated on the X-axis) for 24 hours.

Representative data from assays carried out in triplicate on three occasions. Appropriate drug doses were determined by titration of drugs onto cells which was carried out by Dr Gemma Kelly before this project was initiated [178] and unpublished data. Cell viability was determined by FACS staining for Annexin V-FITC and PI. Statistical comparisons were carried out using a Students T-test.

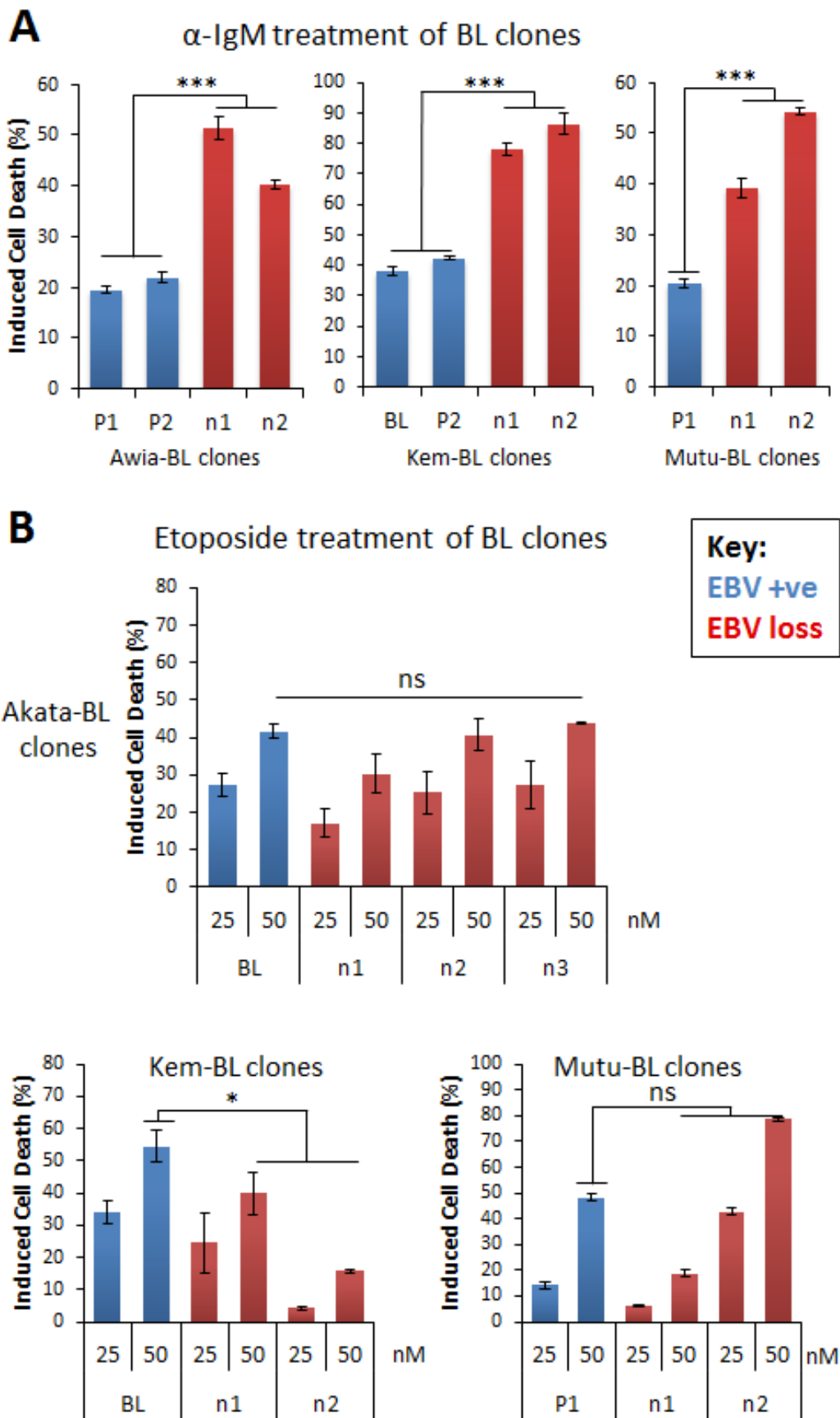


Figure 3.7

In contrast, Etoposide poisons the topoisomerase II enzyme, which can snip and unwind tangled DNA, causing a build-up of the enzyme on the DNA and an accumulation of strand breaks. When the cell then attempts to replicate and topoisomerase II is removed from DNA the genome is irreparably damaged and the cell dies via the DNA-damage response by induction of p53-signalling pathways [493, 518]. Given the difference in the mechanisms of action of these drugs and the knowledge that p53 function is abrogated in many BLs, including those included in this study [260], we hypothesised that EBV protects BL cells in a p53 independent manner via the intrinsic apoptosis pathway.

3.3.2 Ionomycin: a second calcium-dependent intrinsic apoptosis inducer

Like IgM crosslinking, ionomycin-treatment of BLs and other immature B-cell derived cell lines induces intracellular calcium release and activation of several caspases including Caspase-9 and -3 [519, 520]. Therefore we carried out experiments on ionomycin-treated, paired EBV-positive and loss BL clones to see whether EBV could confer protection to a death inducer that is functionally similar to IgM crosslinking.

We have also used ionomycin to induce apoptosis in previous studies where we examined the anti-apoptotic properties of BHRF1 in BL cells [178], which allowed us to infer the appropriate concentrations of drug to use. Our criteria were to use a dose at which the majority, but not all, of the EBV-loss cells underwent apoptosis in order to be able to clearly detect a difference between EBV-positive and loss cells.

In the four BL backgrounds tested in this study (Akata-BL, Kem-BL, Mutu-BL and Awia-BL) we found that ionomycin consistently induced significantly less cell death in EBV-positive clones compared to those that had lost the virus (Figure 3.8). Although we saw some variation, and the difference was less marked at higher drug concentrations, we found that levels of apoptosis in EBV-loss cells were generally more than double that seen in corresponding EBV-positive clones.

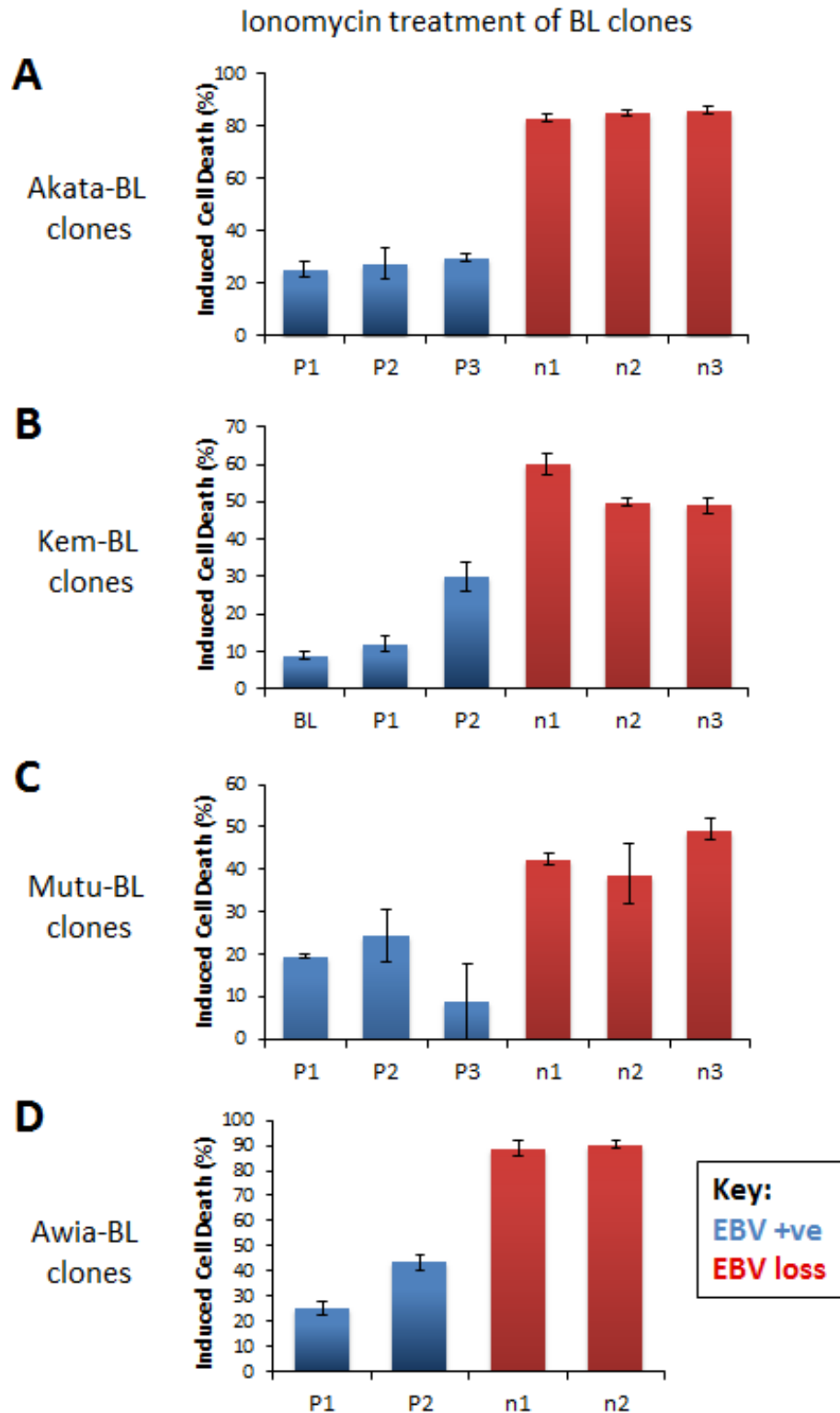


Figure 3.8 Sensitivity of BL clones to ionomycin

A Akata-BL clones + 1 μ g/ml ionomycin **B** Kem-BL clones + 1 μ g/ml ionomycin

C Mutu-BL clones + 2 μ g/ml ionomycin **D** Awia-BL clones + 0.75 μ g/ml ionomycin

All ionomycin treated cells were harvested for analysis 48 hours after assay set up

Representative data from assays carried out in triplicate on at least three occasions

3.3.3 Roscovitine and Staurosporine

Roscovitine is a cyclin dependent kinase (CDK) inhibitor which disrupts the progression of the cell cycle therefore inducing cell death. In a number of tumour cell lines this has been shown to occur via the intrinsic apoptosis pathway [521]. The exact mechanism(s) of Roscovitine-induced apoptosis are not yet clear, however it is clearly able to regulate the expression of a number of Bcl-2 family members [522, 523], and it has also been reported to directly inhibit EBNA-1 leading to EBV episome loss and apoptosis in BL cells [524]. We therefore compared the apoptosis phenotype of our BL clones after Roscovitine treatment and found that EBV-loss cells were consistently more susceptible to Roscovitine-induced apoptosis than were EBV-positive cells (Figure 3.9-A). Interestingly, the difference between positive and loss clones was less pronounced than the α -IgM or ionomycin-induced phenotype, an observation that was found to hold true at two different concentrations of Roscovitine (data not shown).

Staurosporine is a potent inhibitor of a wide variety of protein kinases and can induce apoptosis via both the extrinsic and intrinsic pathways [525]. Although the precise mechanism(s) of action are not yet clear Staurosporine has also been shown to regulate a number of Bcl-2 family members including Puma, Bcl-2, Bcl-XL and Noxa in a variety of cell types [445, 526, 527] including BLs [419]. Like Roscovitine, Staurosporine consistently induced more cell death in BL clones that had lost the virus than in EBV-positive cells, although again the phenotype was less pronounced than for α -IgM or ionomycin (Figure 3.9-B).

3.3.4 Cell death inhibitors

To further investigate our finding that Latency I EBV inhibits the intrinsic apoptosis pathway we compared the response of EBV-positive and loss clones to two different inhibitors of cell death after treatment with an apoptosis inducer. Ionomycin induced the greatest degree of cell death in EBV-loss clones compared to EBV-positive counterparts and so it was used to induce

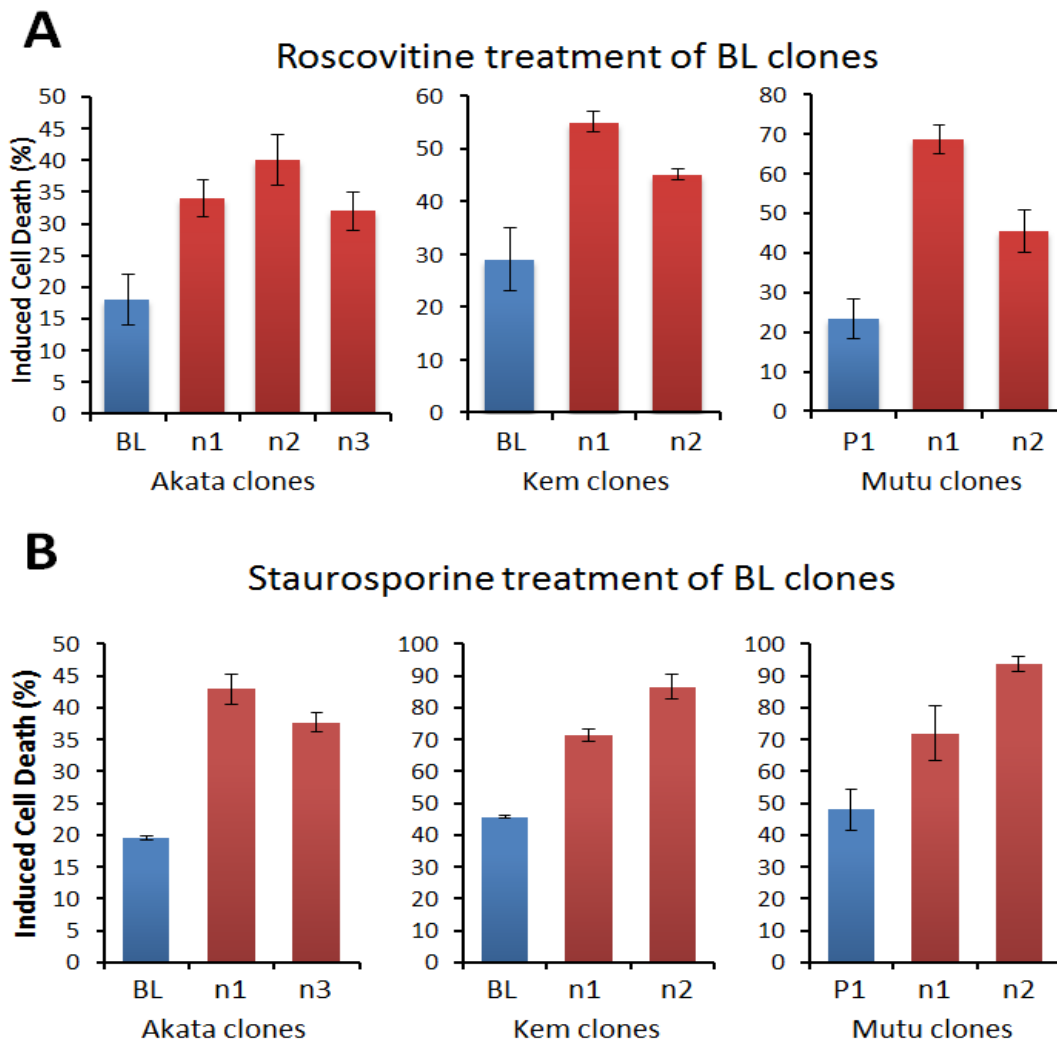


Figure 3.9 Sensitivity of BL clones to Roscovitine and Staurosporine

A Example data of BL clones treated with 50 μ M Roscovitine for 48 hours

B Example data of BL clones treated with 250nM Staurosporine for 24 hours

Representative data from assays carried out in triplicate on three occasions

cell death in these experiments. Q-VD.OPh is a broad-spectrum caspase inhibitor which can block the cleavage of executioner Caspases 3 and 7 as well as several of those upstream [528], whilst Necrostatin is an inhibitor of RIPK1 [529]. RIPK1 is a key signalling molecule that is able to initiate apoptosis as well as alternative forms of cell death including necrosis and necroptosis [530], which can also be induced by calcium activation of calpains [531, 532]. The drug concentrations used in these experiments were chosen from published work looking at

the effect of these inhibitors in Hodgkin and Burkitt lymphoma cell lines respectively [301, 533]. We found that whilst Q-VD.OPh was able to completely block ionomycin-induced cell death in Kem-BL clones Necrostatin had no discernable effect (Figure 3.10-A and 3.10-B), which supports our previous findings that BL cells are dying via caspase-mediated intrinsic apoptosis and allows us to rule out RIPK-1-dependent pathways to cell death as a target for EBV in BL cells. Consistent with our apoptosis data we were unable to detect cleavage of Caspase-3, -7 or -9 in cells treated with both Q-VD.OPh and ionomycin, whereas we did see cleavage of these proteins in cells treated with ionomycin only. Since we found no difference in the apoptosis phenotype of BL clones in the presence or absence of Necrostatin we did not confirm that RIPK1 was inhibited in these assays.

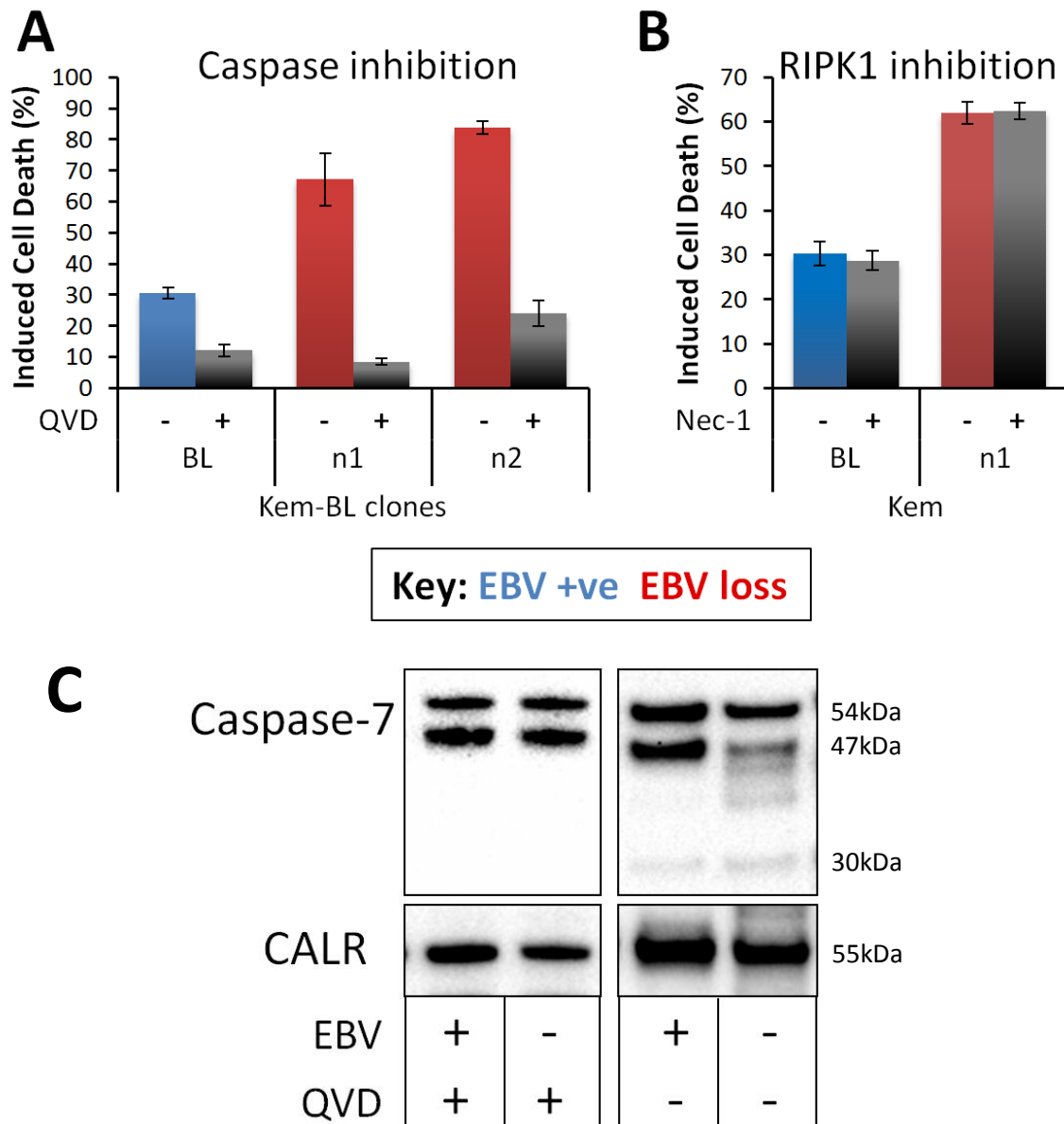


Figure 3.10 Ability of cell death inhibitors to block ionomycin-induced killing

A Example data of Kem-BL clones treated with 1 μ g/ml ionomycin and 25 μ M Q-VD-Oph for 48 hours

B Example data of Kem-BL clones treated with 1 μ g/ml ionomycin and 30 μ M Necrostatin-1 for 48 hours

C Caspase-7 expression and cleavage in Kem-BL clones, clones used were P1 and n1, all cells were treated with 1 μ g/ml Ionomycin in the presence or absence of Q-VD.OPh for 48 hours

Representative data from assays carried out in triplicate on three occasions. Drug concentrations used were chosen from published work [301, 509]

Inhibitor-only and ionomycin-only controls were also included to check for activity of ionomycin and toxicity of inhibitors.

3.3.5 ABT-737

Although our drug sensitivity assays implicate the cellular Bcl-2 family of proteins as likely targets for EBV in BL they do not provide direct evidence that this is the case. ABT-737 is a cell permeable BH3 domain mimic designed to selectively bind and inhibit anti-apoptotic Bcl-2 family members Bcl-2, Bcl-XL and Bcl-w, but not Mcl-1 and A1 [534, 535]. We therefore hypothesised that, if EBV is able to change the dependency of BL cells on any or all of the pro-survivals bound by ABT-737, then EBV-loss cells will exhibit enhanced sensitivity to ABT-737 over their counterpart EBV-positive clones.

We carried out titrations of ABT-737 onto clones of Akata-BL, Kem-BL and Mutu-BL and found that Latency I clones were relatively insensitive to ABT-737, possibly because BLs do not express Bcl-2. Interestingly, there was a difference between EBV-positive and EBV-loss clones and the 50% lethal dose was consistently higher for cells that contained the virus compared to EBV-loss clones (Figure 3.11). The variation between tumour backgrounds and clones from the same background suggests that the precise balance of pro- versus anti-apoptotic proteins may be heterogeneous at the single cell level in BL.

ABT-737 treatment of BL clones

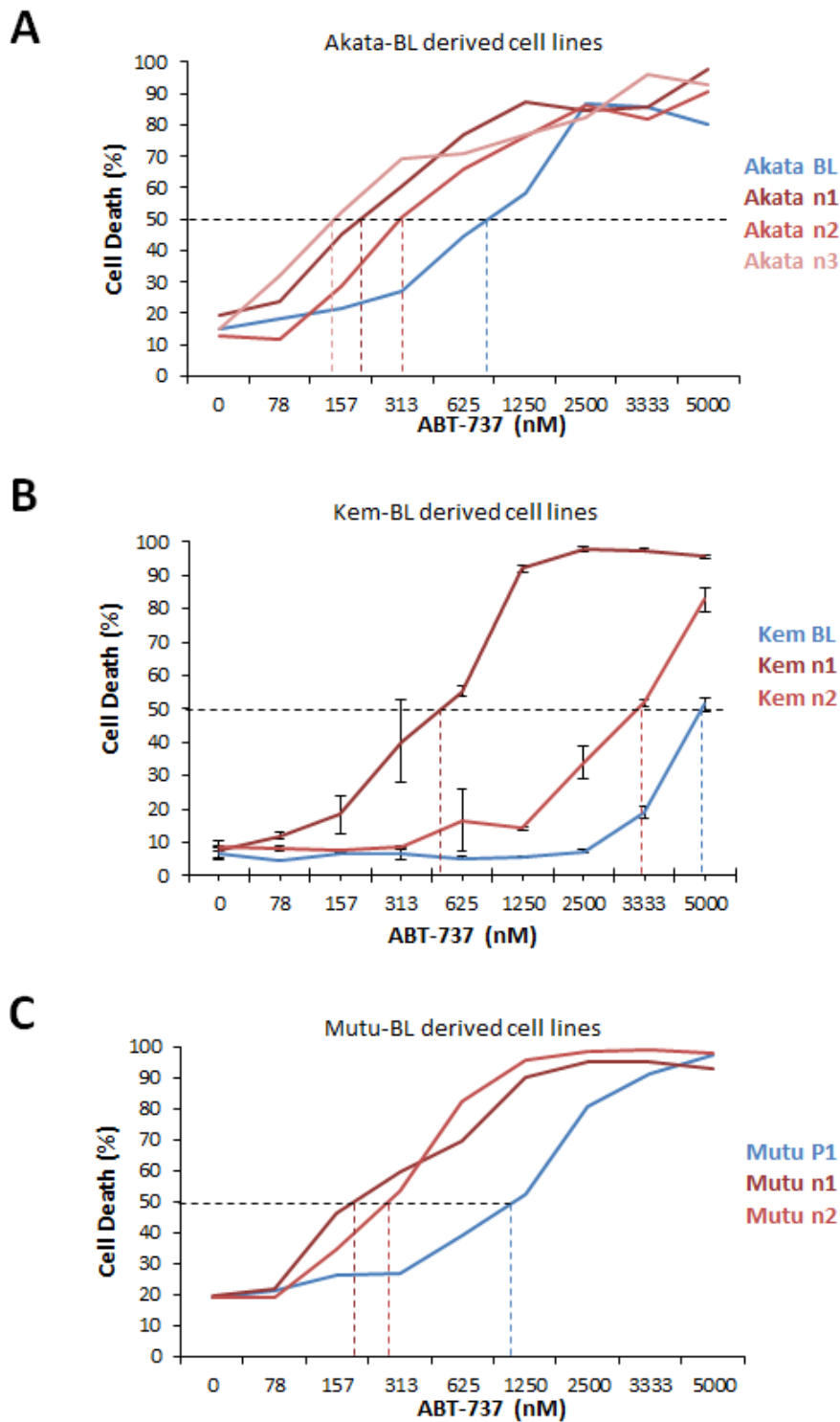


Figure 3.11 Sensitivity of BL clones to ABT-737

A Clones of Akata-BL exposed to serial dilutions of ABT-737 for 24 hours **B** Clones of Kem-BL exposed to serial dilutions of ABT-737 for 24 hours **C** Clones of Mutu-BL exposed to serial dilutions of ABT-737 for 24 hours. Representative data from three independent experiments

3.4 Screening for cellular genes involved in the EBV-loss phenotype

3.4.1 Microarrays

After isolating a small number of EBV-loss clones from several BL tumour backgrounds, Dr Gemma Kelly and Dr Andrew Boyce went on to carry out microarray experiments on two EBV-positive and two EBV-loss clones from each of three tumour backgrounds. Surprisingly, they found that there were no gene expression changes in common between the different backgrounds by rank product analysis (Figure 3.12-A), suggesting that different genes may be important in different patient backgrounds or that the mechanism by which EBV enhances cell survival is not transcriptionally controlled. Unfortunately, since we had expected to find consistent differences, the experiment only included 2 EBV-positive and 2 EBV-loss clones per tumour background. This meant that we were unable to look in more detail at gene expression changes that might be important in individual backgrounds as we would require at least three replicates in order to carry out appropriate statistical analyses.

3.4.2 Protein expression studies

Although some members of the intrinsic apoptosis signalling pathway are transcriptionally regulated, a number of apoptosis related genes are predominantly regulated at the post-transcriptional level [536]. Therefore, we were also interested in looking at apoptosis-related gene expression in EBV-positive and loss cells at the protein level. As part of a previous study we carried out Western blots for selected regulators of apoptosis on EBV-positive and loss cells but were unable to find any consistent differences and so in this study we decided to carry out a more unbiased screen.

Whole cell lysates of BL clones were separated by SDS-PAGE and then stained with Coomassie dye to visualise the total protein in each clone and screen for differences in banding between EBV-positive and EBV-loss cells. Any bands that were found to be considerably different

between clones containing or having lost the virus could then be excised and proteins contained therein could be identified using mass spectrometry.

Unfortunately, we saw no clear differences between EBV-positive and loss clones in any tumour background (Figure 3.12-B). Although, it is important to note this approach would not identify proteins that had modifications that effect function but have little effect on protein expression level or size and that some highly expressed proteins will mask the expression of other proteins of a similar molecular weight.

3.4.3 *MYC*

We also considered that a very small change in expression of a large number of genes could be responsible for the EBV-loss phenotype. Recently it was reported that, rather than regulating a subset of genes by activation or repression, *MYC* is actually a global enhancer of Pol II transcription [251]. We therefore wondered whether *c-myc* levels remain constant between EBV-positive and loss cells; a change that was small in amplitude yet affecting many genes may explain why we saw no obvious differences in overall protein or transcription levels. In clones of Akata-BL, Mutu-BL and Elijah-BL there was no evidence of a difference in *MYC* transcription between EBV-positive and loss clones (Figure 3.12-C). Awia-BL EBV-loss clones were found to express slightly higher levels of *MYC* than did their EBV-positive counterparts, which could presumably lead to increased apoptosis sensitivity in these cells. However, if this difference in *MYC* expression were a direct consequence of EBV-loss we would expect to see it in every cell background which exhibits the EBV-loss phenotype.

Overall these experiments to characterise differences in gene expression between EBV-positive and loss clones did not explain the EBV-loss phenotype or directly indicate any cellular targets of EBV in BL, although we have good evidence that the Bcl-2 family play an important role, either directly or indirectly. There are several possible reasons for this; the pivotal player(s) may be regulated by subtle change in expression level, a post-translational

Figure 3.12 Screening BL clones for gene expression changes associated with EBV-loss

A Summary of data from Affymetrix U133 plus 2.0 microarrays carried out by Dr Andrew Boyce. Data were subjected to rank product analysis using Affymetrix GeneChip Operating Software (GCOS). Fold change cut off was $FC > 1.5$ and the false positive probability threshold was set to 10%. Two EBV-positive and two EBV-loss clones were included for each of the three BL backgrounds included in this analysis (12 clones in total).

B Coomassie staining of whole cell lysates from BL clones separated by SDS-PAGE. Clones of Akata-BL, Mutu-BL and Awia-BL used match those included in the microarray experiments. 20 μ g of total protein was loaded per well.

C Transcription of *MYC* in BL clones determined by q-PCR using the $\Delta\Delta C_t$ relative quantitation method and expressed relative to Akata-BL clone P1. Data shown represent the mean and standard deviation of duplicate wells. GAPDH was used as an endogenous control for normalisation between wells

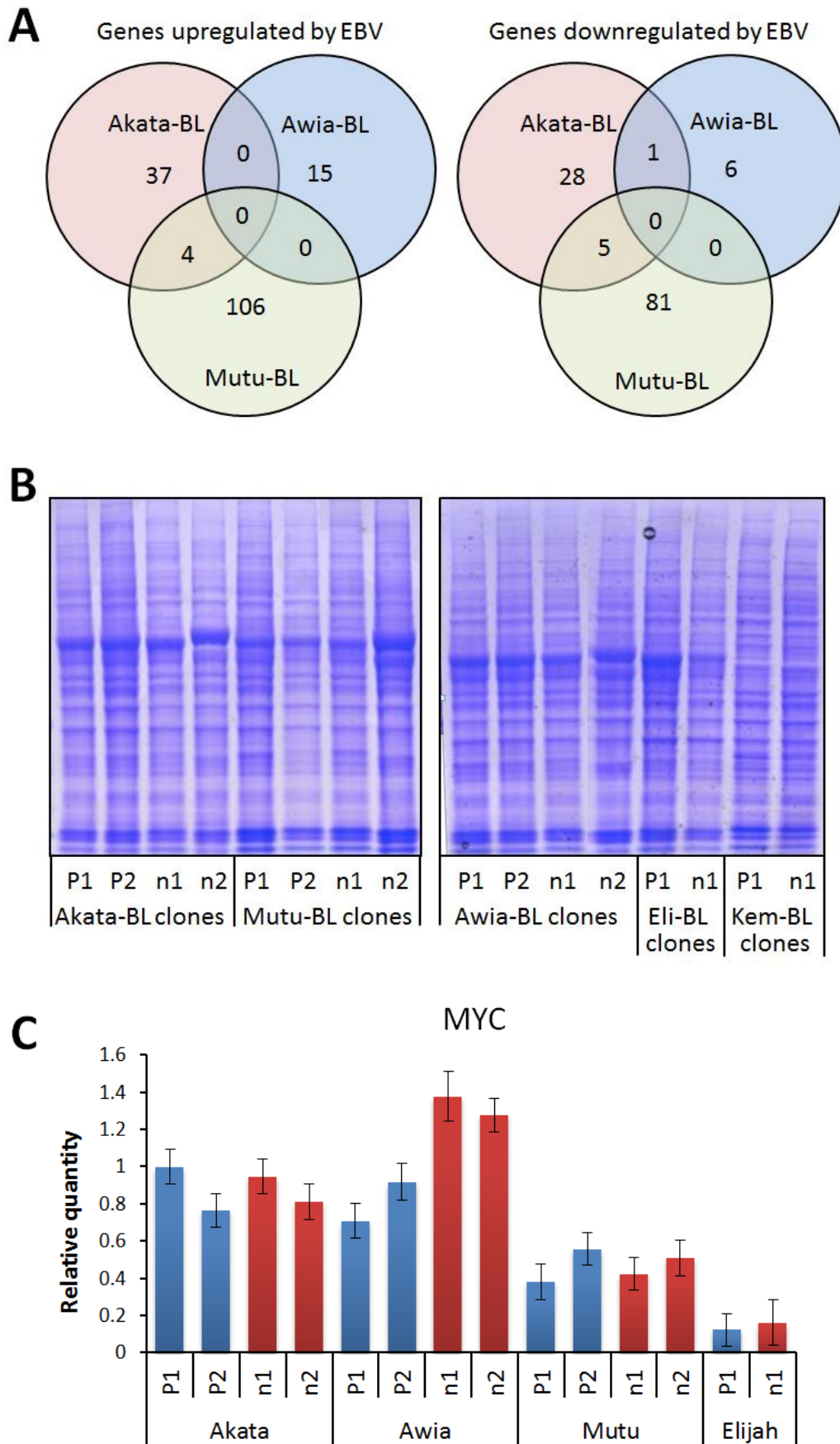


Figure 3.12

modification or a protein-protein interaction, which would not be identified by previous Western blotting, Coomassie staining of lysates or microarrays.

It is also possible that we failed to see consistent differences because the study was carried out on unchallenged cells rather than after apoptosis induction when the EBV-loss phenotype becomes evident. Therefore we sought to take our studies further by investigating the factors affecting EBV-loss and characterising the effect of EBV-loss on BL cells *in vivo* to enable us to better understand the apoptosis sensitivity of EBV-loss clones.

3.5 Investigating the effect of pro-survival signals on EBV-loss

3.5.1 Mechanism of EBV-loss

Although it is clear from the literature that EBV episomes are tethered to the cellular DNA by EBNA1 and segregated into daughter cells in a synchronous, largely symmetrical and non-random manner [295, 296, 537], it is also clear from our work and that of several other groups that EBV-positive cell lines can give rise to spontaneous EBV-loss clones, albeit rarely [178, 309, 538]. Sudgen et al. showed that in an LCL, which relies on EBV for proliferation as well as survival signals, EBV is faithfully maintained at a copy number that is apparently optimal for growth [295]. However, other studies looking at genome segregation have used small *oriP* plasmids in EBV negative cells [312, 318], which may behave differently to wild type virus in cells derived from an EBV-positive tumour. Interestingly, a number of the papers which support faithful partitioning of viral genomes also report instances in which they observed uneven segregation [295, 296].

We therefore wondered whether survival signals within the cell are able to determine how faithfully the genome is passed to daughter cells: is retention of EBV only selected for where the virus provides a survival advantage, and conversely, if the cells obtain a survival advantage

by some other means will that alleviate the need to retain the virus? The EBV-encoded Bcl-2 homologue, BHRF1, is able to robustly inhibit cell death in BL cells induced by various drugs [89, 419, 539] via binding to pro-apoptotic Bcl-2 family proteins [304, 305, 411]. Therefore, to test whether providing BHRF1 in *trans* would relieve the selection pressure for EBV in BLs, we generated EBV-positive Akata-BL and Kem-BL cell lines in which we were able to inducibly express BHRF1 prior to single cell cloning.

3.5.2 Expressing BHRF1 in Latency I BLs

We transduced the parental BL cell lines, Akata-BL and Kem-BL, that are >99% EBV positive by EBER-ISH, with the FTrex-BHRF1-UTG lentivirus, which contains inducible BHRF1 and a constitutive GFP marker (described in Section 2.6.6). Stable, GFP-positive cell lines were then generated by cell sorting. For each tumour background the highest 5% GFP expressers were selected and we also generated matched lines stably transduced with an empty vector control (Figure 3.13-A). Interestingly, the intensity of GFP is far higher in Akata-BL than in Kem-BL. Since the cells were transduced with the same batch of virus under the same conditions, this suggests that Akata-BL is able to take up and integrate lentivirus more efficiently than Kem-BL. When we looked at levels of BHRF1 expression from our construct we found good correlation between GFP and BHRF1; Kem-BL expressed far lower levels than Akata-BL, which expressed similar levels to a Wp-restricted BL and the X50-7 LCL. The highest levels were seen in the highly transducible 293 cells which also expressed very intense GFP (Figure 3.13-B, 3.13- C and data not shown). Unfortunately, we also noted from these experiments that our vector was not as tightly regulated as we had hoped, and we detected 'leaky' expression in uninduced cells at around 10% of the level seen in the doxycycline-treated cells by Western blot. We presume this leaky expression reflects incomplete silencing of the Trex PolIII promoter by the tet repressor leading to low level expression of BHRF1 in all cells. Although since we did not carry out single cell analysis for BHRF1 by FACS we cannot rule out that this result instead reflects a small proportion of cells expressing high levels of BHRF1.

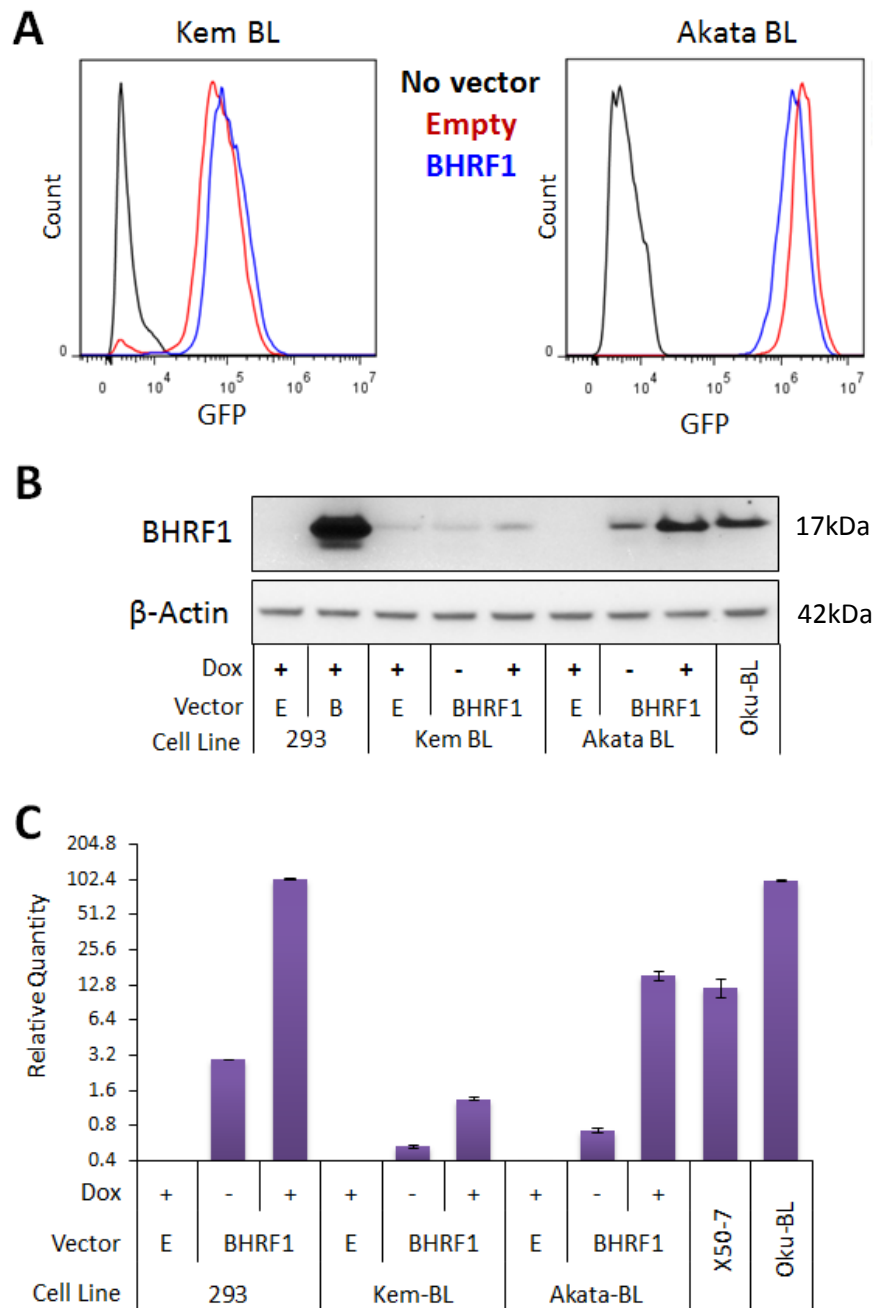


Figure 3.13 Expression of BHRF1 in Latency I BLs

A GFP expression in transduced Kem-BL and Akata-BL cells

B Western blot for BHRF1 in transduced cells. The faint band seen in the Kem-BL + Empty vector lane is probably due to spill-over from the 293 + BHRF1 lane as this sample has been shown to be negative for BHRF1 by Western blot and PCR

C Transcription of BHRF1 in transduced cell lines. Note that due to the range in expression levels between low and high expressers a \log_2 scale has been used. Values shown are the mean and standard deviation of duplicate wells. Data was analysed using the $\Delta\Delta C_t$ relative quantitation method relative to Oku-BL and normalised to GAPDH.

E = empty vector control, B= FTrex-BHRF1-UTG

3.5.3 Single cell cloning of BHRF1-expressing BLs

Since BHRF1 has been shown to strongly inhibit apoptosis even when expressed at low levels [89, 539], we went on to look at whether this Bcl-2 homologue could have any effect on the outgrowth of single cell BL clones. Cells were grown in media supplemented with acyclovir to inhibit lytic viral replication and 1 μ g/ml doxycycline or DMSO as a vehicle-only control for 3 weeks (9 passages) prior to cloning and were then plated out at 1 cell per well into 96-well plates. Interestingly, during the early stages of the experiment, the plates containing BHRF1-expressing cells appeared to expand more quickly than the empty vector cells however, after three weeks, when cells were harvested, the number of outgrowing clones had become similar for each experimental group. The average viral load of each clone was enumerated by q-PCR and then the data for all conditions were compared. Wells in which no virus was detected were classified as EBV-loss clones, and the remaining clones were designated as having a high or low viral load if they were found to contain more than twice the number of genomes as the parental cells, or less than 10 genomes per cell, respectively. An example of average viral loads of BL clones across a single 96-well plate is shown in Figure 3.14.

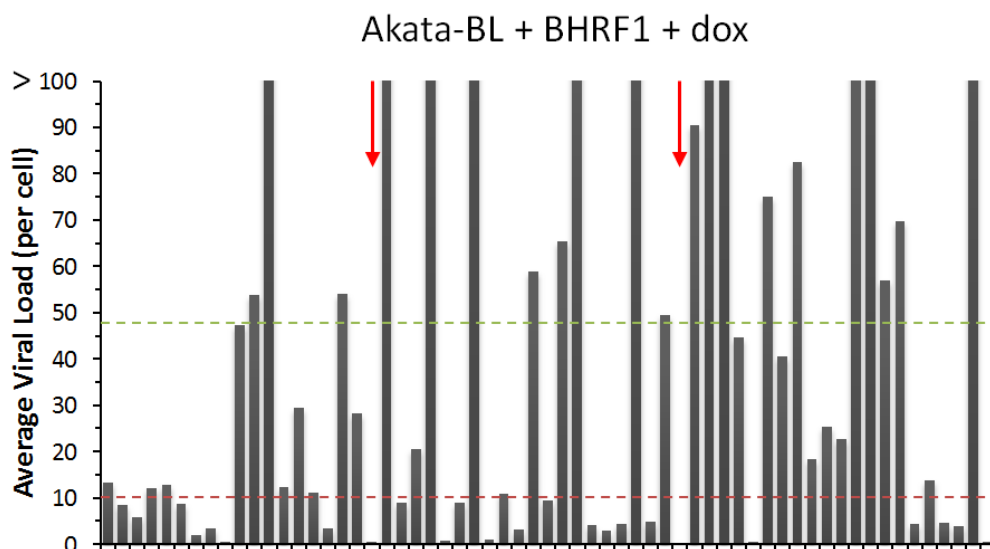


Figure 3.14 Average viral loads in clones of BHRF1-expressing Akata-BL cells

Average copy number of BALF5 DNA normalised to β 2M (see Section 2.3.2)

--- = 10; --- - viral load of parental BL; \rightarrow - EBV-loss (no EBV DNA)

The compiled data from our BHRF1 cloning experiments is presented in Table 3.2. Overall, the range and mean of viral loads detected was quite similar to that reported for the initial cloning experiments of the parental cell lines (see Table 3.1), although there did seem to be a slight tendency for BHRF1 expressing cells to have a higher viral load. In BHRF1-expressing Akata-BL, we noted that more clones had viral loads that were classified as very high or very low and that the frequency of EBV loss also increased slightly however, the numbers of clones analysed were insufficient to draw firm conclusions. Importantly, in Akata-BL, even the highest rate of genome loss was lower than in our initial cloning experiments and Kem-BL never gave rise to EBV-loss clones, even in the presence of BHRF1. Therefore, although the presence of a strong anti-apoptotic signal may slightly increase uneven genome segregation, its presence does not cause EBV to be lost from cells within the time frame of this experiment.

Vector	Dox	N°	Range	Mean	High Load (%)	Low Load (%)	EBV Loss (%)
Kem-BL derived clones							
Empty	+	130	4-371	44.3	26 (20%)	15 (12%)	0 (0%)
BHRF1	-	138	2-407	45.5	19 (14%)	12 (9%)	0 (0%)
	+	146	3-427	50.2	27 (18%)	19 (13%)	0 (0%)
Akata-BL derived clones							
Empty	+	103	0-320	48	18 (17%)	19 (18%)	2 (1.9%)
BHRF1	-	99	0-362	58	30 (30%)	18 (18%)	2 (2.0%)
	+	80	0-360	62	20 (25%)	24 (30%)	3 (3.8%)

Table 3.2 Compiled data from BHRF1 single cell cloning experiments

Viral loads calculated using DNA q-PCR for EBV BALF5 and β 2M as described in Section 2.3.2

High viral load = >2x average viral load of parental (untransduced) cell line

Low viral load = <10 genomes per cell

3.5.4 Apoptosis phenotype of BHRF1-expressing BL clones

To confirm that BHRF1 was able to confer protection to Latency I BL cells, and to investigate whether the varying levels of expression in different cell lines affected apoptosis sensitivity, we carried out apoptosis assays on our stable cell lines that were used for single cell cloning experiments. All cell lines were induced with doxycycline for 48 hours prior to assay set up and assays were then carried out as described in Section 2.2.3. In both Akata-BL and Kem-BL it was clear that BHRF1 protects against ionomycin-induced apoptosis and the degree of protection correlates with the amount of BHRF1 in the cells (Figure 3.15). BHRF1-expressing Akata-BL was substantially protected from ionomycin-induced apoptosis, and uninduced cells were only slightly more sensitive to cell death induction than cells induced by Doxycycline treatment, supporting the notion that BHRF1 acts as a potent pro-survival signal even when present at a very low level compared to a Wp-BLs or LCLs. In Kem-BL the BHRF1 phenotype was less marked, in-keeping with the lower expression levels we observed in this cell line. However,

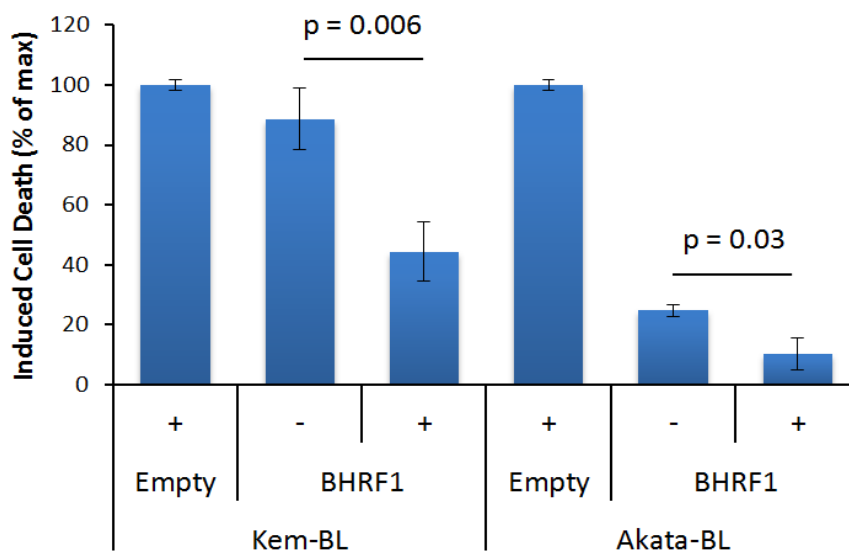


Figure 3.15 Survival of BHRF1-expressing Latency I BL cells versus control cell lines

All cells were treated with 1µg/ml ionomycin (+) or a vehicle-only control (-) for 48 hours, mean and SD of triplicate measurements are shown. Assays were carried out on three occasions. Statistical comparisons were made using a two-tailed Student's T-test.

DOX-induced BHRF1-expressing Kem cells were still substantially protected from ionomycin induced apoptosis, although in this case uninduced cells were not significantly protected when compared to an empty vector control.

3.6 Investigating the tumorigenicity of BL clones *in vivo*

3.6.1 Design of *in vivo* studies

The Takada group, which originally reported the spontaneous loss of EBV, also reported that the loss of EBV from Akata-BL rendered the cells non-tumorigenic in nude mice [309], a finding that was later supported by more detailed studies using SCID mice [310, 327]. Therefore, we were interested as to whether this held true for EBV-loss clones derived from other tumour backgrounds. Although both nude and SCID mice lack functional B and T cells and are thus severely immunodeficient, they also retain some mature lymphocytes, such as NK cells, which can cause xenotransplanted cells to be rejected. The NOD/SCID/IL2 γ KO, or NSG mouse is the current breed of choice for xenotransplantation studies as it harbours a knock out of the IL2 receptor common gamma chain in addition to the NOD/SCID mutations. This results in failure to produce several interleukins which are required for the proper functioning of NK cells, dendritic cells and macrophages. Therefore the functional immune repertoire of NSG mice is restricted to neutrophils and monocytes; B and T cells are absent and NK cells are crippled, whilst dendritic cells and macrophages are partially functional [507].

Although other groups had injected BL cells subcutaneously (SC) into the flanks of mice we primarily chose to inject cells into the peritoneum (IP) to allow the tumour cells to diffuse and circulate within the animal. We also injected fewer cells (up to 2×10^6 IP) into our mice than the Sample and Takada groups (10^7) on the advice of our colleagues at the WEHI, who routinely transplant lymphoid cells into NSG mice and because we felt that this would better reflect the

conditions of our *in vitro* experiments. Figure 3.16 shows a diagram of the set-up for our experiments using clones of Kem-BL and Mutu-BL.

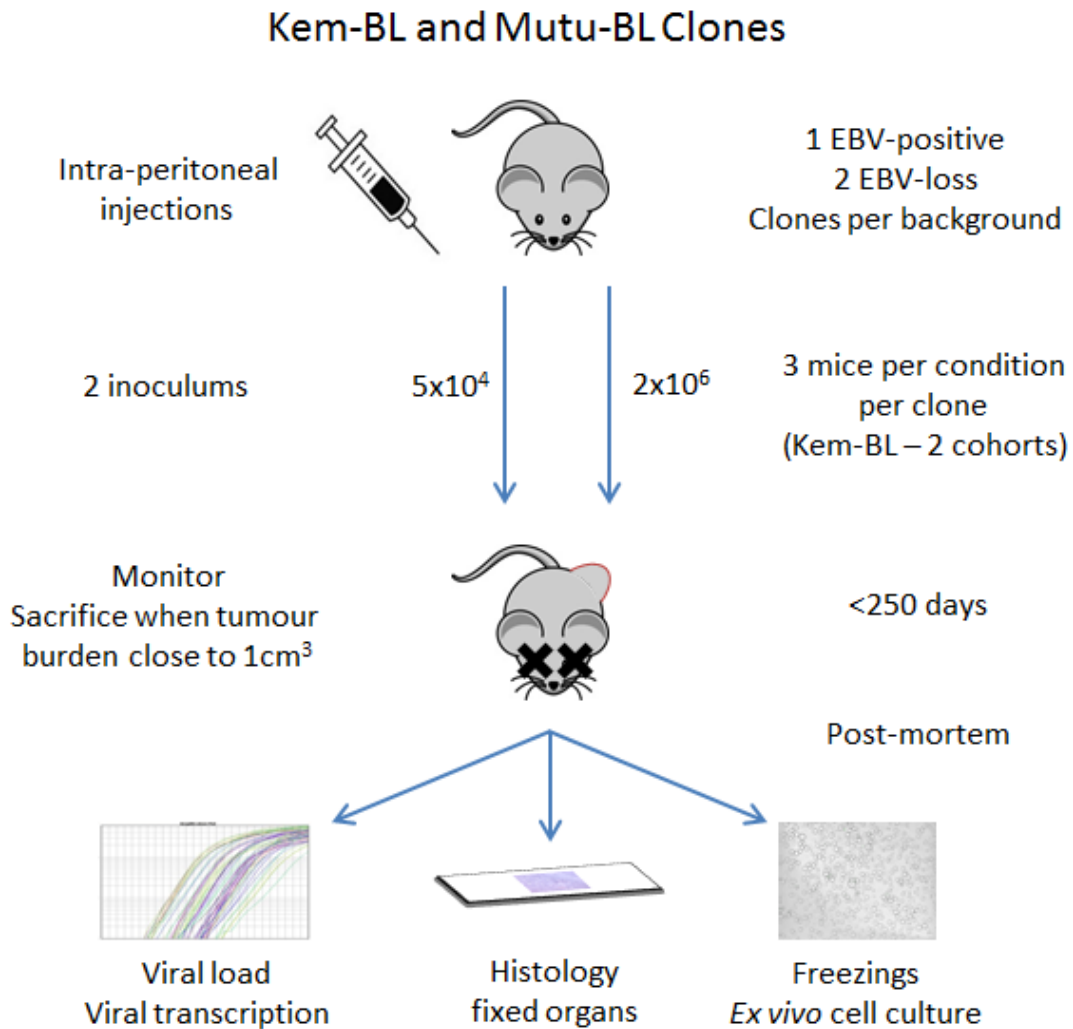


Figure 3.16 Experimental workflow of *in vivo* experiments using EBV-positive and loss clones of Kem-BL and Mutu-BL

Clones of Kem-BL and Mutu-BL were injected IP at two inoculums. For each cell line one positive and two loss clones were included. Mice were monitored for signs of tumour growth and sacrificed when tumour burden reached approximately 1 cm^3 , in accordance with the Walter and Eliza Hall Institute Animal Ethics Committee guidelines.

3.7 Features of BL xenograft tumours in NSG Mice

3.7.1 Sites of tumour formation

Consistent with human BL, clones of Kem-BL and Mutu-BL gave rise to tumours at various sites, including the ovaries, pancreas, spleen and mammary tissue. However, we never saw ocular, maxillofacial or gastrointestinal tumours, which are also commonly affected sites in human endemic BL [540]. An example of a typical mouse with ovarian, pancreatic and mammary tumours is shown in Figure 3.17-A. Like the human form of BL, we also found that the thymus in BL xenotransplant mice was never affected, and lymph nodes were only involved in 2 cases where the tumour was attached to the mesenteric nodes. Table 3.3 summarises all of the tumours and the incidence with which each site was affected. The growth of BL xenotransplant tumours was also aggressive in NSG mice and the first mouse was sacrificed only 33 days after injection, in-keeping with the rapid growth of BL tumours in human patients and with BL cell line proliferation *in vitro* [541].

3.7.2 Histology – H&E stains

Tumour tissue, major body cavity organs, and sections of sternum and spine from every mouse were fixed and embedded in paraffin for histology. Examples of H&E stained slides of various tumours are shown in Figure 3.17-B. Histological examination revealed that the tumours were largely homogeneous and displayed ‘starry sky’ patterning, the histological hallmark of BL. This is clearly visible in the ovarian, pancreatic and splenic sections in Figure 3.17-B. The tumours also destroyed the natural architecture of the organs and infiltrated into the bone marrow. Analysis of H&E stained sections was carried out by Dr Brandon Aubrey in Melbourne.

We also carried out staining for the proliferation marker Ki67 on sections of ovarian tumours from mice injected with different BL clones to see whether there were any differences between tumours from EBV-positive and loss clones. In every case at least 95% of the cells

stained positive, in line with human BL, and no differences were evident between EBV-positive and EBV-loss tumours, suggesting that these cell lines proliferate similarly *in vivo*.

Kem-BL derived clones					
Site Clone	Ovaries	Pancreas	Spleen	Mammary	Other
BL	75% (9/12)	100% (12/12)	75% (9/12)	17% (2/12)	5x SMFP
n1	83% (10/12)	83% (10/12)	8% (1/12)	17% (2/12)	1x SMFP 1x Fallopian
n2	100% (12/12)	100% (12/12)	50% (6/12)	8% (1/12)	3x SMFP 3x Liver
Total	86% (31/36)	94% (34/36)	44% (16/36)	14% (5/36)	
Mutu-BL derived clones					
Site Clone	Ovaries	Pancreas	Spleen	Mammary	Other
P1	80% (4/5)	100% (5/5)	80% (4/5)	(0/5)	1x Ascites 1x LN
n1	100% (5/5)	80% (4/5)	80% (4/5)	(0/5)	1x Liver 1x Fallopian
n2	100% (6/6)	67% (4/6)	50% (3/6)	17% (1/6)	1x Fallopian 1x LN
Total	94% (15/16)	81% (13/16)	69% (11/16)	6% (1/16)	

Table 3.3 Summary of sites of BL xenograft tumour formation in NSG mice

For each clone the frequency with which tumours occurred at each site is listed both as a percentage (i.e. where 4 of a group of 5 animals that all received cells of the same BL clone developed ovarian tumours the frequency of ovarian tumours in this group is listed as 80%) and as the absolute number of animals in the group. Totals are the total frequency and number of animals which had tumours at each site for each tumour background (data for all three clones pooled).

LN – Lymph node involvement, SMFP – swollen mammary fat pad

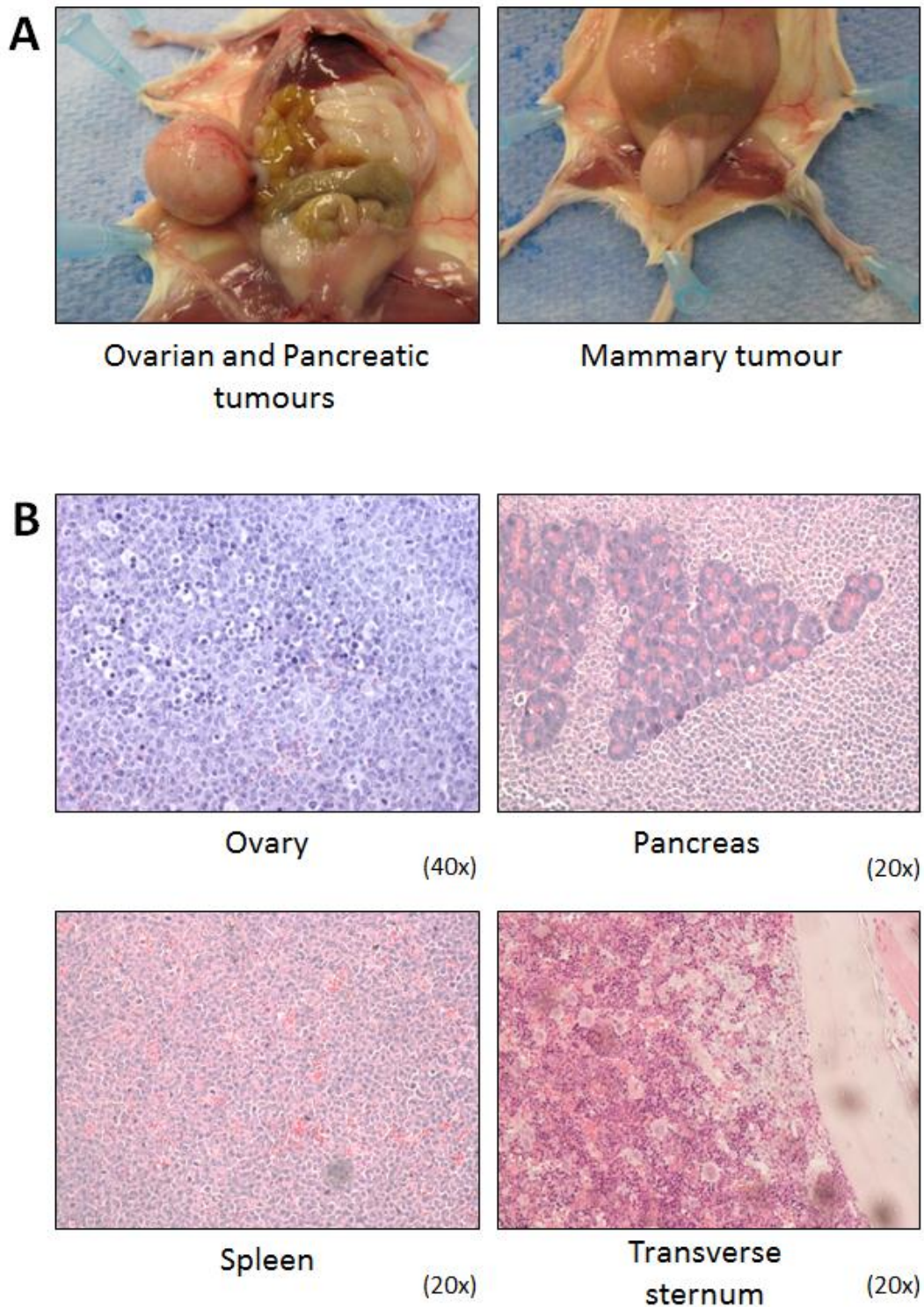


Figure 3.17 Appearance of BL xenograft tumours in NSG mice

A Example of pancreatic, ovarian and mammary tumours in a single mouse showing starry-sky patterning and destruction of normal tissue

B Examples of H&E stained organs from BL xenotransplant mice showing starry-sky patterning, destruction of normal tissue, extra-medullary haemopoiesis (Spleen) and infiltration into bone marrow (Sternum)

3.7.3 Human CD19 FACS

Although the histology and appearance of the tumours was consistent with human BL we wanted to confirm that the tumour cells were of human origin, so we carried out FACS staining for human CD19 on *ex vivo* cells. Tumour samples were passed through a cell strainer before staining and lymphoma cells from an E μ -Myc mouse were included as a negative control whilst EBV-positive Mutu-BL cells that had not been passaged *in vivo* served as a positive control. Figure 3.18 shows staining of controls as well cells of an ovarian tumour from a mouse that was injected with an EBV-positive Mutu-BL clone. We also stained cells from mice injected with EBV-loss clones of Mutu as well as EBV-positive and loss clones of Kem and we included both ovarian and splenic tumours in our analysis. In line with the results shown, we found that virtually all of the *ex vivo* tumour cells were positive for human CD19. This finding is consistent with human BL where there is very little infiltration of non-tumour cells [107].

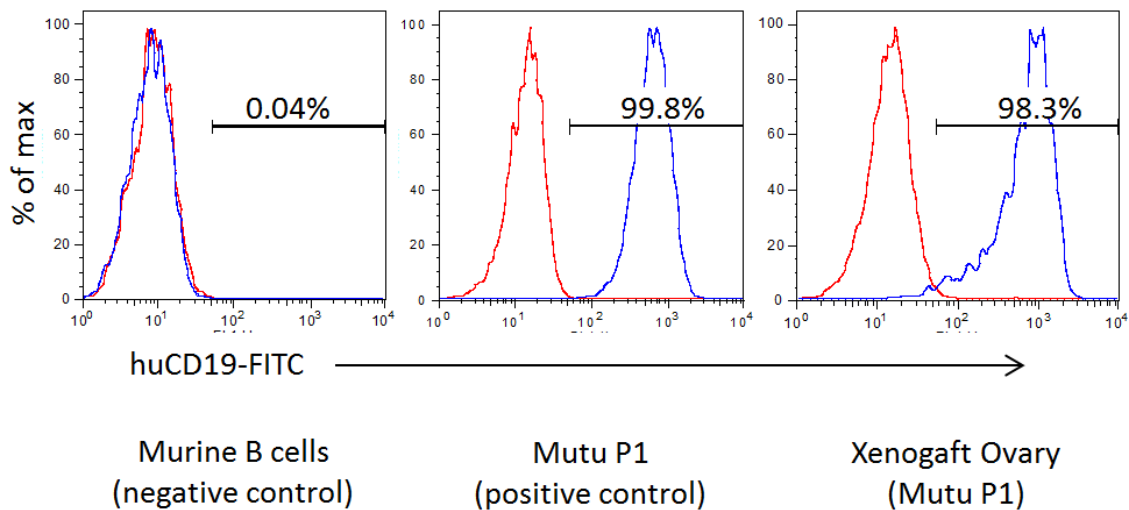


Figure 3.18 Example of CD19 FACS staining of *ex vivo* xenograft cells compared to controls. In each case unstained control cells are shown in red and the experimental sample listed below each panel is shown in blue.

3.8 Survival of BL xenotransplant mice

To determine whether the presence of EBV affects the growth and progression of BL xenograft tumours *in vivo* we plotted the survival data for our two cohorts of Kem-BL injected mice and the single cohort of Mutu-BL injected mice using Kaplan-Meier plots and compared the survival of mice injected with different BL clones by conducting Logrank tests. Figure 3.19-A shows the compiled data for both cohorts of Kem-BL injected mice and Figure 3.19-B shows the data for Mutu-BL injected mice. EBV-loss clones of Kem-BL were significantly less tumorigenic in NSG mice than were EBV-positive cells; mice that received Kem-BL derived EBV-loss cells survived twice as long on average, than those that received EBV-positive cells. Two mice that received Kem n1 cells survived past 250 days, the endpoint of the experiment. Although the effect was less dramatic in mice injected with Mutu n2 than Mutu n1 we still found that EBV-loss clones of Mutu-BL were significantly less tumorigenic than was an EBV-positive clone from the same tumour. Overall, mice injected with EBV-loss clones of Mutu-BL survived at least twice as long as those injected with an EBV-positive counterpart. In this analysis, data for the two inoculums used are pooled however, we found that mice injected with fifty-thousand cells survived only slightly longer than those injected with two million cells (data not shown).

This *in vivo* study is the first to compare the overall survival of mice injected with EBV- positive and loss clones on clones derived from two endemic BL patients and we have found convincing evidence for a role for the virus in an animal model.

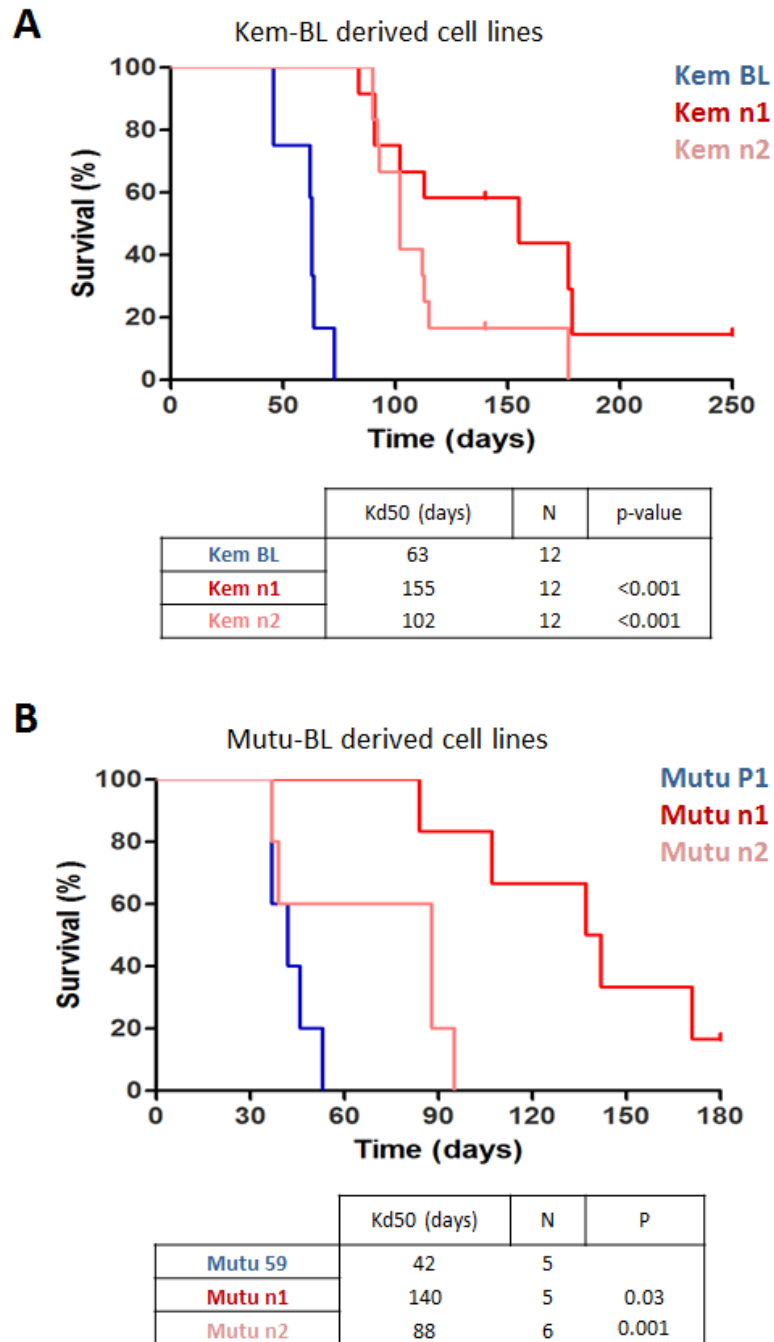


Figure 3.19 Survival analysis of NSG mice injected with BL clones

A Pooled data from two cohorts of mice which were injected with EBV positive Kem-BL cells or one of two EBV-loss clones, Kem n1 and Kem n2

B Data from a single cohort of mice which were injected with an EBV positive Mutu-BL clone, P1, or one of two EBV-loss clones, Mutu n1 and Mutu n2

In each cohort, 3 mice per clone were injected with 5×10^4 cells, and 3 mice per clone received 2×10^6 cells. Kaplan-Meier curves were generated using GraphPad Prism 5 software. From these survival curves median survival (Kd) was calculated and statistical comparisons were carried out. Curves were considered statistically different where the p-value was calculated to be <0.05 using a Log-rank (Mantel-Cox) test.

3.9 Analysis of EBV in xenotransplants

To confirm that EBV retained the Latency I gene expression profile *in vivo* we profiled viral transcription in a range of EBV-positive BL xenotransplant tumour tissue samples derived from both Kem-BL and Mutu-BL. Transcriptional profiling was carried out using microfluidic cards to perform 48 simultaneous q-PCR assays for 45 EBV-encoded genes as well as three cellular controls on RNA extracted from *ex vivo* cells. Data were analysed using the $\Delta\Delta\text{Ct}$ method, normalised to GAPDH, and expressed relative to a standard cell line, as described in Section 3.2.2. Examples of the gene expression profiles we generated are shown in Figure 3.20. Of the sample we tested, the majority had Latency I-like gene expression profiles similar to that of xenografts 65 and 77. However, one Mutu-BL derived tumour; xenograft number 54, expressed high levels of Latency III transcripts and so was excluded from the study. We also checked that viral DNA was retained *in vivo* at a similar viral load to that of the matched EBV-positive clone before transplantation (data not shown).

3.10 Akata-BL xenotransplants

All of the xenotransplant data in this thesis pertains to mice injected with clones of Kem-BL and Mutu-BL because, to our surprise, our clones of Akata-BL appear to be non-tumorigenic in NSG mice. The animals that were injected intraperitoneally were monitored for over 180 days before they were taken ill with an unrelated bacterial infection of the lungs. After this we tried injecting mice with a higher number of cells under the skin of the abdomen to more closely recapitulate previously published studies. Again we found that all of the animals were tumour-free at six months and so were discarded. Since previous reports state that EBV-loss clones caused no tumours in nude and SCID mice and only EBV-positive cells were able to cause tumours we would not have expected to detect tumours in animals injected with EBV-loss

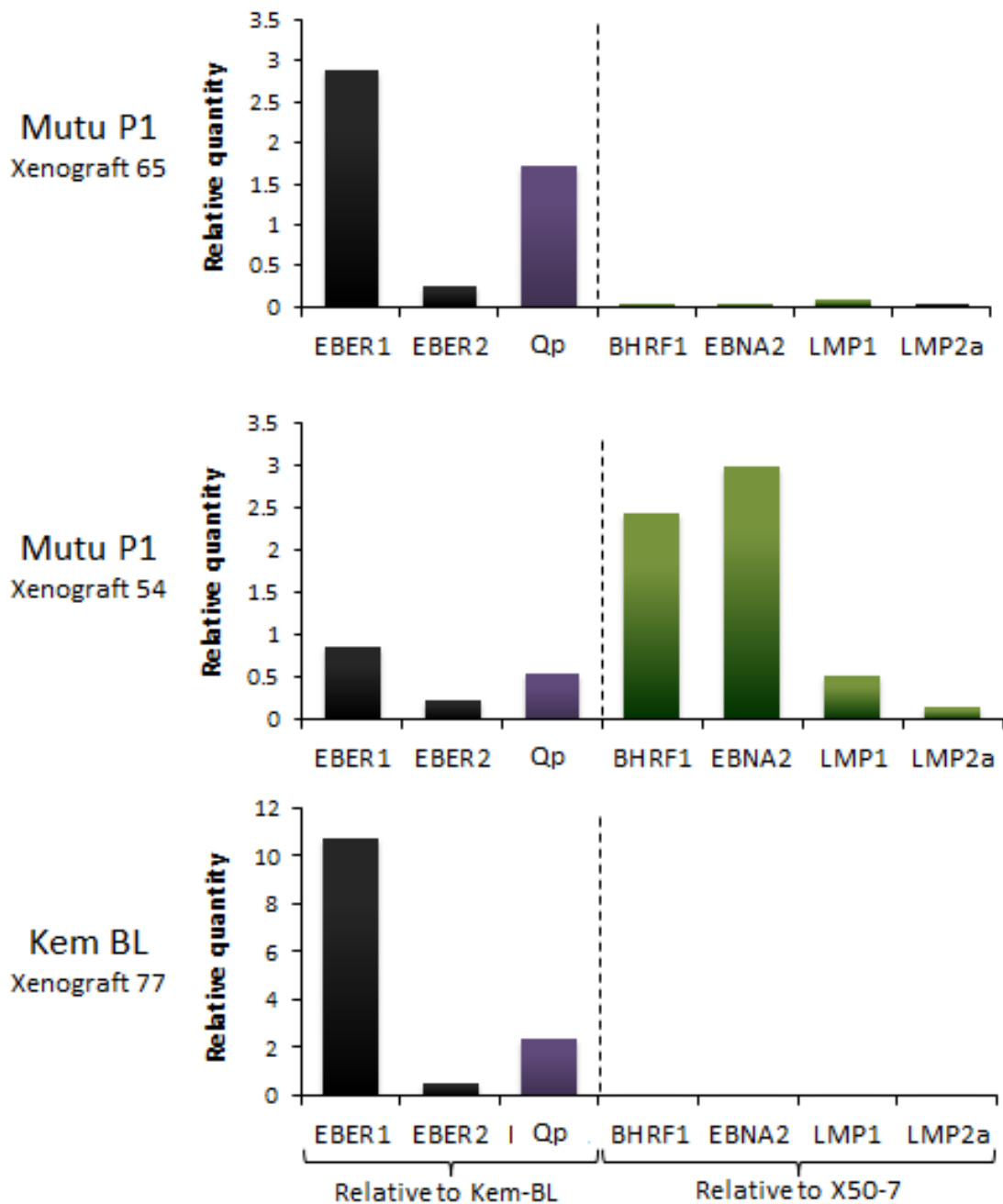


Figure 3.20 Quantitative PCR on xenotransplanted BL cells *ex vivo*

Example data gene expression profiling of *ex vivo* tumour cells from xenotransplanted NSG mice. Xenografts 65 and 77 express Latency I-associated transcripts EBNA1 and EBERs, whilst Latency III-associated BHRF1, EBNA2 and LMPs are almost undetectable. Xenograft 54 expresses BHRF1, EBNA2 and LMPs in addition to EBNA1 and EBERs, consistent with a Latency III gene expression programme.

EBNA1 refers to spliced transcript originating from the Qp promoter that is only found in Latency I cells

clones, but we are still not able to understand why EBV-positive Akata-BL cells caused no tumours. However, it is interesting to note there are indications in the literature of there being significant phenotypic variability between clones of Akata-BL in other respects. For example; the efficiency of lytic cycle induction upon α -IgG treatment can vary from as little as 5% up to 75%, depending on the particular batch of Akata-BL cells used [126, 542].

Conclusions I

Our large-scale single cell cloning of 12 well-characterised endemic BL cell lines is the most comprehensive study of spontaneous EBV-loss to date. We have confirmed both the rare occurrence of such loss, which indicates that the presence of the virus is highly selected for, and the consistently detrimental phenotype that EBV-loss confers, in agreement with the published findings of several groups [99, 178, 182, 298, 309, 310]. Whilst EBV-loss clones appear to be unhindered in their ability to survive under optimal culture conditions, they are significantly more sensitive to a range of apoptosis inducers compared to their EBV-positive Latency I counterparts. This is the first study to carry out a detailed analysis of multiple clones derived from a range of classical Latency I BLs. Consistent with the finding that p53 signalling is frequently abrogated in BL [260], we find that EBV-loss sensitises BL clones to agents that induce cell death in a p53-independent manner via the intrinsic apoptosis signalling pathway. Interestingly, the EBV-loss phenotype did not correlate with any consistent difference in transcription, global protein expression, or c-myc status in comparisons of healthy EBV-positive and loss clones.

Additionally, the viral Bcl-2 homologue, BHRF1, strongly inhibits intrinsic apoptosis in BL cells [89, 178], yet its ectopic expression does not lead to an increase in the rate of EBV-loss over a number of passages. This suggests that EBV-loss is truly a rare occurrence, rather than a frequent occurrence that is rarely detected because EBV-loss clones are unable to survive the

process of single cell cloning. These experiments also imply that, whilst the segregation of EBV genomes to daughter cells is uneven [295], EBV is extremely efficient at ensuring that multiple copies of the virus are inherited by each cell during mitosis.

We have also expanded on the very limited studies of the effect of EBV-loss from BL cells *in vivo*; confirming that the presence of EBV is associated with enhanced tumorigenicity and reduced survival in NSG mice injected with clones of Kem-BL and Mutu-BL. These new experiments clearly demonstrate that EBV is able to make an ongoing contribution to the aggressive phenotype of BL. Surprisingly, although we confirmed that EBV-loss clones of Akata-BL are non-tumorigenic in immunocompromised mice, we were also unable to engraft EBV-positive Akata-BL cells in contrast to the findings of the Takada and Sample groups [309, 310, 327, 339, 340]. Although we noted that, in experiments carried out by the Takada group, mice were injected with pools of six different EBV-positive clones and that one of four mice included in one study and one of seven in a second study, failed to develop tumours [310, 339]. We have since found that NSG mice injected with very early passage Akata-BL cells can develop tumours, although these experiments are ongoing and we have not examined these mice in detail unlike those injected with clones of Kem-BL and Mutu-BL, and therefore those results are not included in this thesis.

We conclude that EBV contributes to the pathogenesis of BL by inhibiting intrinsic apoptosis, thereby allowing c-myc to drive the aggressive growth of the tumour despite also activating pro-apoptotic signalling pathways. We therefore went on to investigate the precise mechanism by which EBV confers this phenotype by examining the anti-apoptotic potential of the Latency I-associated viral genes; EBNA1, the non-coding EBER RNAs and the BART microRNAs.

4. Results Part II

INVESTIGATING THE ROLE OF LATENCY I

EBV-ENCODED GENES IN APOPTOSIS

4.1 Outline of Latency I gene re-expression studies

Having confirmed and built upon previous studies to show that loss of EBV from BL cell lines is rare and consistently detrimental to their survival, we went on to consider the possible role of each of the viral genes that are normally expressed within EBV-positive BLs. At least 85% of all BLs occurring in endemic areas are thought to express the Latency I pattern of gene expression in which only the EBNA1 protein, the EBER RNAs and the BART miRNAs are consistently expressed [156, 505]. In our next set of experiments we therefore re-expressed each in turn to test whether individual Latency I genes can restore apoptosis resistance to EBV-loss clones.

To achieve this we used a lentiviral expression system, originally developed by Marco Herold, which can be used to express both coding and non-coding transcripts [483]. This allowed us to study gene expression in difficult to transfect cells and to select and enrich for transduced cells by FACS since these vectors constitutively express GFP. Additionally, once selected, the cell lines remain stable in long term culture as the lentiviral provirus particles integrate into the genome of the target cell [543].

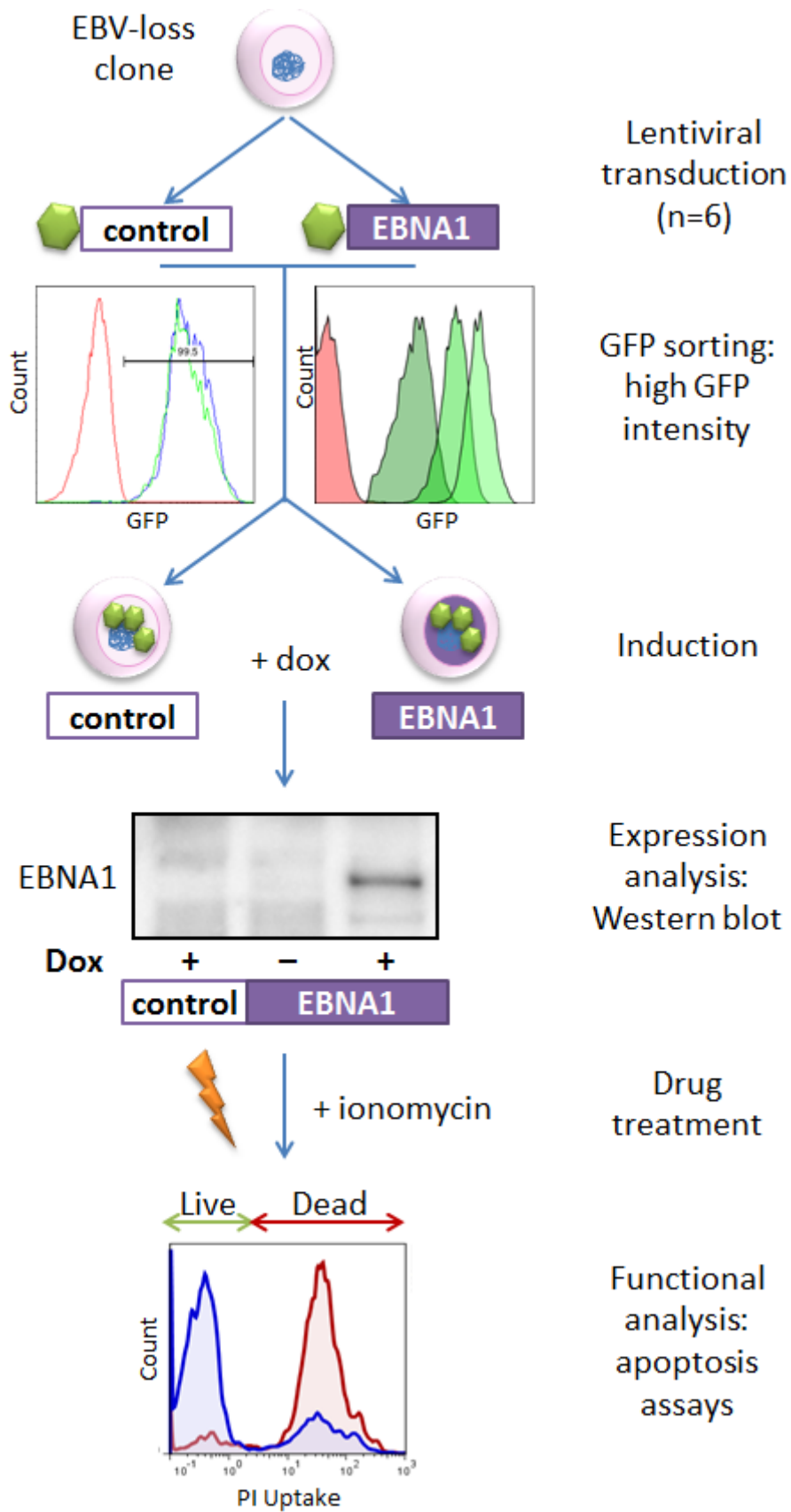


Figure 4.1 Workflow for EBNA1 re-expression experiments.

4.2 EBNA1

4.2.1 Expressing EBNA1 in EBV-loss BL clones

EBNA1 is the only EBV-encoded protein expressed in all EBV-associated malignancies and has previously been reported to have anti-apoptotic properties [298, 320]; therefore we wanted to determine whether EBNA1 contributes to the EBV-loss phenotype.

We used the FTrex-UTG lentivirus containing a full length EBNA1 sequence (fully described in Section 2.6.2) to inducibly express EBNA1 in 6 EBV-loss clones derived from 3 patient backgrounds; a workflow for these experiments is shown in Figure 4.1. Once stable cell lines had been generated, EBNA1 protein expression was measured by Western blot compared to EBV-positive cell lines. We did not examine the dose responsiveness of these vectors to doxycycline as we and others have previously found that they are maximally induced even in the presence of low doses (1-10ng/ml) of doxycycline [164, 483], although we did investigate whether extending induction times might cause EBNA1 to accumulate in EBV-loss cells.

After sorting cells for high GFP expression we found that we were consistently able to achieve comparable levels to those seen in in the respective EBV-positive parental BL lines after 24 hours of induction. There was no increase in levels of EBNA1 protein in cells that had been induced for 14 days; in fact found there appeared to be less EBNA1 in Kem-BL cells that had been induced for longer (Figure 4.2-A & 4.2-B).

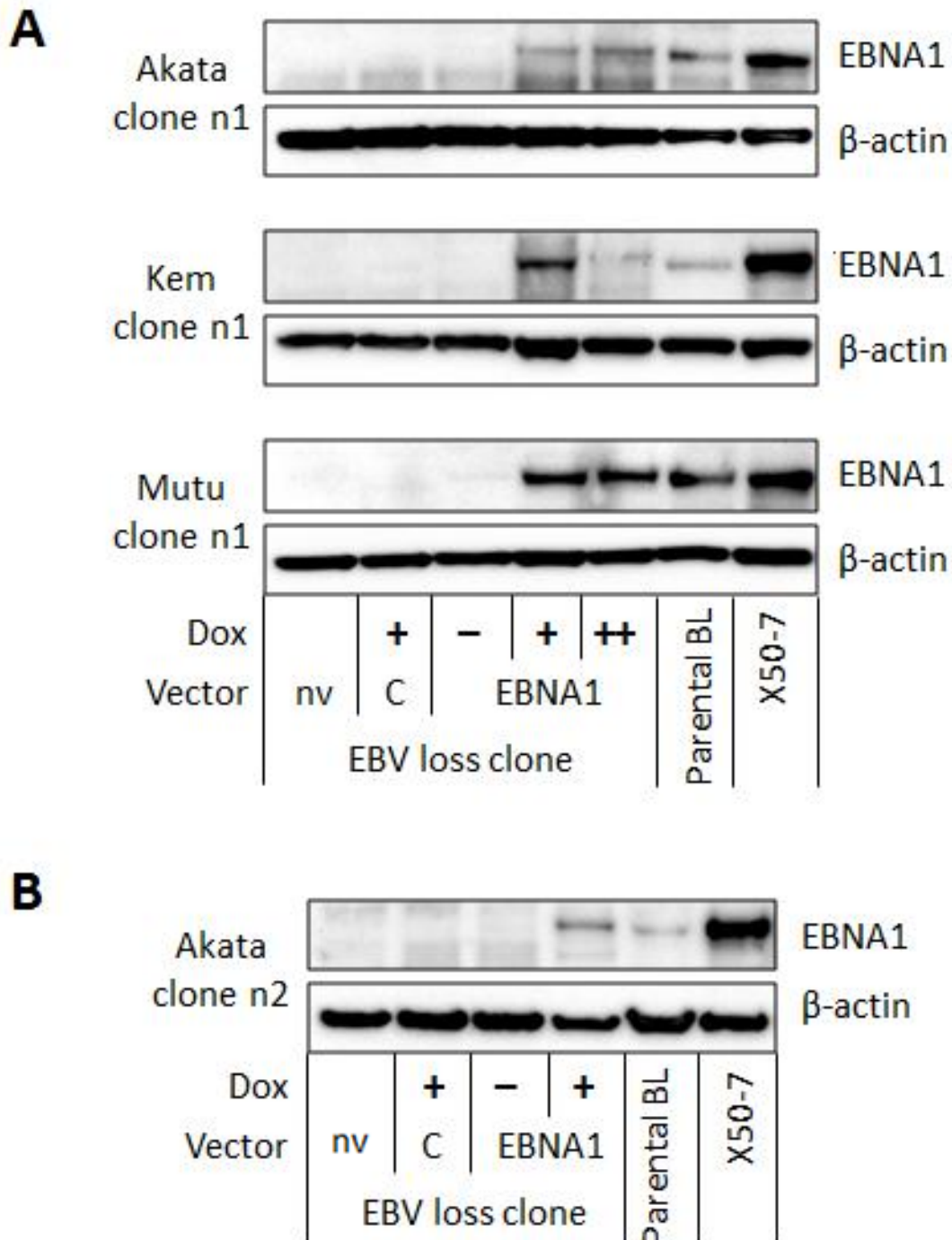


Figure 4.2 EBNA1 expression in FTrex-EBNA1-UTG transduced BL clones

A Examples of EBNA1 expression in clones from different BL backgrounds. Cells containing the EBNA1 lentivirus or an empty control (C) were induced for 24 hours (+) or 14 days (++) and no vector (nv) and uninduced (-) controls were also included.

B Example of EBNA1 expression in an alternative clone of Akata-BL

Media was supplemented with 1µg/ml DOX or DMSO as a vehicle only control
 EBNA1 in the X50-7 sample was calculated to be 55kDa and beta-actin 42kDa

4.2.2 EBNA1 Reporter Assays

In order to confirm that our EBNA1 construct could not only express physiological levels of EBNA1 protein, but that this protein was also functional, we carried out reporter assays to measure the ability of EBNA1 to transactivate luciferase expression from an EBNA1-responsive reporter in EBV-loss BL cells. EBNA1 transactivation activity was determined using the FR-*tk*-luciferase reporter construct [544], which contains the firefly luciferase under control of the Herpes simplex type I thymidine kinase promoter (HSV-I-*tk*) 2 kilobases upstream of the EBV *oriP* family of repeats (FR), which is comprised of 20 repeats of a 30bp EBNA1 binding site (a schematic of the system is shown in Figure 4.3). EBNA1 has previously been shown to increase expression from this promoter by >20-fold in a range of cell types including BLs [545].

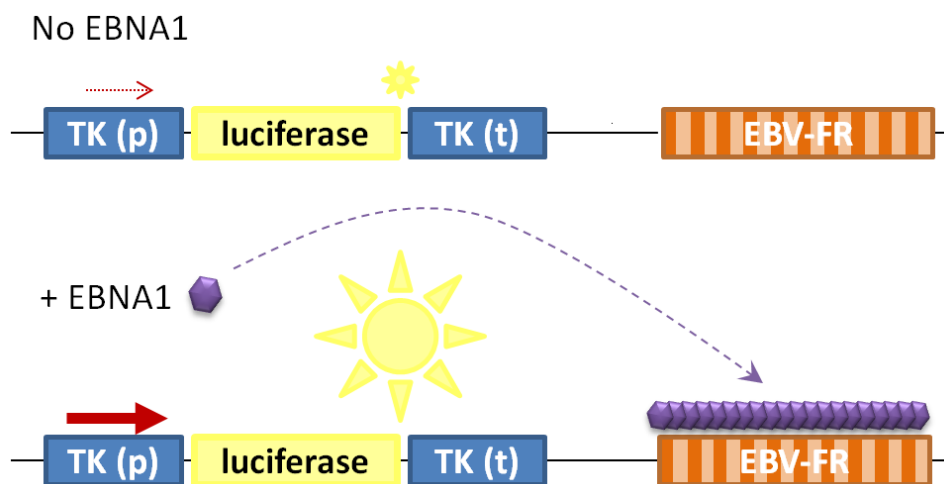


Figure 4.3 Schematic of EBNA1 FR-tk-reporter system

Containing the HSV-I-*tk* promoter, TK(p), terminator, TK(t), family of repeats, EBV-FR, and firefly luciferase

As shown in Figure 4.4, EBNA1 was able to potently increase luciferase expression from the HSV-I-*tk* promoter in EBV-loss Akata by around 200-fold compared to DOX-induced cells transduced with an empty vector control lentivirus, suggesting that it is functional in these cells. Interestingly, there is also some transactivation of HSV-I-*tk* evident in the uninduced EBNA1 cells, which is in line with our other experiences of using this vector where low levels of the gene of interest were constitutively expressed.

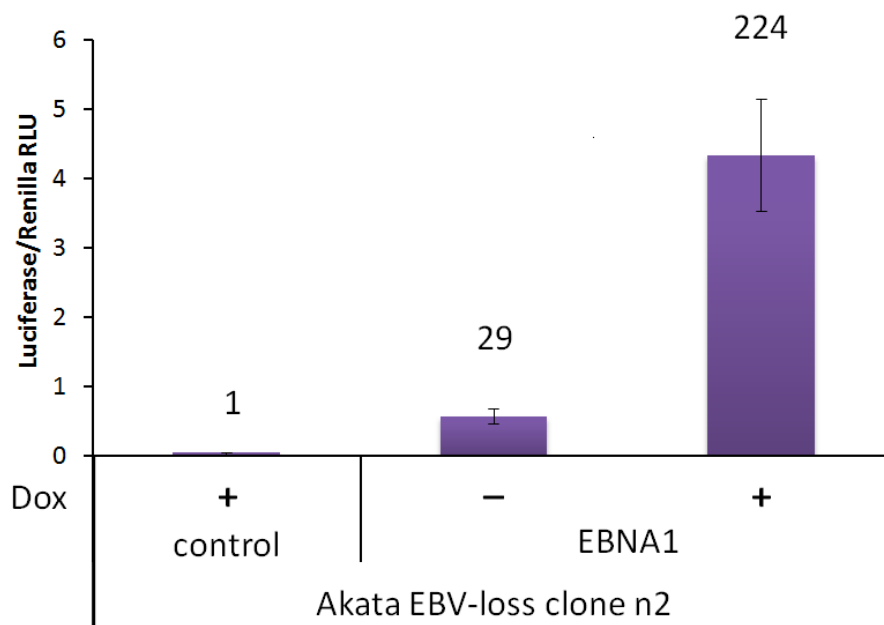


Figure 4.4 Luciferase reporter activation by EBNA1 in EBV-loss Akata cells

Data plotted are mean and standard deviation of three separate transfections carried out in duplicate. Promega Dual-Luciferase reporter reagents were used according to the manufacturer's instructions (see Section 2.9) and firefly luciferase activity was normalised to *Renilla* luciferase activity to allow us to control for variation in transfection efficiency

4.2.3 The apoptosis phenotype of EBNA1-expressing EBV-loss clones

To determine whether EBNA1 could protect EBV-loss cells from cell death, EBNA1-expressing EBV loss cells were compared to empty vector transduced controls in apoptosis assays. All cultures were induced with doxycycline 24 hours prior to assay set up and experiments were carried out on three independent occasions, as described in Section 2.2.3. Apoptosis was induced using ionomycin in these assays as this gave the most robust and consistent results in our screen of responses to various apoptosis-inducing stimuli (see Section 3.3) and was quantified as percentage increase in PI-positive cells per sample compared to untreated controls.

Figure 4.5-A-C shows representative data from experiments carried out on two EBV-loss clones derived from each of Akata-BL, Kem-BL and Mutu-BL, respectively. Although there was some variation between different EBV loss clones transduced with either FTrex-EBNA1-FLAG-UTG or the empty vector control, there was no consistent evidence that EBNA1 confers apoptosis protection across all 3 tumour backgrounds. Interestingly, there tended to be slightly less cell death in both EBNA1-expressing Akata clones than in matched controls and conversely, slightly more cell death in EBNA1-expressing Mutu clones than their matched controls. This difference was significant within replicates from a single experiment using a Student's T-test, hinting that EBNA1 may contribute differently to different tumours. However, when data from 3 independent experiments was pooled, the difference between EBNA1-expressing and control cells was not statistically significant (Figure 4.5-D). Therefore, we conclude that EBNA1 does not consistently confer apoptosis protection to BL cells and is therefore not solely responsible for the EBV-loss phenotype.

Figure 4.5 Apoptosis phenotype of FTrex-EBNA1-UTG transduced BL clones

A Examples of apoptosis in EBNA1-expressing and control vector-transduced Akata-BL clones after treatment with 1µg/ml Ionomycin + 1µg/ml DOX for 48 hours

B Examples of apoptosis in EBNA1-expressing and control vector-transduced Kem-BL clones after treatment with 1µg/ml Ionomycin + 1µg/ml DOX for 48 hours

C Examples of apoptosis in EBNA1-expressing and control vector-transduced Mutu-BL clones after treatment with 2µg/ml Ionomycin + 1µg/ml DOX for 48 hours

A-C representative data from single experiments carried out in triplicate. In each case mean and standard deviation of triplicate measurements are shown

D Comparison of apoptosis data from three independent experiments in EBNA1-transduced and control Akata EBV-loss clone n5 cells. Pooled data from three independent experiments (denoted **1**, **2** and **3**), mean and standard deviation of triplicate measurements are shown

Cells were treated with a dose of Ionomycin at which the corresponding untransduced EBV-loss BL clone undergoes 60-80% apoptosis by the experimental end-point (48 hours), whilst their EBV-positive counterparts undergo around half as much apoptosis. Using a dose in which there is a clear and broad difference in the apoptosis phenotype of protected and unprotected cells should allow us to confidently identify small or subtle changes in apoptosis susceptibility between experimental groups.

P-values were calculated using two-tailed Student's T-tests

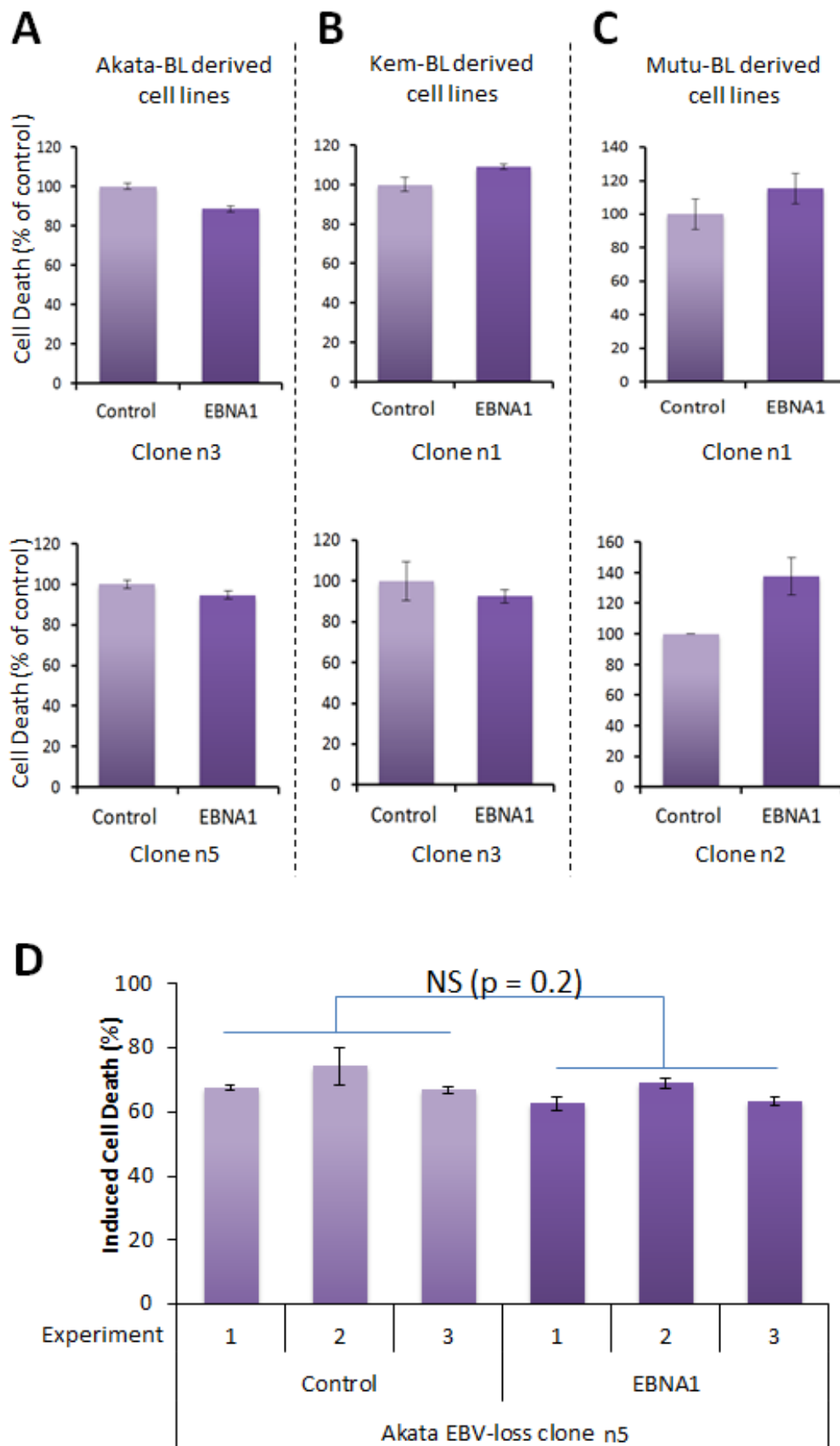


Figure 4.5

4.3 EBERs

4.3.1 Expressing the EBER RNAs in EBV-loss BL clones

The non-coding EBER RNAs are abundantly expressed in all EBV-associated malignancies and have previously been reported to have anti-apoptotic properties in B cells and T cells and to confer tumorigenicity to EBV-loss Akata cells *in vivo* [546]. Therefore we investigated whether they were able to confer apoptosis resistance to our panel of EBV loss clones.

Initially, the EBERs were cloned individually into the same lentiviral backbone as was used to re-express EBNA1 in Section 4.2, except that a tet-responsive human H1 promoter was used instead of the Trex promoter because EBERs can be transcribed *in vitro* by RNA polymerase III (Pol III) but not Pol II [547] (construct described in detail in Section 2.6.2). Transduced cells were enriched for high GFP expression by cell sorting before being induced with doxycycline and RNA expression measured by quantitative PCR and Northern blot. Surprisingly, although the levels of EBER RNA expressed from these constructs looked to equal or exceed endogenous levels in EBV-infected cell lines by q-PCR (Figure 4.6-A) Northern blotting could only detect weak signals even in those lines expressing the highest levels of EBERs by q-PCR (Figure 4.6-B).

Since there have previously been reports of poor termination of non-coding RNAs by Pol III [548, 549], we decided to test whether our transcripts were failing to terminate by carrying out q-PCR assays to compare the total numbers of EBER transcripts with transcripts that ran through the termination sequence. For each EBER we designed an alternative reverse primer to be used with the conventional forward primer and probe in q-PCR; by comparing the conventional assay to the run through assay we could quantify the relative amount of appropriately terminated transcripts being generated. We found that the vast majority of our transcripts were running through the termination sequence (Figure 4.6-C), which explains why

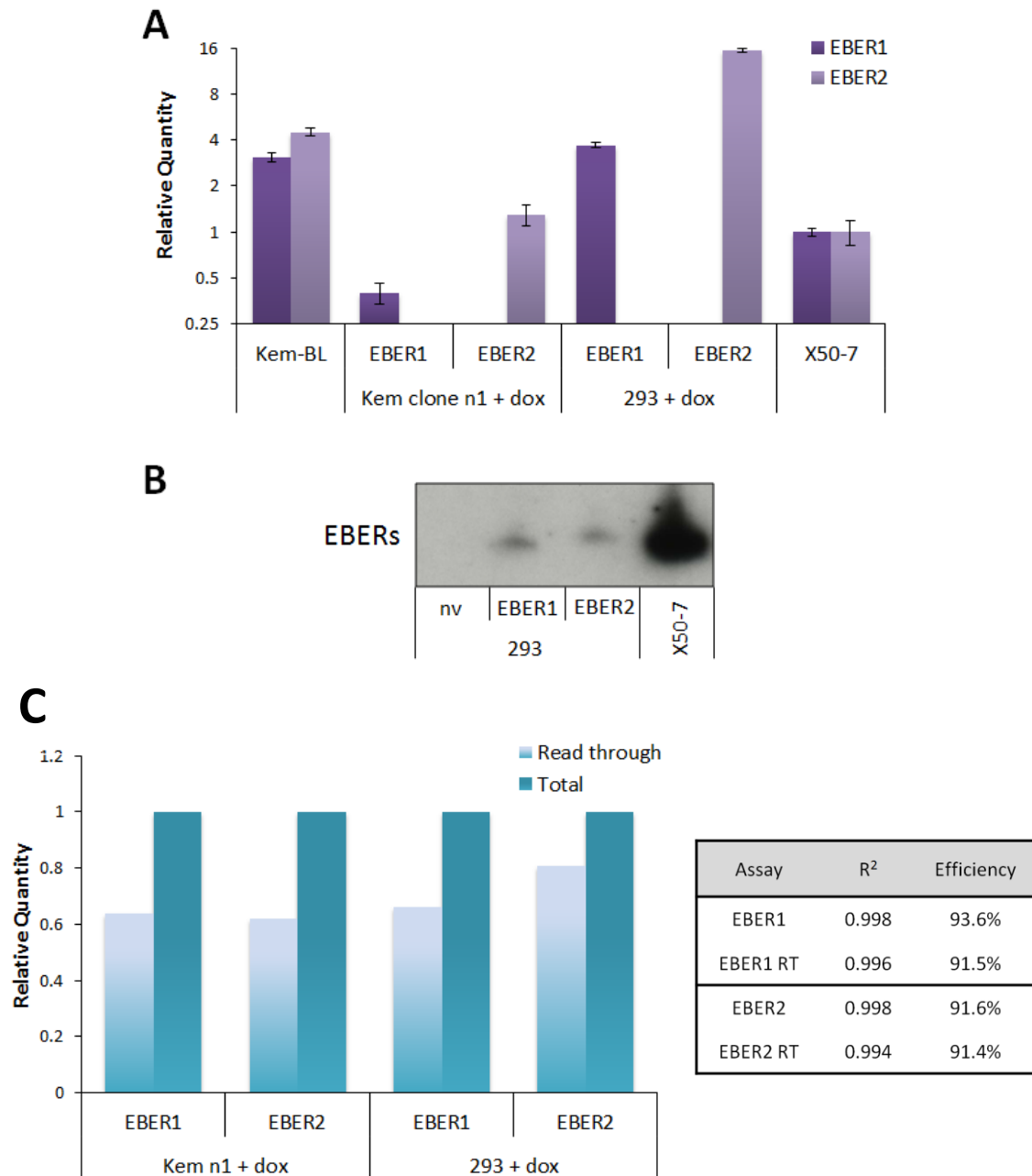


Figure 4.6 Expression of EBER RNAs in FH1-EBER1/2-UTG transduced cells

A EBER q-PCR measured in duplicate and expressed relative to the X50-7 LCL

B Northern blot of EBER RNA in FH1-EBER1/2-UTG transduced 293s, nv = no vector control

C 'Read through' q-PCR, samples were measured in duplicate relative to DNA plasmid standards. Total EBERs was measured using the standard EBER q-PCR assay [90] whereas read-through assays used an alternative reverse primer that bound the backbone of the FH1t-UTG plasmid immediately downstream of the EBER sequence (primer: 5'-GAGGCCAGATCTGGAGCCGA-3'). Standard curve comparisons showed that the standard EBER and read-through assays amplified linearly over several orders of magnitude and with similar efficiency as indicated.

Inductions were carried out using DOX at 1µg/ml

the levels of EBER expression by Northern blot did not correlate with the high levels of transcripts detected by q-PCR.

There are EBER homologues in other viruses which have more complex requirements for efficient termination than the 4 or 5 T tranche thought to be sufficient for EBER termination. For example; the Adenovirus VAs, contain two termination sequences per RNA, which can give rise to VAs of alternative lengths [550, 551], and a distantly related Chicken virus (Chicken embryonic lethal orphan virus, CELO) also contains short RNAs with two termination sequences which give rise to different sized RNAs with different functions [552, 553]. Both the EBERs and CELO RNAs also contain runs of 4 or more T residues within their transcribed sequence which appear not to be sufficient for termination [551], so clearly termination requirements can be complex and varied for different Pol III transcripts.

Interestingly, the EBV genome does indeed contain a second polyT after each conventional EBER termination sequence [547] (Figure 4.7). Unfortunately however, the close proximity of the 'secondary' termination sequences to the conventional termination sequences makes it impossible to distinguish between transcripts using q-PCR and the very strong signals given by Northern blots make it hard to be sure of the exact size of EBER transcripts being produced in EBV-infected cell lines (Figure. 4.6-B). Additionally, it has been reported that tRNA transcripts, which fold similarly to EBERs, associate with ribonucleoproteins such as La, and in some cases, are encoded at loci where secondary termination sequences are present, can be processed by exonucleases which 'nibble' transcripts to the correct length [554, 555]. It would be technically complex and time consuming to determine whether any of these factors are important in the transcription of EBERs and then to generate vectors to efficiently express them individually in an inducible manner. For subsequent experiments therefore, we decided to use an alternative system which contains multiple copies of the EBERs in their endogenous sequence context.

FH1t-EBER1-UTG CATG**TTTT**CTCGAGACGCGTC
 FH1t-EBER2-UTG GCTA**TTTTT**CTCGAGACGCGTC
 EBER1 CATG**TTTT**GATCCAAAC**TTTTGTTTT**AG
 EBER2 GCTA**TTTTTTTGT**GGCTAG**TTTT**GCA
 CELO VA **CTTATTGTCGGTTAGTTCATTTTTCTATTTTTTTT**

Figure 4.7 PolyT tracts in EBV and CELO virus compared to lentivirus constructs

FH1t-EBER1/2-UTG both contain only a single polyT (pink highlight), corresponding to the published EBER termination sequences [524], however there are additional polyT sequences downstream of each EBER in the viral genome, similar to the short and long polyT sequences in CELO VA RNA, which are both required for termination.

EBER DNA accession number J02078.1, CELO VA accession number M12738.1

The EKS10 vector was developed by the Takada group and has been shown to express near-endogenous levels of EBER RNAs in a number of cell types [310, 556]. In this system both EBER RNAs are expressed constitutively from their respective endogenous promoters and stable cell lines are generated by drug-selection of transfected cells (see Section 2.6.3). We generated three pairs of EBER-expressing and empty vector control cell lines on each of three tumour backgrounds; 9 pairs in total.

In each tumour background, two pairs of cell lines were made in a single EBV-loss clone as well as one pair in an alternative EBV-loss clone to allow us to control for variation between transfection and selection procedures and between different loss clones as well as between tumour backgrounds. In all the cell lines generated we could express reasonable amounts of EBER RNAs, approximately 20-60% of that seen in the parental EBV-positive BL cell lines (Figure 4.8). Since EBERs are present at such high copy numbers in EBV-positive BLs, are variable between BL cell lines, and have been reported to be functional at this level of expression by other groups, we deemed this series of transfectants suitable to ascertain whether EBERs can restore the apoptosis protection phenotype to EBV-loss BLs.

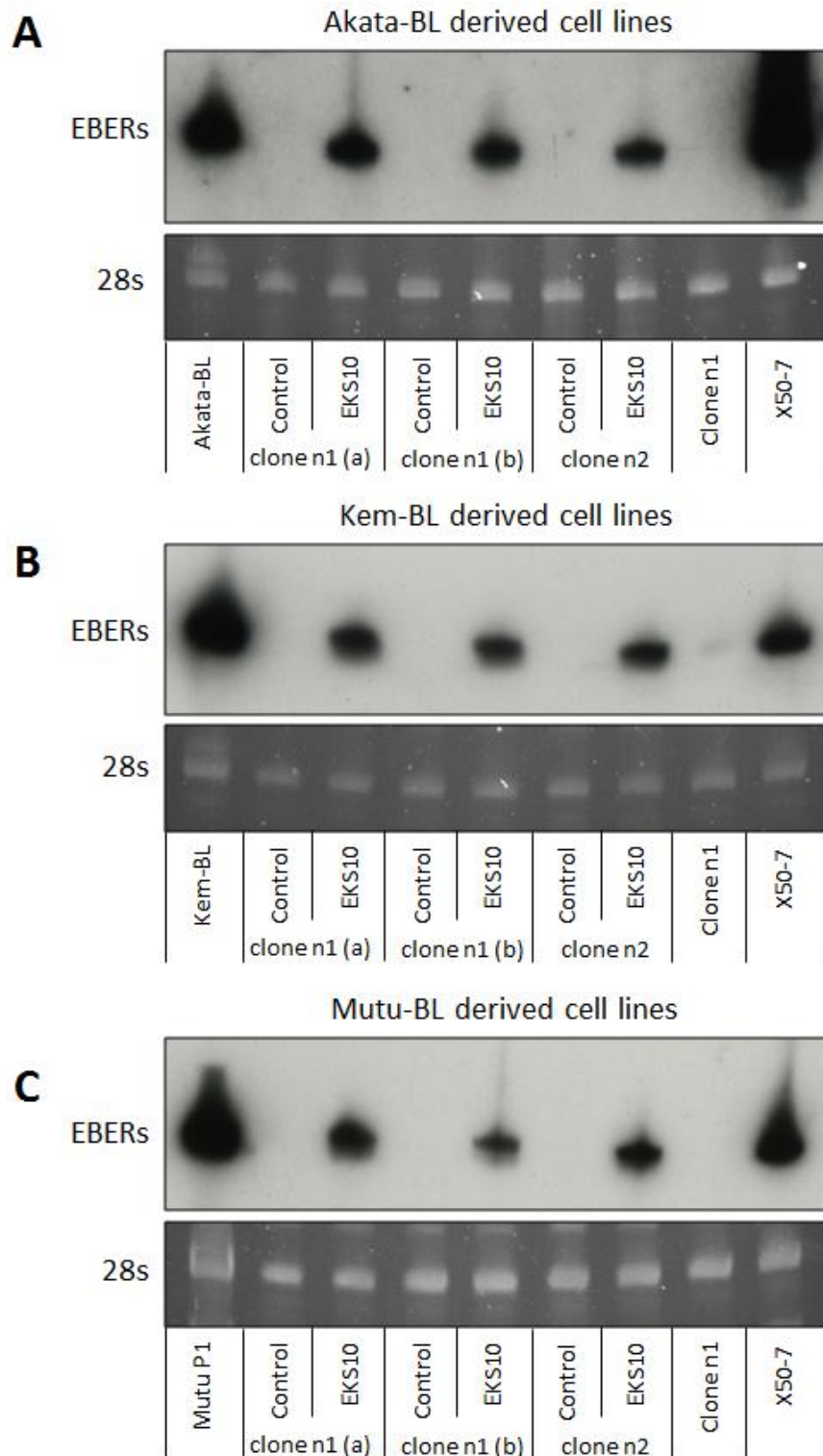


Figure 4.8 EBER RNA expression in EKS10 transfected BL clones

Northern blots carried out as described in Section 2.7.8. Control cells were transfected with pcDNA3 and drug selected under identical conditions to the EBER-encoding EKS10-transfected cells.

All lanes contained 20µg RNA, P³²-labelled DNA was used as a probe, film cassettes were stored at -80°C for 14 days before developing and 28s RNA was used as a loading control.

4.3.2 The apoptosis phenotype of EBER-expressing EBV-loss clones

Apoptosis assays on EBER-expressing cells and empty control cell lines were set up as described in Section 2.2.3 with all samples plated out in triplicate and all experiments carried out on three independent occasions. Cell death was induced by the addition of ionomycin and cells were harvested and analysed by FACS after 48 hours. In contrast to some reports from other groups we found that EBER-expression did not convincingly confer any protection to EBV-loss cells in the Akata, Kem, or Mutu BL backgrounds (Figure 4.9). Although the EBER-expressing Mutu clone n2 cells were less susceptible to ionomycin-induced cell death than were the other EBER-expressing cell lines, the empty vector control line showed a similar phenotype; indicating that this result was due to clonal variation.

4.3.3 Expression and function of human IL-10 in EBV-loss clones

The Takada group reported that EBER-expressing EBV-loss Akata cells could be protected from IFN α and hypoxia-induced cell death [338, 339], and that the mechanism responsible for this was upregulation of cellular IL-10 via activation of RIG-I [342]. Therefore we carried out q-PCR to look at transcription levels of cellular IL-10 in our panel of EBV-positive and loss clones as well as in our EBER-expressing and control EBV-loss cell lines. The assays were carried out in technical and experimental duplicate using an inventoried TaqMan primer and probe set (see Section 2.7.4) that is able to detect human IL-10 mRNA (Genbank reference NM000572.2) and does not cross react with the EBV-encoded IL-10 homologue, BcRF1. Surprisingly, we found no evidence that IL-10 is more highly expressed in either EBV-positive or EBER-expressing EBV-loss BL cell lines compared to EBER-negative cells (Figure 4.10-A, 4.10-B and data not shown). We also found that, whilst the addition of exogenous IL-10 could modestly protect BL cells from ionomycin-induced cell death, it could not fully reverse the EBV-loss phenotype; irrespective of

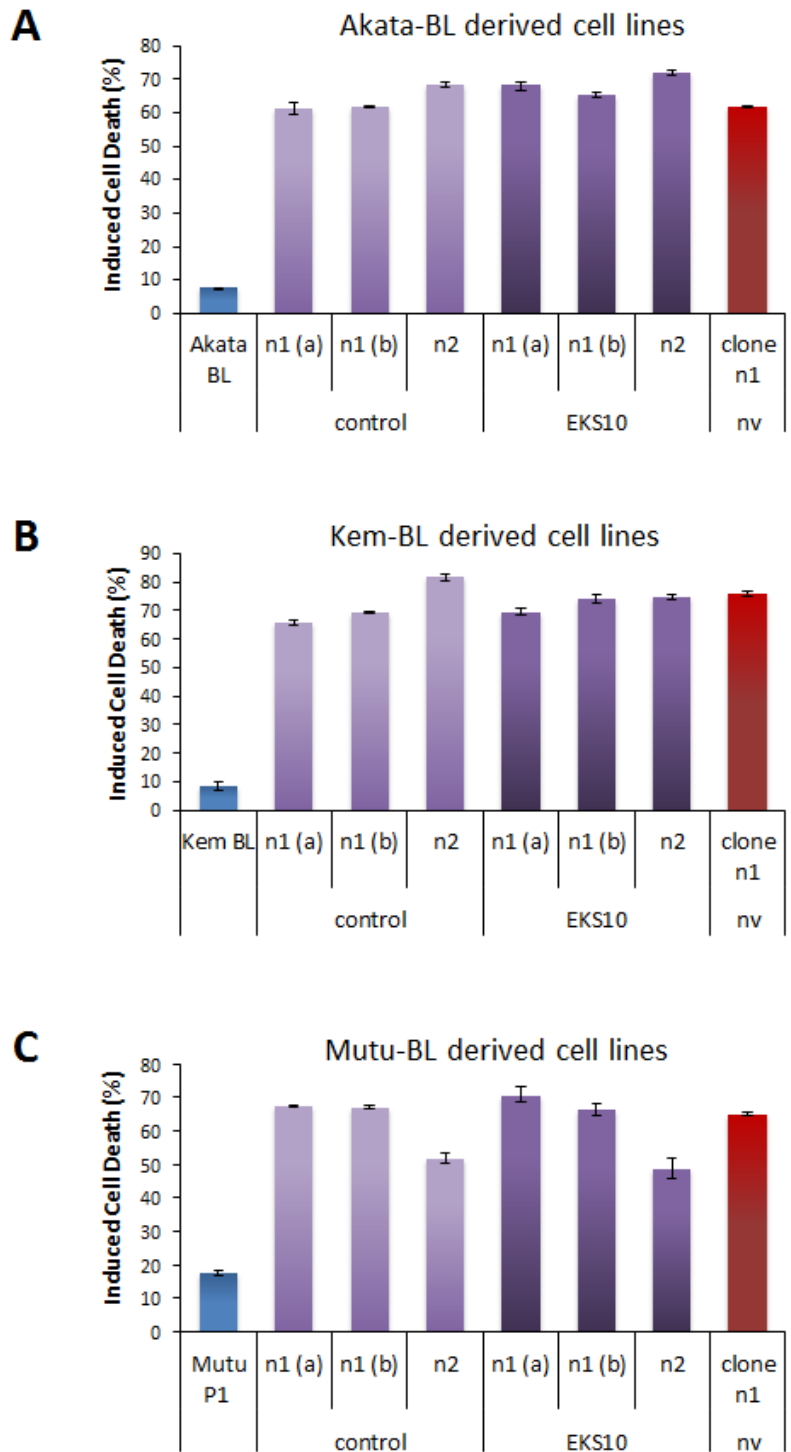


Figure 4.9 Apoptosis phenotype of EKS10 transfected BL clones

A Akata-BL-derived cell lines **B** Kem-BL-derived cell lines, both induced using 1µg/ml ionomycin **C** Mutu-BL-derived cell lines, apoptosis induced using 2µg/ml ionomycin

All data representative, assays carried out on three separate occasions.

n1 (a) and (b) = two different transfectants made in the same EBV-loss clone (n1)

n2 = transfectants made in a second EBV-loss clone, n2

clone n1 nv = EBV-loss clone n1 cells, no vector control

Akata/Kem/Mutu BL/P1 = EBV-positive control for the respective BL backgrounds

EBER status (Figure 4.11-A and 4.11-B). We could also never induce any apoptosis in BL clones by addition of IFN α , even using ten times the amount that is used by the Takada group, nor enhance the effect of ionomycin treatment (data not shown) and so were unable to investigate whether EBERs can affect cell survival by modulating IFN signalling in BL cell lines.

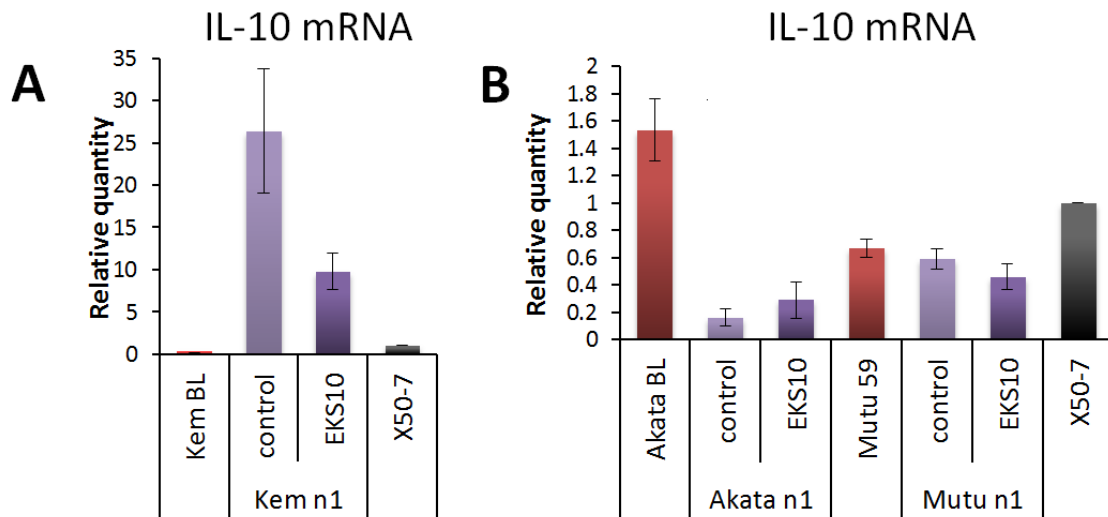


Figure 4.10 IL-10 mRNA expression in EBV-positive and negative BL cell lines

A IL-10 mRNA in EKS10 transfectants of Kem EBV-loss clone n1 and controls, relative to X50-7

B IL-10 mRNA in EKS10 transfectants of Akata EBV-loss clone n1 and Mutu EBV loss clone n1 and controls, relative to X50-7.

Data from one pair of transfectants is shown for each tumour background, but all transfectants generated were tested. Relative quantities were calculated using the $\Delta\Delta C_t$ method, mean and standard deviation of duplicate measurements is shown

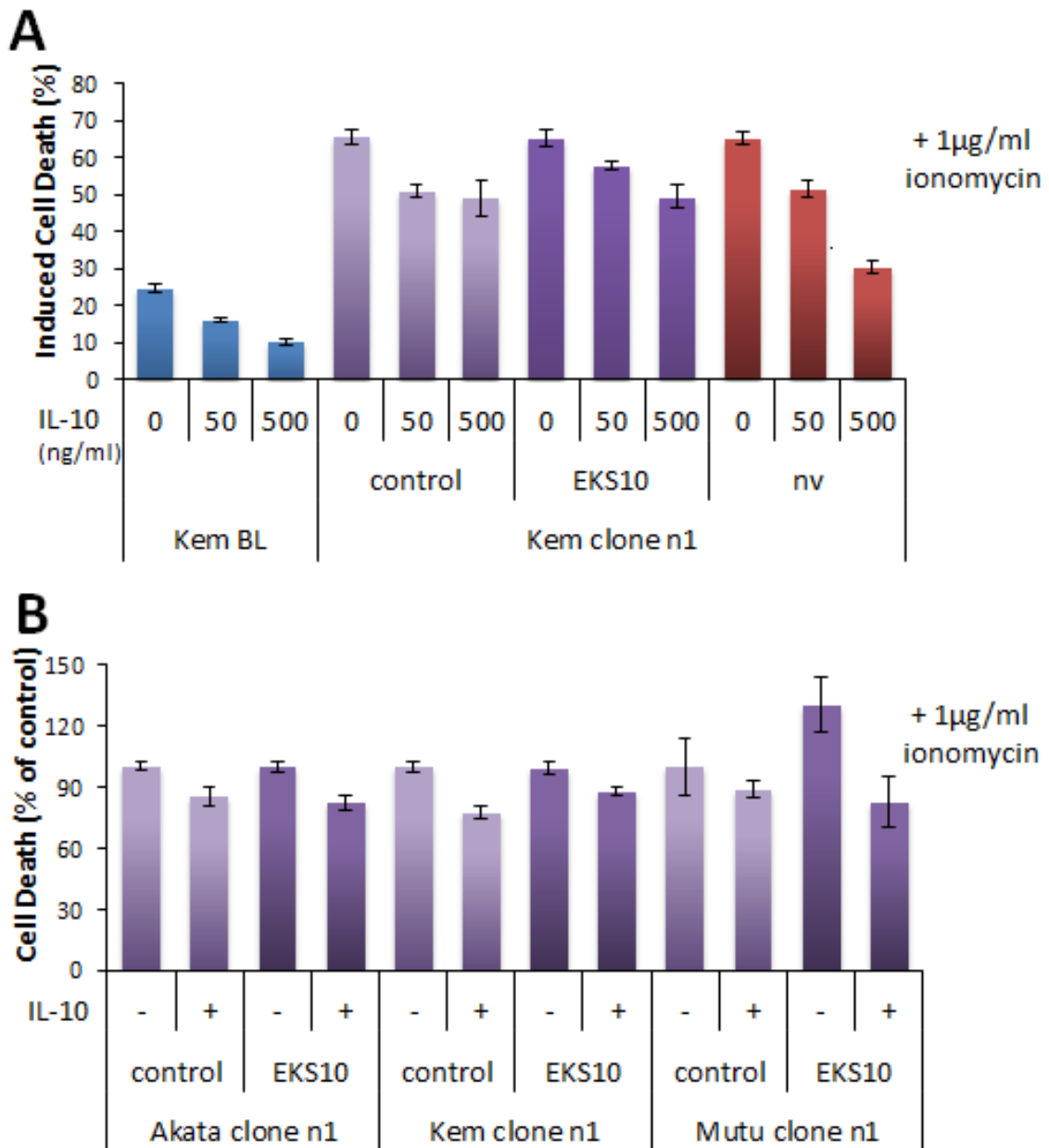


Figure 4.11 IL-10 function in BL clones

A Effect of 0,50 or 500ng/ml IL-10 on ionomycin-treated Kem-BL-derived cell lines comparing EBV-positive parental cells (Kem-BL), and loss clone n1 either untransfected (nv), containing control vector (control) or expressing EBERs (EKS10). Mean and standard deviation of triplicate measurements is shown

B Apoptosis in ionomycin-treated EBER expressing cells supplemented with IL-10 comparing EBV-loss clones from different backgrounds, IL-10 added at 50ng/ml. Mean and standard deviation of triplicate measurements is shown

All assays carried out in triplicate on 3 separate occasions

4.3.4 Further investigations into EBER function in BL cells

In order to further explore possible reasons for the disparity between our findings and the reports of others we carried out a number of other tests on our EBER-expressing cell lines. EBER FACS using a commercially-available PNA probe (Figure 4.12) showed that the majority (60<75%) of EKS10-transfected cells stained positive for EBERs. This may suggest either that some cells in the culture were EBER negative, or that some cells express low levels, below the threshold of detection. Whilst we may expect either of these two possibilities to influence the apoptosis phenotype of the cells, we would still expect to see a difference between EBER-expressing and control cells in apoptosis assays if the EBER RNAs were able to confer resistance to EBV-loss clones.

Finally, to determine whether EBER RNAs were able to confer a growth advantage to EBV-loss BL cells which could have been masked in our apoptosis experiments we carried out proliferation assays on healthy EBER-expressing cells versus empty vector control cells. We found that our stably transfected cell lines grew identically in culture over a seven day period in all three tumour backgrounds tested, indicating that EBERs provide no growth advantage to BL clones *in vitro* (Figure 4.13).

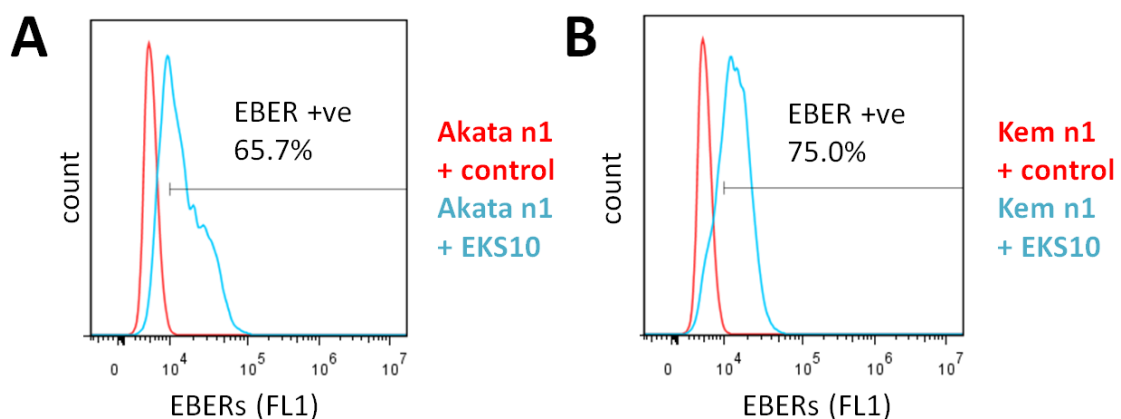


Figure 4.12 EBER FACS in EKS10 transfectants **A** EBER FACS comparing EKS10 and control transfectants of Akata n1 **B** EBER FACS comparing EKS10 and control transfectants of Kem n1 EBV-positive and untransfected controls were also included. Each sample was prepared and analysed in duplicate. Cells were hybridised to an EBER-specific FITC-labelled PNA probe or a scrambled sequence negative control PNA-FITC probe

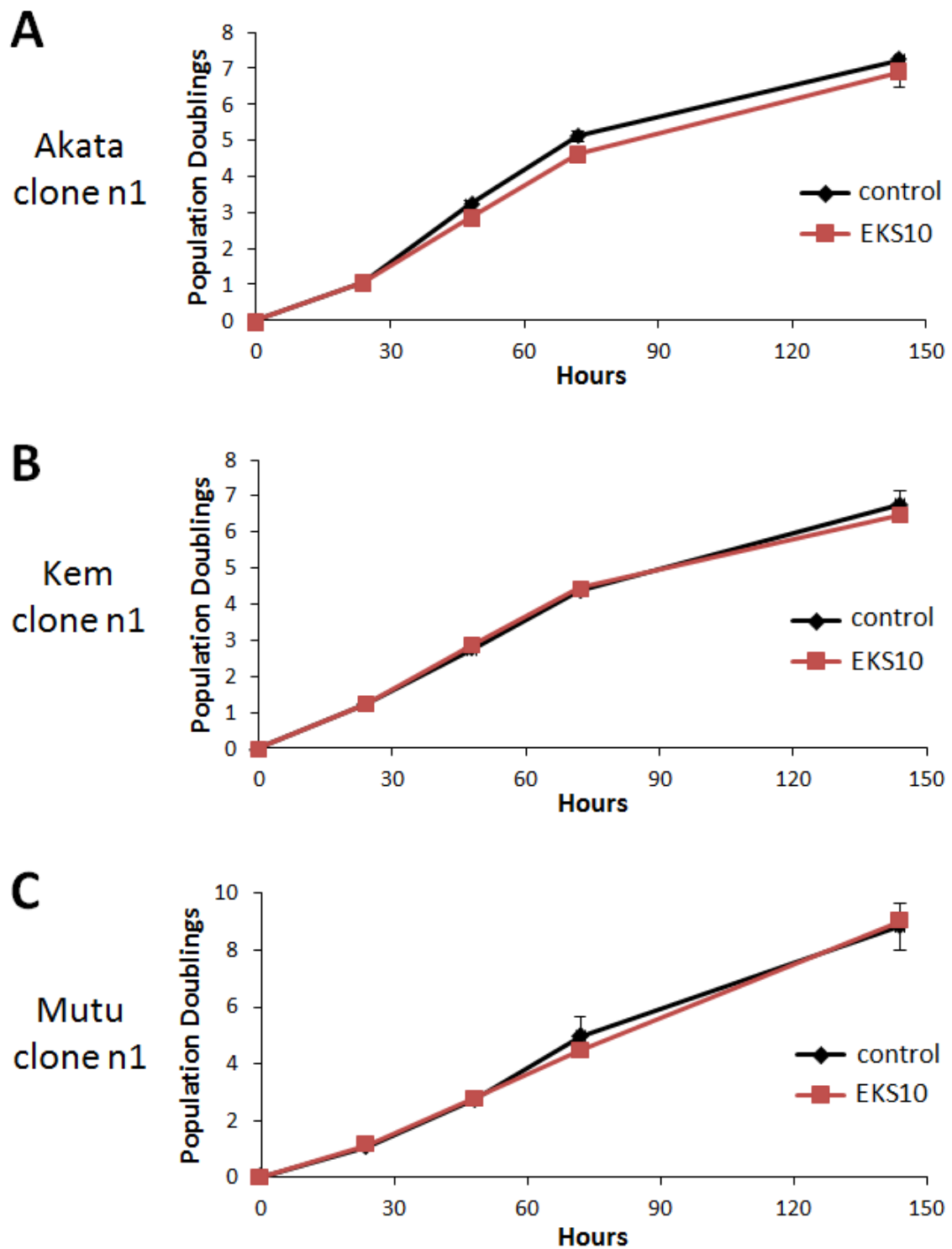


Figure 4.13 Proliferation in EBER-expressing EBV-loss clones

Growth of EBER-expressing and empty-vector transfected control cells

A Transfectants of Akata EBV-loss clone n1 **B** Transfectants of Kem EBV-loss clone n1

C Transfectants of Mutu EBV-loss clone n1

Population doublings calculated from absolute cell counts and calculated as cells/ml divided by cells/ml at time 0, all measurements were made in triplicate and assays were carried out on two occasions

4.4 BART microRNAs

4.4.1 Expressing the BART mRNAs in EBV-loss clones

Although the EBV BamHI A rightward transcript-derived microRNAs (EBV miR BARTs) were first identified in EBV-positive epithelial cells where they are very highly expressed [352], they are also expressed at tens to hundreds of copies each per cell in LCLs and BL cell lines [94, 168, 171]. *In silico* binding predictions carried out by several groups using several different algorithms found likely seed sequence matches for miR BARTs in a large number of 3' UTRs of apoptosis-related genes [99, 168, 365, 366, 371], suggesting that miR BARTs may modulate apoptosis in BL cells. Additionally, some recently published functional studies have suggested that miR BARTs can downregulate pro-apoptotic proteins in epithelial cells [365, 366], and may be able to partially rescue apoptosis in BL cells [99].

After ruling out either the EBNA1 protein or EBER RNAs, we therefore considered that the miR BARTs may be responsible for the EBV-loss phenotype. The primary transcripts derived from the BamHI A locus are long and complex; the exons span over 22kb of the viral genome and a number of different splice variants have been described, only some of which are thought to give rise to the BART miRs [373]. The BART miRs reside in intronic regions arranged in two clusters, with the exception of miR BART 2 which is located several kilobases downstream of

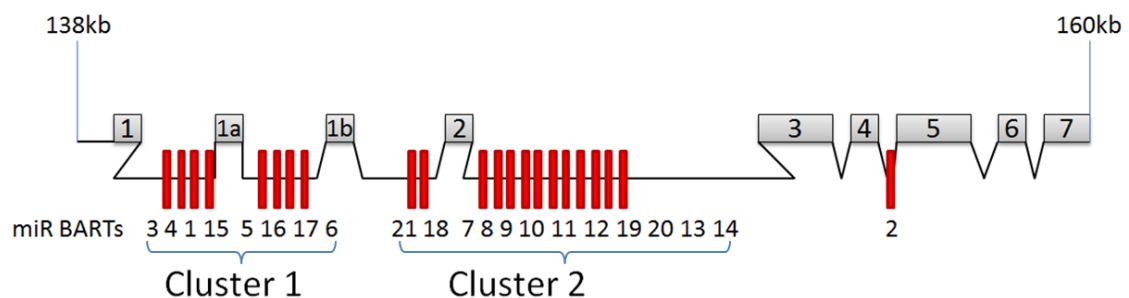


Figure 4.14 Schematic of organisation of BART miRNAs in EBV genome. Grey boxes denote BamHI A region exons and the position of the BARTs region relative to the B95.8/Raji-repaired EBV genome sequence (Accession number M80517.1)

the other miRs (Figure 4.14). Since cloning the entire BamA locus is beyond the capacity of any lentivirus system we opted to generate two separate lentiviruses, each encoding one cluster of the miRs and so two separate genomic fragments were inserted into the F-UTG lentiviral backbone, driven by the PolII Trex promoter (see Section 2.6.4).

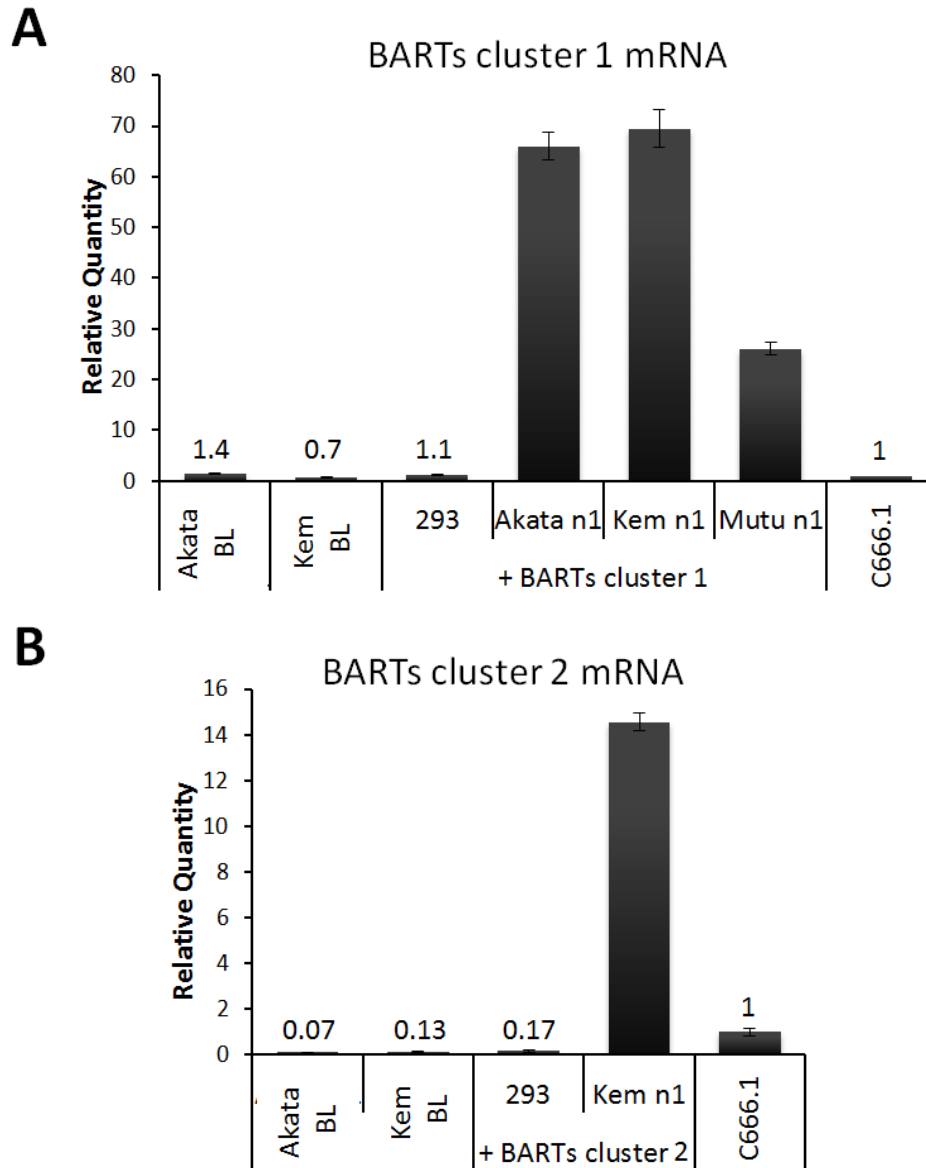


Figure 4.15 BARTs primary transcripts in FTrex-BARTs-UTG transduced BL cells

A BARTs cluster 1 (exon 1-1a) mRNA in EBV-positive cell lines and transduced cells

B BARTs cluster 2 (exon 2-3) mRNA in EBV-positive cell lines and transduced 293 and Kem n1 cells

All transduced cells treated with 1µg/ml DOX for 48 hours

Once miR BARTs cluster 1 and cluster 2 transduced EBV-loss cell lines had been generated we measured expression of our inserts by q-PCR, using a primer/probe set directed within the exon 1-1a and 2-3 introns, respectively. Interestingly, we found high levels of both cluster 1 and cluster 2 mRNA expression in EBV-loss BL cells, compared to their EBV-positive counterparts and 293 cells transduced with the same constructs (Figure 4.15-A and 4.15-B). This was surprising and could not be simply explained by differences in lentiviral transduction as 100% of cells expressed GFP after sorting and cells of the same clone transduced with different constructs expressed similar levels of GFP (Figure 4.16). This implies that the primary BARTs transcripts may not be processed correctly in BL cells; leading them to accumulate, but are more efficiently processed and therefore degraded in HEK 293 cells. Notably the Raab-Traub laboratory has previously reported a disconnect between the level of primary miR BART transcripts and the mature microRNAs in a range of EBV-positive cell lines [373].

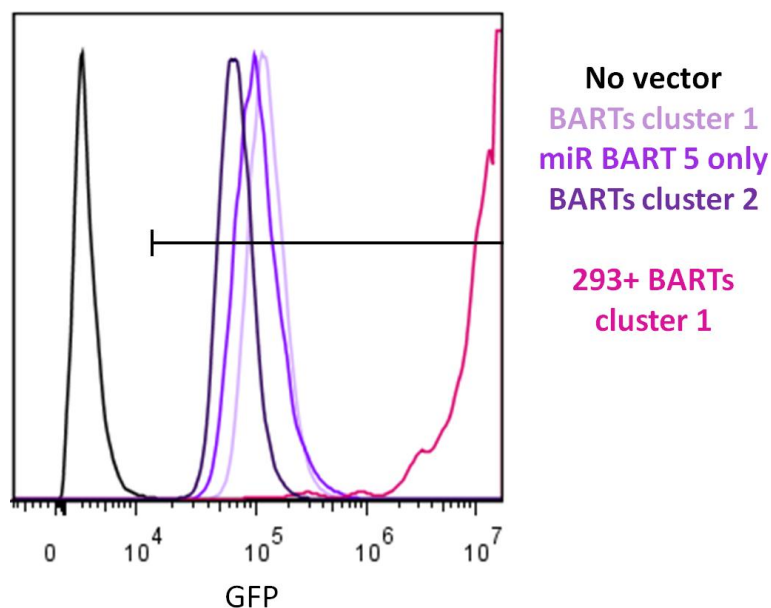


Figure 4.16 Expression of GFP in BART FT-UTG transduced cells

No vector, BARTs cluster 1, miR BART 5 and cluster 2 transduced cells shown in purple are all in Kem clone n1 cells and had been sorted for GFP expression. 293 cells transduced with the BARTs cluster 1 vector (shown in pink) were not sorted as these cells efficiently take up and integrate high levels of lentivirus; this is reflected in the fluorescence intensity of GFP. Representative FACS data of experiments carried out on multiple occasions, all cell lines shown in this figure (except no vector control) were determined to be >99% GFP positive

4.4.2 Expressing the BART microRNAs in EBV-loss clones

When we went on to look at expression of the mature miRs in EBV loss BLs using stem-loop q-PCR assays we found that although we could restore similar levels of miRs to that seen in Akata-BL, we could not restore levels similar to other BLs, such as Kem-BL, which express higher levels of miR BARTs than Akata-BL (Figure 4.17-A). To test whether this was a feature of the construct design, we also made a construct containing pre-miR BART 5 alone driven by a Pol III promoter (see Section 2.6.4), using an identical strategy to that of Choy and colleagues who had used their construct to show an anti-apoptotic function for miR BART 5 in epithelial cells [365]. We looked at miR BART 5 expression from this construct compared to the cluster 1 vector and found that, whilst we could substantially increase mature miR expression, we were still unable to achieve levels comparable to that typically seen in of Latency I BLs, demonstrated here by comparison to Kem-BL (Figure 4.17-B). Interestingly, in 293 cells transduced with our miR BART expression vectors, we were able to achieve expression of mature BART miRs at levels comparable to, or in excess of, those seen in Latency I BLs (Figure 4.18). This may be due to more efficient entry and integration of lentivirus particles and/or more efficient processing of primary transcripts to mature miRs in epithelial cells, although we have not investigated this further.

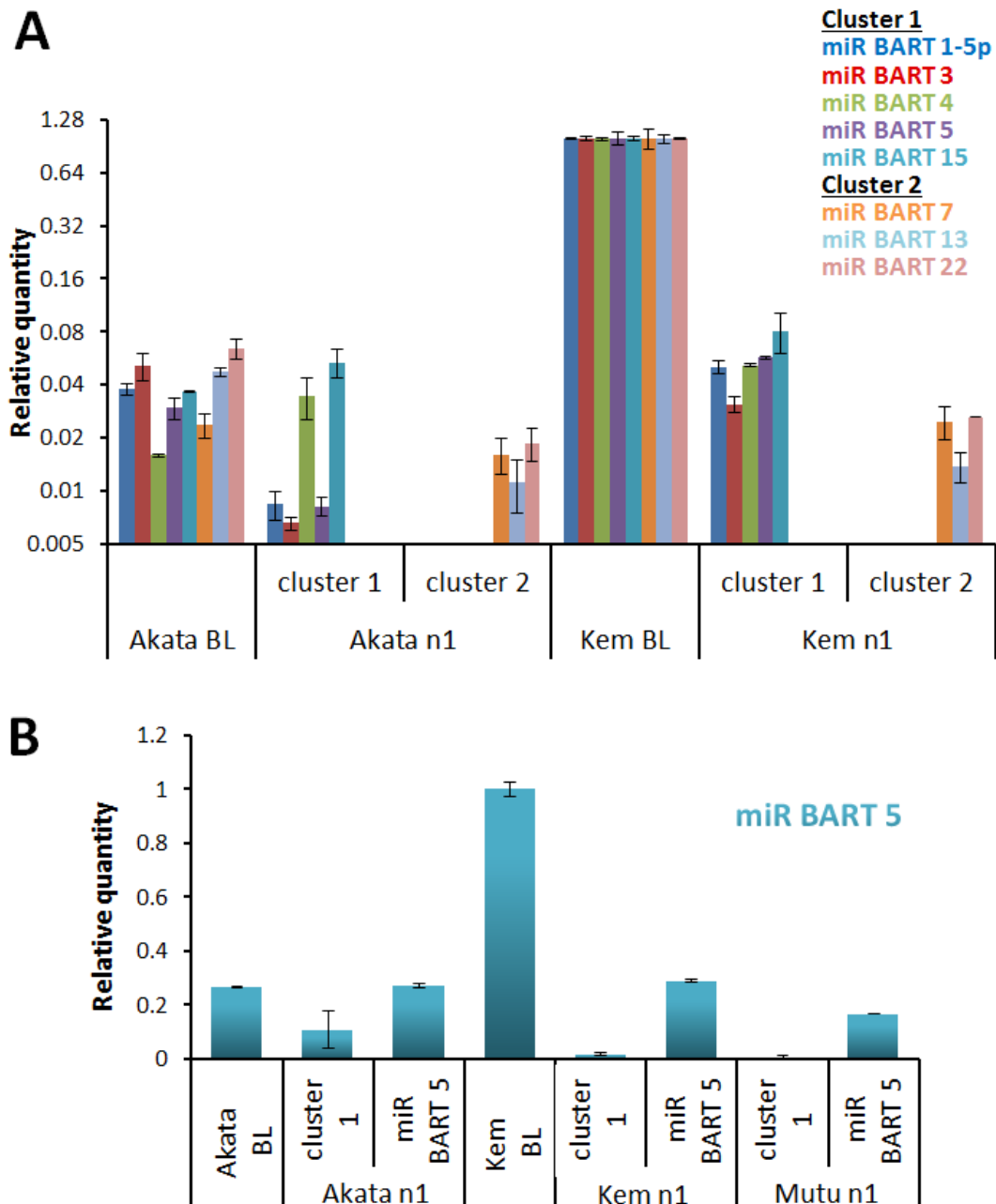


Figure 4.17 Expression of mature BART miRs in transduced BL cells by stem-loop q-PCR

A Example miR BART expression in Akata loss clone n1 and Kem loss clone n2 transduced with either the cluster 1 or cluster 2 BARTs expression vectors compared to EBV-positive parental cell lines. Normalised to EBV-positive Kem-BL cells, Log_2 scale has been used due to the variation in magnitude of difference in miR expression between individual miRs and between different cell lines

B Comparison of miR BART 5 expression from either the cluster 1 construct or the miR BART 5 only lentivirus in EBV-loss cells compared to Latency I cell lines. Normalised to Kem-BL

N.B. A subset of BART miRNAs was measured because of the number of assays and therefore cost involved in measuring all of the miRNAs within our constructs. The assays chosen detect some of the more highly expressed miRs in our panel of Latency I BL cell lines. All data shown are mean and standard deviation of duplicate measurements and analysis was carried out using the $\Delta\Delta\text{Ct}$ relative quantification method

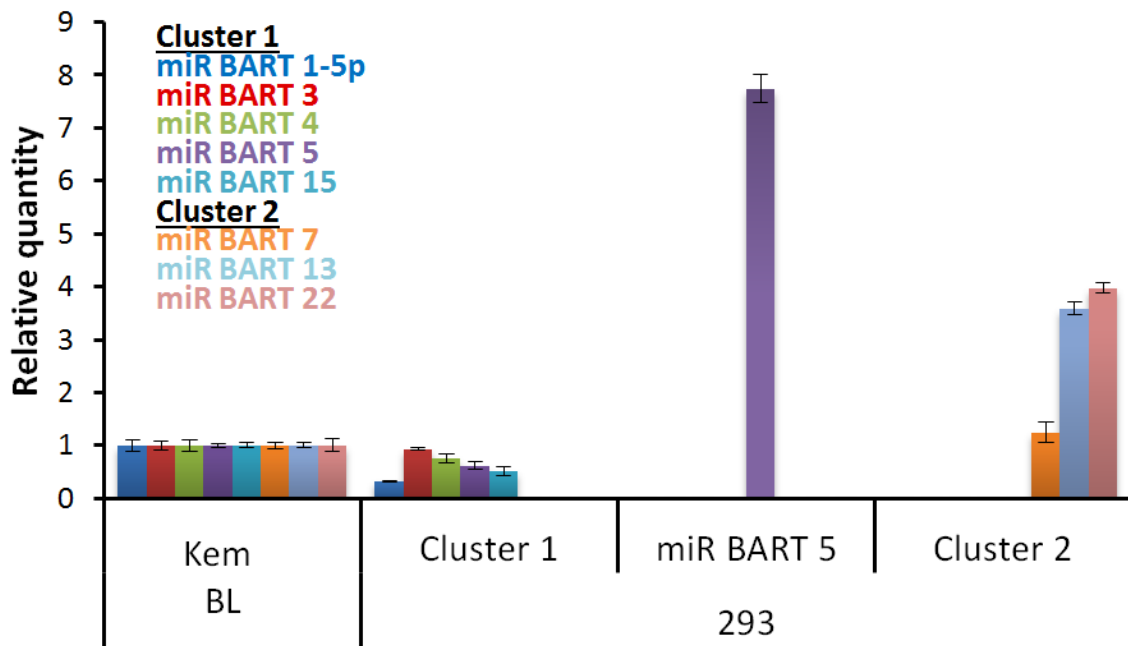


Figure 4.18 Expression of miR BARTs in lentivirus-transduced 293 cells by stem-loop q-PCR. Each miR is expressed relative to Kem-BL, which expresses relatively high levels of miR BARTs compared to other EBV-positive BLs. Data are mean and standard deviation of duplicate measurements and analysis was carried out using the $\Delta\Delta C_t$ relative quantification method.

4.4.3 The apoptosis phenotype of miR BART-expressing BL clones

Since we could achieve similar levels of expression of the EBV BART miRs to that seen in Akata-BL, which also exhibits sensitivity to apoptosis upon loss of the viral genome, we carried out apoptosis assays on miR BART lentivirus-transduced EBV-loss BL cell lines. Although there was some variation between individual experiments in all BL backgrounds tested (Figure 4.19-A), we could never show a convincing or reproducible effect on ionomycin-induced cell death due to the expression of BART miRs in EBV-loss clones (Figure 4.19-B). In total, 5 sets of miR BART expressing cell lines were made and tested; two derived from EBV-loss clones of Akata-BL, two derived from Kem-BL and one in a loss clone of Mutu-BL. A set of cell lines consisted of cells stably transduced with each of the empty, BARTs cluster 1, miR BART 5 only and BARTs cluster 2 lentiviruses.

Figure 4.19 Effect of miR BARTs on the apoptosis phenotype of EBV-loss clones

A Experimental variation in apoptosis assays carried out a set of BARTs transduced Akata clone n1 cell lines. Numbers **1,2** and **3** refer to the experiment number and **nv** denotes 'no vector' control EBV-loss BL clones

B Representative data from apoptosis assays carried out on BART lentivirus transduced clones of Akata-BL and Kem-BL. Control cells contained the empty F-UTG lentivirus

All assays were carried out in triplicate in at least three independent experiments, apoptosis was induced using 1µg/ml ionomycin and miR BART expression was induced using 1µg/ml DOX. Mean and standard deviation from triplicate measurements are plotted, cell lines were compared using a Student's T-test, but since there were no statistically significant consistent differences p-values are not shown

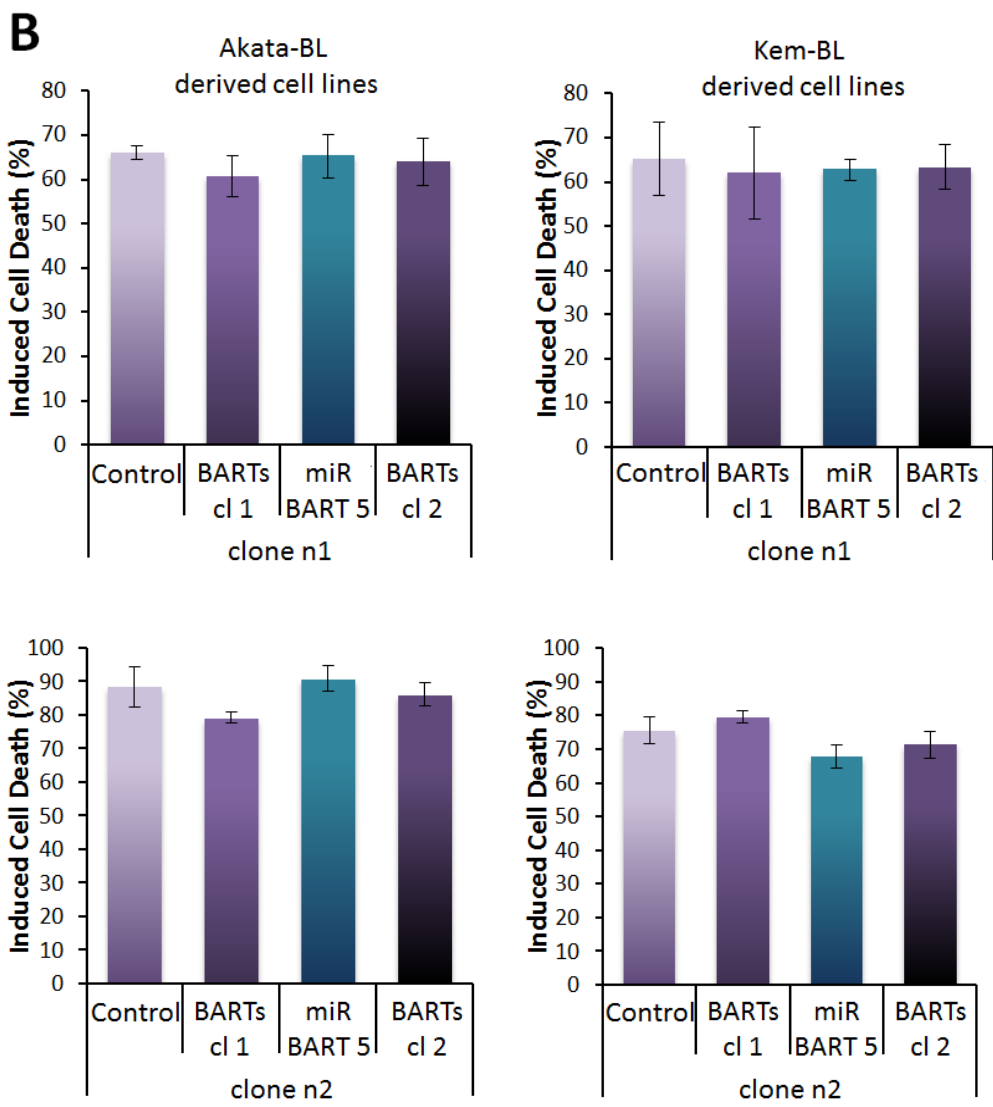
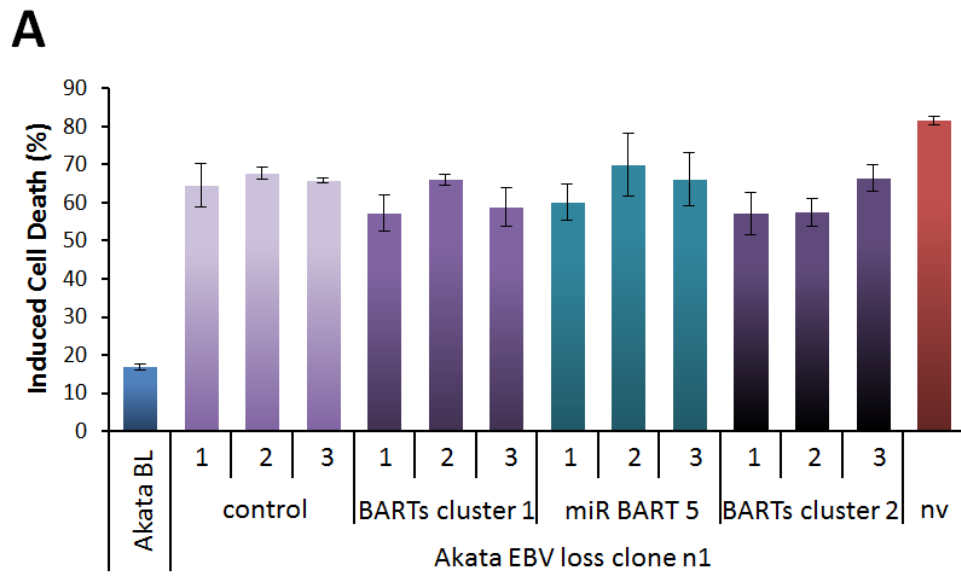


Figure 4.19

4.4.4 Regulation of pro-apoptotic BH3-only proteins by miR BARTs

Although we could show no effect of miR BART expression on the ionomycin-sensitivity of EBV-loss BLs we sought to determine whether the viral miRs were able to modulate the expression of the pro-apoptotic proteins Bim and Puma as has previously been reported in epithelial cell models [365, 366]. In DOX-induced 293 cells, which express similar levels of miR BARTs to EBV-positive cell lines, we were able to show that both miR BART 5 alone and the cluster 2 miRs were able to downregulate Puma protein levels (Figure 4.20-A). Despite this result being seemingly paradoxical since miR BART 5 is within the cluster 1 miRs, this finding does agree with the work of the Raab-Traub group, who reported the same finding in HK1 cells [366]. However, we were unable to show any downregulation in 293 cells of the Bim tumour suppressor protein, which was also reported by this group. In contrast to our finding in 293 cells we found no evidence of downregulation of Puma by the miR BARTs in EBV-loss clones (Figure 4.20-B), which suggests that the targets for miR BARTs in may vary according to cell type, especially since this is coupled with our finding that miR BARTs-transduced BL cells are not protected from apoptosis.

Interestingly, we found that total Puma transcription, using a q-PCR assay which is able to bind all verified Puma mRNAs, seemed to increase in BART-expressing 293 cells, which appears to be in direct discordance with protein expression levels (Figure 4.20-C). This is likely to be due to an increase in transcription of the β -isoform (Figure 4.20-D) that is predicted to be 8-9kDa smaller than Puma- α and did not appear to be detected by the antibody used for these Western blots. We also found that Puma transcription appeared to be unchanged in miR BART-expressing EBV-loss cells compared to EBV-positive and untransduced controls (data not shown).

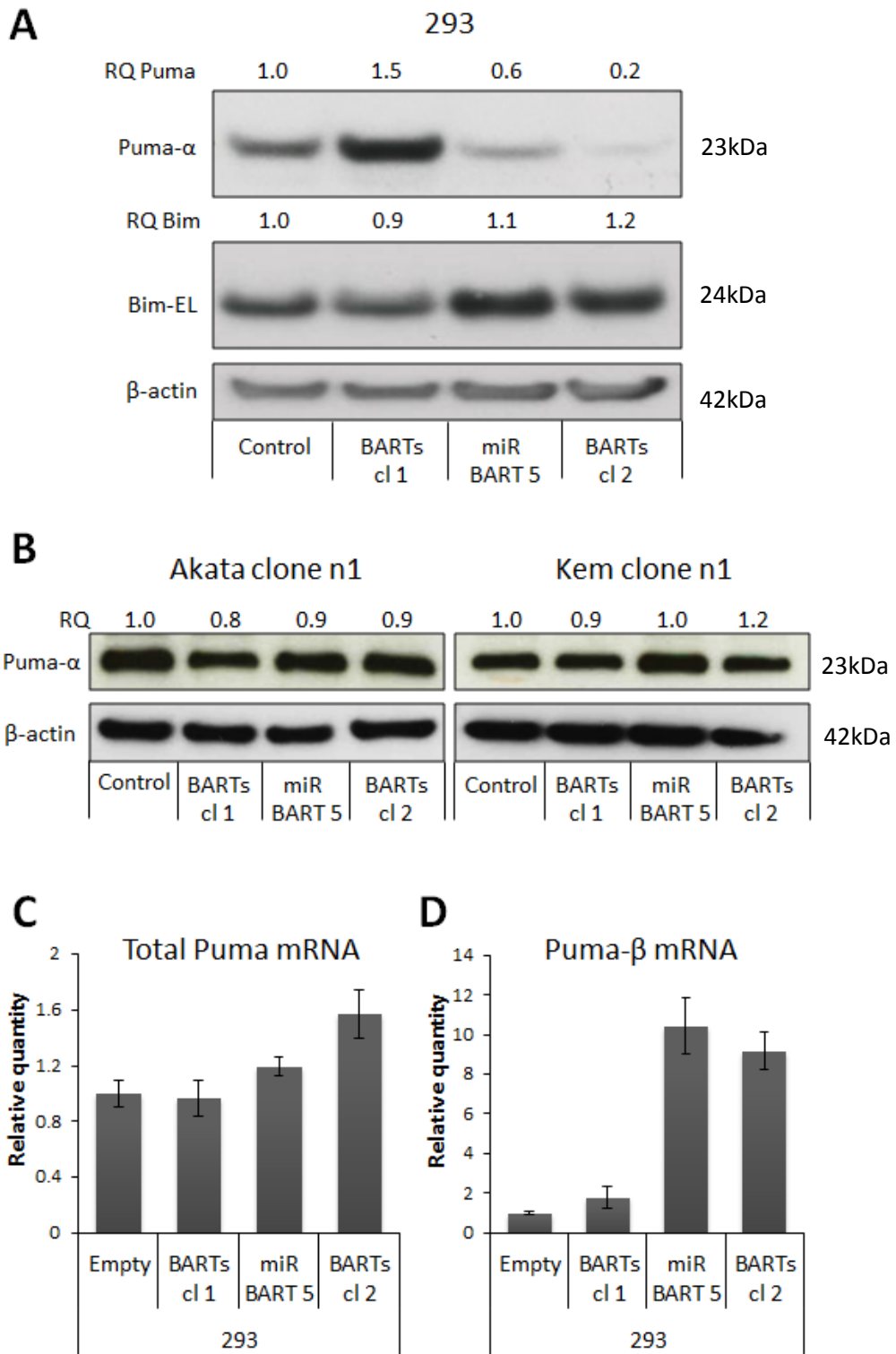


Figure 4.20 Regulation of pro-apoptotic BH3-only proteins by miR BARTs

A Western blot of Puma- α and Bim-EL expression in miR BARTs-expressing 293s

B Western blot of Puma- α expression in miR BARTs-expressing EBV-loss cells

C Relative expression of total Puma mRNA in miR BARTs-expressing 293s

D Relative expression of Puma- β mRNA in miR BARTs-expressing 293s

All inductions carried out using 1 μ g/ml DOX for 48 hours

4.5 Reinfected EBV-loss clones: the Akata virus

4.5.1 Generating Latency I EBV-loss reinfecteds with Akata strain rEBV

Having found that re-expression of EBNA1, EBER RNAs or clusters of BART miRs individually cannot restore apoptosis protection to EBV-loss BLs, we went on to test whether re-infection with EBV could rescue the phenotype. The Takada group who first reported that loss of EBV from Akata-BL cells could sensitise them to apoptosis [309], also showed that re-infecting EBV-loss Akata with an Akata virus BAC could restore protection to the cells [310, 338, 557], and so we set out to repeat this using the same virus strain in EBV-loss clones of Kem-BL and Mutu-BL as well as in Akata-BL.

When our research group first attempted re-infection of EBV-loss clones with Akata strain recombinant EBV (rEBV) we found that, of cells that did take up the virus, the vast majority expressed Latency III-associated viral genes such as EBNA2 and LMP1, which are not expressed in the parental BL cell lines. Subsequently, Latency I reinfecteds could only be isolated from one EBV-loss clone of Mutu-BL in these experiments, which was surprising given that Shimizu and colleagues had reported being able to easily generate EBNA1 positive, EBNA2/LMP1 negative clones from re-infected EBV-loss Akata-BL cells [557].

The Akata BAC carries both GFP and neomycin resistance as markers of infection and so reinfected cells were drug selected for several weeks, sorted for GFP and then screened by q-PCR for the presence of viral DNA. If the viral load was found to be similar to that of an EBV-positive BL (10-100 copies per cell on average) then the cell line was analysed for viral gene expression. However, if viral DNA was detectable at a low level (0.1-10 copies per cell on average) the cells were single cell cloned and then re-screened by q-PCR. At this stage, cell lines and clones that were carrying multiple copies of the EBV genome per cell were analysed by q-PCR, Western blot, FACS and IF to fully characterise viral gene expression. If the reinfected EBV-loss cells were found to have similar gene expression to their EBV-positive

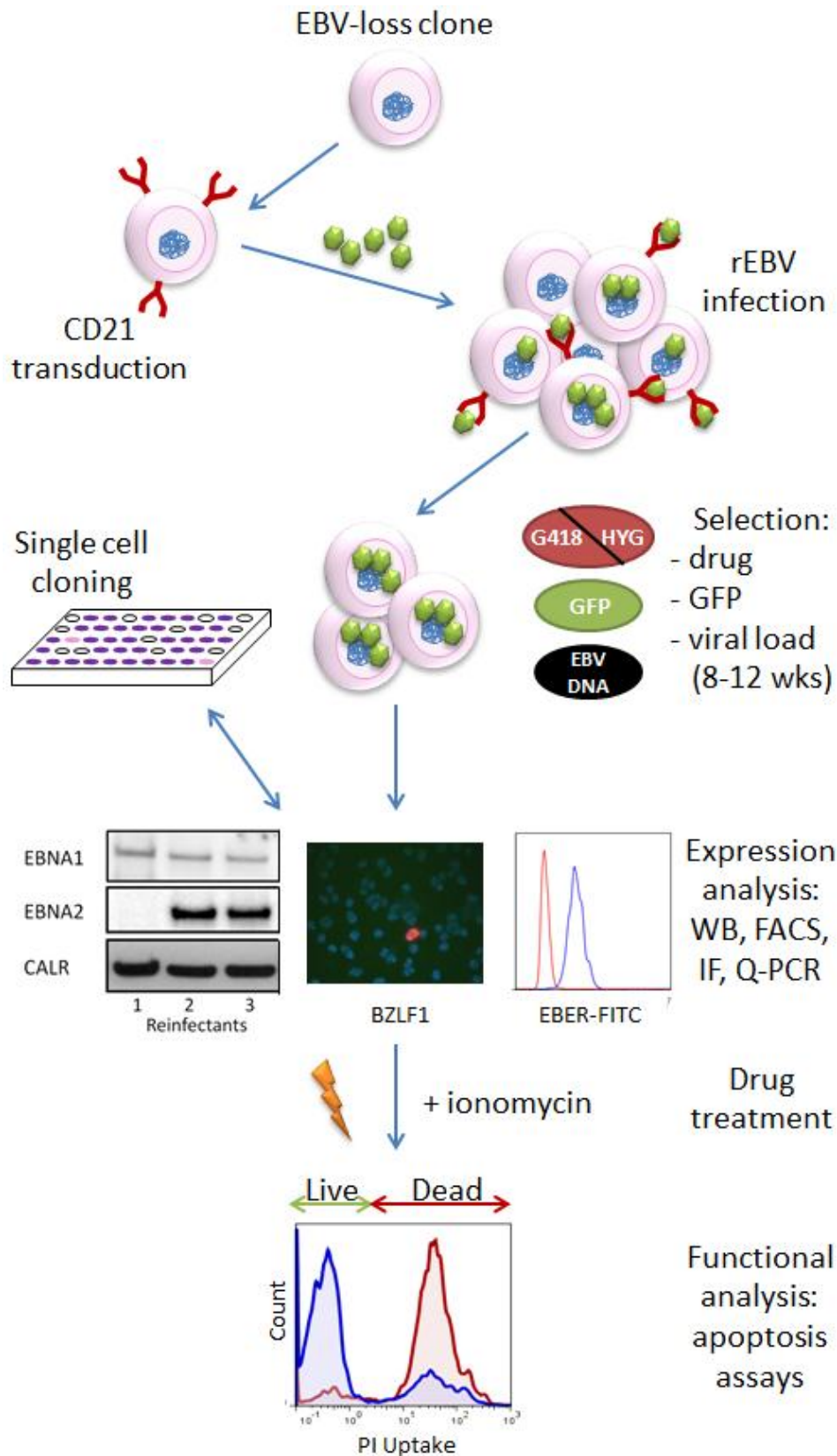


Figure 4.21 Experimental workflow used for re-infection of EBV-loss clones with rEBV. Akata virus rEBV positive cells were selected for on the basis of neomycin resistance using G418 conditioned media whereas 2089-derived rEBV infected cells were selected for on the basis of hygromycin (HYG) resistance

counterparts (i.e. Latency I) they were then used in apoptosis assays to determine whether reinfection had affected the sensitivity of the cells to ionomycin-induced apoptosis. The experimental protocol is depicted in Figure 4.21.

4.5.2 Viral protein expression in Akata virus EBV-loss reinfecteds

After drug selection, all of the cultures that were reinfected with the Akata virus were found to be 100% positive for GFP by FACS, suggesting that every cell contained transcriptionally active virus (Figure 4.22-A). In agreement with the Takada group, every clone that was subsequently selected for gene expression studies expressed EBNA1 protein and the majority of the clones were negative for LMP1 and BHRF1 by Western blot (Figure 4.22-B).

Unfortunately a number of the reinfected clones did express EBNA2 (Figure 4.22-B) and the propensity of reinfecteds to express EBNA2 varied between EBV-loss clones. For example, we were never able to isolate Latency I cells from one of our Akata-BL EBV-loss clones, whereas others gave rise to Latency I cells after only a single attempt. Accordingly, some clones were subjected to several independent infection experiments in order to yield Latency I reinfecteds which expressed only EBNA1 protein by Western blot. We also showed that our reinfecteds had a similar amount of lytic activity to the parental cell lines, as only 1-2% of cells were BZLF1 positive by IF (Figure 4.22-C).

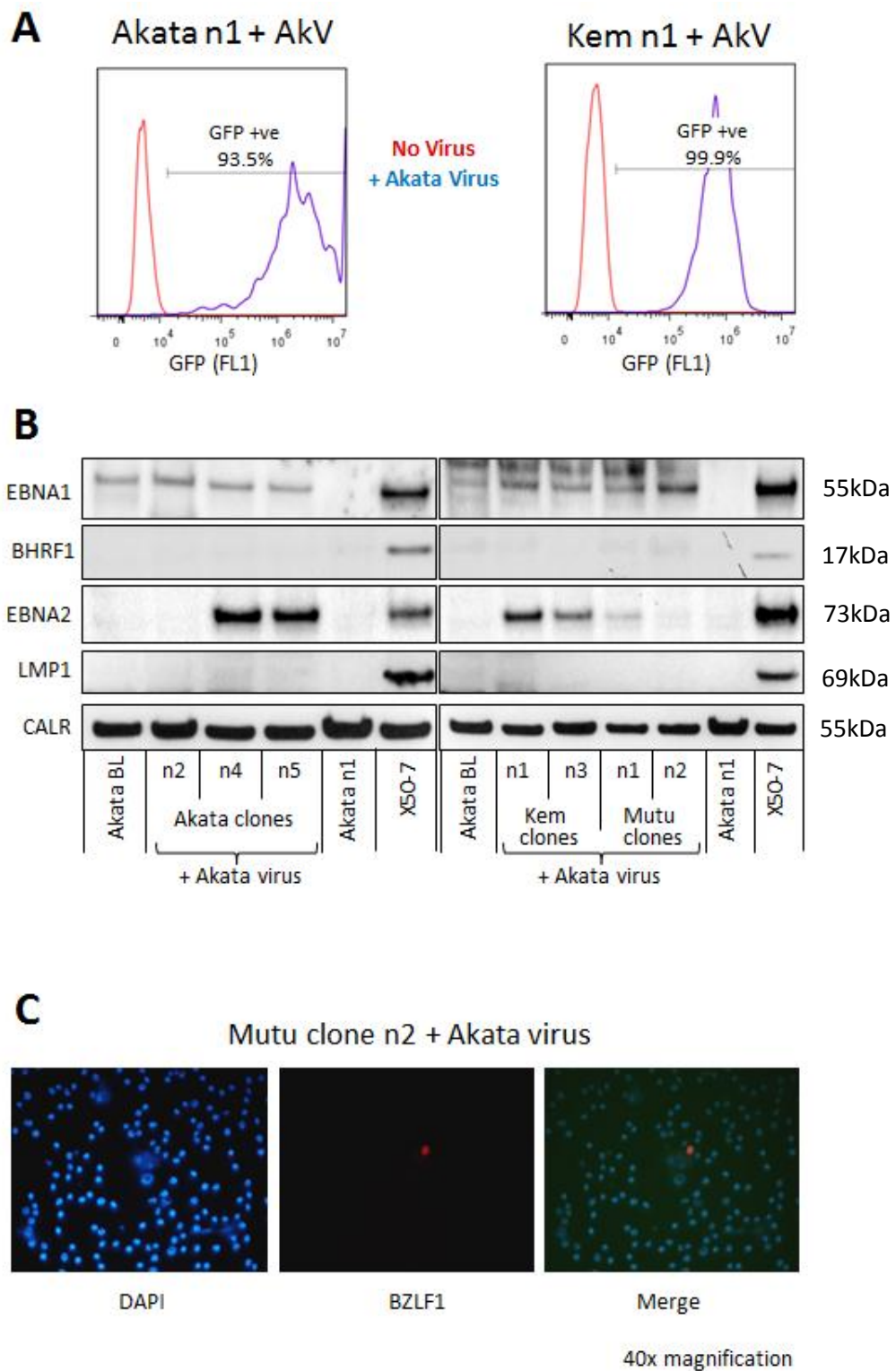


Figure 4.22 Viral protein expression in Akata virus EBV-loss reinfectants

A Example overlays of FACS plots showing EBV-encoded GFP expression in Akata virus reinfected Akata n1 cells and Kem n1 cells

B Example Western blots of Latency I-associated genes in Akata virus reinfectants from a single experiment. Clones that expressed only EBNA1 protein (eg Akata n2 and Mutu n2) were carried forward for use in apoptosis experiments and others were discarded.

C Example BZLF1 immunofluorescence in Akata virus reinfected EBV-loss Mutu n2 cells

4.5.3 Viral transcription in Akata virus EBV-loss reinfecteds

We also profiled viral transcription in our reinfecteds using a panel of 18 q-PCR assays encompassing Latency I, Latency III and lytic cycle-associated genes, in order to more fully characterise gene expression in these cell lines. The method used was identical to that described earlier in this thesis (see Figures 3.3 and 3.20), whereby we expressed the quantities of the individual transcripts relative to either Latency I Kem-BL, the X50-7 LCL, or 100% BZLF1-positive AKBM cells to ascertain how similar the gene expression profiles were to Latency I, Latency III or lytic cells, respectively. In the representative results shown in Figure 4.23; Qp-driven EBNA1 transcripts were expressed relative to Kem-BL; BHRF1, EBNA2, LMP1 and LMP2A were expressed relative to X50-7 and BZLF1 was expressed relative to lytic AKBM cells. Reassuringly, we found that all of the cell lines that were negative for EBNA2 by Western blot had Latency I-like transcriptional profiles.

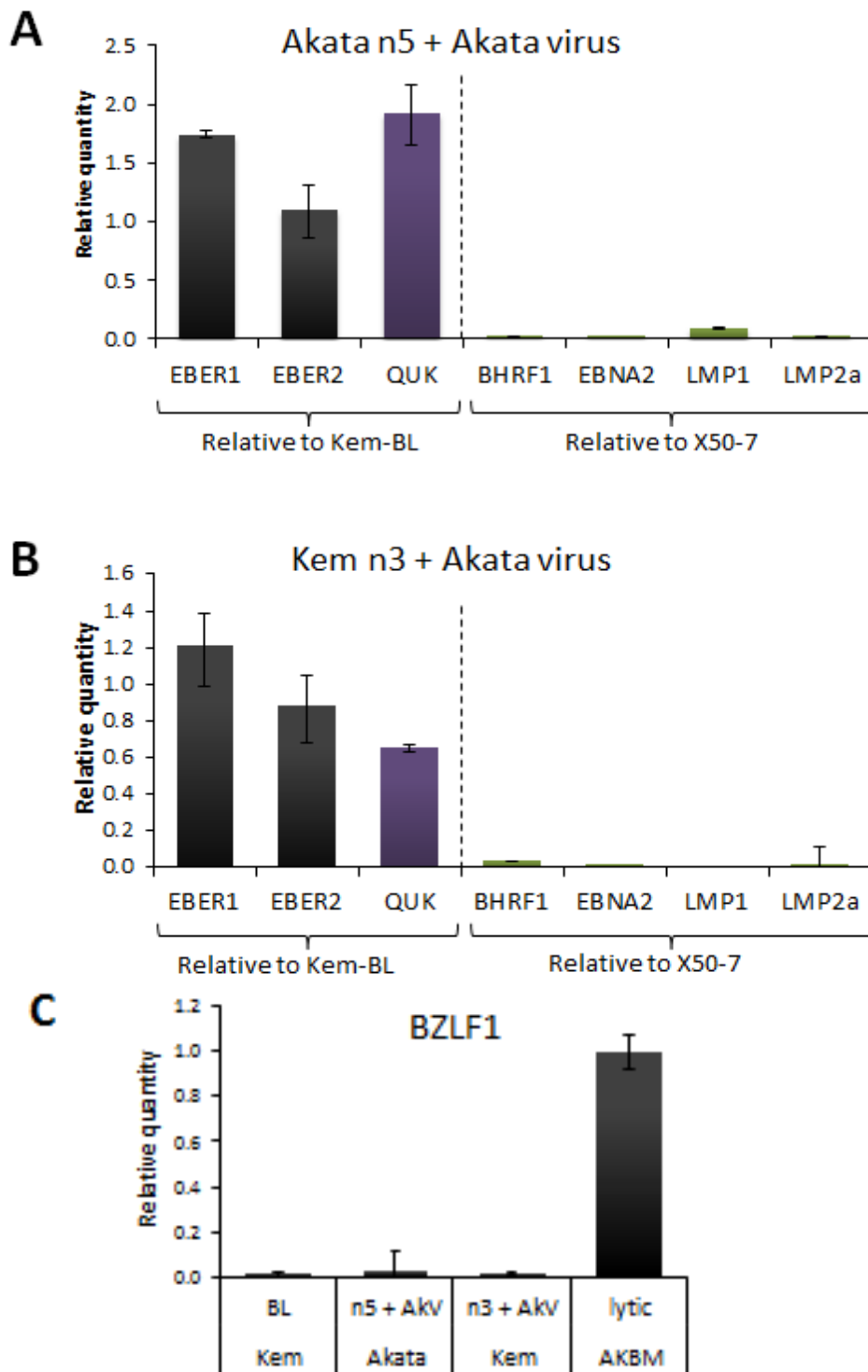


Figure 4.23 Transcription of viral genes in Akata virus EBV-loss reinfectants by q-PCR

A Transcription of Latency I and Latency III-associated genes in Akata clone n5 + Akata rEBV

B Transcription of Latency I and Latency III-associated genes in Kem clone n3 + Akata rEBV

A and B expressed relative to Kem-BL or X50-7 as indicated

C BZLF1 expression from two representative reinfectant lines and Kem-BL, relative to 100% BZLF1-positive AKBM cells

All assays carried out in duplicate, mean and standard deviation are plotted, relative quantitation was calculated using the $\Delta\Delta C_t$ method **AkV** = Akata virus

4.5.4 Expression of viral microRNAs in Akata virus EBV-loss reinfecteds

Since the BART miRs may play a role in the apoptosis phenotype of Latency I BL cells [99], we wanted to know whether they are expressed to levels similar to Latency I BLs in EBV-loss cells reinfected with rEBV. We therefore measured the expression of several miR BARTs by stem-loop q-PCR. Representative data from two cell lines that were found to express comparatively high or low levels of miR BARTs, respectively, is shown in Figure 4.24. In general, we found that our reinfected cell lines express relatively low levels of miR BARTs, around 5-20% of that seen in Kem-BL however, since the levels in reinfecteds were still higher than those seen in Akata-BL, which also displays the EBV-loss phenotype we were not overly concerned about this finding. Interestingly, these levels were similar to levels of miR BARTs expressed in EBV-loss clones transduced with our miR BART lentiviruses.

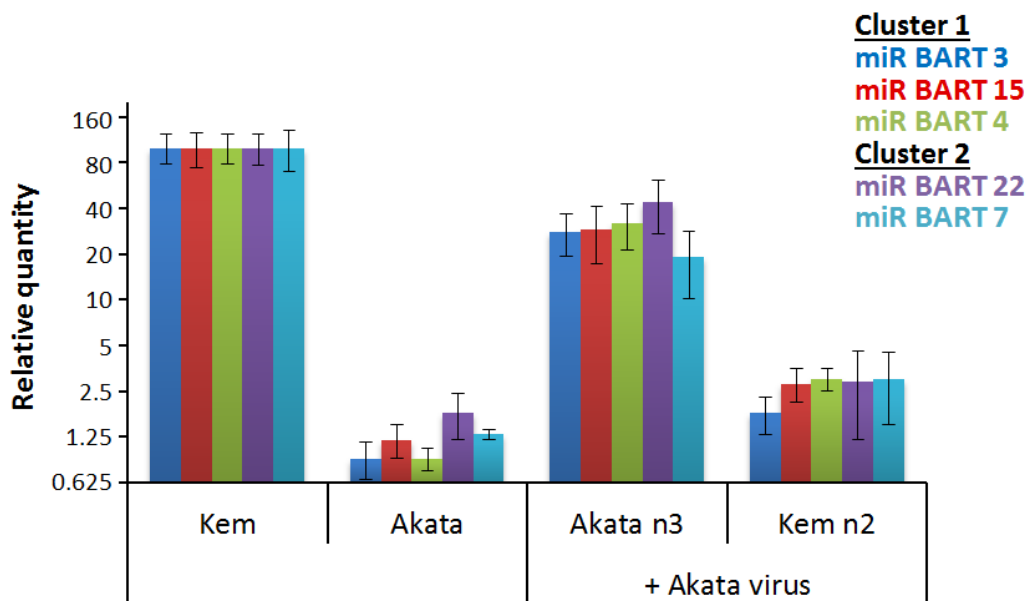


Figure 4.24 Expression of BART miRNAs in Akata virus EBV-loss reinfecteds by stem loop q-PCR

Expressed relative to Kem-BL using the $\Delta\Delta C_t$ method and plotted on a log₂ scale due to the magnitude of difference in expression levels between different cell lines. All measurements were carried out in duplicate and mean and standard deviation of a representative experiment are shown.

4.5.5 The apoptosis phenotype of Akata virus EBV-loss reinfectants

We successfully isolated Latency I reinfectants from three different EBV-loss clones each of Akata-BL, Kem-BL and Mutu-BL, numbering 9 reinfectant cell lines in total. In apoptosis assays we found, in agreement with the Takada and Sample groups, that reinfection with the Akata rEBV was able to completely and consistently rescue the EBV-loss phenotype, protecting the EBV-loss cells to a level that was indistinguishable from that of the parental BL cell lines (Figure 4.25-A and 4.25-B).

However, a full rescue of the EBV-loss phenotype only occurred in 6 of the 9 cell lines generated. In two of the three remaining cell lines (Akata n5 + Akata rEBV, and Kem n1 + Akata rEBV), we did see a substantial and significant amount of protection that was consistent in all assays, nevertheless the reinfectant cells were never protected to quite the same degree as EBV-positive parental cells (Figure 4.25-C). Surprisingly, the final cell line in this set, Akata n2 + Akata rEBV, could not be rescued by reinfection with the Akata virus and exhibited an identical phenotype to uninfected cells of the same loss clone (Figure 4.25-D), despite expressing EBNA1, EBERs and miR BARTs. Interestingly, we could find no correlation between the protection conferred by reinfection with Akata rEBV and viral gene expression. For example; the lowest miR BART-expressing reinfectant, Kem n2, was fully protected (see Figures 4.24 and 4.25-B). Since we used the same panel of EBV-loss clones for all of our Latency I gene expression and reinfection assays, we conclude that the EBV-loss phenotype can be rescued by multiple, but not individual, Latency I-associated genes, although clonal variation between EBV-loss isolates also affects the apoptosis phenotype of BL cells.

Figure 4.25 Apoptosis phenotype of Akata virus EBV-loss reinfectants

A Example of experimental variability in Kem clone n3 Akata rEBV reinfected cells. Data from three independent experiments carried out in triplicate

B Representative apoptosis data from Akata rEBV reinfected EBV-loss cells in the Akata-BL, Kem-BL and Mutu-BL backgrounds.

C Representative apoptosis data from Akata n5 + Akata virus, which was not fully rescued

D Representative apoptosis data from Akata n2 + Akata virus, which was not protected

All measurements were carried out in triplicate and mean and standard deviation of a representative experiment are shown for panels B, C and D. Statistical analysis was carried out using a two-tailed Students T-test

AkV = Akata virus

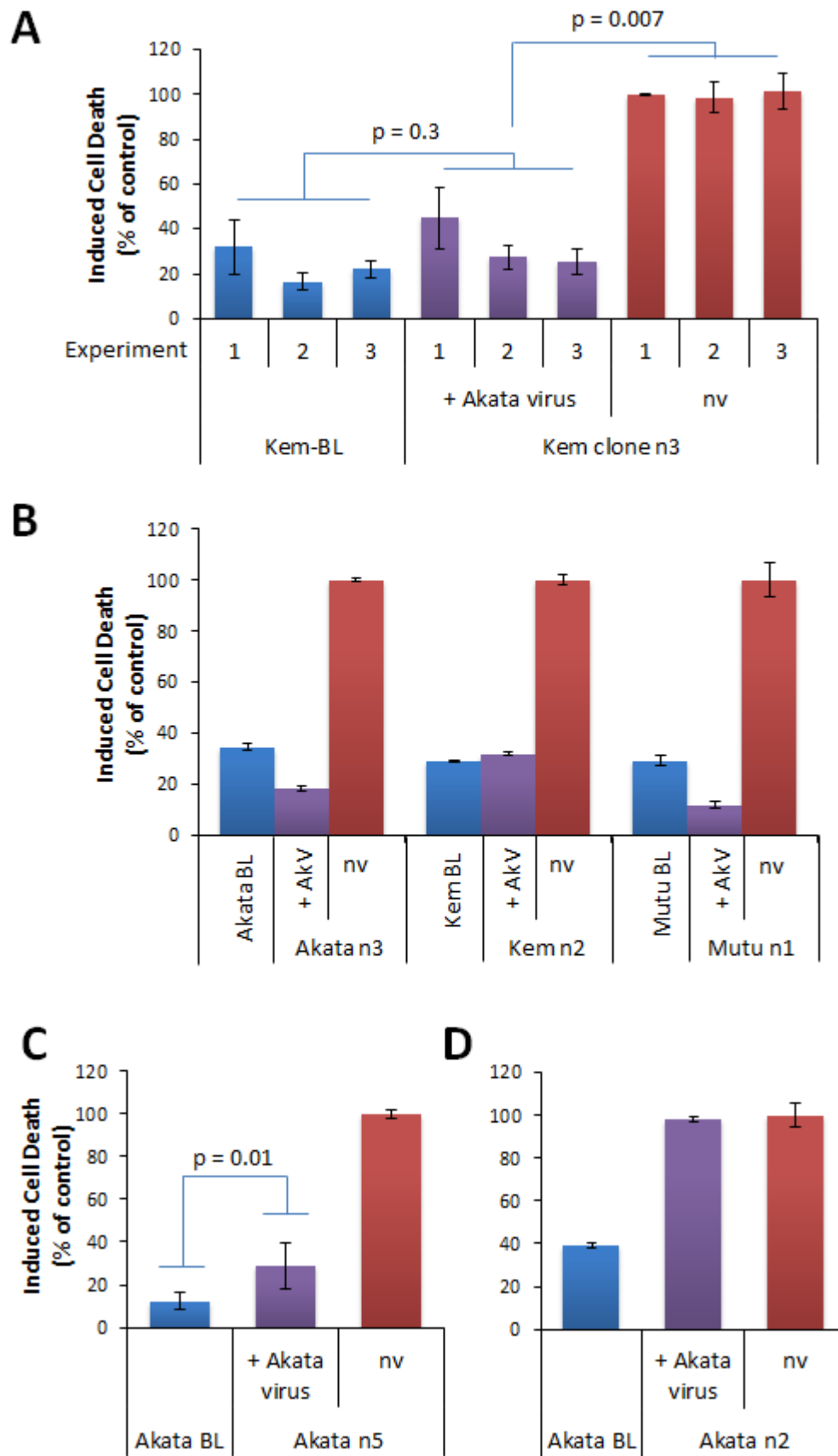


Figure 4.25

4.6 Reinfected EBV-loss clones: the B95.8 rEBV

4.6.1 Generating Latency I EBV-loss reinfecteds with CpWp-KO strain rEBV

During primary infection of resting B cells, expression of the majority of the latent genes, (i.e., EBNA1, 2, 3A, 3B, 3C, LP and BHRF1), is initially driven by the Wp promoter and later from the Cp promoter, whilst LMP1 and LMP2 are transactivated by EBNA2 [85, 86]. We therefore theorised that knocking out the Wp Cp promoters would force the virus to consistently and permanently adopt a Latency I expression pattern, driving EBNA1 expression from the Qp promoter as it is in EBV-positive BLs. Such a virus (a C promoter and W promoter knock out; CpWp-KO) had already been generated by Dr Rose Tierney for use in another project [485] and so we carried out reinfections of EBV-loss BLs using the CpWp-KO 2089 rEBV. Like the Akata BAC, EBV-loss cells were drug selected for several weeks at which point clones carrying rEBV were screened for viral gene expression (see Figure 4.21).

In comparison to the Akata virus fewer CpWp-KO infected cultures survived drug selection and viral loads in CpWp-KO reinfecteds tended to be low (<10 genomes per cell) (data not shown). We also found in some cultures which were single cell cloned, that almost every clone had an average of 1-2 genomes per cell by q-PCR, suggesting that the EBV genome in these cells may have been integrated rather than episomal. Although generating reinfecteds using the CpWp-KO virus was less efficient than we had hoped, we were able to isolate a total of six cell lines with a genome load of at least 8 genomes per cell; 3 in EBV-loss clones of Akata-BL, 2 in EBV-loss clones of Kem-BL and 1 from an EBV-loss clone of Mutu-BL.

4.6.2 Viral protein expression in CpWp-KO virus reinfecteds

Figure 4.26-A shows Western blots carried out on a representative set of CpWp-KO reinfecteds that were generated and screened at the same time. As expected, EBNA1 was

generally detectable in cells that were found to contain viral DNA, but we could never detect any EBNA2, BHRF1 or LMP1. In one reinfectant, Akata n3 + CpWp-KO virus, EBNA1 protein was not detectable however, we later showed that this cell line actually had a viral load of less than one copy per cell, and so may have contained a mixture of EBV-positive and EBV-loss cells (data not shown). This was not investigated further and the cell line was not used in apoptosis assays. As with the Akata virus, we found that only 1-2% of reinfected cells were BZLF1 positive by IF suggesting that these lines support a similar level of lytic viral gene expression to parental EBV positive BLs (Figure 4.26-B).

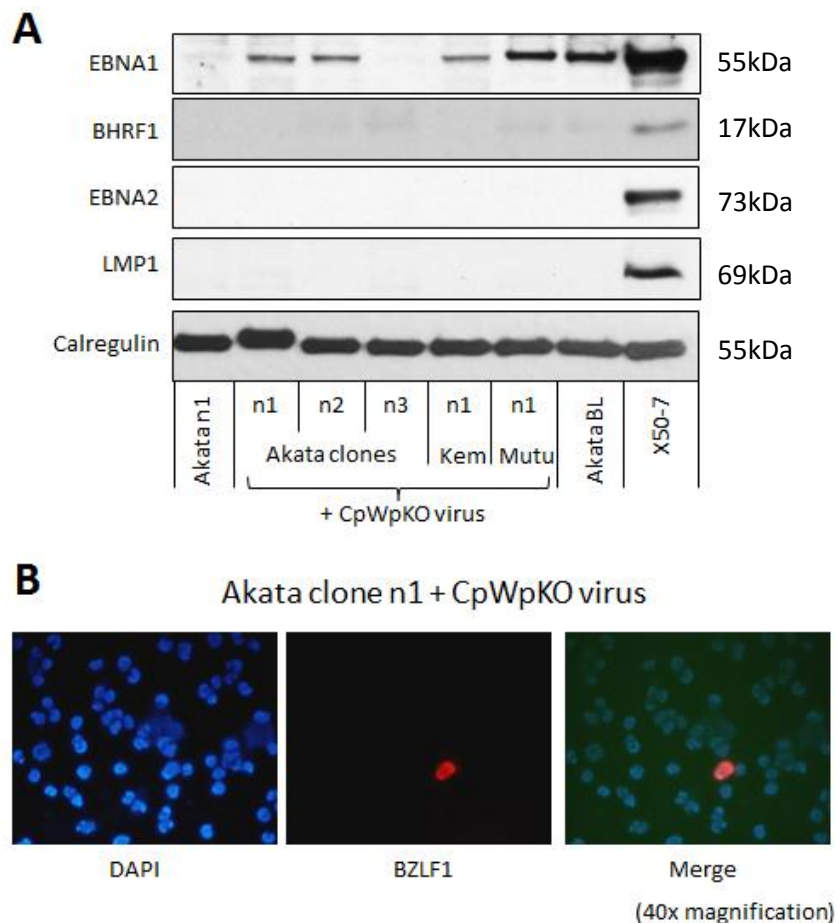


Figure 4.26 Protein expression in CpWp-KO reinfectants

A Representative Western blots with calregulin as a loading control. Antibodies: EBNA1 – Human serum (AMo), BHRF1 – 5B11 mouse monoclonal, EBNA2 – PE2 mouse monoclonal, LMP1 – CS1-4 mouse pooled clones

B Representative immunofluorescence images showing nuclear staining (DAPI, blue) and a BZLF1 positive cell (red) surrounded by latent (BZLF1 negative) cells. Antibody was mouse monoclonal α -BZLF1 made by Martin Rowe as detailed in the methods section

4.6.3 EBER *in situ* hybridisation in CpWp-KO virus reinfectants

Although the CpWp-KO virus carries a GFP marker, for reasons not fully understood it is not reliably expressed in B cells, therefore we measured EBER expression at the single cell level to ensure that every cell in CpWp-KO cell lines contained transcriptionally active virus. Reinfected cells and controls were hybridised to an EBER-specific fluorescently-labelled probe or a negative control probe in solution before being analysed by FACS. Of the six reinfectants that were used in apoptosis assays, at least 98% of cells were EBER positive in every case. Representative data from 2 of the 6 lines and uninfected controls is shown in Figure 4.27.

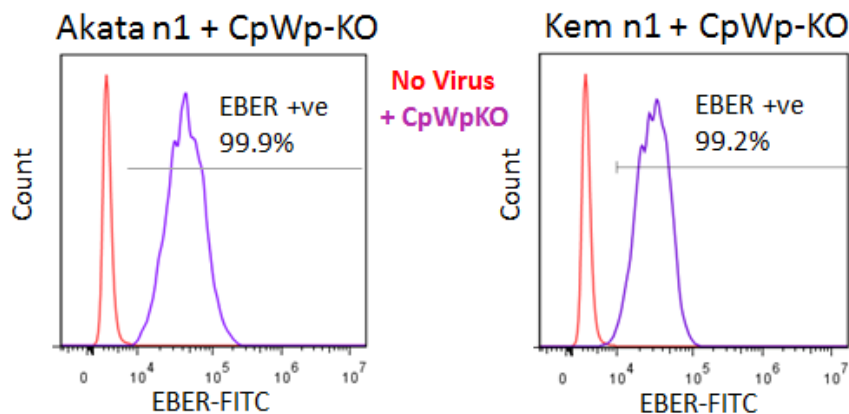


Figure 4.27 Representative EBER FACS in CpWp-KO reinfectants

Red = uninfected EBV-loss cells, **purple** = CpWp-KO reinfectants

EBER RNA was detected using an EBER-specific, FITC-conjugated PNA probe. Cells of the relevant reinfectant hybridised to a scrambled control PNA-FITC probe and EBV-positive EBER-PNA-FITC stained cells were included as additional controls

4.6.4 Viral transcription in CpWp-KO virus EBV-loss reinfected cells

Viral transcription in the CpWp-KO reinfected cells was measured using both standard q-PCR and microfluidic dynamic array chips, which can be used to run up to 48 different q-PCR assays on each of 48 different samples in a single run. Example data from two CpWp-KO reinfected cells that were analysed on a microfluidic chip is shown in Figure 4.28-A. Using the same relative quantitation strategy as was used for the Akata virus reinfected cells we found that CpWp-KO reinfected cells exhibited a Latency I-like expression pattern and consistent with our Western blots, BHRF1, EBNA2 and LMP1 transcripts were low or undetectable in comparison to X50-7. We did detect a small number of LMP2A transcripts, suggesting that these cell lines contained intact terminal repeat regions, indicative of the presence of episomal virus particles [558]. Again, BZLF1 transcript levels indicated a similar amount of lytic activity to that found in the parental EBV-positive cells (Figure 4.28-B).

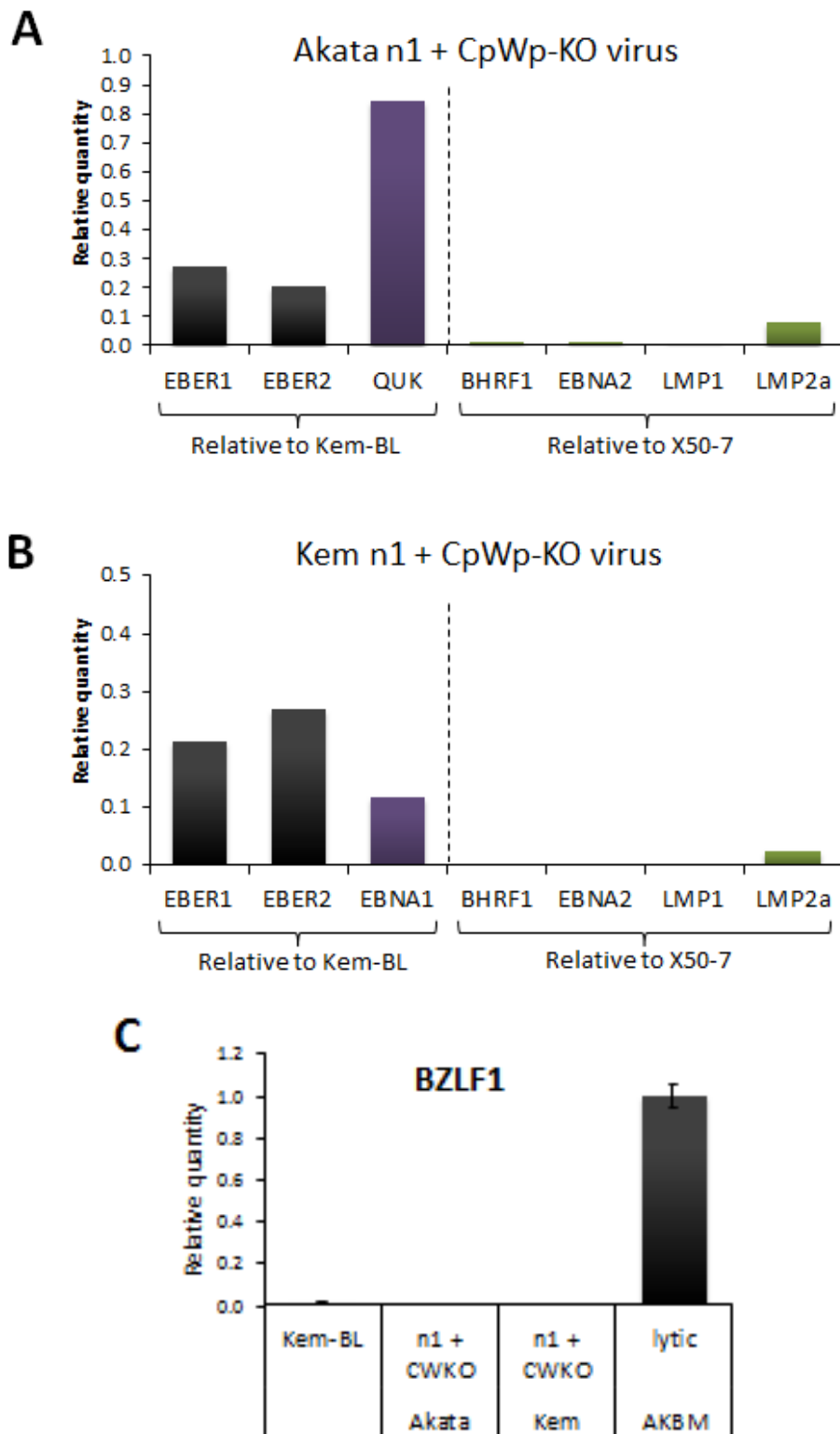


Figure 4.28 Viral transcript expression in CpWp-KO reinfectants by microfluidic q-PCR

A Transcription of Latency I and Latency III-associated genes in Akata clone n1

B Transcription of Latency I and Latency III-associated genes in Kem clone n1

A and B expressed relative to Kem-BL or X50-7 as indicated using $\Delta\Delta C_t$ method

C BZLF1 transcription in Akata n1 and Kem n1 compared to lytic Akata (AKBM)

Data from microfluidic chip q-PCR carried out in duplicate

4.6.5 Expression of viral microRNAs in CpWp-KO EBV-loss reinfectants

Since the CpWp-KO virus is a derivative of the B95.8 EBV strain it harbours a 12kb deletion in the BamHI A locus, and therefore only contains a small subset of the miR BARTs which lie outside the deletion [559, 560]. When we checked expression of those that remain in the virus (miR BARTs 3, 4, 1 and 15) we found that they were also expressed at low levels compared to Kem-BL (<5% of Kem-BL levels), but were still comparable to, or higher than, levels in Akata-BL (Figure 4.29).

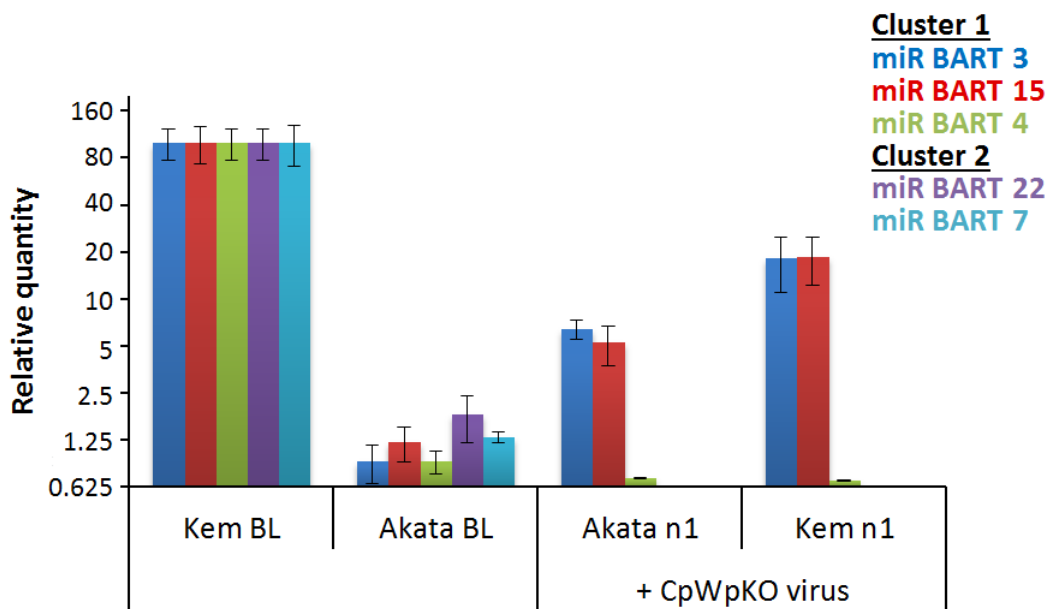


Figure 4.29 Expression of BART miRNAs in CpWp-KO EBV-loss reinfectants

Expressed relative to Kem-BL and plotted on a log₂ scale due to magnitude of difference in expression levels between different cell lines. All measurements were carried out in duplicate and mean and standard deviation of a representative experiment are shown.

4.6.6 Phenotype of EBV-loss clones reinfected with CpWp-KO virus

We next carried out apoptosis assays on the six CpWp-KO virus reinfected EBV-loss clones that had >8 viral genomes per cell and expressed Latency I. Although we found convincing evidence of apoptosis protection in 5 of the 6 strikingly, and in contrast to what was observed with the Akata-virus, we were unable to restore any of the 5 to their parental phenotype. Four of the reinfected cells were considerably protected; their uninfected EBV-loss counterparts underwent more than twice the amount of cell death in response to identical stimulus. However, the reinfected cells were always noticeably and significantly less protected than their EBV-positive counterparts. This characteristic was found to be consistent between individual experiments (Figure 4.30-A) and across different tumour backgrounds (Figure 4.30-B). In the 5th CpWp-KO reinfected cell that showed apoptosis protection the effect was further reduced; the Kem n1 CpWp-KO reinfected cell was only slightly protected from ionomycin-treatment compared to isogenic EBV-loss cells, though this difference was statistically significant (Figure 4.30-C). Interestingly, this was one of the same clones to which the Akata virus restored only partial apoptosis resistance (a CpWp-KO reinfected cell was never isolated from the second clone which exhibited this phenotype).

In the sixth CpWp-KO reinfectant, Akata n2, the presence of the virus had no discernible effect and the cells were phenotypically identical to the uninfected EBV-loss clone (Figure 4.29-D). Intriguingly, Akata n2 is the same clone that could not be protected by reinfection with the Akata virus, suggesting that this clone is fundamentally different to the other EBV-loss clones, perhaps reflecting the acquisition of a cellular mutation *in vitro*. Clearly, although the CpWp-KO virus is able to confer apoptosis protection to EBV-loss BLs it is incapable of fully compensating for the loss of the endogenous virus from these cells.

Figure 4.30 Apoptosis data from CpWp-KO reinfected EBV-loss clones

A Comparison of data from three independent experiments carried out in triplicate on CpWp-KO reinfected Akata n1 cells and controls to demonstrate consistency of phenotype

B CpWp-KO reinfected Akata n3, Kem n2 and Mutu n1 cells in which the virus conferred partial protection

C CpWp-KO reinfected Kem n1 cells in which the virus conferred only slight protection

D CpWp-KO reinfected Akata n2 cells in which the virus conferred no protection

All assays were carried out in triplicate on three occasions and data shown are the mean and standard deviation. Statistical analyses were carried out using a two-tailed Students T-test

CW-KO = CpWp-KO virus, nv = no virus (uninfected)

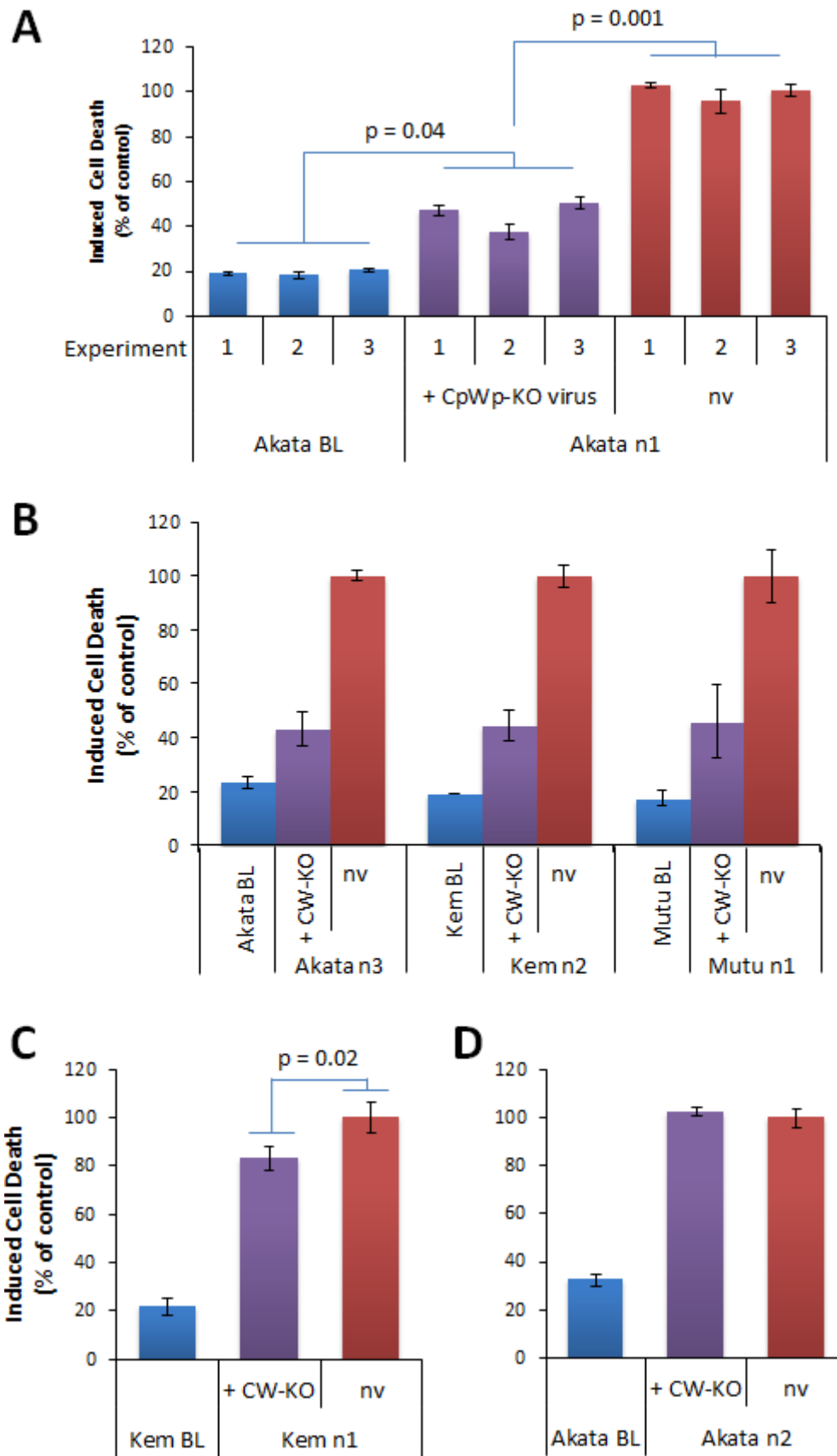
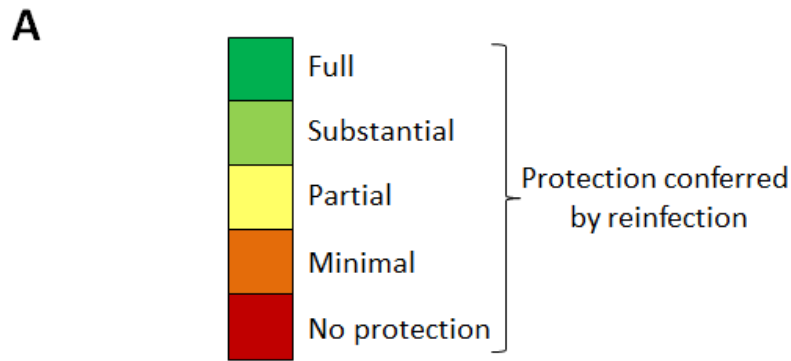


Figure 4.30

4.6.7 Comparison of apoptosis in CpWp-KO and Akata rEBV reinfectants

Figure 4.31-B is a graphical summary of all of the CpWp-KO and Akata virus reinfectants that were generated and used in apoptosis assays in this study. The relative amount of protection conferred to each clone by each virus is represented using a colour grading system (Figure 4.31-A). Although we could not generate a complete set of reinfectants (derivatives of every EBV-loss clone reinfected with each of the two virus strains), this representation clearly demonstrates that reinfected EBV-loss clones with the Akata virus tends to restore full or almost full protection from ionomycin-induced cell death, whereas the CpWp-KO virus is only ever able to restore partial protection at best. Interestingly, those clones which deviate from this general rule do so for both virus strains; most notably the Akata n2 EBV-loss clone could not be rescued by infection with either Akata or CpWp-KO rEBV. The Kem n1 clone could only be partially restored, although the differential amount of protection conferred by re-infection with Akata virus relative to CpWp-KO virus was evident. It is possible that this phenomenon is caused by these clones having acquired additional genetic mutations under conditions of cellular stress during single cell cloning, although we have not investigated this hypothesis.



B

Cell Line	Virus	CpWp-KO virus	Akata virus
Akata-BL clones	n1	Partial	ND
	n2	No protection	No protection
	n3	Partial	Full
	n5	ND	Substantial
Kem-BL clones	n1	Minimal	Substantial
	n2	Partial	Full
	n3	ND	Full
Mutu-BL clones	n1	Partial	Full
	n2	ND	Full
	n3	ND	Full

Figure 4.31 Apoptosis phenotypes of CpWp-KO and Akata virus reinfectants

A Key to colour chart:

No protection = statistically indistinguishable from uninfected EBV-loss cells

Full = statistically indistinguishable from parental EBV-positive cells

Substantial = small significant difference between EBV-positive and reinfected (more than 70% protected)

Partial = intermediate phenotype between EBV-positive and loss (~50% protected)

Minimal = small but significant difference between EBV-loss and reinfected (less than 30% protected)

B Comparison table, ND = not done due to being unable to isolate a Latency I reinfected in this clone

4.7 Loss of Akata rEBV from Akata clone n5 reinfected cells

In one reinfected cell line, Akata n5 + Akata rEBV, which was substantially, but never fully protected from ionomycin-induced apoptosis we wanted to determine the level of heterogeneity in viral gene expression between cells in the culture, as we hypothesised that this could explain the phenotype we had observed. First we re-cloned the cell line, and determined EBNA1 levels by Western blot. Interestingly, levels of EBNA1 protein did show some variability, although the protein was still clearly detectable in every clone (Figure 4.32-A). To test whether these varying levels of EBNA1 could affect the phenotype of the cells we carried out apoptosis assays on two clones which expressed high EBNA1 compared to two which expressed the lowest levels of EBNA1. We consistently found that one of the low EBNA1-expressing clones was more sensitive to ionomycin-treatment than the other clones, apparently supporting the idea that very low viral gene expression levels might be insufficient to protect EBV-loss clones from apoptosis (Figure 4.32-B). However, further investigation indicated that this interpretation is probably incorrect. During single cell cloning the media used for the cultures was not supplemented with G418 to select for retention of the rEBV genome and so it appeared that, whilst three of the four clones had retained the virus and were still >99% GFP positive, the fourth clone, which showed increased sensitivity to apoptosis, had lost the virus in the majority of the cells and was now only 20% GFP positive (Figure 4.32-C).

Remarkably, loss of the virus had led directly to a loss in protection from apoptosis and so we found that we could directly reverse the EBV-associated apoptosis phenotype in cells that had been infected with and then lost EBV for a second time. Additionally, when we looked at GFP expression in the live population of cells from the sensitive clone after ionomycin treatment, almost all of the surviving cells were GFP-positive. Showing that even in a mixed population, only those cells that contained EBV were able to survive drug treatment, providing direct evidence that the presence of EBV really is responsible for the phenotype we see and is not a consequence of *in vitro* culture, single cell cloning or drug selection.

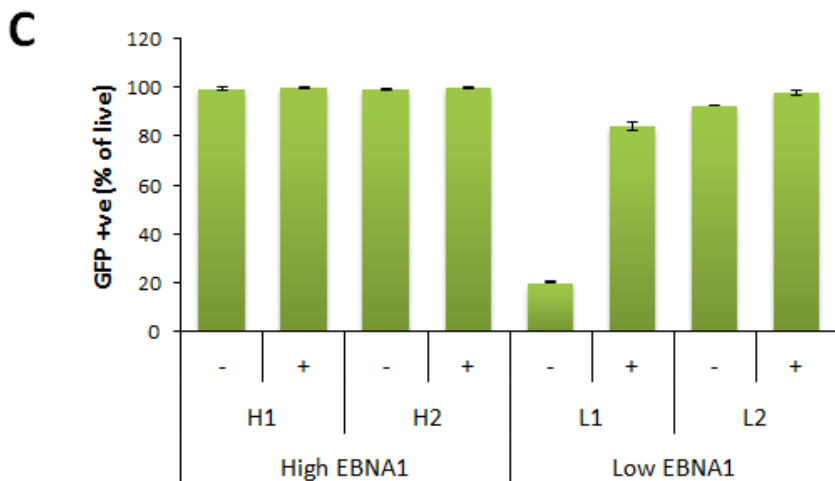
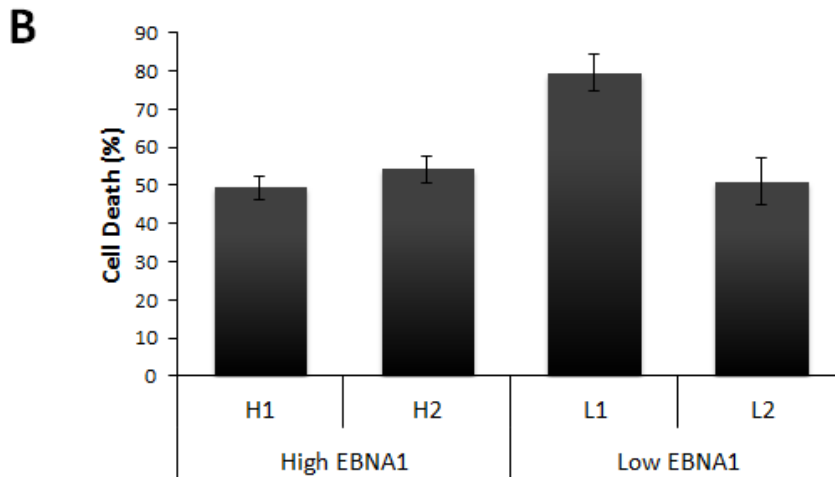
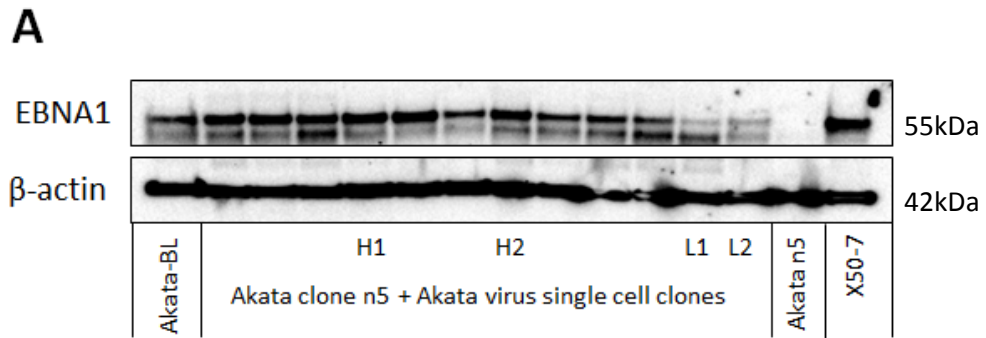


Figure 4.32 Effect of a second EBV-loss event on cell death in Akata n5 subclones
A EBNA1 in subclones of Akata n5 + Akata rEBV, H = high EBNA1, L = low EBNA1. Blotted using AMo human serum which recognised EBV-EBNA1
B Representative apoptosis assay data on Akata n5 + Akata rEBV subclones
C GFP positivity of ionomycin-treated and untreated cell populations
 Plus (+) and minus (-) denote ionomycin treated and untreated, respectively. Apoptosis assays were carried out in triplicate on three occasions and data shown are mean and standard deviation

4.8 Further investigation of viral transcription in Latency I BLs

That the Akata virus strain could protect better than the CpWp-KO virus seemed a very surprising result considering that both ostensibly expressed only Latency I-associated genes. This left us with two hypotheses; that the CpWp-KO simply expressed levels of the Latency I genes that were too low to be effective, or that a factor encoded within the B95.8 deleted region, such as the BART miRs, may be necessary for full restoration of the apoptosis protection phenotype. However, since Latency I genes were expressed to variable levels in Akata virus re-infectants, and expression did not appear to correlate with the amount of apoptosis protection restored, we considered the second hypothesis to be more credible.

We were also intrigued by a paper that had been published by the Flemington group [174], which reported that LF3, a lytic cycle-associated gene encoded on the opposite strand to the miR BARTs in the BamHI A region, is abundantly expressed in latent Mutu-BL and Akata-BL cells. In fact their analysis of polyadenylated transcripts from these cell lines by RNA sequencing showed that LF3 was present in latent BLs at copy numbers in excess of 98% of all cellular genes. In light of this we decided to examine by q-PCR, the expression of LF3 and its sister genes LF1 and LF2, which also reside within the BamHI A region, in EBV-infected cell lines (Figure 4.33).

We assayed a large number of cell lines of various latency types and derived from a range of diseases and found detectable transcripts of LF1 LF2 and LF3 in every sample, including strictly latent cord blood-derived LCLs. Although expression of all three LFs did increase dramatically in AKBM cells induced into lytic cycle compared to uninduced AKBM cells, we also found that the Ct values obtained for LF3 in Latency I BLs were second only to EBER1 (data not shown). This suggested that LF3 may be present in numbers that would average many hundreds of copies per cell, making it unlikely that what we were measuring could be due to the presence of a small number of cells in lytic cycle. In order to absolutely quantify copy numbers of LFs in

EBV-infected cells, we used microfluidic chips to assay 45 EBV genes (including LFs) and 3 endogenous controls simultaneously in a number of Latency I BLs compared to a plasmid DNA standard. The detailed viral gene expression profiling of a large number of EBV-infected cell lines will be published elsewhere [175], but data for the expression of Latency I-associated genes and LFs in a panel of Latency I BLs is shown in Figure 4.34.

All EBV infected cells express EBNA1 as they are dependent upon its presence to maintain the viral genome, but due to the stability and long half-life of the EBNA1 protein it is only transcribed at very low levels [174]; less than 10 copies per cell by our estimates from absolute quantitation studies [175]. Although we see variation between Latency I BLs it is clear that transcripts of LF1, LF2 and LF3 are present in BL cells in at least equivalent abundance to EBNA1, and in some cases, at many times higher levels. Currently, we do not have functional data to support a role for these genes in Latency I BLs as our efforts to this end have been hampered by a lack of reagents. However, the new expression data do suggest that the accepted dogma of Latency I-associated genes may extend beyond the EBERs, EBNA1 protein and BART microRNAs.

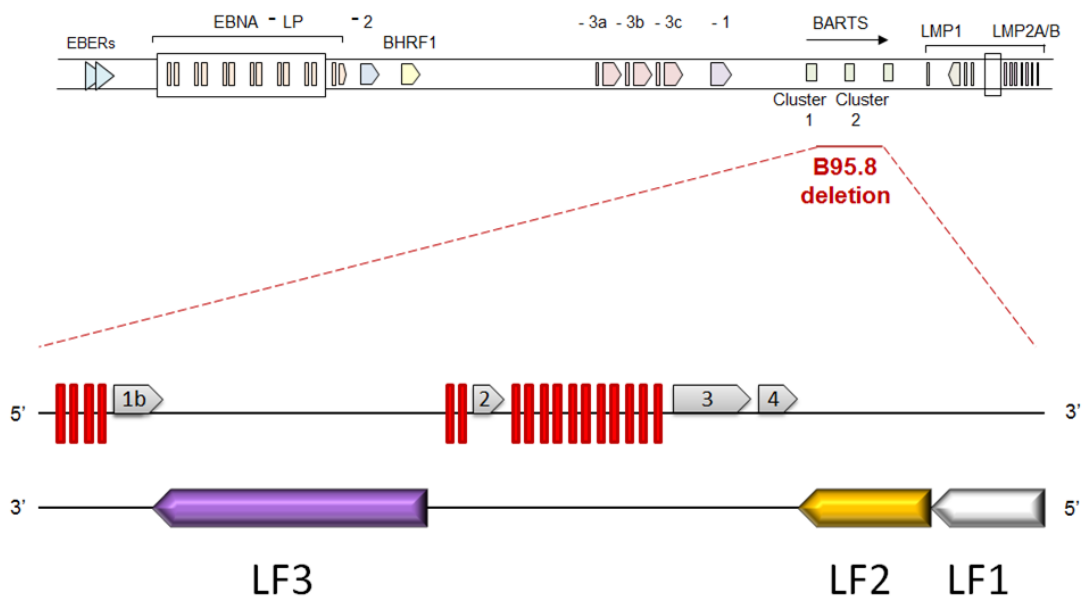
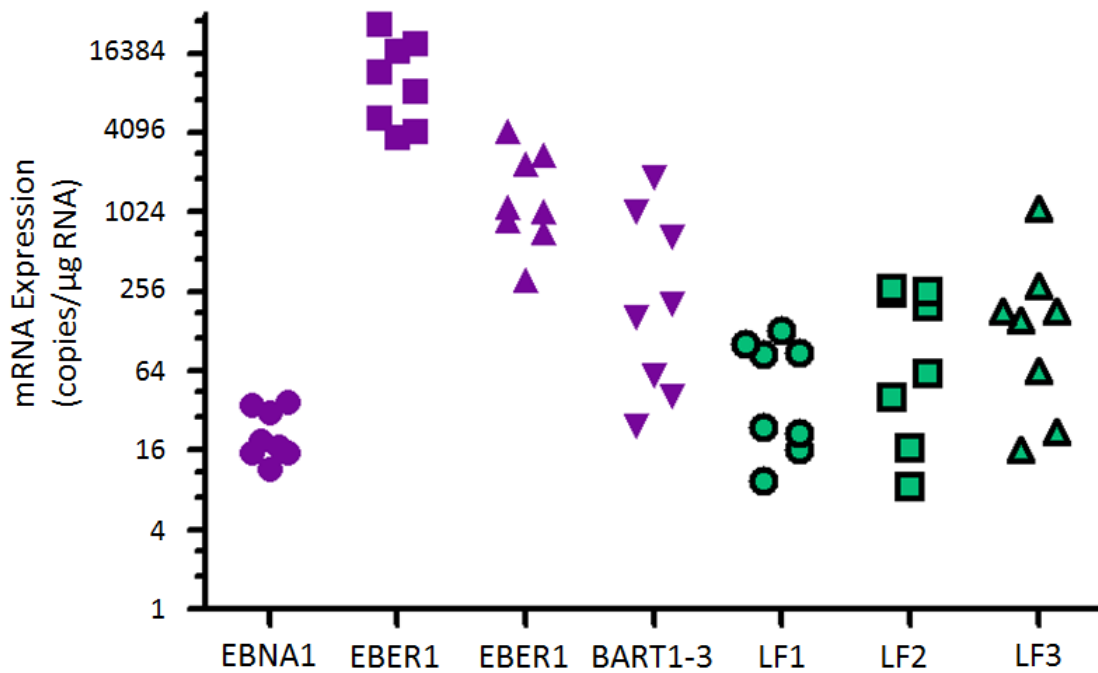


Figure 4.33 Position of LF genes in the BamHI A region of the EBV genome
Schematic of the BamHI A locus showing the relative position of BamHI A exons (grey), miRNAs (red) and putative LF coding regions on the opposite DNA strand



Data from Dr Rosemary Tierney

Figure 4.34 Transcription of Latency I-associated and LF genes in BL cell lines using microfluidic chip q-PCR normalised to plasmid DNA standards in order to quantitate RNA copy number per microgram of total RNA as published in [175]. Values displayed on a Log^2 scale due to the wide variation in copy number between different transcripts and cell lines.

Absolute quantitation of EBV transcripts in 8 Latency I BL cell lines: Rael-BL, Ezema-BL, Sav-BL, Dante-BL, Akata-BL and EBV-positive clones of Kem-BL, Mutu-BL and Awia-BL

NB the LF3 gene is mostly composed of repetitive sequences (known as the PstI repeats), downstream of a unique region. Our q-PCR assay is directed against a section of the unique region of the gene (primer/probe sequences and co-ordinates are listed in the Materials and Methods section of this thesis) so as to ensure that q-PCR values reflect number of whole LF3 transcripts, rather than the number of PstI repeats present.

Conclusions II

We have shown that reinfection of EBV-loss clones with a wild-type, Akata-BL-derived recombinant EBV can fully restore the EBV-positive phenotype, thereby confirming that EBV is directly responsible for the difference in apoptosis sensitivity between EBV-positive and EBV-loss BL clones. Furthermore, our finding that the loss of rEBV from reinfected cells reverses the phenotype and re-sensitises EBV-loss Akata-BL cells to apoptosis indicates that protection is mediated by EBV gene expression and reduces the possibility that this could be an unintended consequence of antibiotic selection.

Consistent with the findings of other groups, we found that ectopic expression of EBNA1 protein was unable to rescue the apoptosis phenotype of EBV-loss cells [327, 339]. Surprisingly, we also found that re-expression of the EBER RNAs or clusters of BART microRNAs did not confer any survival advantage to EBV-loss cells. In contrast, we found that a B95.8-derived rEBV, which harbours a large genomic deletion in comparison to the Akata rEBV, could partially rescue the EBV-loss phenotype, but could not fully restore apoptosis protection unlike the Akata rEBV. We therefore hypothesise that the Latency I-associated genes function cooperatively to inhibit apoptosis in BL and that viral genes encoded within the region of BamHI A locus that is deleted in B95.8 are partially responsible for the EBV-loss phenotype.

We constructed lentiviruses to allow us to inducibly express individual EBERs in EBV-loss cells, but found that these vectors did not efficiently express RNAs of the correct length and thus, we could only restore EBER-expression to a fraction of the level seen in Latency I BL. Interestingly, we are aware that other groups have experienced similar difficulties with EBER-expressing lentiviruses (Joan Steitz and Elizabeth Boulden, personal communications) and we hypothesise that this is due to poor transcription termination. We therefore used the pEKS10 plasmid in our functional assays, as this vector contains the endogenous EBER regulatory regions and can restore EBER expression at comparable levels to Latency I BL cell lines [339].

Consistent with our hypothesis that the EBER RNAs may co-operate with other EBV gene products in order to protect BL cells from apoptosis, the two groups that have reported an anti-apoptotic role for EBV in BL found that ectopic expression of EBERs only partially restored tumorigenicity of EBV-loss clones of Akata-BL in SCID mice. Only around 50% of mice that were injected with EBER-expressing EBV-loss cells developed tumours, and EBER⁺/EBV⁻ cells took significantly longer than an EBV-positive clone to give rise to tumours, suggesting that EBERs may be necessary, but are not entirely responsible for the EBV-loss phenotype [339, 340]. Additionally, the Sample group also reported that, whilst EBERs can contribute to tumorigenicity *in vivo*, they do not restore apoptosis protection to Akata-BL cells *in vitro* [340]. Unfortunately, since our *in vivo* experiments were carried out during a sabbatical visit to the Walter and Eliza Hall Institute, we have been unable to test whether our EBER⁺/EBV⁻ cell lines are more tumorigenic than their EBV-loss counterparts in NSG mice. It is also important to note that the Sample group reported that 2 EBV-loss Akata-BL clones which stably express EBNA1 as well as EBERs were considerably more tumorigenic *in vivo* than the same clones expressing EBERs alone [340]. The authors attribute this finding to the increased level of EBER expression that they detect in the EBNA1⁺/EBER⁺/EBV⁻ cells because cells expressing EBNA1 alone are not tumorigenic, but another interpretation is that the presence of EBNA1 enhances the tumorigenicity of EBER-expressing cells by functional co-operation.

It has been suggested that EBER RNAs might inhibit apoptosis in Akata-BL clones and EBV-negative BJAB Burkitt-like lymphoma cells by upregulation of Bcl-2 and IL-10, or modulation of interferon signalling by inhibition of PKR [310, 339, 342, 561, 562]. However, these findings are contradicted by others [335], and we likewise find no evidence that EBERs are able to carry out these functions in our extensive panel of clones. We therefore infer that any anti-apoptotic function of the EBERs may occur by a previously undescribed mechanism. Alternatively, it is possible that EBER-mediated gene regulation is only evident after the induction of apoptosis in BL cells, and this is investigated in the following chapter.

Although EBV-loss has previously been described in three BL backgrounds, EBERs have only been shown to inhibit apoptosis in a small number of EBV-loss clones derived from the Akata-BL background [327, 340, 341]. Our experiments carried out on nine pairs of EBER-expressing and empty-vector control cell lines derived from three different EBV-loss backgrounds is the most comprehensive study of EBER-function in BL to date. Therefore, we conclude that the EBERs are not solely responsible for the inhibition of apoptosis in Latency I BLs. However, we do suggest that the EBER RNAs are able to co-operate with EBNA1 and the BART microRNAs in protecting BL cells from apoptosis.

This conclusion is further supported by a recent publication from the Sugden group, which showed that apoptosis induced by the forced eviction of EBV from Latency I BLs can be inhibited by the BART miRs [99]. Unfortunately, due to the nature of their experiment (i.e. not comparing BARTs-expressing EBV-loss cells to isogenic empty-vector controls), we are unable to determine whether the BART miRs are able to fully or only partially substitute for the presence of EBV from these data. Interestingly though, this paper did report considerable variation in the phenotype conferred by the BARTs miRs between two EBV-positive clones from two different Latency I BLs. In fact miR BARTs did not improve the survival of a Dante-BL clone as measured by population doublings until four weeks after the start of the experiment, whereas a clone of Sav-BL showed a difference between the control and BART-complemented cells after two weeks. It is likely that a very subtle phenotype such as this would not be detected in our 48 hour assays. We also carried out our experiments on multiple clones from three different tumour backgrounds to control for clonal variation and ascertain the generality of our findings, whereas the published study included only a single clone from each of two BL backgrounds.

Although the BART miRs have been reported to downregulate Bim and Puma in epithelial cells [365, 366], we found, in-keeping with other groups, that these proteins are not regulated by miR BARTs in B cells [99, 168, 371]. However, it is possible that the microRNAs restrain the

expression of these proteins in BL cells rather than downregulating them, and therefore this phenotype would only be detected in assays comparing miR BART-positive and negative cells after apoptosis had been induced; a possibility which is investigated in the following chapter. We have also not investigated whether miR BARTs can regulate Puma and Bim or inhibit cell death when both microRNA clusters are expressed together, as we were unable to clone the entire BamHI A locus into a single vector. We postulate that sequence context may be an important requirement for efficient expression of miR BARTs as we were able to express endogenous levels of miR BART-5 from a lentivirus containing only its pri-miR sequence; we did not investigate this further due to the technical difficulties associated with transducing B cells with a different lentivirus to express each BART miR.

Further to our hypothesis of co-operation between the viral genes, we also noted that the Takada and Sample groups both found that reinfected EBV-loss Akata-BL clones were less tumorigenic than their counterpart EBV-positive clones containing wild type virus [310, 340]. We interpret this as evidence for an anti-apoptotic role for the miR BARTs in this system as the recombinant Akata genome used contained an antibiotic resistance cassette and F-plasmid within the BamHI A locus. In contrast, our reinfection experiments used an Akata virus recombinant that was generated several years later and contains the selection cassette and F-plasmid within the BamHI X locus and consequently has an intact BamHI A locus [488]. Therefore, in order to further investigate our hypothesis of viral gene co-operation we are currently developing a new system for generating and modifying recombinant EBV genomes that will allow us to rapidly create viruses which are unable to express particular transcripts without disruption of other transcripts even within the same loci. This method uses two sequential rounds of temperature-regulated homologous recombination to create 'scar free' mutants that do not retain *flip* or *lox* sites. This approach has proven successful for generating mutant recombinant versions of a variety of viruses including KSHV and murine herpesvirus-68, which are closely related to EBV [563-565].

Using this technology we plan to generate viral genomes that lack the ability to express EBERs or BARTs, although we will be unable to investigate the effect of knocking out EBNA1 due to its essential role in genome maintenance. In addition, we plan to make viruses that are knocked out for LF1, LF2, or LF3, in order to determine whether these transcripts, which appear to be abundantly expressed in BL [174], also contribute to apoptosis inhibition by EBV.

Having shown that Latency I EBV can fully restore apoptosis protection to the majority, but not all, EBV-loss clones from three different tumour backgrounds we next went on to investigate the differences in apoptosis signalling between EBV-positive and loss clones. In these experiments, described in the next chapter, we aimed to identify targets of Latency I genes to further inform us about their possible mechanisms of action and determine whether any differences in apoptosis signalling between clones could explain why two clones were not phenotypically rescued by reinfection with a recombinant EBV. We also hoped to confirm our hypothesis that gene regulation by EBV would only be revealed when comparing EBV-positive and loss clones after apoptosis has been induced.

5. Results Part III

THE ROLE OF CELLULAR GENES IN THE APOPTOSIS- PHENOTYPE OF EBV-LOSS CLONES

5.1 Apoptosis-response of EBV-loss clones to BH3 ligands

Whilst our attempts to identify precisely how EBV genes protect BL cells were hampered by apparent requirements of co-operation, we considered that there may be some consistent pattern to downstream effects on cellular genes. Our earlier experiments, in which we used a range of different drugs to induce apoptosis in BL cells, indicated that that the intrinsic Bcl-2 family-mediated apoptosis pathway is important in the EBV-loss phenotype, so we focussed on determining which members of the Bcl-2 family are important in the response of BL cells to cytotoxic insults. Microarray studies comparing EBV-loss clones to their EBV-positive counterparts or EBV-positive and negative BLs from different patients have found few differences in transcription between cells which do or do not contain the virus, we therefore decided to use functional assays to investigate the role of the Bcl-2 family in BL clones [194, 195, 566].

In 2007, a method was published by which cells could be 'BH3 profiled' that is, the ability of BH3-only proteins to initiate the apoptotic cascade in different cells could be determined [567]. Due to the specificity with which anti-apoptotic Bcl-2 homologues bind to different pro-apoptotic BH3 only proteins, BH3 profiling can reveal which of the anti-apoptotic proteins is critical for the survival of the cells being profiled. This in turn has been shown to correlate directly with the sensitivity of cells with different BH3 profiles to cytotoxic insults [568-570]. We were keen to investigate whether EBV-loss clones might have an altered BH3 profile to their EBV-positive counterparts, which may in turn allow us to resolve the question of which

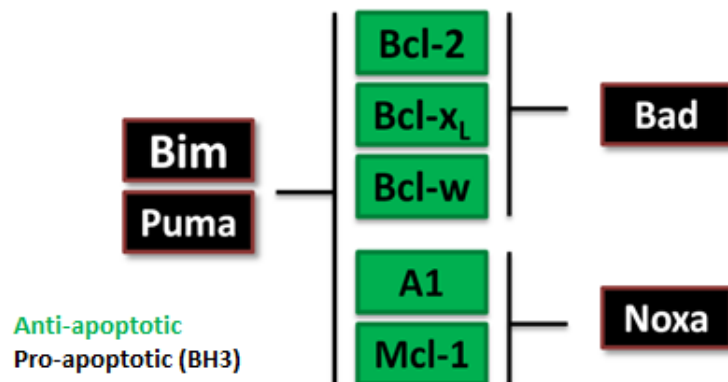
cellular apoptosis regulators EBV may target to inhibit apoptosis in BL and therefore the mechanism by which the virus achieves this.

5.1.1 Expressing Bim_S-derived BH3 ligands in EBV-loss clones

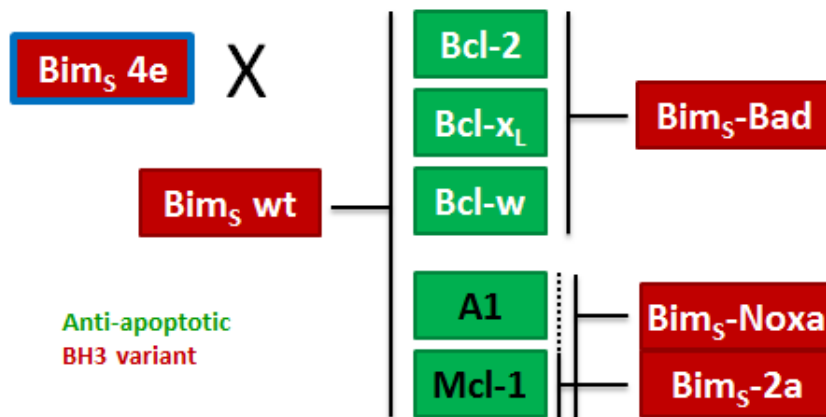
In the BH3 profiling technique published by Letai and colleagues [567], short BH3 peptides (20-25 amino acids of the BH3 domain of the BH3-only protein of interest) are added to permeabilised cells and the amount of mitochondrial membrane depolarisation caused is measured by FACS. However, another group has shown that BH3 peptides of less than 26 amino acids may not bind pro-survival Bcl-2 proteins in the same way as the full length proteins [500]. It is also relatively expensive to have the full range of BH3 peptides synthesised and technically difficult to permeabilise the plasma membrane of cells without affecting the inner cell membranes, including that of the mitochondria, which might impact the subcellular localisation or function of Bcl-2 family member proteins or other regulatory molecules.

Our collaborators at the WEHI developed a similar method which uses whole BH3 variant proteins to induce apoptosis as opposed to BH3 peptides. The variant proteins are all derived from Bim_S, the smallest and most potent isoform of the pro-apoptotic BH3-only protein Bim [450]. In each Bim_S-derived BH3-variant the BH3 domain has been modified either by replacing the entire domain or by mutating specific residues to mimic the binding specificity and affinity of a range of BH3-only proteins. The binding selectivity of several endogenous pro and anti-apoptotic Bcl-2 family members is depicted in Figure 5.1-A and the corresponding Bim_S-derived BH3 variants are shown in Figure 5.1-B. Bim_S-wt is the wild-type Bim_S protein, Bim_S-Bad and Bim_S-Noxa were made by replacing the entire BH3 domain (residues 51-76 of Bim_S-wt) with that of Bad or Noxa respectively, Bim_S-2a is an Mcl-1-specific 2 amino acid mutant of Bim_S-wt and Bim_S-4e is a 4 point mutant of Bim_S-wt which is unable to bind any of the pro-survival Bcl-2 family and serves as a negative control (Table 2.3 contains a detailed description of Bim_S BH3 ligands) [423, 500]. These Bim_S-derivatives have been shown to closely correlate in their

A Endogenous Bcl-2 family member binding



B BH3 variant binding to Bcl-2 homologues



C Affinity (nM) of BH3 variant peptide binding to prosurvival Bcl-2 proteins

	Bcl-2	Bcl-XL	Bcl-w	A1	Mcl-1
Bad	16	5.3	30	>10,000	>10,000
2a	>10,000	>10,000	>10,000	520	19
Noxa	>10,000	>10,000	>10,000	180	24
Bim	2.6	4.6	4.3	4.3	2.4

Data from Biacore solution competition assays carried out by Lin Chen, Erinna Lee and colleagues.

Figure 5.1 Binding specificity and affinity of BH3 proteins and mimetic ligands

A Endogenous Bcl-2 family members **B** BH3 variant binding to Bcl-2 homologues

C Affinity of BH3 peptide binding to pro-survival Bcl-2 proteins, all measurements in nM from Biacore solution competition assays carried out by Lin Chen, Erinna Lee and colleagues at WEHI [398, 472]

binding to Bcl-2 homologues with the full length proteins they mimic in both *in vitro* assays and in cells [500]. Therefore this method can be used to diagnose blocks in the Bcl-2 signalling pathway that can then be overcome using specific BH3 mimetics [301, 434, 571]. The relative binding affinities of each of the BH3 domains inserted into the Bim_S backbone for each of the pro-survival Bcl-2 proteins, as measured by groups who generated this system, are shown in Fig 5.1-C.

5.1.2 Generating Bim_S variant-expressing cell lines

Each of the BH3 variant proteins shown in Figure 5.1-B was cloned into the FTrex-UTG DOX-inducible lentivirus system (as used in previous experiments to re-express viral genes) by Toru Okamoto and Marco Herold, and were kindly made available for my experiments. The BH3 variant Bim_S lentiviruses were then individually transduced into a total of ten cell lines from three tumour backgrounds, comprising; one EBV-positive parental and three loss clones of Akata-BL; one EBV-positive and two EBV-loss clones of Kem-BL and one EBV-positive and two EBV-loss clones of Mutu-BL.

Expression of all of the BH3 variants was similar in the Akata-BL derived cell lines, deviating by less than two-fold between the highest and lowest expressers (Figure 5.2-A). We also found similarly low levels of variation in BH3 variant expression levels in each of the three Akata-BL EBV-loss clones used in these experiments (data not shown). In the Kem-BL background, we found a greater degree of variation in expression of BH3 variants within the same clonal background, up to 8-fold in EBV-positive Kem-BL (Figure 5.2-B), and up to 4-fold variation between different variants in EBV-loss Kem cells (data not shown). In Mutu-BL derived BH3 variant cell lines, we found that levels varied up to around three-fold in all of the clones used (Figure 5.2-C and data not shown).

As mentioned earlier in this thesis, we and others have found that GFP intensity in lentivirus transduced cell lines closely mirrors the level of expression of the gene of interest [484].

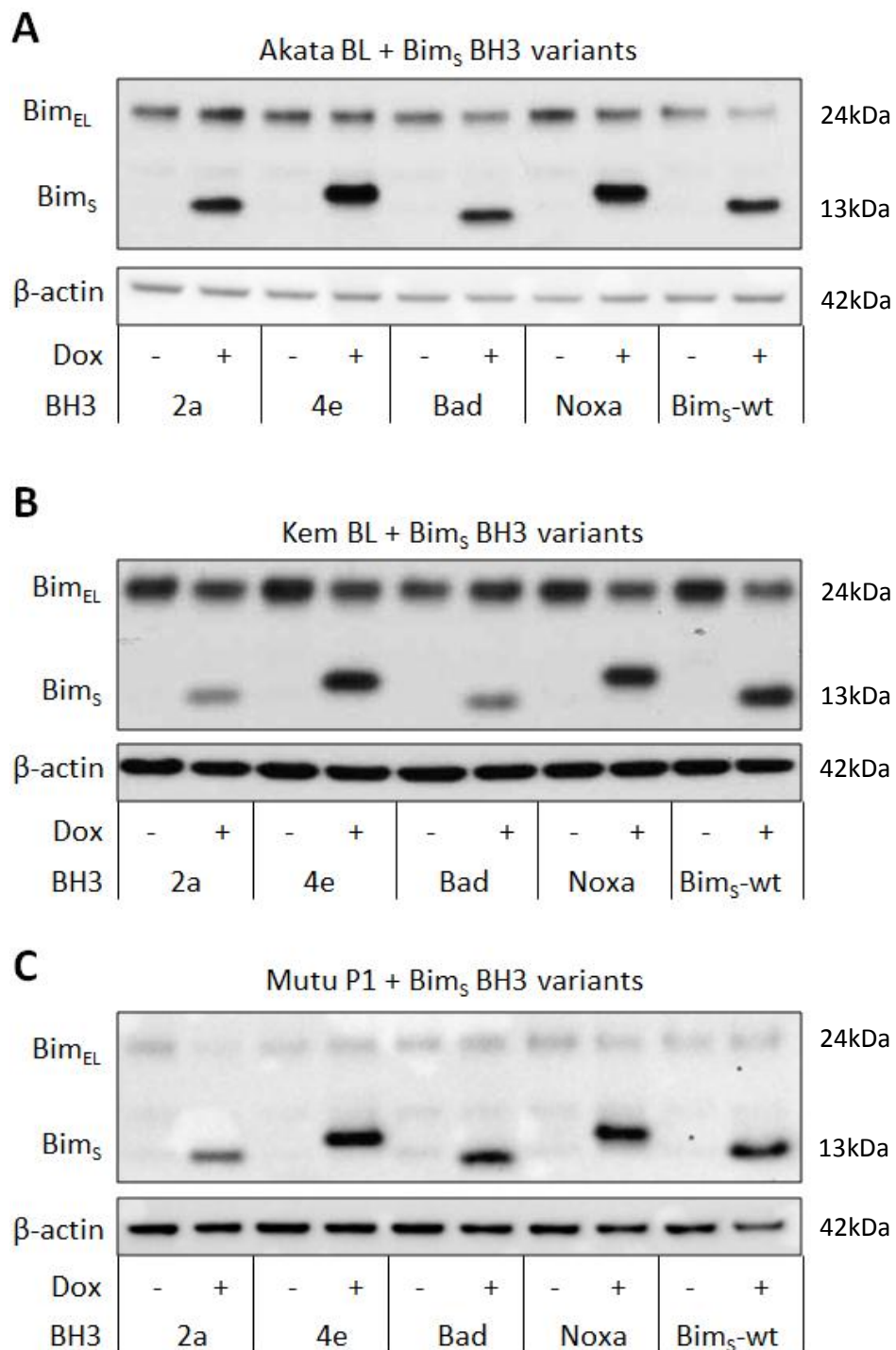


Figure 5.2 Bim_S-variant expression in BL clones

A Akata-BL-derived BH3 variant cell lines **B** Kem-BL-derived BH3 variant cell lines

C Mutu-P1-derived BH3 variant cell lines

Representative data, Bim expression was blotted and relative expression quantified in all ten sets of cell lines used for apoptosis experiments using BioRad ImageLab and normalised to β-actin expression

Induced cells (+) treated with DOX and caspase inhibitor, Q-VD.OPh, for 24 hours

Uninduced controls (-) were treated with Q-VD.OPh alone. Bim antibody (CST #2918, 1/1000) used recognises endogenous Bim_{EL} and Bim_L isoforms as well as Bim_S.

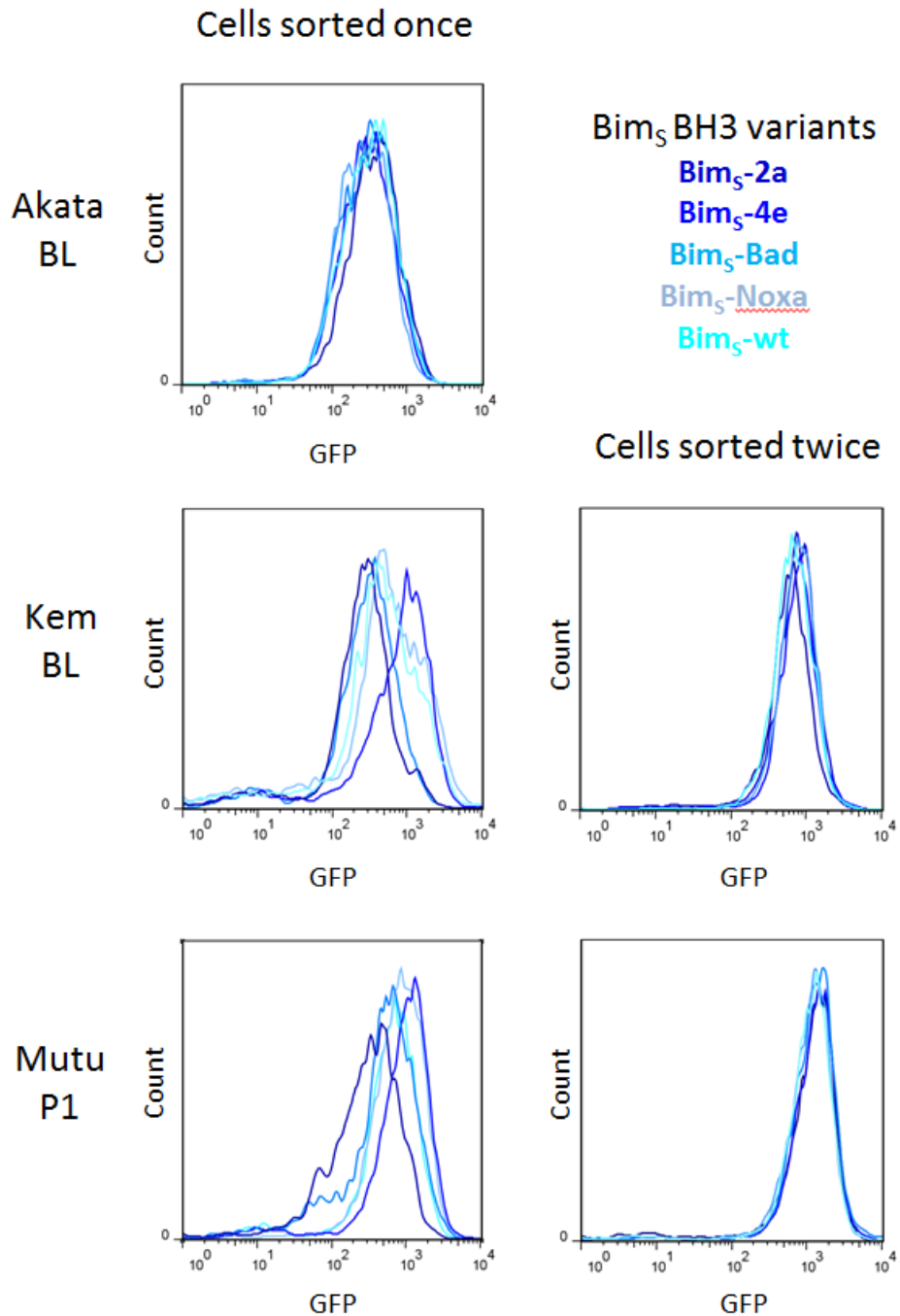


Figure 5.3 GFP intensity in BL clones after successive rounds of GFP sorting

Intensity of GFP expression was quantified by FACS in all ten sets of cell lines used for apoptosis experiments. In this figure GFP profile overlays are shown for Bim₅-variant transduced EBV-positive cells of Akata-BL, Kem-BL and Mutu P1 as an example

Therefore, to remedy the disparity between different BH3 variant cell lines, we enriched the Kem and Mutu-derived cell lines for high GFP expression as described in Section 2.1.4 using identical gating for all cell lines from the same family. After the second round of sorting we found that the intensity of GFP expression in our Bim_S-variant cell lines was almost identical, as shown in Figure 5.3, and so we went on to look at the functional consequence of expressing BH3 variants in BL clones. Unfortunately it was not possible to carry out detailed examination of Bim_S expression in the cells that had undergone a second round of sorting as these experiments were carried out during a short sabbatical visit to the Walter and Eliza Hall Institute (WEHI), as previously noted. However, it has been demonstrated in this thesis and elsewhere that GFP expression closely correlates with that of the gene of interest in this system.

5.1.3 The apoptosis phenotype of Bim_S variant expressing cell lines

In Akata-BL derived cell lines we found that EBV-positive parental cells were protected against Bim_S-Bad, -2a and -Noxa compared to their EBV-loss counterparts, although protection conferred by EBV was most striking in Bim_S-Noxa expressing cells (Figure 5.4-A). Interestingly, EBV-positive Akata-BL cells were sensitive to Bim_S-wt, undergoing similar amounts of cell death to Akata EBV-loss clones expressing the same variant. Although there was a small amount of variation between individual assays this pattern of responses was consistent, suggesting that Akata-BL cells are not solely dependent on any one of the anti-apoptotic Bcl-2 family members being investigated. Instead it appears that, whilst ligation of any one of the pro-survival Bcl-2 proteins by BH3 domains is sufficient to induce cell death in EBV-loss Akata cells, EBV-positive Akata cells are generally more resistant to BH3 and can only be killed when all pro-survival Bcl-2 proteins are depleted by BH3 binding.

In Kem-BL derived cell lines we again found that the EBV-positive parental cells were relatively resistant to Bim_S variant expression compared to two EBV-loss Kem clones (Figure 5.4-B). In contrast to Akata-BL however, we found that Kem-BL and loss clone n2 were completely resistant to Bim_S-Bad expression, whereas loss clone n1 was sensitive. This suggests that whilst survival in parental Kem and n2 cells is Bcl-w, Bcl-XL or Bcl-2 independent, loss of EBV from clone n1 has caused the cells to become dependent on one or more of these

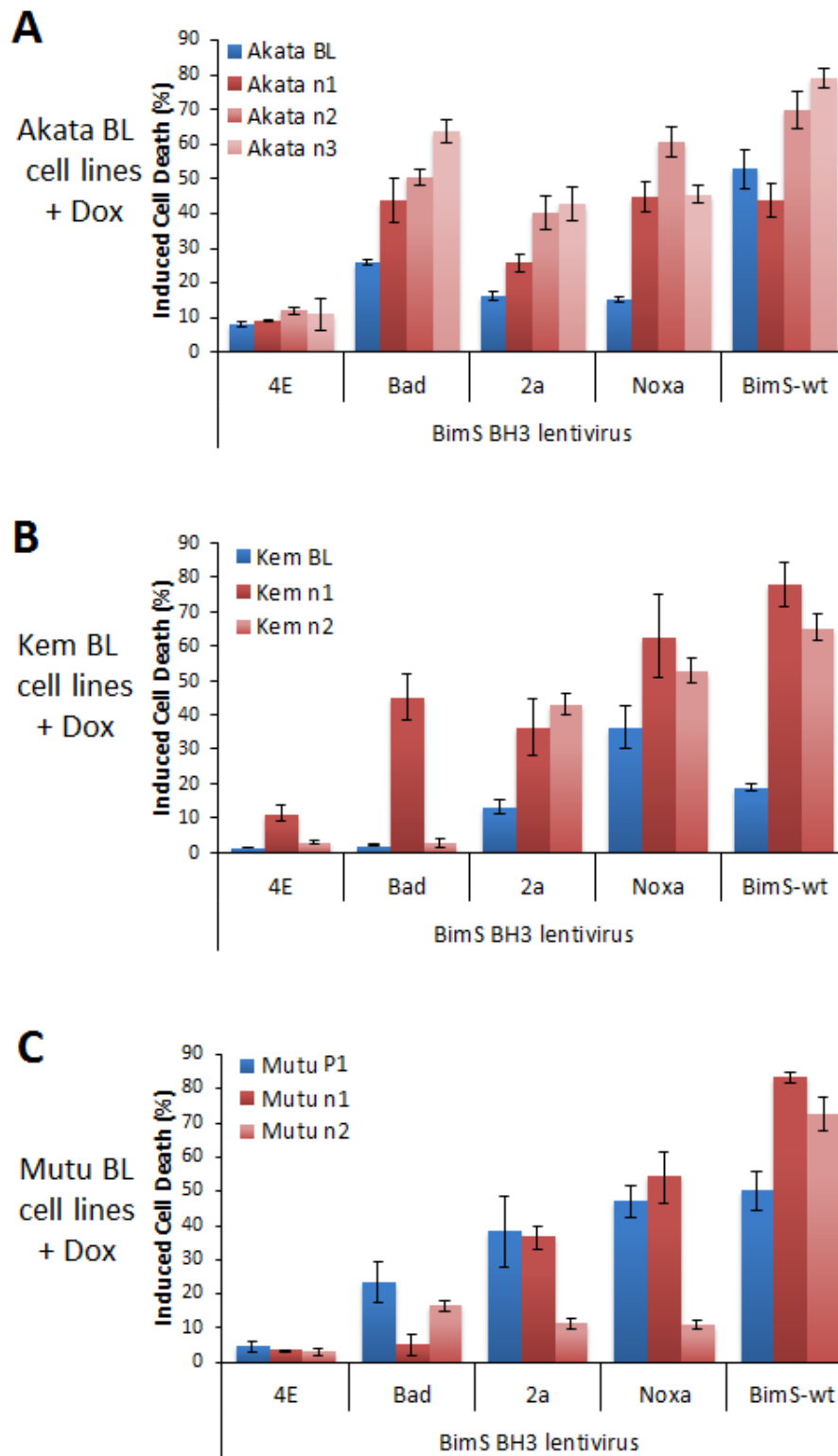


Figure 5.4 The apoptosis phenotype of Bim₅-variant expressing BL clones

A Akata-BL-derived BH3 variant cell lines **B** Kem-BL-derived BH3 variant cell lines

C Mutu-BL-derived BH3 variant cell lines

Cells were treated with 1µg/ml DOX for 72 hours and data shown are mean and standard deviation of triplicate assay wells

Representative data, all assays carried out in triplicate on three separate occasions.

anti-apoptotics in order to compensate. All of the Kem-BL derived cell lines show sensitivity to Bim_S-2a, Bim_S-Noxa and Bim_S-wt, although to a lesser extent in the EBV-positive cells, indicating that Mcl-1 and A1 are important for the survival of Kem-derived cells. The difference in response between EBV-positive and loss cells again implies some sort of general protective effect of EBV on Bcl-2-family signalling.

The EBV-positive Mutu clone P1 showed a gradual increase in sensitivity to BH3 variant expression with a similar hierarchy to that seen in Akata-BL suggesting a modest dependence on Mcl-1, A1 and Bcl-XL (Figure 5.4-C). Mutu EBV-loss clone n1 exhibited a similar profile, except that it was resistant to Bim_S-Bad and so does not appear to be dependent on Bcl-XL, Bcl-2 or Bcl-w, but conversely displayed increased sensitivity to Bim_S-Noxa and Bim_S-wt indicating a greater and more profound dependence on A1 in this clone. EBV-loss Mutu clone n2 showed a marked and surprising resistance to both Bim_S-2a and Noxa, but retained sensitivity to Bim_S-wt, possibly indicating that this clone has also partially adapted to compensate for the loss of EBV, but is still unable to survive strong apoptotic signals as well as EBV-infected Mutu cells.

5.1.4 Summary of BH3 variant re-expression studies

Using Bim_S proteins with variant BH3 domains we were able to demonstrate the ability of EBV to protect BL clones against intrinsic apoptosis signals in all three of the BL backgrounds tested however, there was considerable heterogeneity in responses to individual BH3 variants in different clones. Figure 5.5 is a graphical summary of the data obtained from all of the Bim_S variant induced apoptosis assays carried out in this study, in which each clone/BH3 variant response has been graded and then colour coded according to the average amount of cell death induced across three independent experiments (Figure 5.5-A). Expressing the data in this way clearly shows that, rather than selectively targeting any one member of the Bcl-2 family,

A

Induced Cell Death (%)

0-19	20-29	30-49	50-69	70-100
------	-------	-------	-------	--------

B

		Akata BL derived cell lines			
		Akata BL	n1	n2	n3
BH3 Ligand	4e	5	5	8	1
	Bad	24	37	47	60
	2a	11	21	37	36
	Noxa	12	40	58	52
	BimS wt	40	47	70	78

C

		Kem BL derived cell lines		
		Kem BL	n1	n2
BH3 Ligand	4e	1	13	1
	Bad	1	50	1
	2a	10	35	58
	Noxa	27	51	69
	BimS wt	45	42	76

D

		Mutu BL derived cell lines		
		Mutu 59	n1	n2
BH3 Ligand	4e	1	1	1
	Bad	15	5	12
	2a	27	34	12
	Noxa	42	45	25
	BimS wt	48	77	72

Figure 5.5 Summary of BH3 variant expression studies in BL clones**A** Legend showing grading of induced cell death and corresponding colour code **B**Akata-BL-derived cell lines **C** Kem-BL-derived cell lines**D** Mutu-BL-derived cell lines All values refer to the mean of three experiments

EBV appears to inhibit apoptosis by a general dampening of signalling through the intrinsic apoptosis pathway (Figure 5.5-B, C & D).

The Bcl-2 family are dynamic and highly sensitive to changes within the cell [391, 392], which makes them robust enough to control cell death effectively, but also difficult to subvert. Thus, a mechanism of global repression of Bcl-2 signalling allows EBV to affect a consistent outcome despite diversity in gene expression between individuals, between cells within one individual, and under different conditions, which may be critical for the virus to persist *in vivo*. This hypothesis also accounts for the finding that EBV-positive cells are not entirely resistant to BH3-induced killing; apoptosis signalling in these cells is diminished, but not crippled.

5.2 The cellular apoptosis response in BL clones: preliminary data

5.2.1 Assay design and validation

Although these functional assays provided us with a direct way of measuring the relative importance of individual proteins in Bcl-2 family regulated apoptosis we were still unable to decipher the exact mechanism by which EBV inhibits this pathway in BL clones. Since we had already carried out microarray studies on BL clones from 4 patient backgrounds we thought that the phenotype was unlikely to be explained by transcriptional differences between EBV-positive and loss clones however, total protein staining of BL clones and previous Western blotting studies had also suggested there are very few differences in protein expression profiles between clones from the same background (see Section 3.4). This led us to reconsider our initial microarray and protein expression studies and speculate that, rather than eliciting a permanent change in protein or transcript expression, perhaps EBV induces gene expression changes only under circumstances of cellular stress. We therefore decided to investigate transcriptional and protein expression changes in EBV-positive and loss BL clones that had

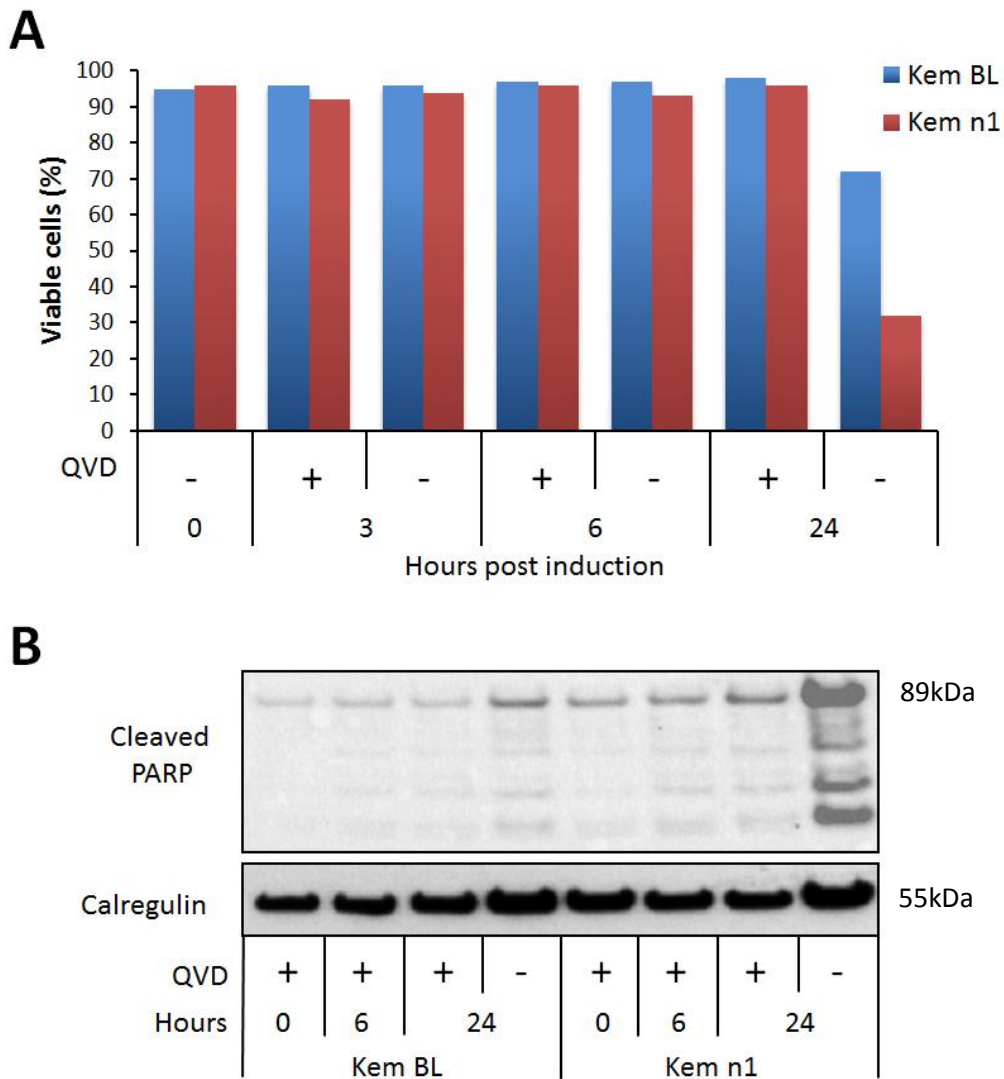


Figure 5.6 Cell death in Kem-BL and loss clone n1 after apoptosis induction by 1 μ g/ml ionomycin in the presence or absence of 25 μ M Q-VD.OPh

A Representative cell viability assay data

B Expression of PARP protein, PARP cleavage is a defining characteristic of apoptosis

Representative data, assays carried out on three occasions. QVD = Q-VD.OPh

been induced to undergo apoptosis, to investigate our hypothesis that genotypic changes which would explain the phenotypic difference would be evident upon intrinsic apoptosis induction in these cells.

First we carried out a small pilot study to ascertain whether this approach was likely to be successful and to determine the most appropriate experimental parameters as the assay had to be scaled up for RNA and protein analysis. Since we found the clearest difference between

EBV-positive Kem-BL and loss clone n1 in our functional assays these cell lines were used in these initial experiments. Although our aim was to profile gene expression changes in response to the initiation of cell death, we also wanted to minimise the number of dead cells in our samples as this could give misleading results. Earlier in this study we showed that the pan-caspase inhibitor, Q-VD.OPh, can completely block ionomycin induced cell death in BL clones and so we carried out apoptosis time courses on cells treated with ionomycin alone or in the presence of Q-VD.OPh to establish the kinetics of apoptosis in these cells, an example of which is shown in Figure 5.6-A.

The cells remained >90% viable up to 6 hours after apoptosis induction regardless of EBV-status and in the absence of Q-VD.OPh. However, at 24 hours post induction, whilst the Q-VD.OPh treated cells remained viable, cells with no caspase-inhibition had undergone a considerable amount of apoptosis, though EBV-positive cells characteristically less so than the EBV-loss clone (Figure 5.6-A). We then carried out Western blotting for PARP on these samples and found that PARP expression did not increase in any of the Q-VD.OPh-treated cells, confirming that QVD is able to completely block caspase activation in this system. In cells treated with ionomycin only, PARP upregulation and cleavage was evident at 24 hours, as expected, and occurred to a greater degree in EBV-loss cells (Figure 5.6-B).

We also examined the expression of the EBV lytic genes in EBV-positive Kem cells as it has been reported in the literature that ionomycin-treatment can induce lytic reactivation in BLs [572]. We found that all 3 of the lytic cycle-associated genes that were assayed (BZLF1, BHRF1 and LF3), were upregulated after ionomycin addition, but not at early time points (<6 hours) and not in Q-VD.OPh treated cells. This suggests that lytic cycle is only triggered after the cell is already committed to programmed cell death (Figure 5.7). Therefore we decided to only include cells that had been treated with Q-VD.OPh in subsequent experiments, to rule out any complications of viral lytic gene expression and to minimise indirect cellular gene expression changes associated with either lytic cycle or late stage apoptosis.

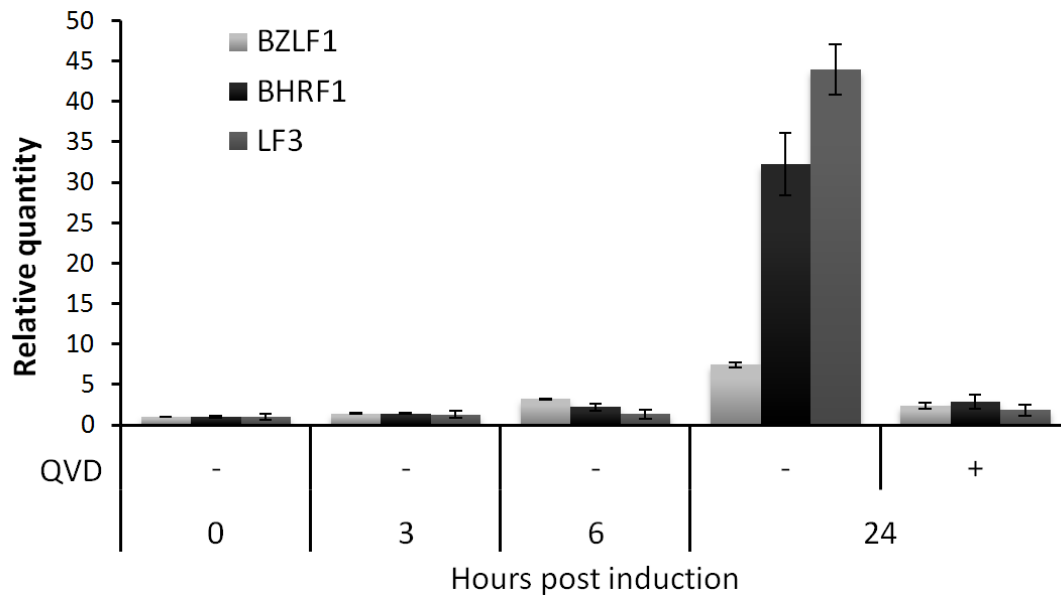


Figure 5.7 Lytic gene expression in Kem-BL after apoptosis induction with 1 μ g/ml ionomycin in the presence or absence of 25 μ M Q-VD.OPh, quantified by q-PCR relative to baseline expression levels of each transcript in Ionomycin-only treated cells (-) at time 0 measurements carried out in duplicate and quantified using the $\Delta\Delta$ Ct method, mean and SD shown
QVD = Q-VD.OPh

5.2.2 Bcl-2 family expression in drug-treated EBV-loss clones

Next, we looked for changes in expression of Bcl-2 family genes by q-PCR and Western blot and although many of the proteins and transcripts that we investigated were unaffected by ionomycin-treatment, we did observe several interesting responses. At the protein level, the alpha isoform of Puma was gradually upregulated in EBV-loss Kem n1 cells over time, but was unchanged in EBV-positive Kem-BL. Conversely, Mcl-1_L was expressed at low levels and the s-isoform was gradually degraded over time in the n1 clone compared to Kem-BL cells (Figure 5.8). It is interesting that healthy Kem-BL and Kem n1 cells express both the long (L) and short (S) isoforms of Mcl-1 because Mcl-1_S has been shown to bind and antagonise the action of Mcl-1_L and is therefore pro-apoptotic [573, 574]. Although the disappearance of Mcl-1 in the EBV-loss Kem n1 cells may be responsible for the apoptosis phenotype it is also possible that it does not affect the fate of the cells since both the long (pro-survival) and short (pro-apoptotic)

isoforms are both degraded in Kem n1 cells in response to apoptosis induction. If this finding were to be confirmed in a wider panel of EBV-loss versus EBV-positive clones it would be important to examine the relative contributions of the different isoforms of Mcl-1 to the apoptosis phenotype of the cells.

In accordance with the Western blot data Puma transcripts were also clearly upregulated in Kem n1, but were relatively unchanged in Kem BL (Figure 5.9-A). Mcl-1 expression did not change at the mRNA level, suggesting that its disappearance in ionomycin-treated Kem n1 cells may be due to degradation (Figure 5.9-B). Interestingly, Noxa transcripts were upregulated in both EBV-positive and loss Kem cells, showing around a 4-fold increase in both cell lines after 3 hours, although transcript levels continued to rise only in the EBV-loss cells, reaching an 8-fold increase compared to time 0 by 24 hours (Figure 5.9-C). Unfortunately, our Noxa antibody gave poor results in Western blot and so we were unable to conclude whether or not there was a concomitant change at the protein level (data not shown).

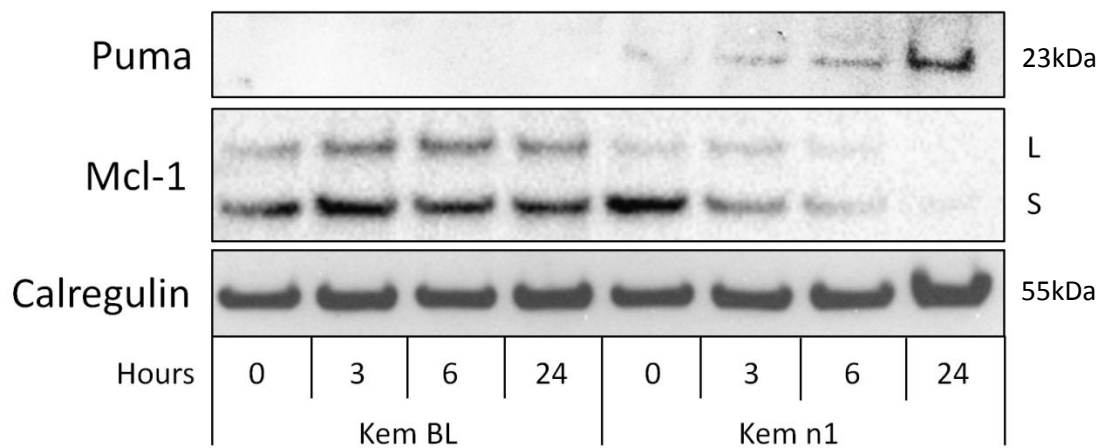


Figure 5.8 Time course of Puma- α and Mcl-1 protein expression in Kem-BL and Kem n1 cells after treatment with 1 μ g/ml ionomycin and 25 μ M Q-VD.OPh

Representative data, assays carried out on three occasions. Hours = hours since addition of ionomycin + Q-VD.OPh

L denotes Mcl-1 long isoform (40kDa) and S denotes the short isoform (32kDa)

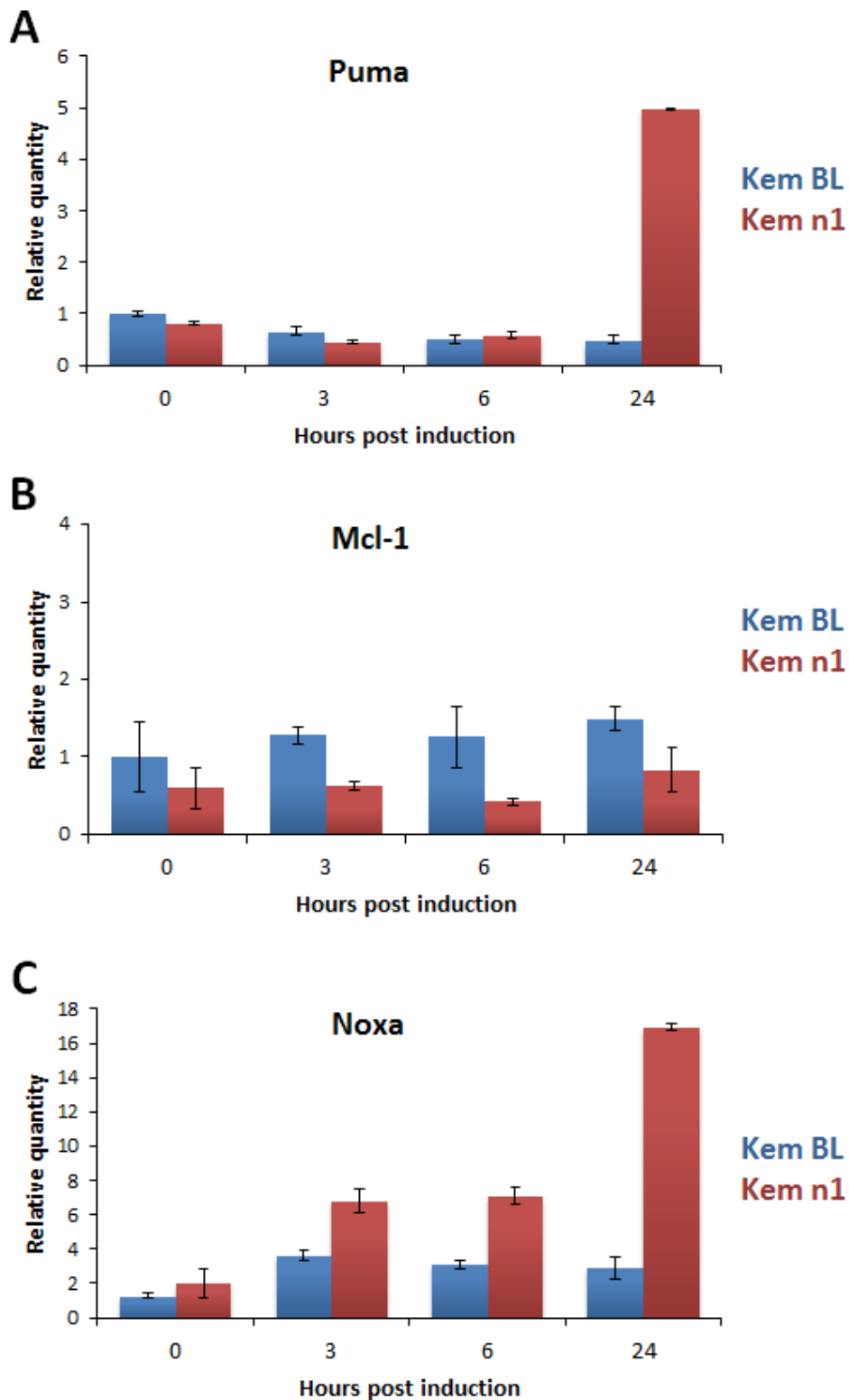


Figure 5.9 Time course of Puma, Mcl-1 and Noxa transcription in Kem-BL cells after treatment with 1 μ g/ml ionomycin and 25 μ M Q-VD.OPh

Representative q-PCR data, assays carried out on three occasions. Mean and standard deviation of duplicate measurements is shown. Data analysed using the $\Delta\Delta$ Ct method and expressed relative to expression levels in Kem-BL at time 0.

TaqMan assays used are able to detect all known protein coding isoforms

5.3 The cellular apoptosis response in BL clones: q-PCR arrays

5.3.1 Experimental set-up

As we had hypothesised, our preliminary data identified genes that were expressed differently between treated EBV positive and loss cells that would have been missed by looking only at untreated cells. Interestingly, only a minority of the Bcl-2 family members assayed changed in their expression over the time points we looked at and the changes we did find; possible degradation of one isoform and almost total lack of a second isoform of Mcl-1, and upregulation of two BH3-only Bcl-2 homologues, suggest that the underlying mechanism may be complex, involving multiple interacting components of the same pathway.

To investigate whether these changes were consistent between clones and to determine the impact of EBV on the orchestration of cell death in BL cells we carried out scaled up apoptosis assays on 6 clones of Kem-BL. As depicted in Figure 5.10, Kem-BL clones (three EBV-positive and three EBV-loss) were induced with ionomycin in the presence of Q-VD.OPh in three separate time course experiments and cells were harvested at 0, 6 and 48 hours. The final time point was changed from 24 hours to 48 hours after further optimisation because we saw the clearest difference in viability between EBV-positive and loss cells in ionomycin-only controls (i.e. without QVD) at this time point. We also omitted the 3 hour time point used in preliminary experiments to minimise sample number since changes in gene expression were more pronounced at 6 hours and there was very little difference in cell viability between 0 and 6 hours in ionomycin-only controls.

To analyse transcription in these samples we used commercially available microfluidic q-PCR cards pre-loaded with 93-apoptosis-related mRNA targets and 3 endogenous control genes. This allowed us to cost-effectively measure a large number of targets simultaneously, which have all previously been shown to regulate apoptosis and can be transcriptionally regulated. Expression of apoptosis-related proteins in these samples was then further investigated using Western blot and FACS.

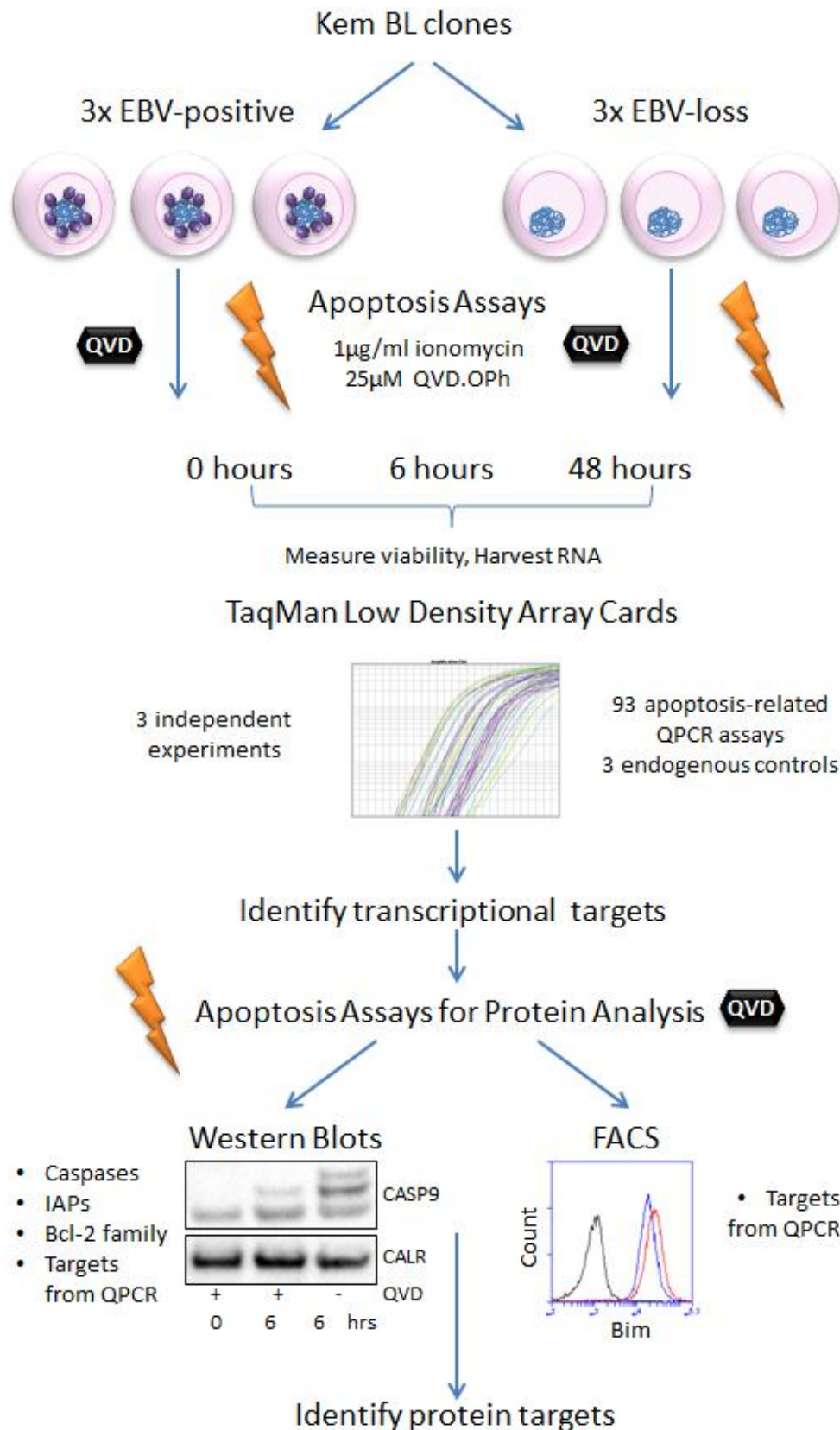


Figure 5.10 Workflow used for experiments to investigate cellular gene changes in response to apoptotic stimulus in clones of Kem-BL

5.3.2 Apoptosis response of Kem-BL clones in scaled-up assays

Before we ran samples on microfluidics cards we wanted to check that all of the clones behaved similarly in scaled up apoptosis assays to our small scale and preliminary experiments. Figure 5.11 shows the viability of the cells harvested for q-PCR arrays as well as ionomycin-only treated controls over three independent experiments. As in the small scale assays, there is a clear difference in viability between the EBV-positive and EBV-loss clones, although there is some variability between different clones for example; clone P1 is always the most protected and clone n3 is always the most sensitive, followed by clone n1.

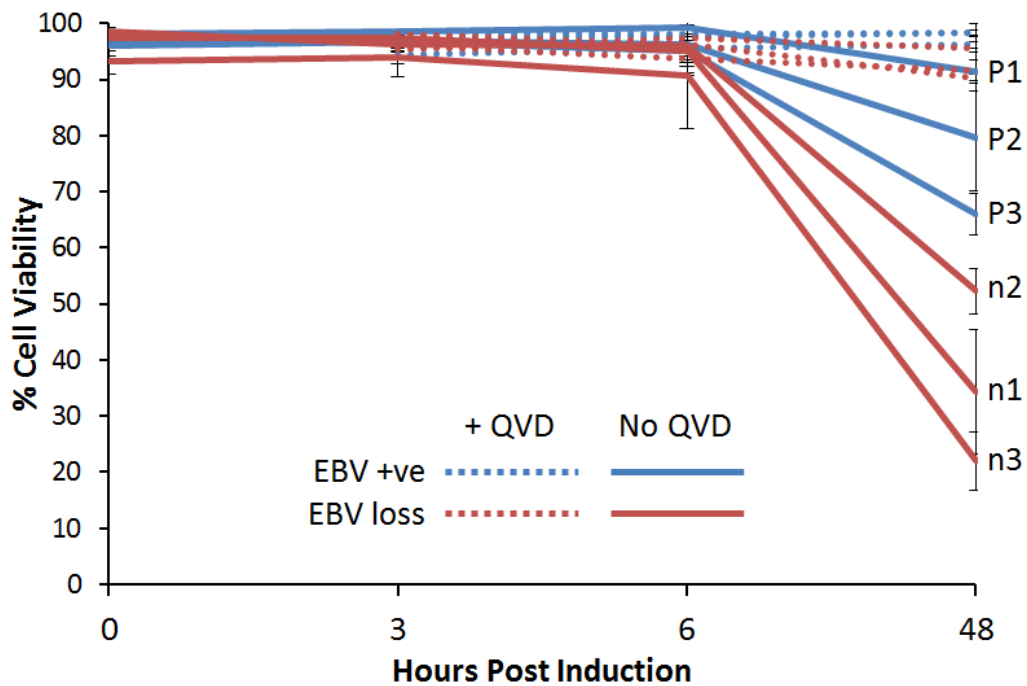


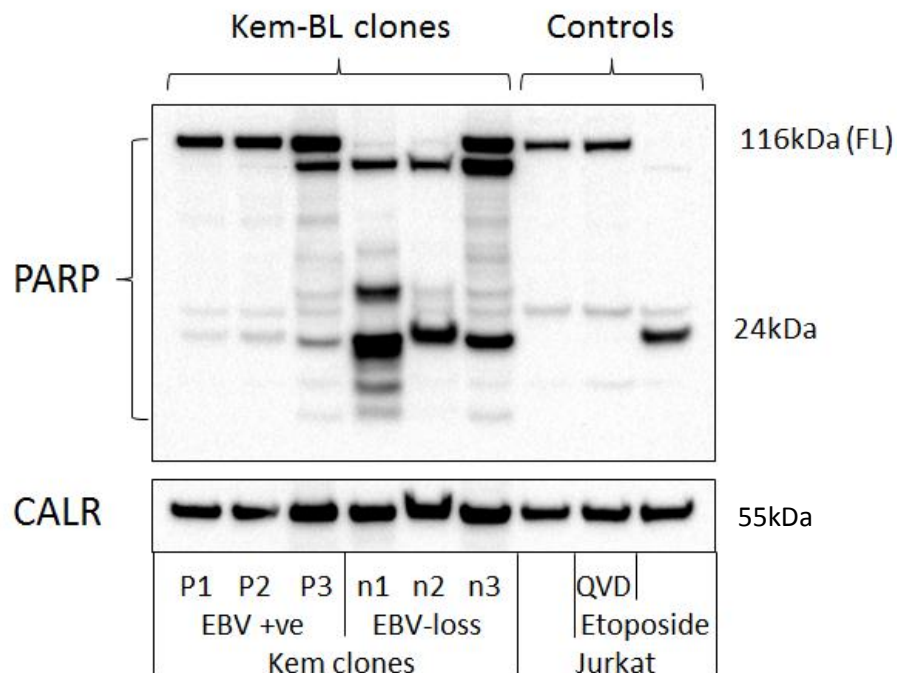
Figure 5.11 Viability of EBV-positive and loss clones of Kem-BL in scaled-up apoptosis assays

Viability of cells was assessed using trypan blue staining in duplicate, mean and standard deviation from three independent experiments is shown

We also checked that Q-VD.OPh still completely blocked late stage apoptosis in all six clones of Kem-BL. Cells were treated with either ionomycin alone as a positive control (Figure 5.12-A), or ionomycin and Q-VD.OPh (Figure 5.12-B), for 48 hours and were then harvested for Western blot analysis. Blots were probed using an antibody against PARP which recognises both the full length protein and its cleavage products. PARP can be cleaved by a number of proteases as a consequence of cell stress and therefore PARP cleavage is considered a hallmark of apoptosis [575, 576]. In agreement with our preliminary experiments, QVD-treatment completely blocked PARP cleavage and PARP expression was similar in all Kem-BL clones in the presence of caspase inhibition. As expected, EBV-loss cells treated with ionomycin in the absence of Q-VD.OPh exhibited far more PARP cleavage than their EBV-positive counterparts. Interestingly, individual EBV loss clones appeared to show distinctive PARP cleavage patterns, which may be indicative of variation in the proteases responsible for cleaving PARP in different clones [577]. We also included treated or untreated Jurkat cells as controls, as many commercial antibodies, including our PARP antibody, have data available for Jurkat. Jurkat cells were harvested after 5 hours of treatment with either vehicle only, Etoposide and Q-VD.OPh as control for caspase inhibition or Etoposide alone as a positive control for apoptosis.

A

Kem BL clones + ionomycin only

**B**

Kem BL clones + ionomycin + QVD.OPh

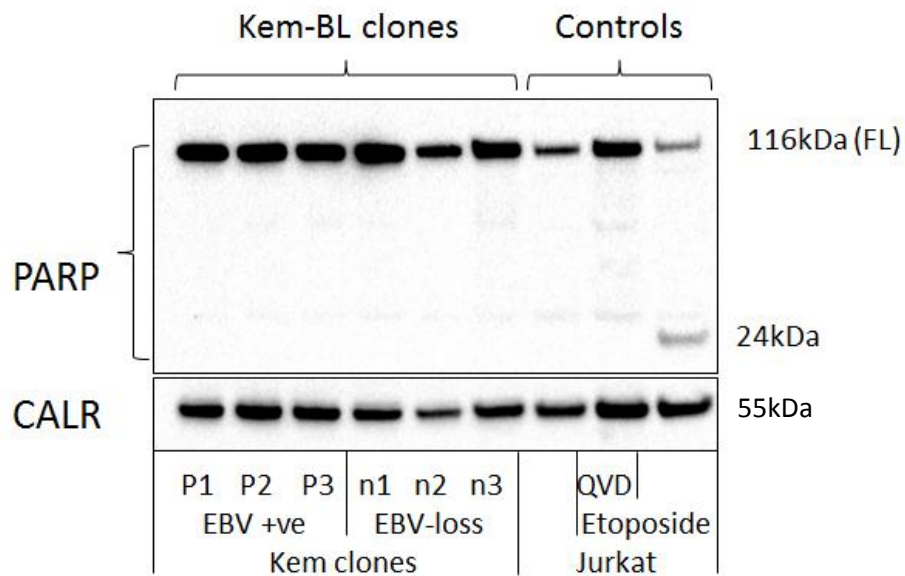


Figure 5.12 Western blots of PARP expression and cleavage in Kem-BL clones treated with ionomycin only (**A**) or ionomycin and Q-Vd.OPh (**B**) for 48 hours showing that PARP cleavage is completely inhibited in Q-Vd.OPh treated cells and that EBV-loss clones undergo a greater degree of PARP cleavage than their EBV-positive counterparts. Jurkat cells are included as controls for healthy cells (lane 7), and apoptosis induction in the presence (lane 8) or absence of Q-Vd.OPh (lane 9)

QVD = Q-Vd.OPh, CALR = calregulin loading control FL = full length

5.3.3 Analysis of similarity between clones of Kem-BL in q-PCR arrays

Since the assays on q-PCR array cards are run simultaneously on a single batch of sample material we were able to globally compare the ΔCt values (gene of interest – endogenous controls) for all of the targets loaded on the cards between different members of the same experimental group. This allows us to assess the overall similarity of one clone to another in terms of its apoptosis-related gene expression. We would expect all clones of one type (EBV-positive or EBV-loss) to respond in the same way to apoptotic stimuli, and therefore have an almost linear relationship to one another. By plotting the ΔCt values of one clone against another on a scatter graph and then performing linear regression, a value describing the similarity of the two clones, known as the signal correlation coefficient, can be calculated.

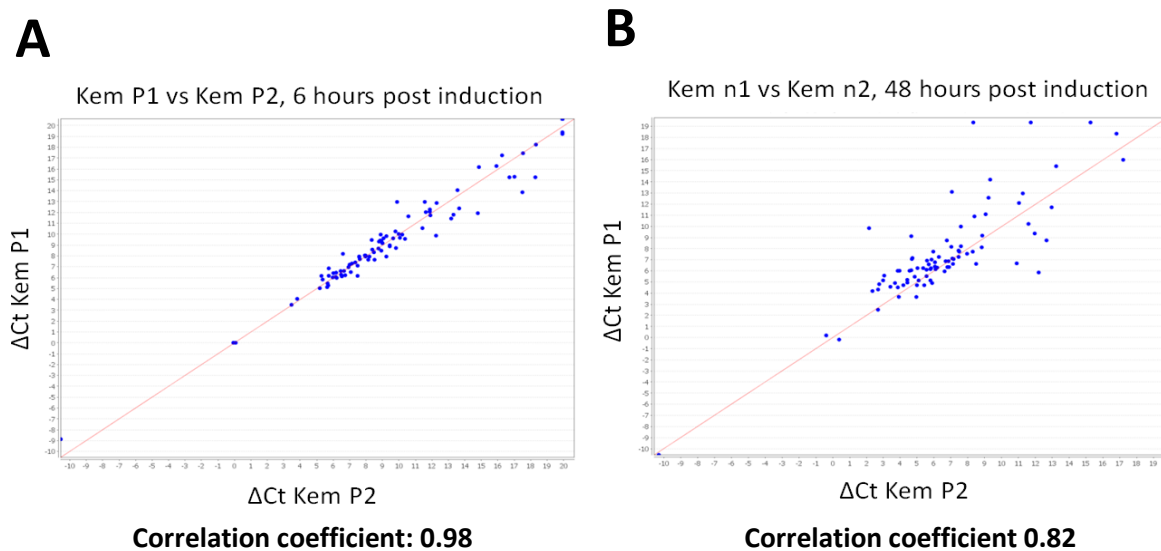


Figure 5.13 Global gene expression comparisons from q-PCR arrays

Example plots of ΔCt values for each individual assay present on the microfluidic card in one sample (Kem P1) versus another sample (Kem P2)

A EBV-positive clones P1 and P2 at 6 hours (in this example the correlation efficient is the highest between two samples and therefore they are most similar)

B EBV-loss clones n1 and n2 at 48 hours (in this example the correlation efficient is one of the lowest between two samples and therefore they are less more divergent from one another in their gene expression pattern, although the relatively high coefficient of 0.82 reflects that overall these two genetically related clones are still highly similar)

Examples of global signal comparisons between two pairs of Kem-BL clones are shown in Figure 5.13. EBV-positive clones P1 and P2 after 6 hours of ionomycin-treatment, were almost identical in their gene expression (correlation coefficient of 0.98) (Figure 5.13-A), whereas a comparison of gene expression in EBV-loss clones n1 and n2 after 48 hours of treatment showed less similarity (correlation coefficient of 0.82) (Figure 5.13-B). A summary of the similarity in all possible pairings of each of the three clones in each experimental group is shown in Figure 5.14. On the whole, the samples show a high level of similarity to one another (89% similarity overall) as would be expected in cells derived from a single individual. However, it is noticeable that the EBV-loss clones are less similar to one another compared to the EBV-positive clones; 84.9% and 93.1% overall similarity, respectively. It is also interesting that the gene expression profiles of all Kem-BL clones tended to increase in their similarity after drug treatment compared to time 0.

		Time Post Induction (hours)		
		0	6	48
EBV Positive Clones	P1 vs P2	0.89	0.98	0.87
	P1 vs P3	0.96	0.98	0.95
	P2 vs P3	0.90	0.98	0.87
EBV Loss Clones	n1 vs n2	0.83	0.88	0.82
	n1 vs n3	0.77	0.85	0.85
	n2 vs n3	0.80	0.94	0.90

Signal Correlation 

>0.91 >0.86 >0.81 >0.76

Figure 5.14 Summary of similarity between pairs of EBV-positive and EBV-loss clones of Kem-BL based on signal correlation coefficients.

Signal correlation values (in white) were also colour graded for clarity, as per the key (below the table)

5.3.4 Grouped pairwise analyses

To assess the impact of EBV on apoptosis response on clones of Kem-BL, we grouped our samples according to EBV-status and then carried out pairwise analyses between the grouped data sets. Changes in gene expression were considered significant if the fold change was greater than 2 and the significance calculated to be less than $p=0.05$. Pairwise comparisons were plotted as a function of fold change (x-axis) versus significance of change (y-axis), known as a volcano plot. This allows for quick identification of genes that change significantly between two samples and to what magnitude, and also gives an overall view of the proportion of the genes that are differentially expressed between two samples.

All gene expression data were normalised to an average of ACTB and GAPDH. 18S was also included as an endogenous control but we found that it was expressed at very different levels to the other targets so it was excluded from the analyses (average Ct values: 18S – 12, endogenous controls - 20, targets - 24). Importantly, expression of the two endogenous control genes used did not change in response to drug treatment and varied by less than 2Cts between all of the samples analysed.

We created volcano plots for every possible pairing of the 6 groups of samples (EBV-positive and EBV-loss at each of 0, 6 and 48 hours) to look for changes which might explain the EBV-loss phenotype. Figure 5.15-A shows an example volcano plot comparing EBV-loss clones at 6 hours to the same cells at time 0. Up and downregulated genes are shown on either side of the parallel black lines; green dots on the left-hand side signify genes that are more than 2-fold downregulated, and red dots on the right-hand side are upregulated more than 2-fold, whilst the blue line marks the cut off for significance ($P<0.05$). Although 31 genes are changed across all three EBV-loss clones after 6 hours of drug treatment only RELB is changed significantly. In EBV-loss clones at 48 hours the vast majority of the genes change in their expression and of those, 15 change significantly (Figure 5.15-B|). Carrying out the same comparison on the

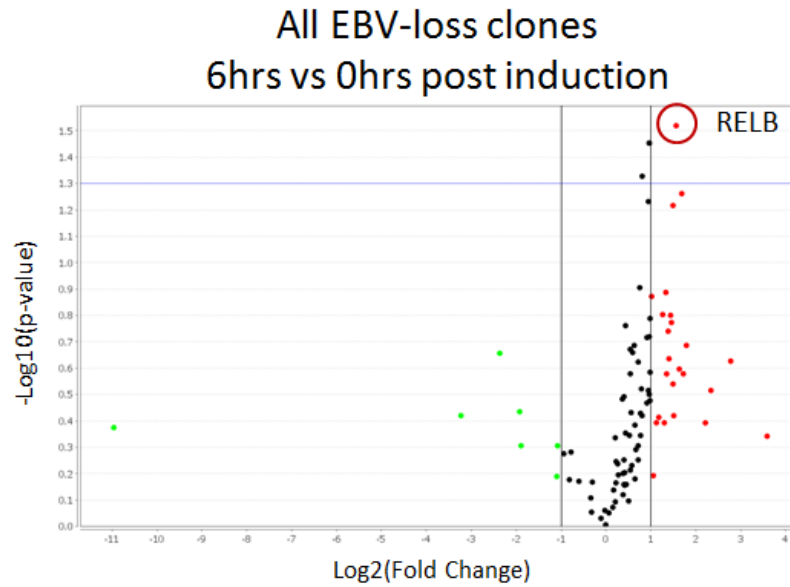
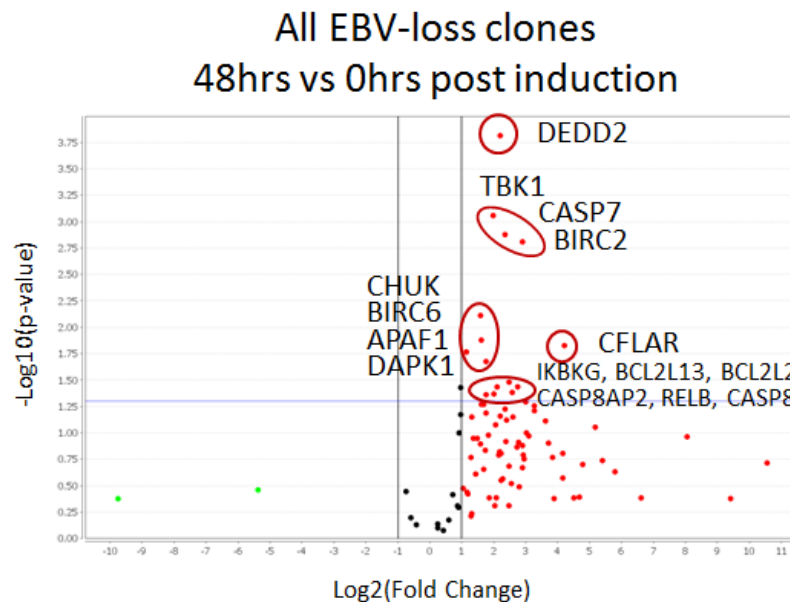
A**B**

Figure 5.15 Magnitude and significance of gene expression changes in Kem-BL derived EBV-loss clones after treatment with ionomycin and Q-VD.OPh

A EBV-loss clones, 6 hours vs 0 hours **B** EBV-loss clones, 48 hours vs 0 hours

Assays were carried out in technical and experimental triplicate and analysed using DataAssist software from Applied Biosystems. Cut-offs used were: Fold Change ≥ 2 and p-value in a two-tailed Students T-test ≤ 0.05

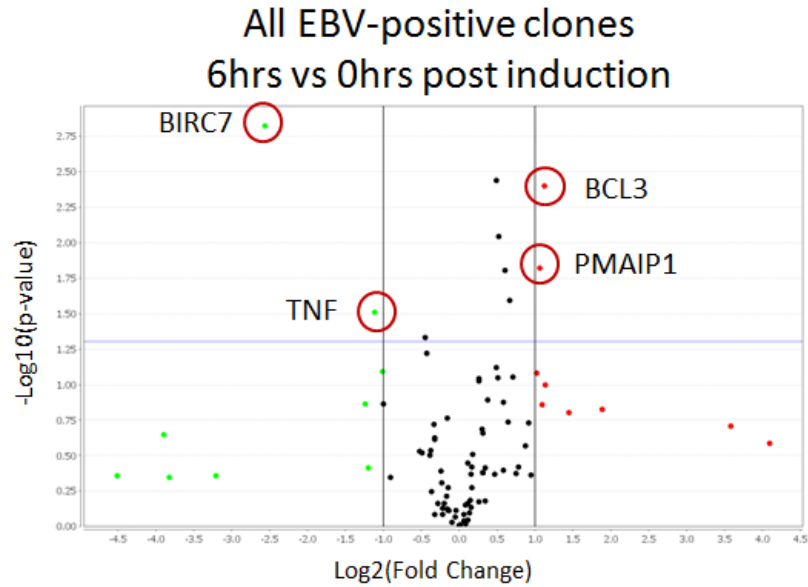
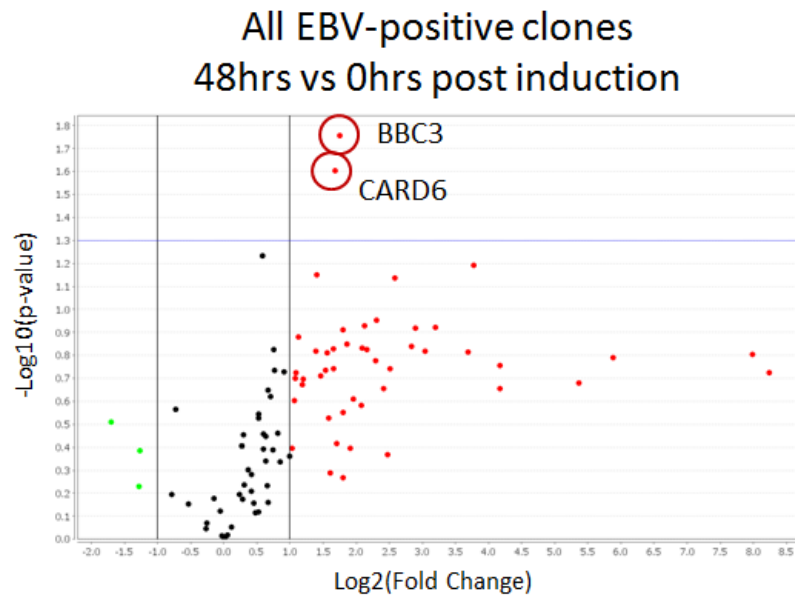
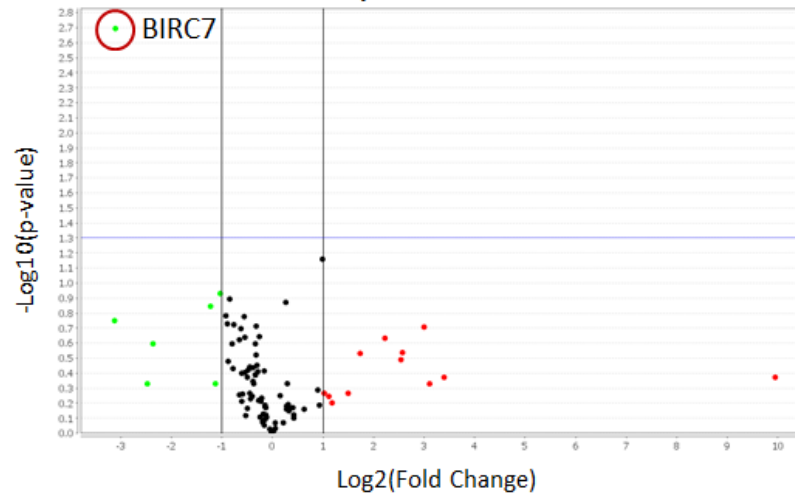
A**B**

Figure 5.16 Magnitude and significance of gene expression changes in Kem-BL derived EBV-positive clones after treatment with ionomycin and Q-VD.OPh

A EBV-positive clones, 6 hours vs 0 hours **B** EBV-positive clones, 48 hours vs 0 hours
Assays were carried out in technical and experimental triplicate and analysed using DataAssist software from Applied Biosystems. Cut-offs used were: Fold Change \geq 2 and p-value in a two-tailed Students T-test \leq 0.05

A

EBV-loss versus EBV-positive clones
0hrs post induction

**B**

EBV-loss versus EBV-positive clones
48hrs post induction

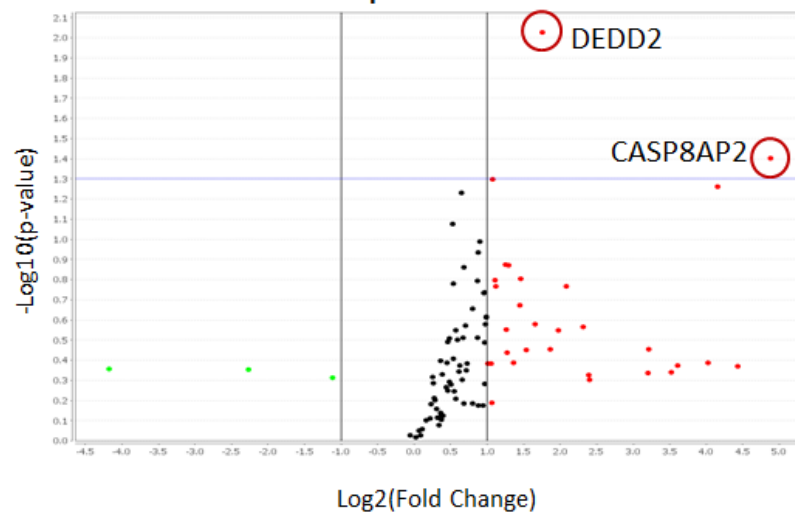


Figure 5.17 Magnitude and significance of gene expression changes in Kem-BL derived EBV-positive and loss clones after treatment with ionomycin and Q-VD.OPh

A EBV-loss versus EBV-positive clones at time 0 (comparison of baseline gene expression profiles) **B** EBV-loss versus EBV-positive clones at 48 hours post induction Assays were carried out in technical and experimental triplicate and analysed using DataAssist software from Applied Biosystems. Cut-offs used were: Fold Change ≥ 2 and p-value in a two-tailed Students T-test ≤ 0.05

EBV-positive clones shows that only 18 genes are changed >2-fold, 40% fewer than in EBV-loss clones, and of those only BIRC7, TNF, BCL3 and PMAIP1 (Noxa) are changed significantly at 6 hours (Figure 5.16-A). Again, more genes are changed in their regulation at 48 after apoptosis induction, but in the EBV-positive cells only BBC3 (Puma) and CARD6 are significantly different (Figure 5.16-B).

Figure 5.17 shows gene expression change comparisons between EBV-positive and loss clones at time 0 and 48 hours after apoptosis induction. As might be expected, only a only a single gene, BIRC7 (c-IAP2), varies in its expression between EBV-positive and loss cells at time 0 (Figure 5.17-A), but surprisingly there are only two significant changes in gene expression between EBV-positive and loss cells after 48 hours (Figure 5.17-B). Interestingly, the same two genes, DEDD2 and CASP8AP2, were also significantly upregulated in EBV-loss clones at 48 hours as well as when compared to their untreated counterparts.

A summary of all the significant changes identified by grouped pairwise comparisons is shown in Table 5.1, which also lists commonly used aliases of the shortlisted genes. Many of the gene expression changes are quite moderate, less than 5-fold, although there must be consistency across different clones within the group as levels of significance in some cases are very high. To identify exactly how many of the gene changes were consistent across every clone within a particular group we next carried out pairwise analyses of individual clones.

Gene	Gene Aliases	Fold Change	p-value	
EBV +ve Untreated vs EBV Loss Untreated				
BIRC7	LIVIN	0.12	0.002	***
EBV +ve Untreated vs EBV +ve 6hr ionomycin				
BCL3		2.17	0.004	***
PMAIP1	Noxa	2.08	0.015	*
TNF	TNF- α	0.46	0.031	*
BIRC7	LIVIN	0.17	0.0015	***
EBV +ve Untreated vs EBV +ve 48hr ionomycin				
BBC3	Puma	3.36	0.018	*
CARD6		3.21	0.025	*
EBV loss Untreated vs EBV loss 6hr ionomycin				
RELB		2.96	0.03	*
EBV loss Untreated vs EBV loss 48hr ionomycin				
CFLAR	c-FLIP	18.58	0.015	*
BIRC2	c-IAP1	7.47	0.0016	***
CASP8	Caspase-8	6.7	0.037	*
RELB		6.01	0.042	*
CASP8AP2	FLASH	5.6	0.033	*
CASP7	Caspase-7	5.12	0.0013	***
DEDD2	FLAME-3	4.58	0.00016	***
BCL2L2		4.3	0.037	*
BCL2L13	Bcl-RAMBO	3.99	0.043	*
TBK1		3.94	0.00087	***
IKBKG	Nemo	3.39	0.043	*
APAF1		3.37	0.021	*
BIRC6		3.06	0.013	*
CHUK	IKK- α	2.99	0.0078	**
DAPK1		2.22	0.017	*
EBV loss 48hrs iono vs EBV +ve 48hr ionomycin				
CASP8AP2	FLASH	29.49	0.039	*
DEDD2	FLAME-3	3.38	0.0094	**

Table 5.1 Summary of gene expression changes from grouped pairwise analyses

5.3.5 Pairwise analyses of individual clones

All possible pairwise analyses of all 6 clones at 3 time points was carried out and shortlists made of all transcripts that changed >2-fold. These lists of differentially regulated genes were then compared to one another to identify common changes. Figure 5.18-A shows the number of genes that had changed by 2-fold or more in each EBV-positive clone at 6 hours (left) or 48 hours (right), compared to time 0. At 6 hours 14, 33 and 21 genes had changed at least 2-fold in clones P1, P2 and P3, respectively, whereas at 48 hours 61, 34, and 57 genes had changed in P1, P2 and P3, respectively. This relatively large number of changes in apoptosis-related gene expression was surprising as the grouped analyses had suggested there were relatively few changes in EBV-positive clones. Interestingly, the vast majority of changes were common to at least 2 of the three clones at both 6 and 48 hours, although intriguingly, the number of genes that increased in their expression between 6 and 48 hours was very different for each clone, ranging from an increase of 1 to 47 changed genes.

Figure 5.18-B shows the same comparisons at 6 hours (left) and 48 hours (right) for EBV-loss clones. More genes were changed in all of the EBV-loss clones at both 6 and 48 hours than in EBV-positive clones at the same time points. At 6 hours 19, 38 and 56 genes had changed in clones n1, n2 and n3, respectively, and by 48 hours 83, 78 and 81 genes had changed in n1, n2 and n3, respectively. This finding is consistent with the EBV-loss phenotype, but we were still surprised that so many genes (83-89% of all targets on the card) had changed more than 2-fold.

As in the analysis of EBV-positive clones, the majority of changes were common to at least two of the loss clones at both time points, with 67 changes being common to all three clones at 48 hours. Interestingly, clone n3 looked quite different to the other two clones at 6 hours and this clone was also consistently the least viable of the clones at 48 hours (see Figure 5.11-A). Therefore this clone is likely to be further along the apoptosis pathway in comparison to the other clones at 6 hours and by 48 hours the other clones have 'caught up'.

With this in mind, we decided to pool the data and compare all changes that were common to all three positive clones at 48 hours to the 67 genes that were changed in all of the loss clones (Figure 5.18-C). We found that almost every gene that had changed in the positive clones had also changed in the loss clones. This further suggests that all BL clones undergo the same changes during the commitment to programmed cell death, but with slower kinetics in those clones that contain EBV. The two genes that were changed in all three EBV-positive clones but not all three EBV-loss clones, were also changed in two of the three EBV-loss clones, indicating that one loss clone was an outlier in this response.

Collectively, our transcriptional data suggest that many of the changes we have seen may reflect the degree to which each of the cell lines has committed to apoptosis, rather than being the specific triggers of apoptosis in BL clones however, the data from our q-PCR arrays alone are insufficient to prove this hypothesis. We therefore went on to further investigate the significant changes from the grouped analyses in order to look more closely at the kinetics of gene expression change in EBV-positive and loss clones, and to identify whether the changes we had seen at the transcriptional level are also evident at the protein level.

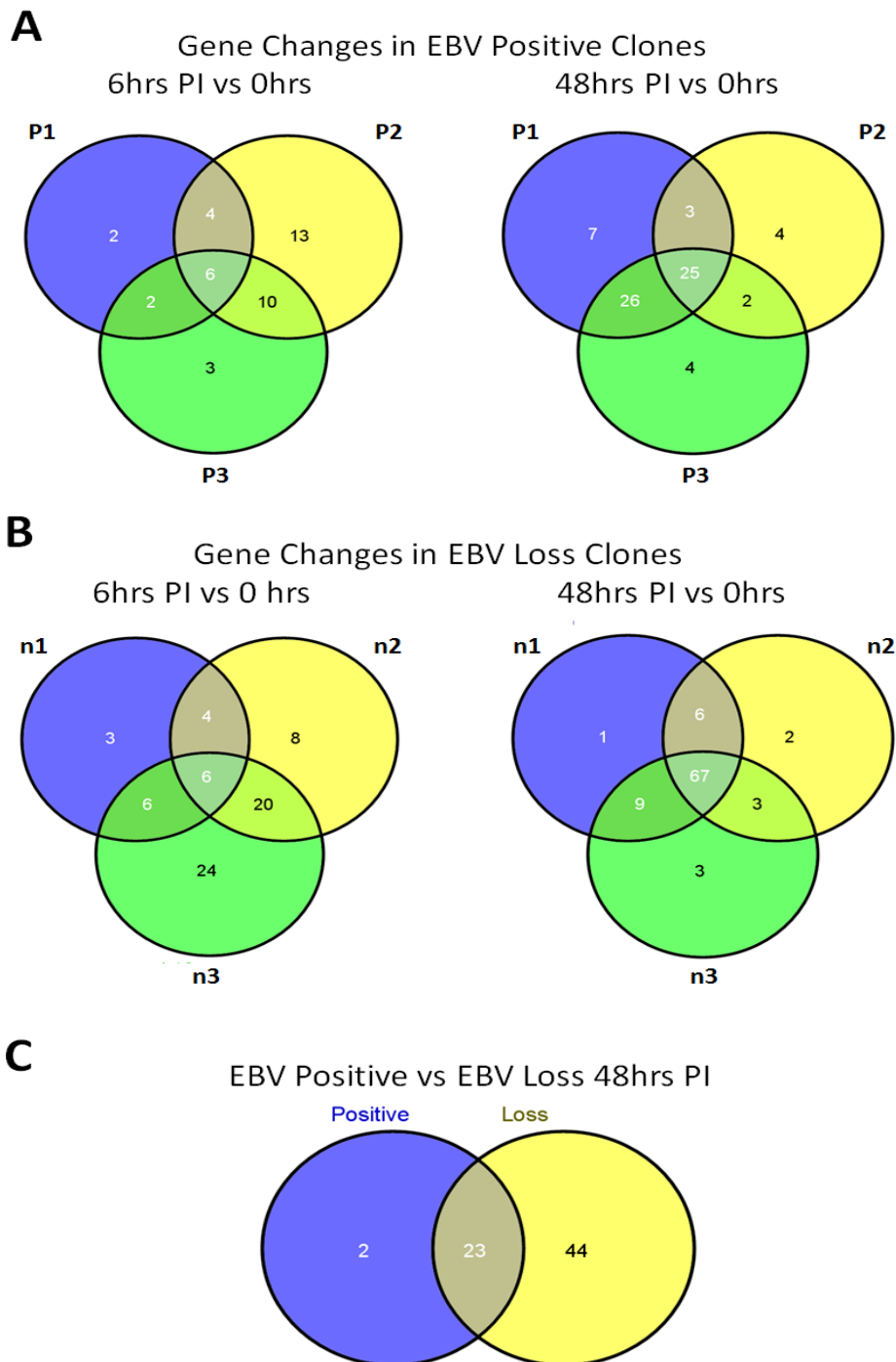


Figure 5.18 Overlap in gene expression changes of 2-fold or more in individual clones of Kem-BL
A concordance between gene expression changes in 3 EBV-positive clones at 6 (left) or 48 hours (right) after apoptosis induction
B concordance between gene expression changes in 3 EBV-loss clones at 6 (left) or 48 hours (right) after apoptosis induction
C concordance between gene expression changes in 3 EBV-positive clones versus EBV-loss clones 48 hours after apoptosis induction
 Made using VENNY software (Oliveros, J.C. (2007) VENNY. An interactive tool for comparing lists with Venn Diagrams <http://bioinfogp.cnb.csic.es/tools/venny/index.html>)

5.3.6 Relative quantitation

By carrying out q-PCR arrays rather than traditional microarrays, we were also able to calculate with greater accuracy the relative quantities of all of the targets at every time point compared to a reference sample. We therefore plotted the mean of the three EBV-positive and three EBV-loss clones at each time point, for all of the 21 significantly differentially regulated targets identified by the grouped pairwise analyses (Table 5.1), using Kem clone P1 at 0 hours as the reference sample.

Caspase-7 (CASP7), in conjunction with the other 'executioner' Caspases; -3 and -6, is responsible for the majority of the proteolytic destruction of cell substrates during apoptosis [384, 578]. In our screen, Caspase-7 was upregulated over 4-fold in EBV-loss clones after treatment with ionomycin however, it was also upregulated in some of the EBV-positive clones, although not significantly (Figure 5.19-A). Given the critical and important role of Caspase-7 in apoptosis it is not surprising that many viruses encode caspase inhibitors (reviewed in [579]), although no caspase inhibitor has been described so far for EBV. Our data imply that EBV may block transcription of Caspase-7 rather than inhibiting its proteolytic function.

BIRC2 (c-IAP1) is part of the IAP family of apoptosis regulators which bind to and inhibit cleavage of caspases [580]. We found that BIRC2 was significantly upregulated over 7-fold in EBV-loss cells following ionomycin treatment, which may suggest that its NF- κ B signalling capacity, rather than its ability to inhibit apoptosis is important in this context (Figure 5.19-B) [581]. Similarly to Caspase-7, BIRC2 was only significantly upregulated at the 48 hour time point and we again also saw a response in the EBV-positive cells, albeit more variable and of a lesser magnitude.

CFLAR, also known as c-FLIP, a master regulator of apoptosis, was upregulated 18.6-fold in ionomycin-treated EBV-loss cells at 48 hours compared to time 0 (Figure 5.19-C). FLIP proteins

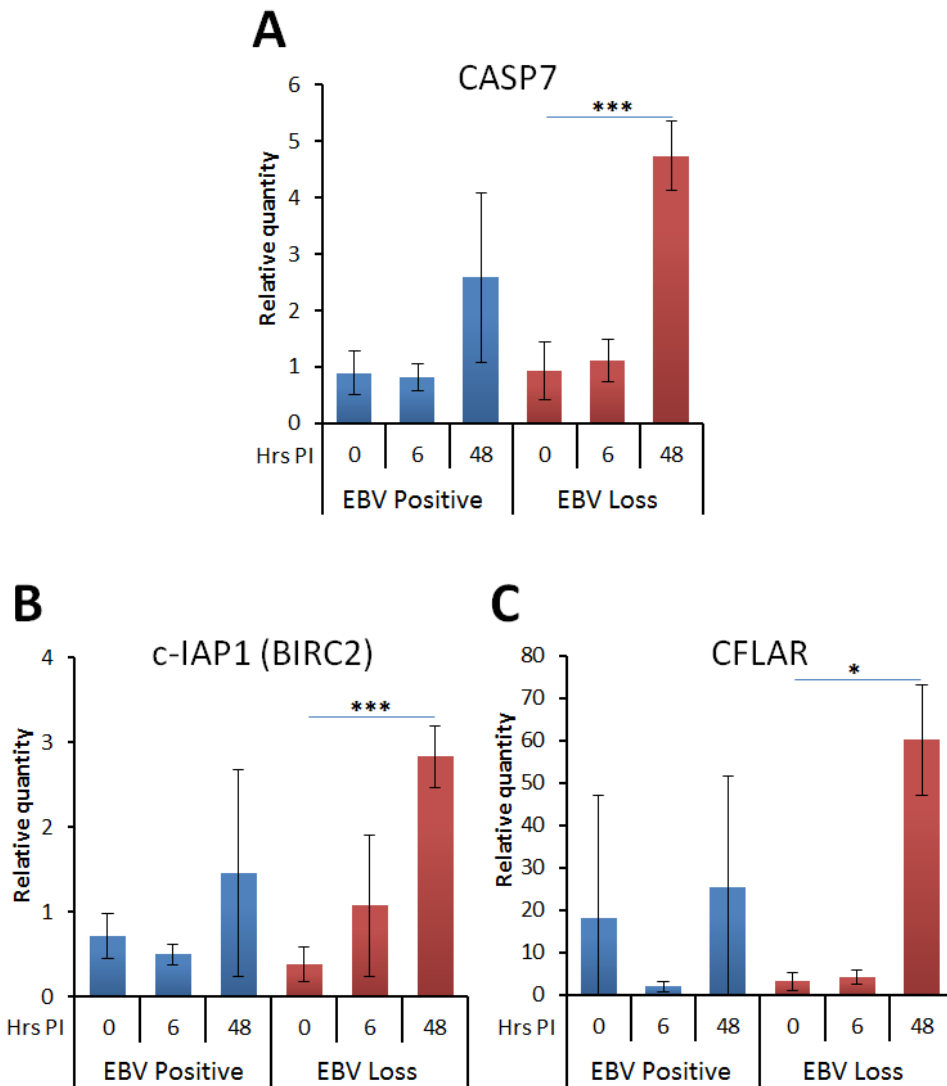


Figure 5.19 CASP7, c-IAP1 and CFLAR transcription measured by q-PCR using the $\Delta\Delta C_t$ method

A Caspase-7 **B** Cellular inhibitor of apoptosis 1 **C** CFLAR, also known as c-FLIP
 Data expressed as relative quantitation with Kem-BL, 0 hours as the reference sample. Mean and SD from 3 different clones in 3 independent experiments. Statistical comparisons carried out using a two-tailed Student's T-test

are known to be targeted by many viruses, and some, such as KSHV, a close relative of EBV, encode viral homologues of FLIP (v-FLIPs), [582, 583], although EBV itself does not. FLIP proteins, like IAPs, block the activation of the caspase cascade [584], providing a second example of EBV-loss clones upregulating a gene with known anti-apoptotic functions after ionomycin treatment.

Overall, this pattern of gene expression, where the target of interest was only significantly changed in EBV-loss cells at the 48 hour time point and was also upregulated, albeit more

variably and to a lesser degree, in the EBV-positive group, was also evident in many of the other genes (both pro- and anti-apoptotic) that we had shortlisted (data not shown). This is consistent with our hypothesis that the majority of the changes identified by these arrays may be downstream effects of cell death initiation, even in the absence of PARP cleavage or loss of viability. Therefore, although these gene expression changes provide important clues to the signalling mechanisms by which BL cells commit to cell death, they are probably not the initiators of the response, and are therefore unlikely to be direct targets for EBV in this setting. In our preliminary assays, Puma (BBC3) was significantly upregulated in EBV-loss clone n1 versus EBV-positive Kem-BL after ionomycin treatment (Figure 5.8 and 5.9-A) yet, in our q-PCR arrays Puma was identified as being significantly upregulated in EBV-positive cells at 48 hours, but not EBV-loss clones. Consistent with many of our other shortlisted genes, relative quantitation data showed that Puma is upregulated in both EBV-positive and loss cells, but to a greater extent in EBV-loss clones. In this case however, the response in the EBV-loss clones is more variable than in EBV-positive cells and so the differential regulation is classed as significant only in the EBV-positive group (Figure 5.20).

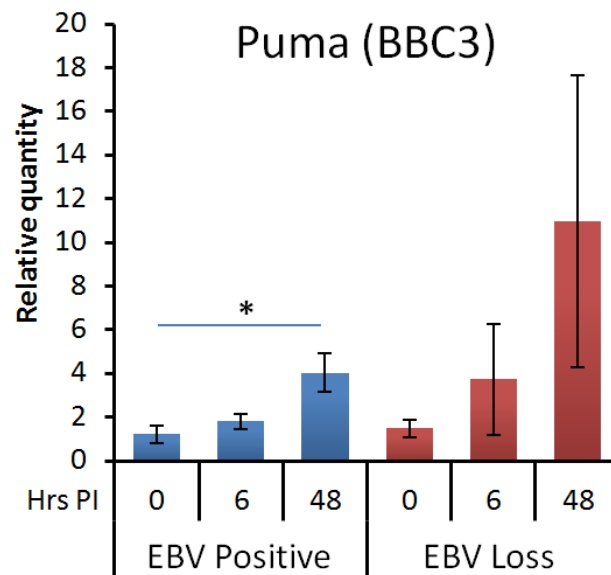


Figure 5.20 Relative quantitation of Puma expression transcription measured by q-PCR using the $\Delta\Delta C_t$ method
 Data expressed as relative quantitation with Kem-BL, 0 hours as the reference sample. Mean and SD from 3 different clones in 3 independent experiments. Statistical comparisons carried out using a two-tailed Student's T-test

DEDD2, also known as FLAME3, was one of only two genes found to be significantly changed in EBV-loss clones at 48 hours versus both untreated cells and treated EBV-positive clones. DEDD2 was upregulated 4.6-fold in treated EBV-loss cells whilst there was almost no change in EBV-positive cells (Figure 5.21-A). Little is known about the function of DEDD2, although its role in cell death is thought to occur via binding to FLIP proteins, [585, 586] and Caspases-8 and -10 [587].

CASP8AP2 (FLASH) was the second of two genes found to be significantly upregulated in EBV-loss clones at 48 hours versus both untreated cells and EBV-positive clones at 48 hours post induction (Figure 5.21-B). Unlike many other genes identified in this screen, upregulation of FLASH appeared to begin early after apoptosis induction and, by 48 hours shows a more than 5-fold increase over time 0 and an almost 30-fold increase over EBV-positive cells at the same time point. Interestingly, although there seems to be some early activation of FLASH in EBV positive cells this appears to be reversed by 48 hours.

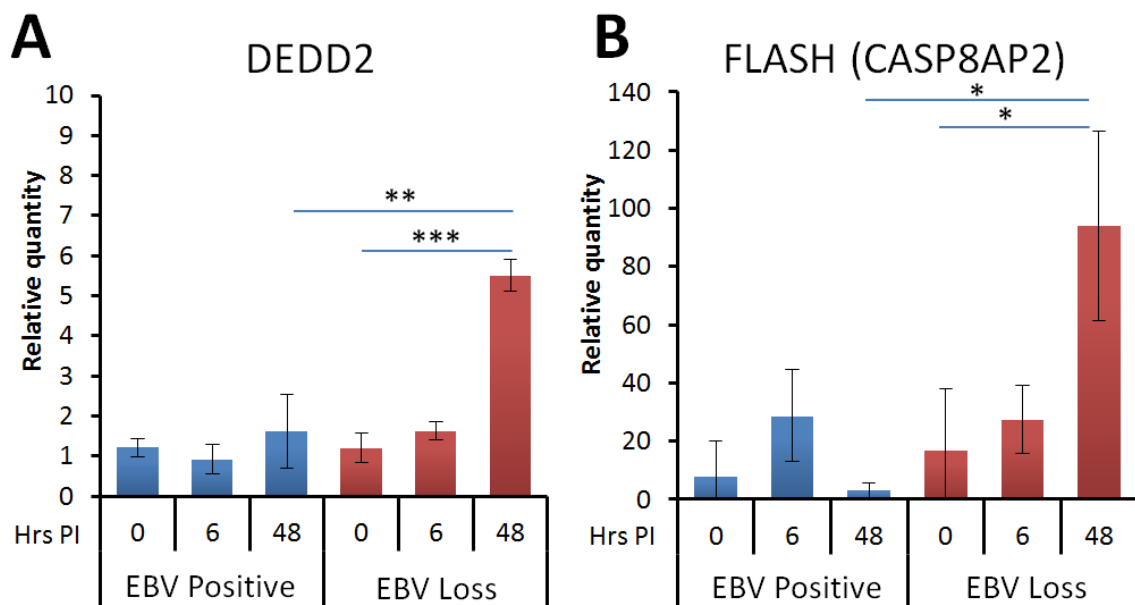


Figure 5.21 Relative quantitation of DEDD2 and FLASH measured by q-PCR using the $\Delta\Delta C_t$ method

A DEDD2 **B** CASP8AP2 more commonly referred to as FLASH

Data expressed as relative quantitation with Kem-BL, 0 hours as the reference sample. Mean and SD from 3 different clones in 3 independent experiments.

Statistical comparisons carried out using a two-tailed Student's T-test

Our q-PCR arrays showed that, even in viable cells in the absence of caspase cleavage, a large number of apoptosis-related genes change in their expression in response to apoptosis initiation, and that many of the changes may be common between all BL cells regardless of EBV status. Of the shortlisted genes, only DEDD2 and CASP8AP2 appeared to change specifically in EBV-loss cells and not EBV-positives. Additionally, EBV-loss cells consistently underwent more rapid and dramatic apoptosis activation than their EBV-positive counterparts, suggesting that, as well as possibly transcriptionally regulating DEDD2 and CASP8AP2, EBV may have a role in targeting some upstream cell fate-determining 'master switch' and / or that the target(s) of the virus are not transcriptional. We therefore went on to characterise expression of a variety of apoptosis-related proteins in treated and untreated Kem-BL clones by Western blot.

5.4 Apoptosis-related changes in clones of Kem-BL at the protein level

5.4.1 Western blotting experimental set up

Western blotting allows us to gain qualitative, and to some degree, quantitative data about gene expression and may be used to detect increases in protein synthesis or accumulation due to stabilisation, decreases due to a block in synthesis, degradation, cleavage events and in some cases, protein modifications indicated by a shift in protein size. Other technologies, such as antibody arrays or proteomics were considered for this study as this would allow us to look at a greater number of proteins, and in the case of proteomics, would be totally unbiased, but the number of samples required to draw reliable conclusions would make both techniques prohibitively expensive. The alternative option of running only a few samples may give misleading results, as we would have to sacrifice the number of clones included, the number of time points or the number of experimental replicates.

Every antibody used in his study has either been previously validated on other samples by us, or been used in publications from at least two different research groups. Details of antibodies used can be found in Section 2.8.2. Since small changes in expression are difficult to quantify by Western blot, we screened Kem-BL clones at 48 hours after apoptosis induction to look for changes that were consistent in all three clones of one group and were specific to either EBV-positive or EBV-loss cells. Jurkat samples were included on every blot to allow for normalisation between different blots and to act as controls for healthy, apoptotic and pre-apoptotic (caspase-inhibitor treated) cells. All changes in protein expression were normalised to calregulin levels as it was found to be expressed at similar levels at every time point in preliminary experiments, whereas β -actin levels clearly decreased in response to apoptosis induction (data not shown). Protein quantitation and normalisation was carried out using the BioRad ImageLab software. Densitometry data was normalised to the loading control calregulin and expressed relative to expression levels of the protein of interest in healthy (untreated) Jurkat cells or untreated Kem P1 cells in cases where the protein of interest was not expressed/undetectable in untreated Jurkat cells.

5.4.2 Caspases

Caspases are activated when they are cleaved from their full length, inactive form, whereupon their destructive proteolytic activity is unleashed. Our q-PCR arrays identified Caspase-7 and Caspase-8 as being more highly upregulated in EBV loss clones than their EBV-positive counterparts upon treatment with ionomycin in the presence of Q-VD.OPh. The Q-VD.OPh peptide is able to bind and inhibit cleavage of initiator Caspases-4, -8, -9, -10 and -12, as well as executioner Caspases-3, -6 and -7, although its activity varies depending on the experimental system used [588-590]. As previously mentioned, a number of viruses inhibit caspase expression and/or function, and a recent publication showed that EBV-encoded miR

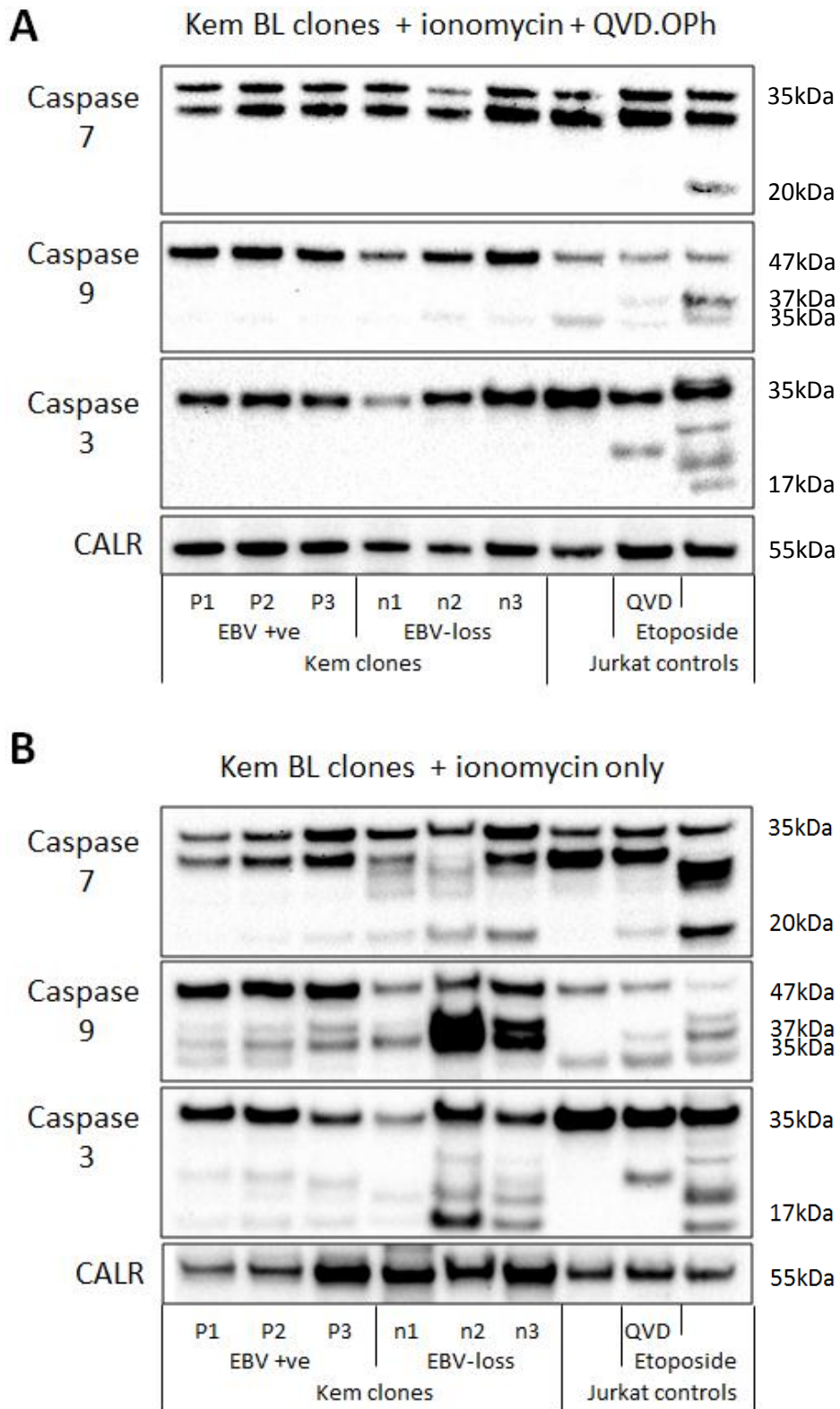


Figure 5.22 Caspase-3, -7 and -9 Western blots on EBV-positive and loss Kem-BL clones 48 hours after apoptosis induction
A Kem-BL clones treated with 1 μ g/ml ionomycin to induce apoptosis and 25 μ M QVD.OPh to block caspase cleavage
B Kem-BL clones treated with ionomycin only

BARTs can inhibit Caspase-3 promoter activity in BL cells [99]. Since Q-VD.OPh does not affect caspase transcription, we examined the expression and activation of several caspases in our panel of BL clones in order to further investigate whether EBV regulated caspase expression in BL clones.

In Q-VD.OPh-treated cells Caspases 3, 7 and 9 remained in their inactive, full length forms and we found no significant difference in protein expression levels between EBV-positive and loss clones, suggesting that EBV does not inhibit transcription of Caspases 3, 7 or 9 in Kem-BL (Figure 5.22-A). Unfortunately, we were unable to determine levels of Caspase-8 expression by Western blot as our antibody gave very poor and inconsistent results, and so we were unable to validate our transcriptional data in this case.

Cleavage of Caspases 3, 7 and 9 was evident in EBV-loss clones in the absence of Q-VD.OPh, but to a lesser extent or not at all in EBV-positive Kem-BL clones (Figure 5.22-B). Whilst this is supportive of a hypothesis of caspase inhibition by EBV, this is also consistent with the fact that there is simply more apoptosis occurring in the EBV-loss cells. Therefore we think that this is likely to be a downstream effect of cell death rather than directly related to presence or absence of EBV; a hypothesis that is corroborated by the fact that we see a similar effect in all three of the caspases investigated. Interestingly, and similarly to our PARP blots, we saw differences in the patterns of caspase cleavage products individual in different clones, indicating that there may be variation in which upstream proteases are responsible for cleaving and activating caspases in different clones.

5.4.3 Targets from q-PCR arrays

DEDD2, CFLAR, CARD6 and CASP8AP2 were all significantly upregulated in EBV-loss clones following ionomycin treatment in our q-PCR array experiments, we therefore examined whether levels of the corresponding proteins correlated with our transcriptional findings

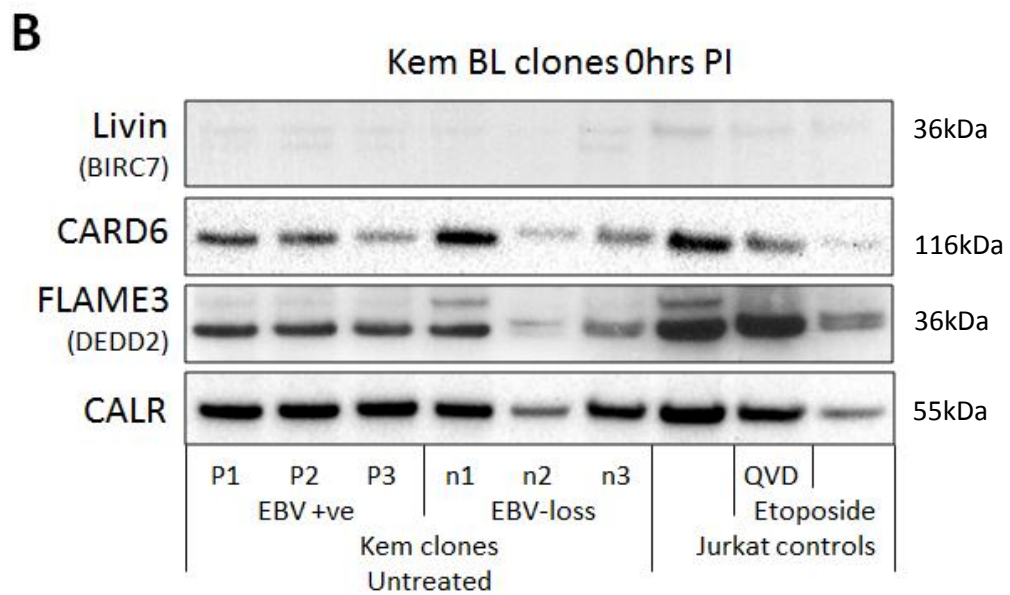
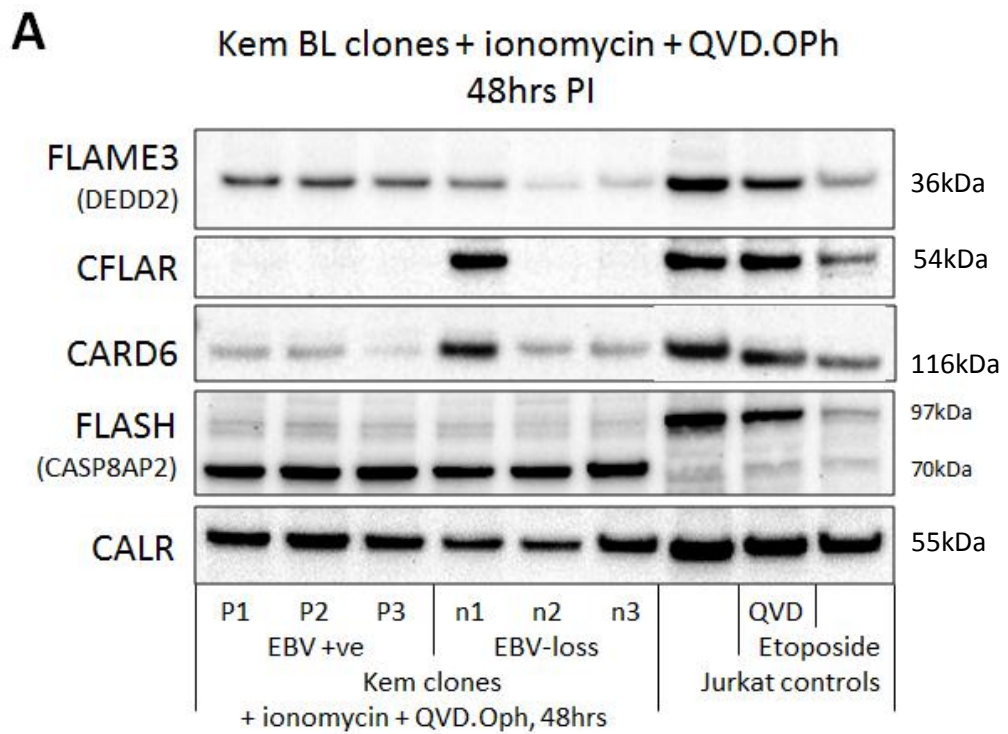


Figure 5.23 Protein expression of targets identified by q-PCR array
A Kem-BL clones treated with 1 μ g/ml ionomycin to induce apoptosis and 25 μ M Q-VD.OPh to block caspase cleavage 48 hours
B Kem-BL clones at 0 hours

(Figure 5.23). The FLAME3 protein, encoded by DEDD2, appeared to be more highly expressed in EBV-positive clones than those that had lost the virus after apoptosis induction, which is in direct contradiction to the change in DEDD2 transcription seen in our arrays (Figure 5.23-A). Surprisingly, there was also no evidence that CFLAR or CARD6 were more highly expressed in EBV-loss clones overall, although both were abundant in loss clone n1. Unfortunately, we were unable to obtain satisfactory staining with our FLASH antibody; the FLASH protein is predicted to run at around 200kDa however, the only clear bands on our blots ran at 70kDa or 97kDa in Kem or Jurkat, respectively [591]. We are unclear how to interpret this blot data, but we noted that, FLASH, encoded by CASP8AP2, is thought to induce apoptosis via downregulation of Mcl-1 and CFLAR [592], which we similarly see no evidence of in our EBV-loss clones (Figure 5.23-A & 5.25).

BIRC7, which encodes Livin, was significantly lower in EBV-loss clones at time 0 compared to EBV-positives at the same time point at the transcript level, but this was not evident at the protein level (Figure 5.23-B). CARD6 was transcribed at significantly higher levels in EBV-positive cells at 48 hours versus time 0 and DEDD2 (FLAME3) was specifically upregulated in EBV-loss clones at 48 hours versus time 0. However, when we compared our staining for these proteins in our untreated samples to ionomycin-treated cells, using the Jurkat controls as a reference point, we could see no evidence that these findings held true at the protein level (Figure 5.23-A & 5.23-B).

Whilst it was disappointing that we could not corroborate our transcriptional data with levels of protein expression we are still able to draw useful conclusions from these experiments. It is interesting that there appear to be widespread transcriptional changes in BL clones following apoptosis induction that occur in the absence of caspase or PARP activation and do not necessarily lead to changes in protein expression. This robust and complex response to stress signals, in-keeping with our Bim₅ mutant assays, suggests that the mechanism by which EBV acts is to a generally slow or dampen the progression of the apoptotic cascade. These findings

indicate that a more specific mechanism, whereby the virus inhibits or activates one particular entity within a pathway would surely not be sufficient to effectively subvert this wide-ranging response.

5.4.4 The IAP family

The inhibitor of apoptosis family of proteins (IAPs) were first identified as inhibitors of apoptosis, although it is now known they also play a role in the innate immune response via NF- κ B and ubiquitin signalling [581]. These proteins are frequently deregulated in haematological malignancies and it is hoped that therapies that target IAPs may be useful to treat a number of cancers, we therefore examined the expression of several IAP proteins by Western blot (Figure 5.24) [593]. BIRC2 (c-IAP1) was significantly upregulated in EBV-loss clones in our q-PCR arrays compared to EBV-positives however, we could find no difference between EBV-positive and loss clones in c-IAP1 protein expression. We also found no correlation between XIAP, Livin (BIRC7) or Survivin protein expression and EBV status in Kem-BL clones after apoptosis induction. Therefore, although EBV has previously been reported to regulate IAPs in other systems [321, 594, 595], we find no convincing evidence that EBV regulates IAP protein expression in BL clones in this system.

IAP family proteins

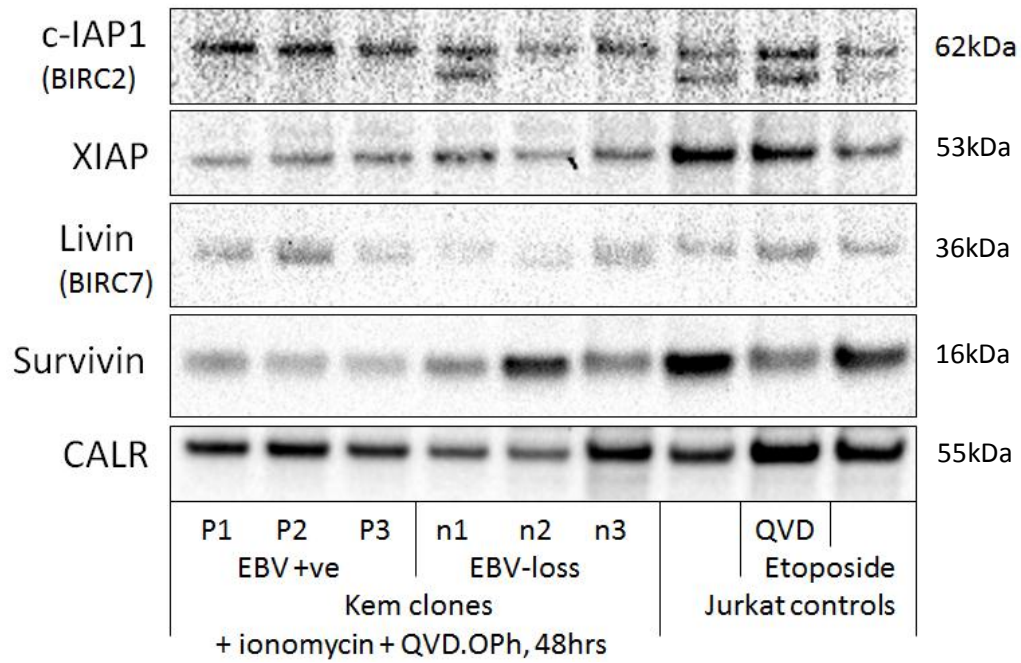


Figure 5.24 Expression of IAP family member proteins in Kem-BL clones
c-IAP1 is predicted to run at 62kDa, corresponding to the upper band on this blot

5.4.5 The Bcl-2 family

Our initial apoptosis assays using a variety of apoptosis inducers indicated that EBV protects BL cells from apoptosis via the intrinsic, or mitochondrial signalling pathway. We therefore examined differences in expression of the Bcl-2 family members, which coordinate the intrinsic apoptosis response. Rather than looking for changes in expression between untreated and treated cells we opted to screen for differences between ionomycin and Q-VD.OPh treated EBV-positive and loss clones. Of the anti-apoptotic Bcl-2 family members we looked at, Bcl-2 itself was undetectable and Bcl-XL was expressed at very low levels in 5 of the 6 clones. Interestingly however, both Bcl-2 and Bcl-XL were expressed in EBV-loss clone n1 (Figure 5.25) the same clone that showed evidence of being Bcl-2 or Bcl-XL dependent in Bim₅ variant studies and could not be fully rescued by reinfection (see Figures 4.29-B & 5.5-C).

Pro-survival Bcl-2 homologues

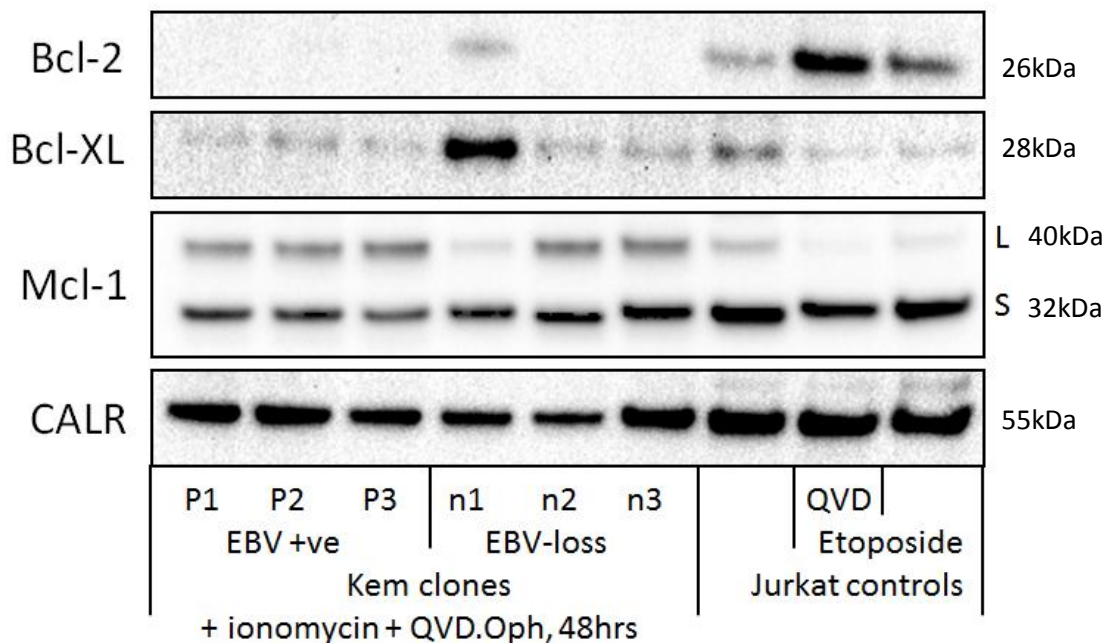


Figure 5.25 Expression of pro-survival Bcl-2 proteins in Kem-BL clones after treatment with ionomycin and Q-VD.OPh

Pro-apoptotic Bcl-2 homologues

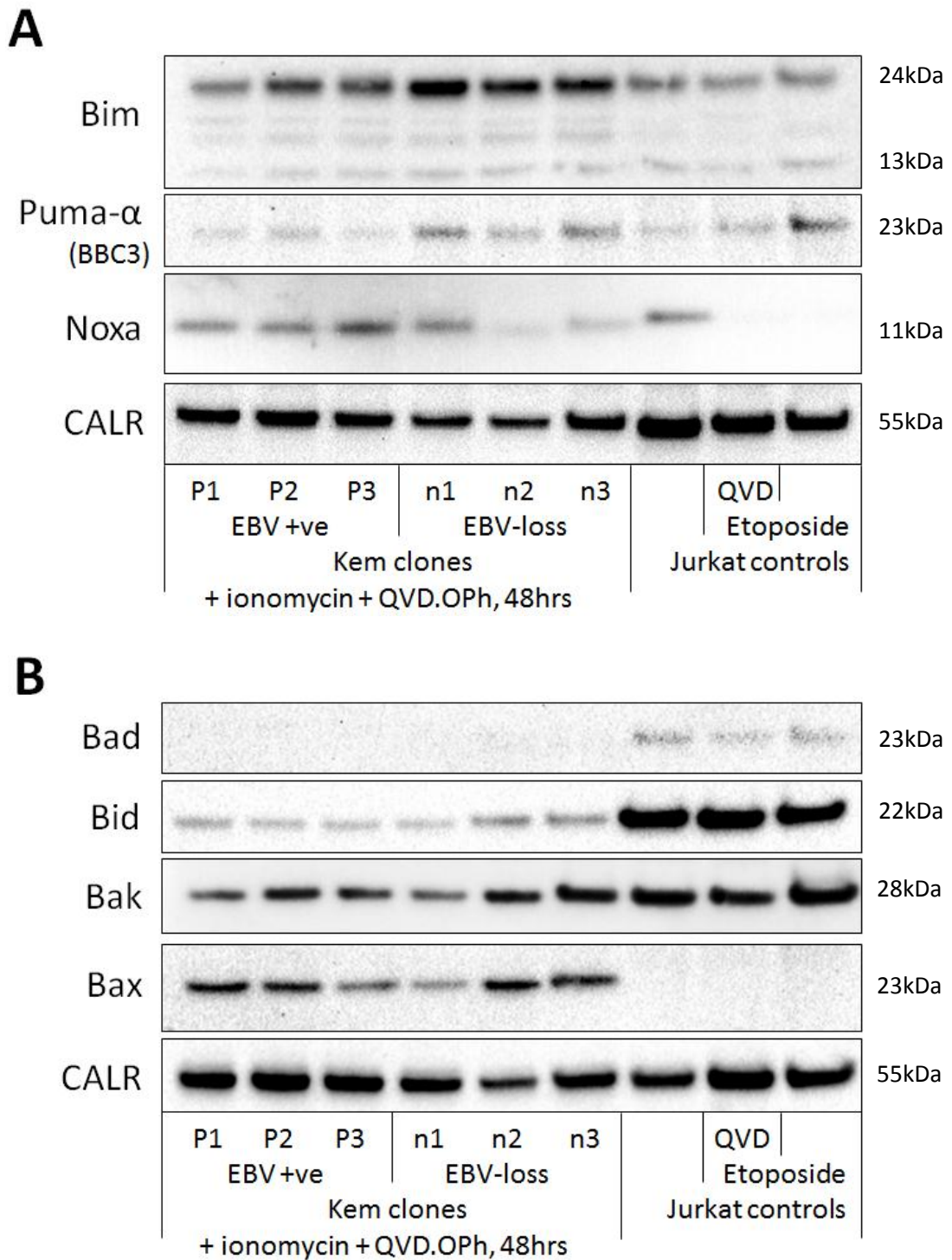


Figure 5.26 Expression of pro-apoptotic Bcl-2 homologues in Kem-BL clones after treatment with ionomycin and Q-VD.OPh

A BH3 only proteins Bim, Puma- α , and Noxa

B BH3-only proteins Bad and Bid and multi-domain effector proteins Bak and Bax

In addition, Mcl-1 was expressed at stable levels in all of the clones except clone n1, in which the L-isoform was barely detectable, in agreement with our earlier findings (Figure 5.8), which further suggests that this clone may have adapted to survive the loss of EBV. Unfortunately, we were unable to find a suitable antibody against A1.

Of the pro-apoptotic BH3 proteins, Bim, Puma and Noxa have all previously been reported to play an important role in apoptosis in BL cells [267, 419, 596]. Both Bim and Puma appeared to be expressed more highly in all of the ionomycin-treated EBV-loss clones versus their EBV-positive counterparts (Figure 5.26-A), confirming our Puma transcriptional data. Paradoxically, since it is a pro-apoptotic protein, Noxa appeared to be less abundant in two of the three EBV-loss clones than EBV-positive clones. The exception to this being clone n1, which as mentioned, also stands out from the other EBV-loss clones in terms of its gene expression and response to challenge with BH3 variant proteins. Bid, Bax and Bcl-2 were also expressed at higher levels in EBV-loss clones n2 and n3, but not n1 (Figure 5.26-B), although these differences were not significant when quantified (Table 5.2) so we would need to confirm this in additional EBV-loss clones. Bad protein was undetectable in clones of Kem-BL.

5.4.6 Summary of Western blotting for apoptosis related proteins

Table 5.2 is a summary of all of the Western blotting we carried out to compare protein expression in EBV-positive and loss clones after treatment with ionomycin and Q-VD.OPh. All quantitation was carried out using ImageLab software from Bio-Rad, relative to untreated Jurkat cells (or untreated Kem-BL if the protein of interest was not expressed in Jurkat) and data were normalised to Calregulin. This analysis identified 7 proteins (highlighted in red) as being upregulated more than 2-fold in EBV-loss clones compared to EBV-positives following apoptosis induction although, due to variation in expression levels between individual cells only 2, Bim and Puma, were deemed significant ($P < 0.05$) using a Student's T-test. If EBV-loss

	EBV Positive			EBV Loss			EBV Loss vs EBV Positive	
	P1	P2	P3	n1	n2	n3	Fold Change	p-value
Anti-apoptotic Bcl-2 Homologues								
Bcl-2	0.02	0.03	0.02	0.5	0.03	0.02	8.3	0.4
Bcl-XL	0.2	0.3	0.2	3.0	0.8	0.5	5.7	0.3
Mcl-1 (total)	1.0	0.9	1.2	0.5	2.5	1.6	1.5	0.5
Mcl-1 (L)	1.7	1.6	2.0	0.4	4.1	2.5	1.3	0.6
Mcl-1 (S)	0.4	0.3	0.3	0.5	1.0	0.7	2.1	0.1
Pro-apoptotic Bcl-2 Homologues								
Bim (total)	0.7	1.0	1.1	2.2	2.8	1.7	2.4	0.04
Puma- α	1.2	1.0	0.7	4.6	6.0	6.3	5.8	0.01
Noxa	0.6	0.4	0.7	0.6	0.1	0.5	0.7	1.0
Bid	0.1	0.05	0.04	0.1	0.2	0.1	2.4	0.2
Bak	0.3	0.4	0.4	0.3	0.9	0.7	1.8	0.3
Bax	0.8	0.6	0.4	0.3	1.5	1.0	1.6	0.4
IAP Family Proteins								
c-IAP1	1.8	1.5	1.6	1.7	1.4	1.2	0.9	0.3
XIAP	0.2	0.3	0.4	0.6	0.4	0.4	1.5	0.1
Survivin	1.3	1.8	0.8	0.7	0.9	1.2	0.7	0.3
Survivin	0.3	0.2	0.2	0.4	1.0	0.3	2.8	0.2
Others – Identified by QPCR Arrays								
FLAME3	0.7	0.7	0.8	0.8	0.2	0.3	0.6	0.3
CFLAR	0	0	0	3.1	0	0		0.4
CARD6	0.9	0.8	0.4	4.7	1.5	1.2	3.6	0.3
FLASH (70kDa)	8.9	8.4	11.5	12.2	15.5	11.1	1.4	0.1

Table 5.2 Summary of apoptosis-related protein expression in Western blots. Data normalised to calregulin loading control and expressed relative to untreated Jurkat cells. Fold change is calculated as the mean of the expression value in the three loss clones divided by the mean expression in the EBV-positive clones at 48 hours after apoptosis induction. P-values were calculated using a two-tailed Student's T-test

clone n1 is excluded from this analysis Mcl-1, Noxa, Bid, Bak, Bax, Survivin and CARD6 would also vary more than two-fold between EBV-positive and EBV-loss clones however, none of these changes is reaches significance due to the lack of replicates.

Compared to the huge number of proteins known to be involved in apoptosis we only looked at a relatively small subset, although we were able to include many key regulators of the intrinsic apoptosis pathway as well as targets identified by our q-PCR arrays. Given the large number of transcriptional changes in Kem-BL clones we were surprised that so few of the proteins we investigated changed in their expression and to fairly modest degrees. Interestingly however, Bim and Puma, which were both significantly differentially expressed between EBV-positive and loss clones, are known to be potent inducers of apoptosis [444, 450], and as previously mentioned, have both previously been reported to be targets of EBV. Additionally, Bim, Puma and Noxa have been shown to play an important and likely co-operative role in MYC-driven lymphomagenesis *in vivo* [274]. Therefore we considered that co-operation between Bim and Puma may be responsible for the EBV-loss phenotype.

5.5 FACS analysis of protein expression changes in Kem-BL clones

Western blotting provided a convenient and effective way to screen for differences in protein expression between EBV-positive and loss clones at late time points after ionomycin and Q-VD.OPh treatment. We had expected to see a number of dramatic differences which would help to illuminate the mechanism of apoptosis inhibition by EBV. Had this been the case we could have then dissected the kinetics and orchestration of apoptosis initiation in these clones in order to better understand the role of the virus in subverting this response. Therefore, although we found consistent and convincing changes in the expression of the Bim and Puma proteins, due to the small number of targets and the modest fold changes we saw, we decided to further investigate their role in the EBV-loss phenotype using a more sensitive technique.

FACS staining offered a number of advantages over Western blotting in these experiments; we were able to quantify both the number of cells expressing our gene of interest and with what intensity, allowing us to quantitate differences even where changes were relatively small. Additionally, although we carried out our initial screen on cells that had been treated for 48 hours, we considered that any specific changes related to the presence or absence of EBV, rather than as a downstream consequence of the widespread activation of apoptosis regulating pathways (as we had seen in our q-PCR screens), would be evident soon after drug treatment. Consequently, and in line with our preliminary experiments where we saw changes in gene expression within a few hours of drug treatment, we decided to look at Bim and Puma expression at 6 hours post induction compared to cells harvested at the beginning of the experiment (0 hours). We also looked at Noxa expression in these cells as Bim, Puma and Noxa have been shown to exhibit synergy in lymphomagenesis [274], and because Noxa has previously been reported to be important in the EBV-loss phenotype [419]. Yet our Western blots, using the same antibody against Noxa showed weak staining that did not corroborate this finding (Figure 5.26-A).

5.5.1 Bim

We found that >90% of cells in every sample analysed stained positive for Bim expression and stained cells were clearly distinguishable from a negative control sample. Additionally, we saw good evidence of upregulation of Bim after 6 hours of ionomycin and Q-VD.OPh treatment (Figure 5.27-A). Overall, although the number of Bim positive cells and intensity of staining was found to be highest in drug treated EBV-loss cells compared to other sample groups, the difference between EBV-positive and loss cells after treatment was not found to be significant (Figure 5.27-B).

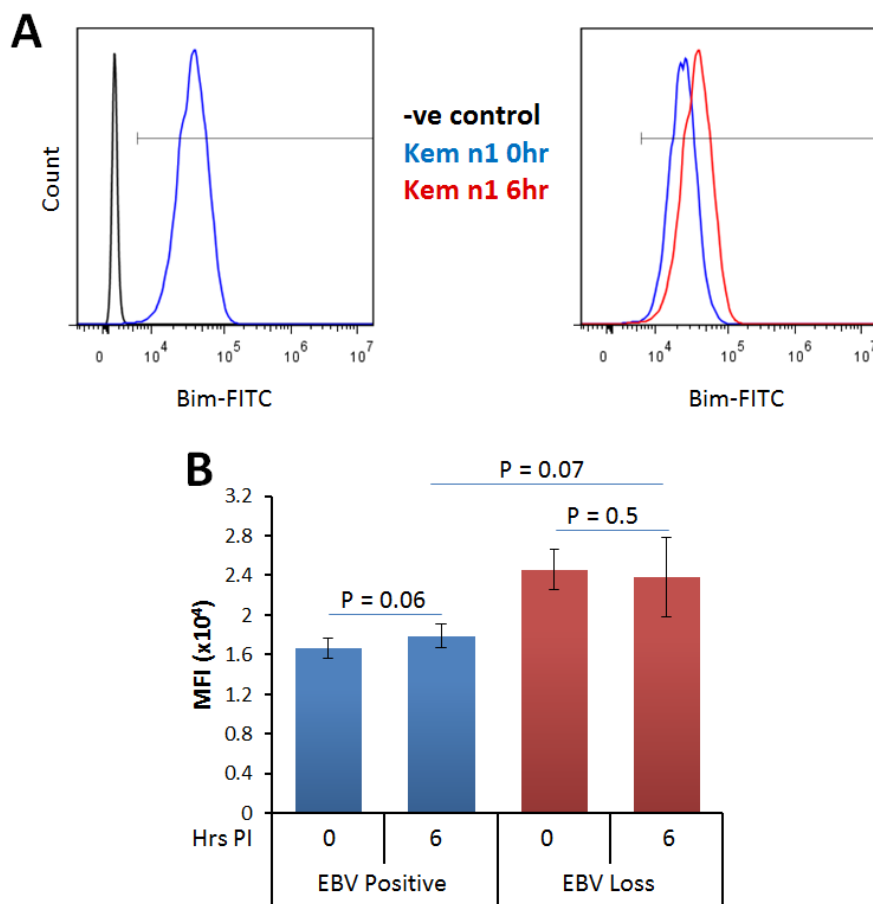


Figure 5.27 FACS analysis of Bim protein expression in Kem-BL clones

A Example staining of untreated EBV-loss clone n1 at time 0 versus isotype control (left) or treated clone n1 cells at 6 hours (right)

B Average mean fluorescence intensity (MFI) of Bim positive cells in each experimental group

Representative data from assays carried out in triplicate on three occasions using three different EBV-positive Kem-BL clones and three different EBV-loss Kem-BL clones. Statistical comparisons were made using a two-tailed Student's T test

5.5.2 Noxa

The Noxa antibody worked well in FACS staining with clear separation between stained samples and negative controls. Surprisingly, we found evidence of Noxa upregulation in EBV-loss cells in response to apoptosis induction (Figure 5.28-A). Although this disagrees with our 48 hour blot data it is consistent with the findings of the Allday group (though their experiments were carried out at 24 hours after apoptosis induction) [419]. This suggests that the low levels of Noxa seen in EBV-loss clones n2 and n3 in Western blots may be due to degradation of the protein as Noxa has been shown to undergo rapid turnover, being degraded by the proteasome without the need for ubiquitin labelling [597, 598]. This finding highlights the importance of shifting our focus to look for more subtle changes than could be distinguished by Western blot that occur early after apoptosis induction.

As we found for Bim, the majority of the cells in our samples stained positively for Noxa and the highest numbers of Noxa positive cells were in the treated EBV-loss cells, although the differences between the groups were again not significant (not shown). The intensity of Noxa staining was also highest in drug treated EBV-loss cells, though again this did not reach statistical significance (Figure 5.2B-B). Although this data suggests that Noxa may also be an important target for EBV in Latency I BL cells and is in-keeping with the published findings of another group [419] it is possible that this antibody may be binding something other than Noxa. Therefore, in order to be confident that Noxa is a target of EBV we would need additional data to corroborate these FACS experiments.

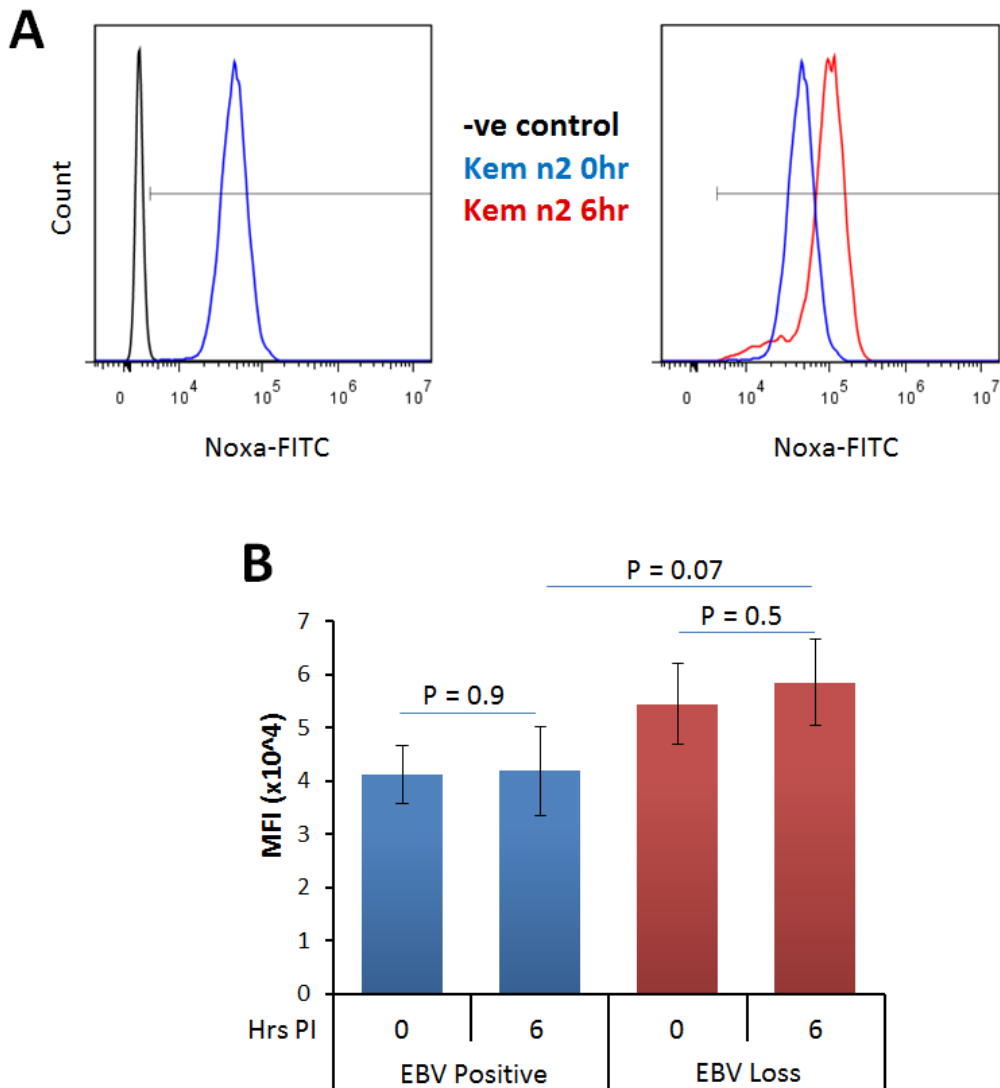


Figure 5.28 Noxa protein expression in Kem-BL clones

A Example FACS staining of untreated EBV-loss clone n2 at time 0 versus isotype control (left) or treated clone n1 cells at 6 hours (right)

B Average mean fluorescence intensity (MFI) of Noxa positive cells in each experimental group

Representative data from assays carried out in triplicate on three occasions using three different EBV-positive Kem-BL clones and three different EBV-loss Kem-BL clones. Statistical comparisons were made using a two-tailed Student's T test

5.5.3 Puma

Unlike Bim and Noxa, Puma staining in Kem-BL clones was weak compared to negative controls, although we did still see clear shifts in Puma expression in response to treatment with ionomycin and Q-VD.OPh (Figure 5.29-A). The low intensity of the staining may be due to the antibody used, although we did also get similar results with an alternative antibody (data not shown). More likely then, since Puma is a potent pro-apoptotic and still gives a single peak in staining, rather than a positive and a negative peak, is that Puma expression is generally low in Kem-BL cells, although we do not have enough data to be certain that this is the reason for this finding.

Like Bim and Noxa, the largest proportion of Puma positive cells were found in the drug treated EBV-loss group, but due to variation between clones and experiments, the difference was only significant when compared to untreated EBV-positive clones (Figure 5.29-B). Similarly, Puma staining was also most intense in this group, though not significantly different to untreated EBV-loss cells or drug-treated EBV-positive cells (Figure 5.29-C).

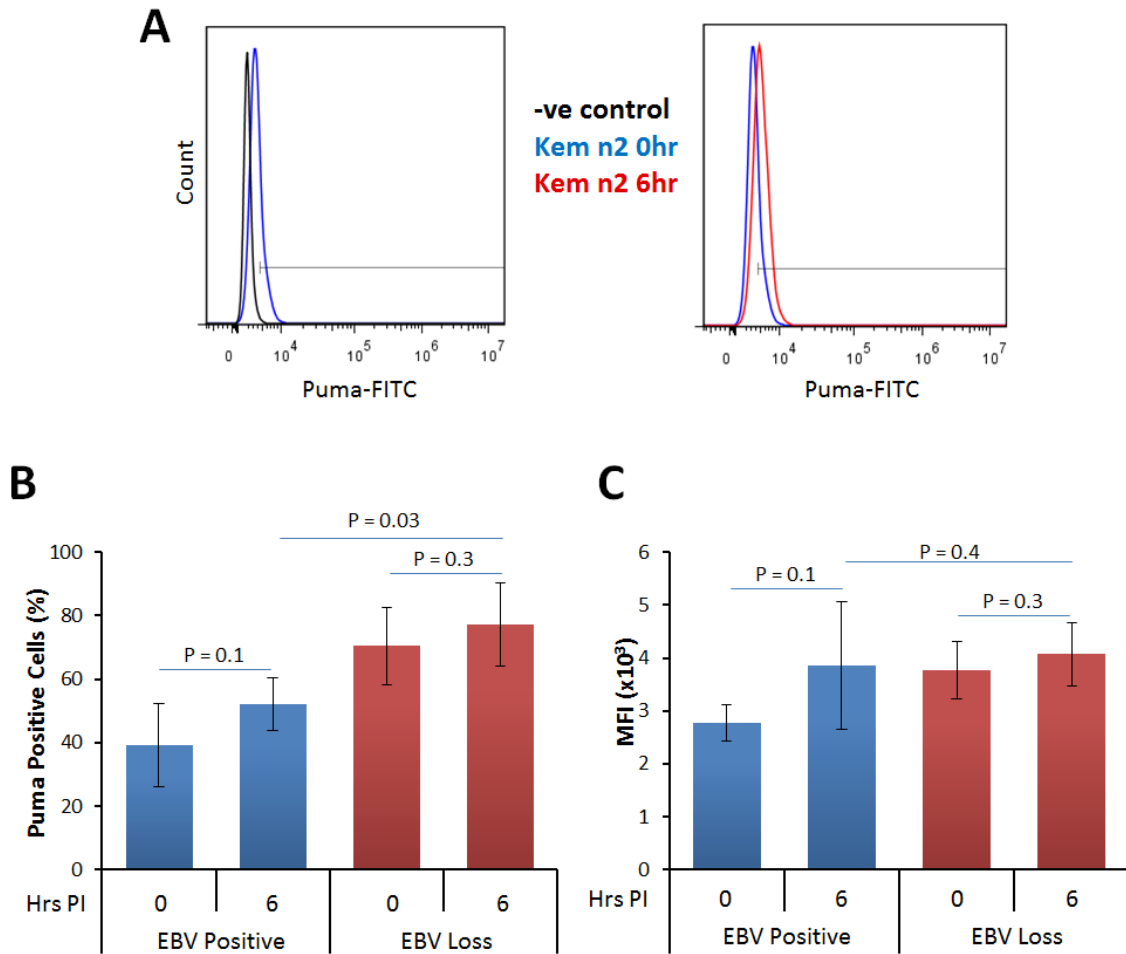


Figure 5.29 Puma protein expression in Kem-BL clones

A Example staining of untreated EBV-loss clone n2 at time 0 versus isotype control (left) or treated clone n1 cells at 6 hours (right)

B Proportion of cells stained Puma positive in each group

C Average mean fluorescence intensity (MFI) of Puma positive cells in each experimental group

Representative data from assays carried out in triplicate on three occasions using three different EBV-positive Kem-BL clones and three different EBV-loss Kem-BL clones.

Statistical comparisons were made using a two-tailed Student's T test

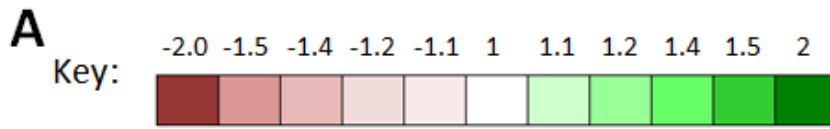
5.5.4 Summary of FACS data

In order to better visualise our FACS staining results, we expressed the all of the data in colour coded tables, organised by experiment (Figure 5.30). For each gene both the fluorescence intensity and the proportion of cells that stained positive were calculated compared to the reference group (EBV-positive cells at 0 hours) and fold-changes were then ranked by magnitude, as per the key in Figure 5.30-A.

For Noxa and Bim (Figures 5.30-B & 5.30-C, respectively) the overall number of stained cells changed very little but the mean fluorescence intensity increased in the drug treated EBV-loss cells compared to the other groups in every experiment. For Puma, both the percentage of cells stained and the intensity of staining were increased in drug-treated EBV-loss cells compared to other groups (Figure 5.30-D).

These data, in conjunction with our q-PCR arrays and Western blot data, show that EBV-loss clones of Kem-BL consistently upregulate pro-apoptotic BH3-only proteins in response to apoptosis induction to a greater degree than their EBV-positive counterparts, even at early time points. That we see this effect in several BH3-only proteins at once suggests that it is co-operation between these proteins which gives rise to the EBV-loss phenotype. This hypothesis fits neatly with our reinfection and ectopic expression studies which suggest that EBV genes work co-operatively to suppress apoptotic signalling in EBV-positive cells. This theory also explains how it is that a virus that is apparently expressing so few genes exerts a consistent phenotype in cells from genetically different individuals and is able to mitigate the barrage of pro-apoptotic signals imposed by the translocation of MYC.

Currently we have no clear indication as to what mechanism(s) EBV might be employing to co-ordinately exert control over the expression of multiple BH3-only proteins. However, it is our hope that more sophisticated viral gene expression systems as well as additional studies to look at possible mechanisms of apoptosis regulation outside of transcription and gross protein expression levels will allow us to finally begin to unravel the subtle, yet important survival advantage EBV affords to BL cells.



B Noxa

Number of Positive Cells					Mean Fluorescence Intensity				
Expt	EBV Positive		EBV Loss		Expt	EBV Positive		EBV Loss	
	0hrs	6hrs	0hrs	6hrs		0hrs	6hrs	0hrs	6hrs
1	1	1.0	0.9	1.0	1	1	1.0	1.3	1.4
2	1	1.0	1.0	1.0	2	1	0.8	1.1	1.1
3	1	1.0	1.0	1.0	3	1	1.2	1.4	1.7

C Bim

Number of Positive Cells					Mean Fluorescence Intensity				
Expt	EBV Positive		EBV Loss		Expt	EBV Positive		EBV Loss	
	0hrs	6hrs	0hrs	6hrs		0hrs	6hrs	0hrs	6hrs
1	1	1.0	1.0	1.0	1	1	1.2	1.1	1.3
2	1	1.0	1.0	1.0	2	1	1.0	1.0	1.2
3	1	1.0	1.0	1.0	3	1	1.1	1.5	1.4

D Puma

Number of Positive Cells					Mean Fluorescence Intensity				
Expt	EBV Positive		EBV Loss		Expt	EBV Positive		EBV Loss	
	0hrs	6hrs	0hrs	6hrs		0hrs	6hrs	0hrs	6hrs
1	1	1.3	1.8	2.0	1	1	1.4	1.4	1.5
2	1	1.4	1.8	2.7	2	1	1.1	1.1	1.2
3	1	2.3	2.9	4.0	3	1	1.0	1.1	1.1

Figure 5.30 Summary of Noxa, Bim and Puma expression in Kem-BL clones at 6 hours post apoptosis induction versus time 0
A Key to grading and colour coding of data, **B** Noxa, **C** Bim, **D** Puma,
 All data from three independent experiments carried out in triplicate
 Expt = experiment number

Conclusions III

This is the first study to our knowledge to have profiled a large number of cellular targets in isogenic EBV-positive and loss clones in response to apoptosis induction, both functionally and by measuring changes in gene expression. This has allowed us to elucidate that EBV functions to suppress apoptosis induction via the Bcl-2 family of intrinsic apoptosis regulators in Latency I BL. This is consistent with the findings of others that subversion of the intrinsic apoptosis pathway is able to synergise with c-myc during lymphomagenesis [266-269, 274].

Our functional assays using Bim_S-variant ligands to induce cell death showed that EBV-loss clones from three tumour backgrounds are increased in their sensitivity to BH3-ligands compared to their EBV-counterparts. Interestingly, these data indicated that no individual pro-survival Bcl-2 protein is activated or inhibited by EBV; instead EBV-positive cells are generally more resistant to induction of the BH3 sensitiser proteins. Although we did observe some variation between different clones, this correlates with our earlier findings that there is some variation in the degree of sensitivity to apoptosis inducing agents, including the BH3 mimetic ABT-737, between different clones. We therefore went on to look in detail at the expression of a range of apoptosis-related genes in response to apoptosis induction, in order to uncover the underlying mechanism at work.

Our detailed analysis of apoptosis-related gene regulation in multiple clones of Kem-BL unexpectedly revealed that EBV suppresses the Bcl-2 signalling pathway by co-ordinately targeting the pro-apoptotic BH3-only proteins Bim, Puma and Noxa. Whilst we were initially surprised by this finding, the reason for such a strategy is clear since the BH3-only proteins exhibit considerable functional overlap and redundancy [599]. Consequently, inhibition of multiple BH3-only proteins allows EBV to subvert apoptotic signalling initiated by any or all of the three apoptosis 'sensor' BH3-only proteins; allowing it to protect against a wide range of stimuli. Additionally, this mechanism of protection allows EBV to inhibit apoptosis even when

multiple BH3-only proteins are activated. If only one of the BH3-only proteins were inhibited by the virus this inhibition could be overcome by other BH3 only proteins either alone or synergistically, as has been shown to occur in BH3-only protein knock-out E μ -myc mice [266, 274].

It is important to note at this point that although we chose to screen our clones at the transcriptional and protein level these techniques have limitations and it is possible that we may have overlooked other important differences between EBV-positive and loss clones that will help to reveal the molecular mechanism of apoptosis protection by EBV in BL. For example, some genes may not change in their total expression, but may translocate or change in activation status between experimental groups. We are particularly interested to know whether there is any difference in surface immunoglobulin expression between EBV-positive and loss cells (either in the presence or absence of an apoptosis-inducer) as this could explain the difference in sensitivity to α -IgM in EBV-positive or loss clones of Mutu-BL, Kem-BL and Awia-BL.

Our investigations into apoptosis-related changes in gene expression also showed that there are widespread changes in a large number of genes during apoptosis initiation, even in viable cells that are unable to activate caspases. This underlines the importance of including multiple clones, carrying out unbiased screening and validating changes at the protein level at both early and late time points. These observations may also explain reports in the literature which identify other apoptosis-related genes as targets for EBV in BL as these studies were carried out in a limited number of clones, only looked at a small number of targets or included non-viable cells in their analysis [99, 313, 419, 600]. Reassuringly however, we note that all of these studies identified individual components of the intrinsic apoptosis signalling pathway as targets for EBV.

Consistent with our findings, data from the Allday and Clybouw groups suggest a role for Bim or Noxa directly, whilst the Takada group postulates a role for Bcl-2 and the Sugden group

instead points to Caspase-3 as a target of EBV. We therefore posit that Noxa and Bim (as well as Puma) are *bona fide* targets of EBV in BL, whilst upregulation of Bcl-2 in some clones of Akata-BL and upregulation of Caspase-3 in Sav-BL clone 1.1 may be indirect consequences of apoptosis induction in these cells. For example, our data show that many NF- κ B family transcripts are deregulated following apoptosis-inhibition in BL cells, several of which are able to upregulate Bcl-2 [601-604], and Caspase-3 is a downstream target of multiple apoptosis-related proteins that can be activated by a plethora of mechanisms [605, 606]. The Sugden group did consider a direct role for Puma and Bim however, since their retroviruses did not appreciably express miR BART-5, no investigation of Puma expression was carried out. Western blots for Bim were carried out and quantitation does show slightly higher expression of Bim in Sav-BL after dnEBNA1 treatment, which is then reduced in miR BART-complemented cells, although these changes are not significant. Interestingly we note that the levels of BART miRs expressed from the retrovirus constructs used in their study are many times lower than those endogenously expressed in Sav-BL as we find that early passage cells from this cell line express hundreds to thousands of copies of BART miRs per picogram of RNA [94], whilst these vectors express only tens to hundreds of copies per 10 picograms of RNA [99]. As mentioned previously, we and others have also found difficulty in expressing miR BARTs to endogenous levels in BL cells, and the low expression of BART microRNAs may explain why the subtle difference in apoptosis phenotype reported by this group between miR BART-complemented and un-complemented cells is primarily detected in Caspase-3; a downstream target of Bim, Puma and Noxa. In summary, although we cannot exclude a direct role for the BART microRNAs in targeting Caspase-3 as we also find differences between Caspase-3 expression in EBV-positive and EBV-loss clones, (but not in healthy cells), we propose that this is a consequence of subtle deregulation of BH3-only protein signalling.

Although we have shown that Bim, Puma and Noxa are all upregulated in EBV-loss clones in response to apoptosis induction, we are currently uncertain of the mechanism by which the

virus controls their expression. Regulation of the BH3-only proteins is known to occur by a diverse and complex range of processes including post-translational modification, sequestration, degradation, and targeting by microRNAs, as well as transcriptional activation or inhibition [434, 443, 444, 447, 449-451, 458, 460-462]. Therefore further investigations are required to determine the precise nature of BH3-protein regulation by EBV. Additionally, because we hypothesise that the Latency I EBV genes co-operate in order to carry out this function, we expect to find that more than one molecular mechanism is responsible for this effect.

6. Discussion and future work

Whilst individual viral genes are able to imitate the functions of multiple cellular genes, it is also established that multiple viral genes can co-operate in order to subvert particular signalling pathways within the cells of their host. In the case of EBV; the EBNA3A, B and C genes that are expressed in Wp-BLs as well as LCLs co-operatively regulate a variety of cellular genes [607]. Whilst it is unsurprising that individual EBNA3s are functionally homologous since they arose from the duplication of a single ancestor EBNA3 gene [608], they must co-operate in a non-redundant manner to carry out some of their essential functions. The most notable examples of this are the epigenetic regulation of Bim and p16^{INK4a} by EBNA3A and C [181, 306, 609]. Interestingly, and like the genes that regulate them, Bim and p16^{INK4a} also show functional overlap, since p16^{INK4a} upregulates the BH3-only protein Puma, whilst downregulating anti-apoptotic Mcl-1 and Bcl-2 [610]. Wp-BLs also express high levels of the Bcl-2 homologue, BHRF1, which strongly inhibits intrinsic apoptosis via binding to BH3-only proteins [89, 304, 411]. Therefore, EBV inhibits Bcl-2 family signalling in Wp-BL via a tripartite mechanism involving the epigenetic silencing of Bim and p16^{INK4a} as well as direct BH3-only protein inhibition by BHRF1.

The growth transformation of B cells by EBV also requires co-operation between viral genes, and this co-operation exhibits an all-or-nothing phenotype. That is; if any one of the essential genes is lacking, the virus is completely inert in transformation assays [107]. Although the essential growth transforming genes of EBV are known to have a range of targets, they also co-ordinately deregulate the Bcl-2 family. LMP1 upregulates the Bcl-2 homologues, Bcl-2, Mcl-1, Bfl-1 and A1 [611-614], and as mentioned, the EBNA3s downregulate Bim and Puma (via p16^{INK4a}), whilst EBNA2 downregulates Bik [615]. Additionally, the EBV-encoded Bcl-2 homologues themselves, (BHRF1 and BALF1) are also essential to transformation in combination [88]. There is clearly a precedent for the combinatorial targeting of the Bcl-2

family by multiple EBV-encoded genes in EBV-infected B cells and we therefore propose that subversion of the Bcl-2 pathway by a combination of Latency I genes is also necessary for the development and maintenance of Latency I BLs.

In this study we find that the Latency I genes of EBV are able to inhibit the intrinsic apoptosis pathway in BL by co-operation and do so by targeting three of the BH3-only proteins. These findings reconcile some of the conflicting data that has been published on this topic and also explain why retention of EBV is highly selected for in BL cells *in vitro* and *in vivo*. Whilst this study includes the most detailed and comprehensive analysis of EBV-loss to date, we are also aware that we have been unable as yet to elucidate the precise mechanisms by which each of the Latency I genes contribute to the inhibition of Bim, Puma and Noxa, respectively.

Since re-expressing individual genes from lentiviruses has proven technically challenging, we are hoping to advance this work using novel recombinant EBV constructs that have been engineered to lack individual transcripts of interest without disturbing the expression of nearby, overlapping or opposite strand transcripts. Although recombinant EBV technology has been available for a number of years, a system by which totally scar-less modified genomes can be made has only recently been developed [563, 564]. By carrying out careful modification of an EBV-BAC containing an intact BamHI A region we aim to create a number of BACs that are mutated for each of the known Latency I genes (except EBNA1), as well as the LF1, 2 and 3 transcripts. We predict that a virus lacking a single Latency I gene, but retaining the rest, will show an apoptosis phenotype intermediate between that of EBV-positive and loss cells, which will enable us to directly prove a contribution for each gene. We will then be able to carry out more detailed investigations into the expression and regulation of Bim, Puma and Noxa in our novel re-infectants in order to unravel the underlying mechanisms by which EBV subverts BH3-only protein signalling in Latency I BL.

As well as genetic co-operation, our studies have also highlighted another important concept in cancer research; that of clonal heterogeneity. It is impossible for us to determine whether

the two EBV-loss clones that could not be phenotypically rescued by Akata rEBV acquired additional mutations *in vitro*. Neither can we know to what degree the tumours from which they are derived exhibited clonal variation *in vivo* or earlier during *in vitro* passage. Equally, we cannot determine the degree of clonal heterogeneity in BLs from the currently published whole genome sequencing studies as SNPs that are present in a minority of cells in the global population would not be identified using these techniques [277-279]. However, we have found that BL biopsy samples can exhibit heterogeneity in viral gene expression at the single cell level ([178] and Rosemary Tierney, unpublished data); and subsequently we infer that there may also be clonal variation in cellular gene expression *in vivo*.

Intratumoral genomic heterogeneity can now be detected using single cell sequencing on biopsy material and variations in gene expression can be detected using single cell q-PCR [616, 617]; therefore we are keen to carry out such studies on fresh BL biopsies. In addition to further investigation of the occurrence and phenotypic consequences of heterogeneity within BLs, genetic studies on new tumour biopsies will also enable us to determine the frequency of cellular mutations in the Bcl-2 family. In these experiments it would be especially interesting to compare EBV-positive and negative tumours as we might expect EBV-negative tumours to necessarily acquire mutations to inactivate Bcl-2 signalling, whereas we would expect EBV-positive tumours, in which the virus inhibits this family, to carry wild type sequences.

Although the recent global analyses of the genetic landscape in BL tell us little about intratumoral heterogeneity, they do underscore the necessity for BLs to overcome Bcl-2-mediated regulation of apoptosis. Three independent studies found that the most common recurrent cellular gene mutations in BL are found in *ID3*, *CCND3* (cyclin D3) and *TCF3* (E2A); all of which converge on the PI3 Kinase signalling pathway in order to carry out their functions in promoting cell survival and proliferation [277-279]. PI3 Kinase (PI3K) acts as a signalling hub for cell fate decisions and is consequently able to cross-talk with the Bcl-2 family [618]. Primarily this has been shown through activation of the extrinsic/intrinsic apoptosis mediator, Bad, by

phosphorylation at serine 136 [619, 620]. However, there is also evidence that PI3K and its signalling partner Akt, can also regulate Bax, and Mcl-1 as well as Puma and Bim via the transcription factor FoxO3a independently of any effect on Bad [447, 621-623]. We found that phosphorylation of Bad at serine 136 was undetectable in our EBV-positive and loss clones, either in resting cells or those induced into apoptosis (data not shown), but we are yet to investigate a role for PI3K in the upregulation of Bim and Puma in these cell lines. Notably, the NGS studies found that mutations in *ID3*, *TCF3* and *CCND3* were more common in sBL versus eBL, further implicating EBV as a substitute for the survival advantage conferred by these cellular mutations.

In addition to studies on human cells we would also like to carry out more detailed analyses on the pathogenesis of BL in mouse models. Currently, *in vivo* studies of EBV in mice use NSG mice with humanised immune systems, in which the lymphoid compartments have been reconstituted via the engraftment of human CD34⁺ stem cells [624]. However, the introduction of CRISPR-Cas9 gene editing techniques has made it possible to rapidly create new mouse strains which carry several different specific mutations in the mouse genome, in order to investigate the complex interplay between common mutations in cancer [625]. Therefore, it may soon be possible to create a mouse which carries modified receptors; rendering it permissive to infection with EBV, as well as specific mutations in Bcl-2 family member genes. Although it should be noted that our understanding of exactly which receptors would need to be adapted is still lacking as mice carrying a humanised version of the CD21 'EBV receptor' remain refractory to infection ([626] and Martin Rowe, personal communication). However, if this could be overcome, and in combination with novel recombinant viruses, these technologies make it possible to consider elegant models with which to illuminate the extremely complex interplay between cellular and microbial genomics in virus-driven cancers as well as to better understand tumorigenesis more generally.

Thus, after 50 years of paradigm-shifting, investigations into the role of EBV in BL may still help us to better understand the subtleties and complexities of cancer. Ultimately this will inform clinicians and lead to improvements in the treatment of BL, which remains woefully unsuccessful in some patient groups and settings. One example that leads directly from this project is that of specific BH3 mimetics. Several BH3 mimetics are being developed and selected for specific binding profiles, enabling them to overcome particular apoptotic 'road blocks'. This method of using BH3 mimetics that are specific to the tumour, for example using ABT-199 to resensitise cells that are over-expressing Bcl-2, leads to apoptosis in the tumour cells, but also alleviates side effects, such as the destruction of platelets, which are common in patients treated with less specific BH3 mimetics, such as ABT-737 [434, 535, 627]. If multiple Bcl-2 family blockades must be overcome to successfully treat BL, this may mean that sophisticated strategies and combinations of chemotherapeutics will be required to improve outcomes in the cohorts of patients for whom BL is currently rapidly fatal.

References

1. Rowe, M., et al., *Burkitt's lymphoma: the Rosetta Stone deciphering Epstein-Barr virus biology*. *Semin Cancer Biol*, 2009. **19**(6): p. 377-88.
2. Klein, G., *Burkitt lymphoma--a stalking horse for cancer research?* *Semin Cancer Biol*, 2009. **19**(6): p. 347-50.
3. Burkitt, D., *A sarcoma involving the jaws in African children*. *Br J Surg*, 1958. **46**(197): p. 218-23.
4. Magrath, I., *Lessons from clinical trials in African Burkitt lymphoma*. *Curr Opin Oncol*, 2009. **21**(5): p. 462-8.
5. Burkitt, D., *Burkitt's lymphoma*. *JAMA*, 1972. **222**(9): p. 1164.
6. Burkitt, D. and G.T. O'Connor, *Malignant lymphoma in African children. I. A clinical syndrome*. *Cancer*, 1961. **14**: p. 258-69.
7. O'Connor, G.T. and J.N. Davies, *Malignant tumors in African children. With special reference to malignant lymphoma*. *J Pediatr*, 1960. **56**: p. 526-35.
8. Wright, D.H., *Cytology and histochemistry of the Burkitt lymphoma*. *Br J Cancer*, 1963. **17**: p. 50-5.
9. Haddow, A.J., *An Improved Map for the Study of Burkitt's Lymphoma Syndrome in Africa*. *East Afr Med J*, 1963. **40**: p. 429-32.
10. Burkitt, D., *A "tumour safari" in East and Central Africa*. *Br J Cancer*, 1962. **16**: p. 379-86.
11. Burkitt, D., *A children's cancer dependent on climatic factors*. *Nature*, 1962. **194**: p. 232-4.
12. Epstein, M.A. and Y.M. Barr, *Cultivation in Vitro of Human Lymphoblasts from Burkitt's Malignant Lymphoma*. *Lancet*, 1964. **1**(7327): p. 252-3.
13. Epstein, M.A. and Y.M. Barr, *Characteristics and Mode of Growth of Tissue Culture Strain (Eb1) of Human Lymphoblasts from Burkitt's Lymphoma*. *J Natl Cancer Inst*, 1965. **34**: p. 231-40.
14. Epstein, M.A., B.G. Achong, and Y.M. Barr, *Virus Particles in Cultured Lymphoblasts from Burkitt's Lymphoma*. *Lancet*, 1964. **1**(7335): p. 702-3.
15. Epstein, M.A., et al., *Morphological and Biological Studies on a Virus in Cultured Lymphoblasts from Burkitt's Lymphoma*. *J Exp Med*, 1965. **121**: p. 761-70.
16. Henle, G. and W. Henle, *Immunofluorescence in cells derived from Burkitt's lymphoma*. *J Bacteriol*, 1966. **91**(3): p. 1248-56.
17. Henle, W., et al., *Herpes-type virus and chromosome marker in normal leukocytes after growth with irradiated Burkitt cells*. *Science*, 1967. **157**(792): p. 1064-5.
18. Pope, J.H., B.G. Achong, and M.A. Epstein, *Cultivation and fine structure of virus-bearing lymphoblasts from a second New Guinea Burkitt lymphoma: establishment of sublines with unusual cultural properties*. *Int J Cancer*, 1968. **3**(2): p. 171-82.
19. de-The, G., et al., *Epidemiological evidence for causal relationship between Epstein-Barr virus and Burkitt's lymphoma from Ugandan prospective study*. *Nature*, 1978. **274**(5673): p. 756-61.
20. Clifford, P., *Treatment of Burkitt's lymphoma*. *Lancet*, 1968. **1**(7542): p. 599.
21. Clifford, P., et al., *Treatment of Burkitt's lymphoma*. *Lancet*, 1968. **2**(7566): p. 517-8.
22. Ziegler, J.L., et al., *Burkitt's lymphoma--a model for intensive chemotherapy*. *Semin Oncol*, 1977. **4**(3): p. 317-23.
23. Manolov, G. and Y. Manolova, *Marker band in one chromosome 14 from Burkitt lymphomas*. *Nature*, 1972. **237**(5349): p. 33-4.

24. Zech, L., et al., *Characteristic chromosomal abnormalities in biopsies and lymphoid-cell lines from patients with Burkitt and non-Burkitt lymphomas*. *Int J Cancer*, 1976. **17**(1): p. 47-56.
25. Adams, J.M., et al., *Cellular myc oncogene is altered by chromosome translocation to an immunoglobulin locus in murine plasmacytomas and is rearranged similarly in human Burkitt lymphomas*. *Proc Natl Acad Sci U S A*, 1983. **80**(7): p. 1982-6.
26. Adams, J.M., et al., *The c-myc oncogene driven by immunoglobulin enhancers induces lymphoid malignancy in transgenic mice*. *Nature*, 1985. **318**(6046): p. 533-8.
27. Schuhmacher, M., et al., *Control of cell growth by c-Myc in the absence of cell division*. *Curr Biol*, 1999. **9**(21): p. 1255-8.
28. Schmidt, E.V., *The role of c-myc in cellular growth control*. *Oncogene*, 1999. **18**(19): p. 2988-96.
29. Hayward, W.S., B.G. Neel, and S.M. Astrin, *Activation of a cellular onc gene by promoter insertion in ALV-induced lymphoid leukemia*. *Nature*, 1981. **290**(5806): p. 475-80.
30. Dalla-Favera, R., et al., *Human c-myc onc gene is located on the region of chromosome 8 that is translocated in Burkitt lymphoma cells*. *Proc Natl Acad Sci U S A*, 1982. **79**(24): p. 7824-7.
31. Neel, B.G., et al., *Two human c-onc genes are located on the long arm of chromosome 8*. *Proc Natl Acad Sci U S A*, 1982. **79**(24): p. 7842-6.
32. Davison, A.J., *Herpesvirus systematics*. *Vet Microbiol*, 2010. **143**(1): p. 52-69.
33. McGeoch, D.J., F.J. Rixon, and A.J. Davison, *Topics in herpesvirus genomics and evolution*. *Virus Res*, 2006. **117**(1): p. 90-104.
34. Wang, F., *Nonhuman primate models for Epstein-Barr virus infection*. *Curr Opin Virol*, 2013. **3**(3): p. 233-7.
35. Pellet, P.a.B.R., *The family Herpesviridae: a brief introduction*. *Fields Virology*, ed. D.a.P.M.H. Knipe. 2007, Philadelphia: Lippincott, Williams and Wilkins.
36. Dolyniuk, M., R. Pritchett, and E. Kieff, *Proteins of Epstein-Barr virus. I. Analysis of the polypeptides of purified enveloped Epstein-Barr virus*. *J Virol*, 1976. **17**(3): p. 935-49.
37. Johannsen, E., et al., *Proteins of purified Epstein-Barr virus*. *Proc Natl Acad Sci U S A*, 2004. **101**(46): p. 16286-91.
38. Mettenleiter, T.C., *Herpesvirus assembly and egress*. *J Virol*, 2002. **76**(4): p. 1537-47.
39. Dai, W., et al., *Unique structures in a tumor herpesvirus revealed by cryo-electron tomography and microscopy*. *J Struct Biol*, 2008. **161**(3): p. 428-38.
40. Jochum, S., et al., *RNAs in Epstein-Barr virions control early steps of infection*. *Proc Natl Acad Sci U S A*, 2012. **109**(21): p. E1396-404.
41. Yamaguchi, J., Y. Hinuma, and J.T. Grace, Jr., *Structure of virus particles extracted from a Burkitt lymphoma cell line*. *J Virol*, 1967. **1**(3): p. 640-2.
42. Dambaugh, T., et al., *Epstein-Barr virus (B95-8) DNA VII: molecular cloning and detailed mapping*. *Proc Natl Acad Sci U S A*, 1980. **77**(5): p. 2999-3003.
43. Baer, R., et al., *DNA sequence and expression of the B95-8 Epstein-Barr virus genome*. *Nature*, 1984. **310**(5974): p. 207-11.
44. Arrand, J.R., et al., *Molecular cloning of the complete Epstein-Barr virus genome as a set of overlapping restriction endonuclease fragments*. *Nucleic Acids Res*, 1981. **9**(13): p. 2999-3014.
45. de Jesus, O., et al., *Updated Epstein-Barr virus (EBV) DNA sequence and analysis of a promoter for the BART (CST, BARF0) RNAs of EBV*. *J Gen Virol*, 2003. **84**(Pt 6): p. 1443-50.
46. Hatfull, G., et al., *Sequence analysis of Raji Epstein-Barr virus DNA*. *Virology*, 1988. **164**(2): p. 334-40.

47. Kintner, C.R. and B. Sugden, *The structure of the termini of the DNA of Epstein-Barr virus*. Cell, 1979. **17**(3): p. 661-71.
48. Raab-Traub, N. and K. Flynn, *The structure of the termini of the Epstein-Barr virus as a marker of clonal cellular proliferation*. Cell, 1986. **47**(6): p. 883-9.
49. Kalla, M. and W. Hammerschmidt, *Human B cells on their route to latent infection--early but transient expression of lytic genes of Epstein-Barr virus*. Eur J Cell Biol, 2012. **91**(1): p. 65-9.
50. Sixbey, J.W., et al., *Detection of a second widespread strain of Epstein-Barr virus*. Lancet, 1989. **2**(8666): p. 761-5.
51. Gratama, J.W. and I. Ernberg, *Molecular epidemiology of Epstein-Barr virus infection*. Adv Cancer Res, 1995. **67**: p. 197-255.
52. Sample, J., et al., *Epstein-Barr virus types 1 and 2 differ in their EBNA-3A, EBNA-3B, and EBNA-3C genes*. J Virol, 1990. **64**(9): p. 4084-92.
53. Edwards, R.H., F. Seillier-Moiseiwitsch, and N. Raab-Traub, *Signature amino acid changes in latent membrane protein 1 distinguish Epstein-Barr virus strains*. Virology, 1999. **261**(1): p. 79-95.
54. Bhatia, K., et al., *Variation in the sequence of Epstein Barr virus nuclear antigen 1 in normal peripheral blood lymphocytes and in Burkitt's lymphomas*. Oncogene, 1996. **13**(1): p. 177-81.
55. McGeoch, D.J. and D. Gatherer, *Lineage structures in the genome sequences of three Epstein-Barr virus strains*. Virology, 2007. **359**(1): p. 1-5.
56. Rickinson, A.B., L.S. Young, and M. Rowe, *Influence of the Epstein-Barr virus nuclear antigen EBNA 2 on the growth phenotype of virus-transformed B cells*. J Virol, 1987. **61**(5): p. 1310-7.
57. Tzellos, S., et al., *A Single Amino Acid in EBNA-2 Determines Superior B Lymphoblastoid Cell Line Growth Maintenance by Epstein-Barr Virus Type 1 EBNA-2*. J Virol, 2014. **88**(16): p. 8743-53.
58. Young, L.S., et al., *New type B isolates of Epstein-Barr virus from Burkitt's lymphoma and from normal individuals in endemic areas*. J Gen Virol, 1987. **68** (Pt 11): p. 2853-62.
59. de Campos-Lima, P.O., et al., *T cell responses and virus evolution: loss of HLA A11-restricted CTL epitopes in Epstein-Barr virus isolates from highly A11-positive populations by selective mutation of anchor residues*. J Exp Med, 1994. **179**(4): p. 1297-305.
60. de Campos-Lima, P.O., et al., *Antigen processing and presentation by EBV-carrying cell lines: cell-phenotype dependence and influence of the EBV-encoded LMP1*. Int J Cancer, 1993. **53**(5): p. 856-62.
61. Lung, M.L., et al., *Epstein-Barr virus genotypes associated with nasopharyngeal carcinoma in southern China*. Virology, 1990. **177**(1): p. 44-53.
62. Abdel-Hamid, M., et al., *EBV strain variation: geographical distribution and relation to disease state*. Virology, 1992. **190**(1): p. 168-75.
63. Brennan, R.M., et al., *Strains of Epstein-Barr virus infecting multiple sclerosis patients*. Mult Scler, 2010. **16**(6): p. 643-51.
64. Knecht, H., et al., *Mutational hot spots within the carboxy terminal region of the LMP1 oncogene of Epstein-Barr virus are frequent in lymphoproliferative disorders*. Oncogene, 1995. **10**(3): p. 523-8.
65. Kwok, H., et al., *Genomic diversity of Epstein-Barr virus genomes isolated from primary nasopharyngeal carcinoma biopsy samples*. J Virol, 2014. **88**(18): p. 10662-72.
66. Tsai, M.H., et al., *Spontaneous lytic replication and epitheliotropism define an Epstein-Barr virus strain found in carcinomas*. Cell Rep, 2013. **5**(2): p. 458-70.

67. Lin, Z., et al., *Whole-genome sequencing of the Akata and Mutu Epstein-Barr virus strains*. J Virol, 2013. **87**(2): p. 1172-82.
68. Shannon-Lowe, C., et al., *Epstein-Barr virus-induced B-cell transformation: quantitating events from virus binding to cell outgrowth*. J Gen Virol, 2005. **86**(Pt 11): p. 3009-19.
69. Fingeroth, J.D., et al., *Epstein-Barr virus receptor of human B lymphocytes is the C3d receptor CR2*. Proc Natl Acad Sci U S A, 1984. **81**(14): p. 4510-4.
70. Wang, X., et al., *Epstein-Barr virus uses different complexes of glycoproteins gH and gL to infect B lymphocytes and epithelial cells*. J Virol, 1998. **72**(7): p. 5552-8.
71. Li, Q., et al., *Epstein-Barr virus uses HLA class II as a cofactor for infection of B lymphocytes*. J Virol, 1997. **71**(6): p. 4657-62.
72. Nemerow, G.R. and N.R. Cooper, *Early events in the infection of human B lymphocytes by Epstein-Barr virus: the internalization process*. Virology, 1984. **132**(1): p. 186-98.
73. Tanner, J., et al., *Epstein-Barr virus gp350/220 binding to the B lymphocyte C3d receptor mediates adsorption, capping, and endocytosis*. Cell, 1987. **50**(2): p. 203-13.
74. Feederle, R., et al., *Epstein-Barr virus BNRF1 protein allows efficient transfer from the endosomal compartment to the nucleus of primary B lymphocytes*. J Virol, 2006. **80**(19): p. 9435-43.
75. Lindahl, T., et al., *Covalently closed circular duplex DNA of Epstein-Barr virus in a human lymphoid cell line*. J Mol Biol, 1976. **102**(3): p. 511-30.
76. Hurley, E.A., et al., *When Epstein-Barr virus persistently infects B-cell lines, it frequently integrates*. J Virol, 1991. **65**(3): p. 1245-54.
77. Hurley, E.A. and D.A. Thorley-Lawson, *B cell activation and the establishment of Epstein-Barr virus latency*. J Exp Med, 1988. **168**(6): p. 2059-75.
78. Alfieri, C., M. Birkenbach, and E. Kieff, *Early events in Epstein-Barr virus infection of human B lymphocytes*. Virology, 1991. **181**(2): p. 595-608.
79. Abbot, S.D., et al., *Epstein-Barr virus nuclear antigen 2 induces expression of the virus-encoded latent membrane protein*. J Virol, 1990. **64**(5): p. 2126-34.
80. Zimmer-Strobl, U., et al., *The Epstein-Barr virus nuclear antigen 2 interacts with an EBNA2 responsive cis-element of the terminal protein 1 gene promoter*. EMBO J, 1993. **12**(1): p. 167-75.
81. Schlager, S., S.H. Speck, and M. Woisetschlager, *Transcription of the Epstein-Barr virus nuclear antigen 1 (EBNA1) gene occurs before induction of the BCR2 (Cp) EBNA gene promoter during the initial stages of infection in B cells*. J Virol, 1996. **70**(6): p. 3561-70.
82. Speck, S.H. and J.L. Strominger, *Analysis of the transcript encoding the latent Epstein-Barr virus nuclear antigen 1: a potentially polycistronic message generated by long-range splicing of several exons*. Proc Natl Acad Sci U S A, 1985. **82**(24): p. 8305-9.
83. Rogers, R.P., M. Woisetschlaeger, and S.H. Speck, *Alternative splicing dictates translational start in Epstein-Barr virus transcripts*. EMBO J, 1990. **9**(7): p. 2273-7.
84. Allday, M.J., D.H. Crawford, and B.E. Griffin, *Epstein-Barr virus latent gene expression during the initiation of B cell immortalization*. J Gen Virol, 1989. **70** (Pt 7): p. 1755-64.
85. Zimmer-Strobl, U., et al., *Epstein-Barr virus nuclear antigen 2 activates transcription of the terminal protein gene*. J Virol, 1991. **65**(1): p. 415-23.
86. Fahraeus, R., et al., *Epstein-Barr virus-encoded nuclear antigen 2 activates the viral latent membrane protein promoter by modulating the activity of a negative regulatory element*. Proc Natl Acad Sci U S A, 1990. **87**(19): p. 7390-4.
87. Rowe, M., et al., *Three pathways of Epstein-Barr virus gene activation from EBNA1-positive latency in B lymphocytes*. J Virol, 1992. **66**(1): p. 122-31.
88. Altmann, M. and W. Hammerschmidt, *Epstein-Barr virus provides a new paradigm: a requirement for the immediate inhibition of apoptosis*. PLoS Biol, 2005. **3**(12): p. e404.

89. Kelly, G.L., et al., *An Epstein-Barr virus anti-apoptotic protein constitutively expressed in transformed cells and implicated in burkitt lymphomagenesis: the Wp/BHRF1 link*. PLoS Pathog, 2009. **5**(3): p. e1000341.
90. Shannon-Lowe, C., et al., *Features distinguishing Epstein-Barr virus infections of epithelial cells and B cells: viral genome expression, genome maintenance, and genome amplification*. J Virol, 2009. **83**(15): p. 7749-60.
91. Gregorovic, G., et al., *Cell gene expression correlating with EBER expression in Epstein-Barr virus infected lymphoblastoid cell lines*. J Virol.
92. Swaminathan, S., B. Tomkinson, and E. Kieff, *Recombinant Epstein-Barr virus with small RNA (EBER) genes deleted transforms lymphocytes and replicates in vitro*. Proc Natl Acad Sci U S A, 1991. **88**(4): p. 1546-50.
93. Yajima, M., T. Kanda, and K. Takada, *Critical role of Epstein-Barr Virus (EBV)-encoded RNA in efficient EBV-induced B-lymphocyte growth transformation*. J Virol, 2005. **79**(7): p. 4298-307.
94. Amoroso, R., Fitzsimmons, L., Thomas, W.A., Kelly, G.L., Rowe, M., and A.I. Bell, *Quantitative studies of Epstein-Barr virus-encoded miRNAs provide novel insights into their regulation*. J Virol, 2010 (**in press**).
95. Seto, E., et al., *Micro RNAs of Epstein-Barr virus promote cell cycle progression and prevent apoptosis of primary human B cells*. PLoS Pathog, 2010. **6**(8).
96. Feederle, R., et al., *The members of an Epstein-Barr virus microRNA cluster cooperate to transform B lymphocytes*. J Virol, 2011. **85**(19): p. 9801-10.
97. Feederle, R., et al., *A viral microRNA cluster strongly potentiates the transforming properties of a human herpesvirus*. PLoS Pathog, 2011. **7**(2): p. e1001294.
98. Wahl, A., et al., *A cluster of virus-encoded microRNAs accelerates acute systemic Epstein-Barr virus infection but does not significantly enhance virus-induced oncogenesis in vivo*. J Virol, 2013. **87**(10): p. 5437-46.
99. Vereide, D.T., et al., *Epstein-Barr virus maintains lymphomas via its miRNAs*. Oncogene, 2014. **33**(10): p. 1258-64.
100. Bird, A.G., et al., *Characteristics of Epstein-Barr virus activation of human B lymphocytes*. J Exp Med, 1981. **154**(3): p. 832-9.
101. Masucci, M.G., et al., *Activation of B lymphocytes by Epstein-Barr virus/CR2 receptor interaction*. European Journal of Immunology, 1987. **17**(6): p. 815-820.
102. Peng, M. and E. Lundgren, *Transient expression of the Epstein-Barr virus LMP1 gene in B-cell chronic lymphocytic leukemia cells, T cells, and hematopoietic cell lines: cell-type-independent-induction of CD23, CD21, and ICAM-1*. Leukemia, 1993. **7**(1): p. 104-12.
103. Rowe, M., et al., *Upregulation of bcl-2 by the Epstein-Barr virus latent membrane protein LMP1: a B-cell-specific response that is delayed relative to NF-kappa B activation and to induction of cell surface markers*. J Virol, 1994. **68**(9): p. 5602-12.
104. Jeon, J.P., et al., *Sustained viral activity of epstein-Barr virus contributes to cellular immortalization of lymphoblastoid cell lines*. Mol Cells, 2009. **27**(2): p. 143-8.
105. Counter, C.M., et al., *Stabilization of short telomeres and telomerase activity accompany immortalization of Epstein-Barr virus-transformed human B lymphocytes*. J Virol, 1994. **68**(5): p. 3410-4.
106. Evans, A.S., and J.C. Niederman, *Epstein-Barr virus*. Viral Infections of Humans. 1989, New York: Plenum Press.
107. Rickinson, A.a.E.K., *Fields Virology*. Fourth ed. Epstein-Barr Virus, ed. D.a.P.M.H. Knipe. Vol. 2. 2001, Philadelphia: Lippincott, Williams and Wilkins. 3063.
108. Gratama, J.W., et al., *EBNA size polymorphism can be used to trace Epstein-Barr virus spread within families*. J Virol, 1990. **64**(10): p. 4703-8.
109. Thomas, R., et al., *Evidence of shared Epstein-Barr viral isolates between sexual partners, and low level EBV in genital secretions*. J Med Virol, 2006. **78**(9): p. 1204-9.

110. Thorley-Lawson, D.A. and A. Gross, *Persistence of the Epstein-Barr virus and the origins of associated lymphomas*. N Engl J Med, 2004. **350**(13): p. 1328-37.
111. Anagnostopoulos, I., et al., *Morphology, immunophenotype, and distribution of latently and/or productively Epstein-Barr virus-infected cells in acute infectious mononucleosis: implications for the interindividual infection route of Epstein-Barr virus*. Blood, 1995. **85**(3): p. 744-50.
112. Karajannis, M.A., et al., *Strict lymphotropism of Epstein-Barr virus during acute infectious mononucleosis in nonimmunocompromised individuals*. Blood, 1997. **89**(8): p. 2856-62.
113. George, J. and L. Claflin, *Selection of B cell clones and memory B cells*. Semin Immunol, 1992. **4**(1): p. 11-7.
114. Liu, Y.J., et al., *Sequential triggering of apoptosis, somatic mutation and isotype switch during germinal center development*. Semin Immunol, 1996. **8**(3): p. 169-77.
115. Miyashita, E.M., et al., *Identification of the site of Epstein-Barr virus persistence in vivo as a resting B cell*. J Virol, 1997. **71**(7): p. 4882-91.
116. Miyashita, E.M., et al., *A novel form of Epstein-Barr virus latency in normal B cells in vivo*. Cell, 1995. **80**(4): p. 593-601.
117. Faulkner, G.C., et al., *X-Linked agammaglobulinemia patients are not infected with Epstein-Barr virus: implications for the biology of the virus*. J Virol, 1999. **73**(2): p. 1555-64.
118. Chaganti, S., et al., *Epstein-Barr virus persistence in the absence of conventional memory B cells: IgM+IgD+CD27+ B cells harbor the virus in X-linked lymphoproliferative disease patients*. Blood, 2008. **112**(3): p. 672-9.
119. Tierney, R.J., et al., *Epstein-Barr virus latency in blood mononuclear cells: analysis of viral gene transcription during primary infection and in the carrier state*. J Virol, 1994. **68**(11): p. 7374-85.
120. Chen, F., et al., *A subpopulation of normal B cells latently infected with Epstein-Barr virus resembles Burkitt lymphoma cells in expressing EBNA-1 but not EBNA-2 or LMP1*. J Virol, 1995. **69**(6): p. 3752-8.
121. Chen, H., et al., *Expression of Epstein-Barr virus BamHI-A rightward transcripts in latently infected B cells from peripheral blood*. Blood, 1999. **93**(9): p. 3026-32.
122. Hochberg, D., et al., *Demonstration of the Burkitt's lymphoma Epstein-Barr virus phenotype in dividing latently infected memory cells in vivo*. Proc Natl Acad Sci U S A, 2004. **101**(1): p. 239-44.
123. Luka, J., B. Kallin, and G. Klein, *Induction of the Epstein-Barr virus (EBV) cycle in latently infected cells by n-butyrate*. Virology, 1979. **94**(1): p. 228-31.
124. Angel, P., et al., *Phorbol ester-inducible genes contain a common cis element recognized by a TPA-modulated trans-acting factor*. Cell, 1987. **49**(6): p. 729-39.
125. Flemington, E. and S.H. Speck, *Autoregulation of Epstein-Barr virus putative lytic switch gene BZLF1*. J Virol, 1990. **64**(3): p. 1227-32.
126. Takada, K. and Y. Ono, *Synchronous and sequential activation of latently infected Epstein-Barr virus genomes*. J Virol, 1989. **63**(1): p. 445-9.
127. Faggioni, A., et al., *Calcium modulation activates Epstein-Barr virus genome in latently infected cells*. Science, 1986. **232**(4757): p. 1554-6.
128. Feng, W.H., et al., *Chemotherapy induces lytic EBV replication and confers ganciclovir susceptibility to EBV-positive epithelial cell tumors*. Cancer Res, 2002. **62**(6): p. 1920-6.
129. Fahmi, H., et al., *Transforming growth factor beta 1 stimulates expression of the Epstein-Barr virus BZLF1 immediate-early gene product ZEBRA by an indirect mechanism which requires the MAPK kinase pathway*. J Virol, 2000. **74**(13): p. 5810-8.
130. Takada, K., *Cross-linking of cell surface immunoglobulins induces Epstein-Barr virus in Burkitt lymphoma lines*. Int J Cancer, 1984. **33**(1): p. 27-32.

131. Tovey, M.G., G. Lenoir, and J. Begon-Lours, *Activation of latent Epstein-Barr virus by antibody to human IgM*. *Nature*, 1978. **276**(5685): p. 270-2.
132. Laichalk, L.L., et al., *The dispersal of mucosal memory B cells: evidence from persistent EBV infection*. *Immunity*, 2002. **16**(5): p. 745-54.
133. Brandtzaeg, P., I.N. Farstad, and G. Haraldsen, *Regional specialization in the mucosal immune system: primed cells do not always home along the same track*. *Immunol Today*, 1999. **20**(6): p. 267-77.
134. Shannon-Lowe, C. and M. Rowe, *Epstein Barr virus entry; kissing and conjugation*. *Curr Opin Virol*, 2014. **4**: p. 78-84.
135. Young, L.S., et al., *Differentiation-associated expression of the Epstein-Barr virus BZLF1 transactivator protein in oral hairy leukoplakia*. *J Virol*, 1991. **65**(6): p. 2868-74.
136. Sinclair, A.J., *Epigenetic control of Epstein-Barr virus transcription - relevance to viral life cycle?* *Front Genet*, 2013. **4**: p. 161.
137. Niller, H.H., H. Wolf, and J. Minarovits, *Epigenetic dysregulation of the host cell genome in Epstein-Barr virus-associated neoplasia*. *Semin Cancer Biol*, 2009. **19**(3): p. 158-64.
138. Kalla, M., et al., *AP-1 homolog BZLF1 of Epstein-Barr virus has two essential functions dependent on the epigenetic state of the viral genome*. *Proc Natl Acad Sci U S A*, 2010. **107**(2): p. 850-5.
139. Woellmer, A., J.M. Arteaga-Salas, and W. Hammerschmidt, *BZLF1 governs CpG-methylated chromatin of Epstein-Barr Virus reversing epigenetic repression*. *PLoS Pathog*, 2012. **8**(9): p. e1002902.
140. Gruffat, H. and A. Sergeant, *Characterization of the DNA-binding site repertoire for the Epstein-Barr virus transcription factor R*. *Nucleic Acids Res*, 1994. **22**(7): p. 1172-8.
141. Gutsch, D.E., K.B. Marcu, and S.C. Kenney, *The Epstein-Barr virus BRLF1 gene product transactivates the murine and human c-myc promoters*. *Cell Mol Biol (Noisy-le-grand)*, 1994. **40**(6): p. 747-60.
142. Ragozy, T. and G. Miller, *Autostimulation of the Epstein-Barr virus BRLF1 promoter is mediated through consensus Sp1 and Sp3 binding sites*. *J Virol*, 2001. **75**(11): p. 5240-51.
143. Hammerschmidt, W. and B. Sugden, *Identification and characterization of oriLyt, a lytic origin of DNA replication of Epstein-Barr virus*. *Cell*, 1988. **55**(3): p. 427-33.
144. Anvret, M. and G. Miller, *Copy number and location of Epstein-Barr Viral genomes in neonatal human lymphocytes transformed after separation by size and treatment with mitogens*. *Virology*, 1981. **111**(1): p. 47-55.
145. Aman, P., B. Ehlin-Henriksson, and G. Klein, *Epstein-Barr virus susceptibility of normal human B lymphocyte populations*. *J Exp Med*, 1984. **159**(1): p. 208-20.
146. Hansson, M., K. Falk, and I. Ernberg, *Epstein-Barr virus transformation of human pre-B cells*. *J Exp Med*, 1983. **158**(2): p. 616-22.
147. Heath, E., et al., *Epstein-Barr virus infection of naive B cells in vitro frequently selects clones with mutated immunoglobulin genotypes: implications for virus biology*. *PLoS Pathog*, 2012. **8**(5): p. e1002697.
148. Kanegane, H., et al., *Chronic persistent Epstein-Barr virus infection of natural killer cells and B cells associated with granular lymphocytes expansion*. *Br J Haematol*, 1996. **95**(1): p. 116-22.
149. Shapiro, I.M., et al., *Infection of the human T-cell-derived leukemia line Molt-4 by Epstein-Barr virus (EBV): induction of EBV-determined antigens and virus reproduction*. *Virology*, 1982. **120**(1): p. 171-81.
150. Sixbey, J.W., et al., *Replication of Epstein-Barr virus in human epithelial cells infected in vitro*. *Nature*, 1983. **306**(5942): p. 480-3.

151. Young, L.S., et al., *Epstein-Barr virus receptors on human pharyngeal epithelia*. *Lancet*, 1986. **1**(8475): p. 240-2.
152. Rickinson, A.B., *Co-infections, inflammation and oncogenesis: future directions for EBV research*. *Semin Cancer Biol*, 2014. **26**: p. 99-115.
153. Frederico, B., et al., *Myeloid infection links epithelial and B cell tropisms of Murid Herpesvirus-4*. *PLoS Pathog*, 2012. **8**(9): p. e1002935.
154. Milho, R., et al., *A heparan-dependent herpesvirus targets the olfactory neuroepithelium for host entry*. *PLoS Pathog*, 2012. **8**(11): p. e1002986.
155. Xing, L. and E. Kieff, *Epstein-Barr virus BHRF1 micro- and stable RNAs during latency III and after induction of replication*. *J Virol*, 2007. **81**(18): p. 9967-75.
156. Cai, X., et al., *Epstein-Barr virus microRNAs are evolutionarily conserved and differentially expressed*. *PLoS Pathog*, 2006. **2**(3): p. e23.
157. Young, L., et al., *Expression of Epstein-Barr virus transformation-associated genes in tissues of patients with EBV lymphoproliferative disease*. *N Engl J Med*, 1989. **321**(16): p. 1080-5.
158. MacMahon, E.M., et al., *Epstein-Barr virus in AIDS-related primary central nervous system lymphoma*. *Lancet*, 1991. **338**(8773): p. 969-73.
159. Auperin, I., et al., *Primary central nervous system malignant non-Hodgkin's lymphomas from HIV-infected and non-infected patients: expression of cellular surface proteins and Epstein-Barr viral markers*. *Neuropathol Appl Neurobiol*, 1994. **20**(3): p. 243-52.
160. Brooks, L., et al., *Epstein-Barr virus latent gene transcription in nasopharyngeal carcinoma cells: coexpression of EBNA1, LMP1, and LMP2 transcripts*. *J Virol*, 1992. **66**(5): p. 2689-97.
161. Brooks, L.A., et al., *Transcripts from the Epstein-Barr virus BamHI A fragment are detectable in all three forms of virus latency*. *J Virol*, 1993. **67**(6): p. 3182-90.
162. Deacon, E.M., et al., *Epstein-Barr virus and Hodgkin's disease: transcriptional analysis of virus latency in the malignant cells*. *J Exp Med*, 1993. **177**(2): p. 339-49.
163. Xu, Z.G., et al., *The latency pattern of Epstein-Barr virus infection and viral IL-10 expression in cutaneous natural killer/T-cell lymphomas*. *Br J Cancer*, 2001. **84**(7): p. 920-5.
164. Fox, C.P., et al., *A novel latent membrane 2 transcript expressed in Epstein-Barr virus-positive NK- and T-cell lymphoproliferative disease encodes a target for cellular immunotherapy*. *Blood*. **116**(19): p. 3695-3704.
165. Young, L.S., C.W. Dawson, and A.G. Eliopoulos, *The expression and function of Epstein-Barr virus encoded latent genes*. *Mol Pathol*, 2000. **53**(5): p. 238-47.
166. Hammarskjold, M.L. and M.C. Simurda, *Epstein-Barr virus latent membrane protein transactivates the human immunodeficiency virus type 1 long terminal repeat through induction of NF-kappa B activity*. *J Virol*, 1992. **66**(11): p. 6496-501.
167. Fukuda, M. and R. Longnecker, *Latent membrane protein 2A inhibits transforming growth factor-beta 1-induced apoptosis through the phosphatidylinositol 3-kinase/Akt pathway*. *J Virol*, 2004. **78**(4): p. 1697-705.
168. Skalsky, R.L., et al., *The viral and cellular microRNA targetome in lymphoblastoid cell lines*. *PLoS Pathog*, 2012. **8**(1): p. e1002484.
169. Nachmani, D., et al., *Diverse herpesvirus microRNAs target the stress-induced immune ligand MICB to escape recognition by natural killer cells*. *Cell Host Microbe*, 2009. **5**(4): p. 376-85.
170. Rowe, D.T., et al., *Restricted expression of EBV latent genes and T-lymphocyte-detected membrane antigen in Burkitt's lymphoma cells*. *EMBO J*, 1986. **5**(10): p. 2599-607.
171. Pratt, Z.L., et al., *The microRNAs of Epstein-Barr Virus are expressed at dramatically differing levels among cell lines*. *Virology*, 2009. **386**(2): p. 387-97.

172. Uozaki, H. and M. Fukayama, *Epstein-Barr virus and gastric carcinoma--viral carcinogenesis through epigenetic mechanisms*. *Int J Clin Exp Pathol*, 2008. **1**(3): p. 198-216.
173. Oh, S.T., et al., *A naturally derived gastric cancer cell line shows latency I Epstein-Barr virus infection closely resembling EBV-associated gastric cancer*. *Virology*, 2004. **320**(2): p. 330-6.
174. Lin, Z., et al., *Quantitative and qualitative RNA-Seq-based evaluation of Epstein-Barr virus transcription in type I latency Burkitt's lymphoma cells*. *J Virol*, 2010. **84**(24): p. 13053-8.
175. Tierney, R.J., et al., *Unexpected patterns of Epstein-Barr virus transcription revealed by a High throughput PCR array for absolute quantification of viral mRNA*. *Virology*, 2015. **474**: p. 117-30.
176. Kelly, G., A. Bell, and A. Rickinson, *Epstein-Barr virus-associated Burkitt lymphomagenesis selects for downregulation of the nuclear antigen EBNA2*. *Nat Med*, 2002. **8**(10): p. 1098-104.
177. Pajic, A., et al., *Antagonistic effects of c-myc and Epstein-Barr virus latent genes on the phenotype of human B cells*. *Int J Cancer*, 2001. **93**(6): p. 810-6.
178. Kelly, G.L., et al., *Three restricted forms of Epstein-Barr virus latency counteracting apoptosis in c-myc-expressing Burkitt lymphoma cells*. *Proc Natl Acad Sci U S A*, 2006. **103**(40): p. 14935-40.
179. Kelly, G.L., et al., *Epstein-Barr virus nuclear antigen 2 (EBNA2) gene deletion is consistently linked with EBNA3A, -3B, and -3C expression in Burkitt's lymphoma cells and with increased resistance to apoptosis*. *J Virol*, 2005. **79**(16): p. 10709-17.
180. Garibal, J., et al., *Truncated form of the Epstein-Barr virus protein EBNA-LP protects against caspase-dependent apoptosis by inhibiting protein phosphatase 2A*. *J Virol*, 2007. **81**(14): p. 7598-607.
181. Anderton, E., et al., *Two Epstein-Barr virus (EBV) oncoproteins cooperate to repress expression of the proapoptotic tumour-suppressor Bim: clues to the pathogenesis of Burkitt's lymphoma*. *Oncogene*, 2008. **27**(4): p. 421-33.
182. Vereide, D.T. and B. Sugden, *Lymphomas differ in their dependence on Epstein-Barr virus*. *Blood*, 2011. **117**(6): p. 1977-85.
183. Souza, T.A., et al., *Peripheral B cells latently infected with Epstein-Barr virus display molecular hallmarks of classical antigen-selected memory B cells*. *Proc Natl Acad Sci U S A*, 2005. **102**(50): p. 18093-8.
184. Pegtel, D.M., et al., *Functional delivery of viral miRNAs via exosomes*. *Proc Natl Acad Sci U S A*, 2010. **107**(14): p. 6328-33.
185. Parkin, D.M., *The global health burden of infection-associated cancers in the year 2002*. *Int J Cancer*, 2006. **118**(12): p. 3030-44.
186. Parkin, D.M., et al., *The international incidence of childhood cancer*. *Int J Cancer*, 1988. **42**(4): p. 511-20.
187. Cohen, J.I., et al., *Epstein-Barr virus: an important vaccine target for cancer prevention*. *Sci Transl Med*, 2011. **3**(107): p. 107fs7.
188. Hippocrate, A., L. Oussaief, and I. Joab, *Possible role of EBV in breast cancer and other unusually EBV-associated cancers*. *Cancer Lett*, 2011. **305**(2): p. 144-9.
189. Ascherio, A. and K.L. Munger, *Environmental risk factors for multiple sclerosis. Part I: the role of infection*. *Ann Neurol*, 2007. **61**(4): p. 288-99.
190. Almohmeed, Y.H., et al., *Systematic review and meta-analysis of the sero-epidemiological association between Epstein Barr virus and multiple sclerosis*. *PLoS One*, 2013. **8**(4): p. e61110.
191. Kelly, G.L. and A.B. Rickinson, *Burkitt lymphoma: revisiting the pathogenesis of a virus-associated malignancy*. *Hematology Am Soc Hematol Educ Program*, 2007: p. 277-84.

192. Ogwang, M.D., et al., *Incidence and geographic distribution of endemic Burkitt lymphoma in northern Uganda revisited*. *Int J Cancer*, 2008. **123**(11): p. 2658-63.
193. Nkrumah, F.K., *Changes in the presentation of Burkitt's lymphoma in Ghana over a 15-year period (1969-1982)*. *IARC Sci Publ*, 1984(63): p. 665-74.
194. Hummel, M., et al., *A biologic definition of Burkitt's lymphoma from transcriptional and genomic profiling*. *N Engl J Med*, 2006. **354**(23): p. 2419-30.
195. Dave, S.S., et al., *Molecular diagnosis of Burkitt's lymphoma*. *N Engl J Med*, 2006. **354**(23): p. 2431-42.
196. Jaffe, E.S., N.L. Harris, and H. Stein, *Pathology and Genetics of Tumours of Haematopoietic and Lymphoid Tissues*. WHO Classification of Tumours, Volume 3, Third Edition. 2001, Lyon, France: IARC Press.
197. Frost, M., et al., *Comparative immunohistochemical analysis of pediatric Burkitt lymphoma and diffuse large B-cell lymphoma*. *Am J Clin Pathol*, 2004. **121**(3): p. 384-92.
198. Kuppens, R., *B cells under influence: transformation of B cells by Epstein-Barr virus*. *Nat Rev Immunol*, 2003. **3**(10): p. 801-12.
199. Magrath, I., *Epidemiology: clues to the pathogenesis of Burkitt lymphoma*. *British Journal of Haematology*, 2012: p. no-no.
200. Ogwang, M.D., et al., *Accuracy of Burkitt lymphoma diagnosis in constrained pathology settings: importance to epidemiology*. *Arch Pathol Lab Med*, 2011. **135**(4): p. 445-50.
201. Naresh, K.N., et al., *Lymphomas in sub-Saharan Africa--what can we learn and how can we help in improving diagnosis, managing patients and fostering translational research?* *Br J Haematol*, 2011. **154**(6): p. 696-703.
202. Queiroga, E.M., et al., *Viral studies in burkitt lymphoma: association with Epstein-Barr virus but not HHV-8*. *Am J Clin Pathol*, 2008. **130**(2): p. 186-92.
203. Queiroga, E.M., et al., *Burkitt lymphoma in Brazil is characterized by geographically distinct clinicopathologic features*. *Am J Clin Pathol*, 2008. **130**(6): p. 946-56.
204. Araujo, I., et al., *Expression of Epstein-Barr virus-gene products in Burkitt's lymphoma in Northeast Brazil*. *Blood*, 1996. **87**(12): p. 5279-86.
205. Levine, P.H., et al., *The American Burkitt's Lymphoma Registry: eight years' experience*. *Cancer*, 1982. **49**(5): p. 1016-22.
206. Magrath, I., *The pathogenesis of Burkitt's lymphoma*. *Adv Cancer Res*, 1990. **55**: p. 133-270.
207. Lenze, D., et al., *The different epidemiologic subtypes of Burkitt lymphoma share a homogenous micro RNA profile distinct from diffuse large B-cell lymphoma*. *Leukemia*, 2011. **25**(12): p. 1869-76.
208. Capello, D., et al., *Genome wide DNA-profiling of HIV-related B-cell lymphomas*. *Br J Haematol*, 2010. **148**(2): p. 245-55.
209. Doll, D.C. and A.F. List, *Burkitt's lymphoma in a homosexual*. *Lancet*, 1982. **1**(8279): p. 1026-7.
210. Ziegler, J.L., et al., *Outbreak of Burkitt's-like lymphoma in homosexual men*. *Lancet*, 1982. **2**(8299): p. 631-3.
211. Ziegler, J.L., et al., *Non-Hodgkin's lymphoma in 90 homosexual men. Relation to generalized lymphadenopathy and the acquired immunodeficiency syndrome*. *N Engl J Med*, 1984. **311**(9): p. 565-70.
212. Beral, V., et al., *AIDS-associated non-Hodgkin lymphoma*. *Lancet*, 1991. **337**(8745): p. 805-9.
213. Baird, J.K. and R.W. Snow, *Acquired immunity in a holoendemic setting of Plasmodium falciparum and p. Vivax malaria*. *Am J Trop Med Hyg*, 2007. **76**(6): p. 995-6.
214. Donati, D., et al., *Clearance of circulating Epstein-Barr virus DNA in children with acute malaria after antimalaria treatment*. *J Infect Dis*, 2006. **193**(7): p. 971-7.

215. Moormann, A.M., et al., *Exposure to holoendemic malaria results in elevated Epstein-Barr virus loads in children.* J Infect Dis, 2005. **191**(8): p. 1233-8.
216. Donati, D., et al., *Identification of a polyclonal B-cell activator in Plasmodium falciparum.* Infect Immun, 2004. **72**(9): p. 5412-8.
217. Rochford, R., M.J. Cannon, and A.M. Moormann, *Endemic Burkitt's lymphoma: a polymicrobial disease?* Nat Rev Microbiol, 2005. **3**(2): p. 182-7.
218. Moss, D.J., et al., *A comparison of Epstein-Barr virus-specific T-cell immunity in malaria-endemic and -nonendemic regions of Papua New Guinea.* Int J Cancer, 1983. **31**(6): p. 727-32.
219. Whittle, H.C., et al., *T-cell control of Epstein-Barr virus-infected B cells is lost during P. falciparum malaria.* Nature, 1984. **312**(5993): p. 449-50.
220. Rickinson, A.B., et al., *Reactivation of Epstein-Barr virus-specific cytotoxic T cells by in vitro stimulation with the autologous lymphoblastoid cell line.* Int J Cancer, 1981. **27**(5): p. 593-601.
221. Moormann, A.M., et al., *Exposure to holoendemic malaria results in suppression of Epstein-Barr virus-specific T cell immunosurveillance in Kenyan children.* J Infect Dis, 2007. **195**(6): p. 799-808.
222. Moormann, A.M., et al., *Children with endemic Burkitt lymphoma are deficient in EBNA1-specific IFN-gamma T cell responses.* Int J Cancer, 2009. **124**(7): p. 1721-6.
223. Chattopadhyay, P.K., et al., *Holoendemic malaria exposure is associated with altered Epstein-Barr virus-specific CD8(+) T-cell differentiation.* J Virol, 2013. **87**(3): p. 1779-88.
224. Torgbor, C., et al., *A multifactorial role for P. falciparum malaria in endemic Burkitt's lymphoma pathogenesis.* PLoS Pathog, 2014. **10**(5): p. e1004170.
225. Engels, E.A., et al., *Trends in cancer risk among people with AIDS in the United States 1980-2002.* AIDS, 2006. **20**(12): p. 1645-54.
226. van Leeuwen, M.T., et al., *Continuing declines in some but not all HIV-associated cancers in Australia after widespread use of antiretroviral therapy.* AIDS, 2009. **23**(16): p. 2183-90.
227. Guech-Ongey, M., et al., *AIDS-related Burkitt lymphoma in the United States: what do age and CD4 lymphocyte patterns tell us about etiology and/or biology?* Blood, 2010. **116**(25): p. 5600-4.
228. Ouedraogo, D.E., et al., *Increased T-cell activation and Th1 cytokine concentrations prior to the diagnosis of B-cell lymphoma in HIV infected patients.* J Clin Immunol, 2013. **33**(1): p. 22-9.
229. Epeldegui, M., et al., *Elevated expression of activation induced cytidine deaminase in peripheral blood mononuclear cells precedes AIDS-NHL diagnosis.* AIDS, 2007. **21**(17): p. 2265-70.
230. Muller, J.R., et al., *Persistence of immunoglobulin heavy chain/c-myc recombination-positive lymphocyte clones in the blood of human immunodeficiency virus-infected homosexual men.* Proc Natl Acad Sci U S A, 1995. **92**(14): p. 6577-81.
231. Shiels, M.S., et al., *The epidemic of non-Hodgkin lymphoma in the United States: disentangling the effect of HIV, 1992-2009.* Cancer Epidemiol Biomarkers Prev, 2013. **22**(6): p. 1069-78.
232. van den Bosch, C. and G. Lloyd, *Chikungunya fever as a risk factor for endemic Burkitt's lymphoma in Malawi.* Trans R Soc Trop Med Hyg, 2000. **94**(6): p. 704-5.
233. van den Bosch, C., *A Role for RNA Viruses in the Pathogenesis of Burkitt's Lymphoma: The Need for Reappraisal.* Adv Hematol, 2012. **2012**: p. 494758.
234. van den Bosch, C., et al., *Are plant factors a missing link in the evolution of endemic Burkitt's lymphoma?* Br J Cancer, 1993. **68**(6): p. 1232-5.
235. Stebbing, J., et al., *Use of antidepressants and risk of cancer in individuals infected with HIV.* J Clin Oncol, 2008. **26**(14): p. 2305-10.

236. Kaatsch, P., U. Scheidemann-Wesp, and J. Schuz, *Maternal use of antibiotics and cancer in the offspring: results of a case-control study in Germany*. *Cancer Causes Control*, 2010. **21**(8): p. 1335-45.
237. Sumba, P.O., et al., *Microgeographic variations in Burkitt's lymphoma incidence correlate with differences in malnutrition, malaria and Epstein-Barr virus*. *Br J Cancer*, 2010. **103**(11): p. 1736-41.
238. Carozza, S.E., et al., *Agricultural pesticides and risk of childhood cancers*. *Int J Hyg Environ Health*, 2009. **212**(2): p. 186-95.
239. Rudant, J., et al., *Household exposure to pesticides and risk of childhood hematopoietic malignancies: The ESCALE study (SFCE)*. *Environ Health Perspect*, 2007. **115**(12): p. 1787-93.
240. Hardell, E., et al., *Case-control study on concentrations of organohalogen compounds and titers of antibodies to Epstein-Barr virus antigens in the etiology of non-Hodgkin lymphoma*. *Leuk Lymphoma*, 2001. **42**(4): p. 619-29.
241. Rainey, J.J., et al., *Spatial clustering of endemic Burkitt's lymphoma in high-risk regions of Kenya*. *Int J Cancer*, 2007. **120**(1): p. 121-7.
242. Castillo, J.J., E.S. Winer, and A.J. Olszewski, *Population-based prognostic factors for survival in patients with Burkitt lymphoma: an analysis from the Surveillance, Epidemiology, and End Results database*. *Cancer*, 2013. **119**(20): p. 3672-9.
243. Lenoir, G.M., et al., *Correlation between immunoglobulin light chain expression and variant translocation in Burkitt's lymphoma*. *Nature*, 1982. **298**(5873): p. 474-6.
244. Klein, G., *The role of gene dosage and genetic transpositions in carcinogenesis*. *Nature*, 1981. **294**(5839): p. 313-8.
245. Taub, R., et al., *Translocation of the c-myc gene into the immunoglobulin heavy chain locus in human Burkitt lymphoma and murine plasmacytoma cells*. *Proc Natl Acad Sci U S A*, 1982. **79**(24): p. 7837-41.
246. Shiramizu, B., et al., *Patterns of chromosomal breakpoint locations in Burkitt's lymphoma: relevance to geography and Epstein-Barr virus association*. *Blood*, 1991. **77**(7): p. 1516-26.
247. Pelicci, P.G., et al., *Chromosomal breakpoints and structural alterations of the c-myc locus differ in endemic and sporadic forms of Burkitt lymphoma*. *Proc Natl Acad Sci U S A*, 1986. **83**(9): p. 2984-8.
248. Li, Z., et al., *A global transcriptional regulatory role for c-Myc in Burkitt's lymphoma cells*. *Proc Natl Acad Sci U S A*, 2003. **100**(14): p. 8164-9.
249. Luscher, B. and J. Vervoorts, *Regulation of gene transcription by the oncoprotein MYC*. *Gene*, 2012. **494**(2): p. 145-60.
250. Nie, Z., et al., *c-Myc is a universal amplifier of expressed genes in lymphocytes and embryonic stem cells*. *Cell*, 2012. **151**(1): p. 68-79.
251. Lin, C.Y., et al., *Transcriptional amplification in tumor cells with elevated c-Myc*. *Cell*, 2012. **151**(1): p. 56-67.
252. McCarthy, N., *Tumorigenesis: Megaphone MYC*. *Nat Rev Cancer*, 2012. **12**(11): p. 733.
253. Pelengaris, S., M. Khan, and G. Evan, *c-MYC: more than just a matter of life and death*. *Nat Rev Cancer*, 2002. **2**(10): p. 764-76.
254. Tanaka, H., et al., *E2F1 and c-Myc potentiate apoptosis through inhibition of NF-kappaB activity that facilitates MnSOD-mediated ROS elimination*. *Mol Cell*, 2002. **9**(5): p. 1017-29.
255. You, Z., et al., *c-Myc sensitizes cells to tumor necrosis factor-mediated apoptosis by inhibiting nuclear factor kappa B transactivation*. *J Biol Chem*, 2002. **277**(39): p. 36671-7.
256. Staeger, M.S., et al., *MYC overexpression imposes a nonimmunogenic phenotype on Epstein-Barr virus-infected B cells*. *Proc Natl Acad Sci U S A*, 2002. **99**(7): p. 4550-5.

257. Schlee, M., et al., *c-MYC impairs immunogenicity of human B cells*. *Adv Cancer Res*, 2007. **97**: p. 167-88.
258. Hoffman, B. and D.A. Liebermann, *Apoptotic signaling by c-MYC*. *Oncogene*, 2008. **27**(50): p. 6462-72.
259. Gaidano, G., et al., *p53 mutations in human lymphoid malignancies: association with Burkitt lymphoma and chronic lymphocytic leukemia*. *Proc Natl Acad Sci U S A*, 1991. **88**(12): p. 5413-7.
260. Farrell, P.J., et al., *p53 is frequently mutated in Burkitt's lymphoma cell lines*. *EMBO J*, 1991. **10**(10): p. 2879-87.
261. Vousden, K.H., T. Crook, and P.J. Farrell, *Biological activities of p53 mutants in Burkitt's lymphoma cells*. *J Gen Virol*, 1993. **74** (Pt 5): p. 803-10.
262. Cherney, B.W., et al., *Role of the p53 tumor suppressor gene in the tumorigenicity of Burkitt's lymphoma cells*. *Cancer Res*, 1997. **57**(12): p. 2508-15.
263. Eischen, C.M., et al., *Disruption of the ARF-Mdm2-p53 tumor suppressor pathway in Myc-induced lymphomagenesis*. *Genes Dev*, 1999. **13**(20): p. 2658-69.
264. Lindstrom, M.S., U. Klangby, and K.G. Wiman, *p14ARF homozygous deletion or MDM2 overexpression in Burkitt lymphoma lines carrying wild type p53*. *Oncogene*, 2001. **20**(17): p. 2171-7.
265. Vousden, K.H. and D.P. Lane, *p53 in health and disease*. *Nat Rev Mol Cell Biol*, 2007. **8**(4): p. 275-83.
266. Michalak, E.M., et al., *Puma and to a lesser extent Noxa are suppressors of Myc-induced lymphomagenesis*. *Cell Death Differ*, 2009. **16**(5): p. 684-96.
267. Garrison, S.P., et al., *Selection against PUMA gene expression in Myc-driven B-cell lymphomagenesis*. *Mol Cell Biol*, 2008. **28**(17): p. 5391-402.
268. Egle, A., et al., *Bim is a suppressor of Myc-induced mouse B cell leukemia*. *Proc Natl Acad Sci U S A*, 2004. **101**(16): p. 6164-9.
269. Hemann, M.T., et al., *Evasion of the p53 tumour surveillance network by tumour-derived MYC mutants*. *Nature*, 2005. **436**(7052): p. 807-11.
270. Eischen, C.M., et al., *Bax loss impairs Myc-induced apoptosis and circumvents the selection of p53 mutations during Myc-mediated lymphomagenesis*. *Mol Cell Biol*, 2001. **21**(22): p. 7653-62.
271. Maclean, K.H., et al., *c-Myc augments gamma irradiation-induced apoptosis by suppressing Bcl-XL*. *Mol Cell Biol*, 2003. **23**(20): p. 7256-70.
272. Juin, P., et al., *c-Myc functionally cooperates with Bax to induce apoptosis*. *Mol Cell Biol*, 2002. **22**(17): p. 6158-69.
273. Mitchell, K.O., et al., *Bax is a transcriptional target and mediator of c-myc-induced apoptosis*. *Cancer Res*, 2000. **60**(22): p. 6318-25.
274. Happo, L., et al., *Maximal killing of lymphoma cells by DNA damage-inducing therapy requires not only the p53 targets Puma and Noxa, but also Bim*. *Blood*, 2010. **116**(24): p. 5256-67.
275. Adhikary, S. and M. Eilers, *Transcriptional regulation and transformation by Myc proteins*. *Nat Rev Mol Cell Biol*, 2005. **6**(8): p. 635-45.
276. Dang, C.V., A. O'Donnell K, and T. Juopperi, *The great MYC escape in tumorigenesis*. *Cancer Cell*, 2005. **8**(3): p. 177-8.
277. Love, C., et al., *The genetic landscape of mutations in Burkitt lymphoma*. *Nat Genet*, 2012. **44**(12): p. 1321-5.
278. Schmitz, R., et al., *Burkitt lymphoma pathogenesis and therapeutic targets from structural and functional genomics*. *Nature*, 2012. **490**(7418): p. 116-20.
279. Richter, J., et al., *Recurrent mutation of the ID3 gene in Burkitt lymphoma identified by integrated genome, exome and transcriptome sequencing*. *Nat Genet*, 2012. **44**(12): p. 1316-20.

280. Rowe, M., L. Fitzsimmons, and A.I. Bell, *Epstein-Barr virus and Burkitt lymphoma*. *Chin J Cancer*, 2014. **33**(12): p. 609-19.
281. Burkitt, D., M.S. Hutt, and D.H. Wright, *The African Lymphoma: Preliminary Observations on Response to Therapy*. *Cancer*, 1965. **18**: p. 399-410.
282. Clifford, P., *Further studies on the treatment of Burkitt's lymphoma*. *East Afr Med J*, 1966. **43**(6): p. 179-99.
283. Gerrard, M., et al., *Excellent survival following two courses of COPAD chemotherapy in children and adolescents with resected localized B-cell non-Hodgkin's lymphoma: results of the FAB/LMB 96 international study*. *Br J Haematol*, 2008. **141**(6): p. 840-7.
284. Goldman, S., et al., *Rituximab with chemotherapy in children and adolescents with central nervous system and/or bone marrow-positive Burkitt lymphoma/leukaemia: a Children's Oncology Group Report*. *Br J Haematol*, 2014.
285. Hesseling, P., et al., *Endemic Burkitt lymphoma: a 28-day treatment schedule with cyclophosphamide and intrathecal methotrexate*. *Ann Trop Paediatr*, 2009. **29**(1): p. 29-34.
286. Costa, L.J., et al., *Trends in survival of patients with Burkitt lymphoma/leukemia in the USA: an analysis of 3691 cases*. *Blood*, 2013. **121**(24): p. 4861-6.
287. Blum, K.A., G. Lozanski, and J.C. Byrd, *Adult Burkitt leukemia and lymphoma*. *Blood*, 2004. **104**(10): p. 3009-20.
288. Kamranvar, S.A., et al., *Epstein-Barr virus promotes genomic instability in Burkitt's lymphoma*. *Oncogene*, 2007. **26**(35): p. 5115-23.
289. Gualandi, G., et al., *Enhancement of genetic instability in human B cells by Epstein-Barr virus latent infection*. *Mutagenesis*, 2001. **16**(3): p. 203-8.
290. Lacoste, S., et al., *Chromosomal rearrangements after ex vivo Epstein-Barr virus (EBV) infection of human B cells*. *Oncogene*, 2010. **29**(4): p. 503-15.
291. Epeldegui, M., et al., *Infection of human B cells with Epstein-Barr virus results in the expression of somatic hypermutation-inducing molecules and in the accrual of oncogene mutations*. *Mol Immunol*, 2007. **44**(5): p. 934-42.
292. Thorley-Lawson, D.A. and M.J. Allday, *The curious case of the tumour virus: 50 years of Burkitt's lymphoma*. *Nat Rev Microbiol*, 2008. **6**(12): p. 913-24.
293. Ambinder, R.F., *Gammaherpesviruses and "Hit-and-Run" oncogenesis*. *Am J Pathol*, 2000. **156**(1): p. 1-3.
294. Fialkow, P.J., et al., *Clonal origin for individual Burkitt tumours*. *Lancet*, 1970. **1**(7643): p. 384-6.
295. Nanbo, A., A. Sugden, and B. Sugden, *The coupling of synthesis and partitioning of EBV's plasmid replicon is revealed in live cells*. *EMBO J*, 2007. **26**(19): p. 4252-62.
296. Kanda, T., et al., *Symmetrical localization of extrachromosomally replicating viral genomes on sister chromatids*. *J Cell Sci*, 2007. **120**(Pt 9): p. 1529-39.
297. Sears, J., et al., *The amino terminus of Epstein-Barr Virus (EBV) nuclear antigen 1 contains AT hooks that facilitate the replication and partitioning of latent EBV genomes by tethering them to cellular chromosomes*. *J Virol*, 2004. **78**(21): p. 11487-505.
298. Kennedy, G., J. Komano, and B. Sugden, *Epstein-Barr virus provides a survival factor to Burkitt's lymphomas*. *Proc Natl Acad Sci U S A*, 2003. **100**(24): p. 14269-74.
299. Nasimuzzaman, M., et al., *Eradication of Epstein-Barr virus episome and associated inhibition of infected tumor cell growth by adenovirus vector-mediated transduction of dominant-negative EBNA1*. *Mol Ther*, 2005. **11**(4): p. 578-90.
300. Bellan, C., et al., *Immunoglobulin gene analysis reveals 2 distinct cells of origin for EBV-positive and EBV-negative Burkitt lymphomas*. *Blood*, 2005. **106**(3): p. 1031-6.
301. Kelly, G.L., et al., *Targeting of MCL-1 kills MYC-driven mouse and human lymphomas even when they bear mutations in p53*. *Genes Dev*, 2014. **28**(1): p. 58-70.

302. Adams, C.M. and C.M. Eischen, *Inactivation of p53 is insufficient to allow B cells and B-cell lymphomas to survive without Dicer*. *Cancer Res*, 2014. **74**(14): p. 3923-34.
303. Henderson, S., et al., *Epstein-Barr virus-coded BHRF1 protein, a viral homologue of Bcl-2, protects human B cells from programmed cell death*. *Proc Natl Acad Sci U S A*, 1993. **90**(18): p. 8479-83.
304. Desbien, A.L., J.W. Kappler, and P. Murrack, *The Epstein-Barr virus Bcl-2 homolog, BHRF1, blocks apoptosis by binding to a limited amount of Bim*. *Proc Natl Acad Sci U S A*, 2009. **106**(14): p. 5663-8.
305. Flanagan, A.M. and A. Letai, *BH3 domains define selective inhibitory interactions with BHRF-1 and KSHV BCL-2*. *Cell Death Differ*, 2008. **15**(3): p. 580-8.
306. Paschos, K., et al., *Epstein-barr virus latency in B cells leads to epigenetic repression and CpG methylation of the tumour suppressor gene Bim*. *PLoS Pathog*, 2009. **5**(6): p. e1000492.
307. Bornkamm, G.W., *Epstein-Barr virus and its role in the pathogenesis of Burkitt's lymphoma: an unresolved issue*. *Semin Cancer Biol*, 2009. **19**(6): p. 351-65.
308. Allday, M.J., *How does Epstein-Barr virus (EBV) complement the activation of Myc in the pathogenesis of Burkitt's lymphoma?* *Semin Cancer Biol*, 2009. **19**(6): p. 366-76.
309. Shimizu, N., et al., *Isolation of Epstein-Barr virus (EBV)-negative cell clones from the EBV-positive Burkitt's lymphoma (BL) line Akata: malignant phenotypes of BL cells are dependent on EBV*. *J Virol*, 1994. **68**(9): p. 6069-73.
310. Komano, J., M. Sugiura, and K. Takada, *Epstein-Barr virus contributes to the malignant phenotype and to apoptosis resistance in Burkitt's lymphoma cell line Akata*. *J Virol*, 1998. **72**(11): p. 9150-6.
311. Chodosh, J., et al., *Eradication of latent Epstein-Barr virus by hydroxyurea alters the growth-transformed cell phenotype*. *J Infect Dis*, 1998. **177**(5): p. 1194-201.
312. Kirchmaier, A.L. and B. Sugden, *Dominant-negative inhibitors of EBNA-1 of Epstein-Barr virus*. *J Virol*, 1997. **71**(3): p. 1766-75.
313. Clybouw, C., et al., *EBV infection of human B lymphocytes leads to down-regulation of Bim expression: relationship to resistance to apoptosis*. *J Immunol*, 2005. **175**(5): p. 2968-73.
314. Swart, R., et al., *Latent membrane protein 2A-mediated effects on the phosphatidylinositol 3-Kinase/Akt pathway*. *J Virol*, 2000. **74**(22): p. 10838-45.
315. Biegging, K.T., A.C. Amick, and R. Longnecker, *Epstein-Barr virus LMP2A bypasses p53 inactivation in a MYC model of lymphomagenesis*. *Proc Natl Acad Sci U S A*, 2009. **106**(42): p. 17945-50.
316. Biegging, K.T., et al., *Epstein-Barr virus in Burkitt's lymphoma: a role for latent membrane protein 2A*. *Cell Cycle*, 2010. **9**(5): p. 901-8.
317. Bell, A.I., et al., *Analysis of Epstein-Barr virus latent gene expression in endemic Burkitt's lymphoma and nasopharyngeal carcinoma tumour cells by using quantitative real-time PCR assays*. *J Gen Virol*, 2006. **87**(Pt 10): p. 2885-90.
318. Mackey, D. and B. Sugden, *Applications of oriP plasmids and their mode of replication*. *Methods Enzymol*, 1999. **306**: p. 308-28.
319. Leight, E.R. and B. Sugden, *EBNA-1: a protein pivotal to latent infection by Epstein-Barr virus*. *Rev Med Virol*, 2000. **10**(2): p. 83-100.
320. Saridakis, V., et al., *Structure of the p53 binding domain of HAUSP/USP7 bound to Epstein-Barr nuclear antigen 1 implications for EBV-mediated immortalization*. *Mol Cell*, 2005. **18**(1): p. 25-36.
321. Lu, J., et al., *Epstein-Barr Virus nuclear antigen 1 (EBNA1) confers resistance to apoptosis in EBV-positive B-lymphoma cells through up-regulation of survivin*. *Virology*. **In Press, Corrected Proof**.

322. Frappier, L., *Contributions of Epstein-Barr nuclear antigen 1 (EBNA1) to cell immortalization and survival*. *Viruses*, 2012. **4**(9): p. 1537-47.
323. Wilson, J.B., J.L. Bell, and A.J. Levine, *Expression of Epstein-Barr virus nuclear antigen-1 induces B cell neoplasia in transgenic mice*. *EMBO J*, 1996. **15**(12): p. 3117-26.
324. Wilson, J.B. and A.J. Levine, *The oncogenic potential of Epstein-Barr virus nuclear antigen 1 in transgenic mice*. *Curr Top Microbiol Immunol*, 1992. **182**: p. 375-84.
325. Kang, M.S., et al., *Epstein-Barr virus nuclear antigen 1 does not induce lymphoma in transgenic FVB mice*. *Proc Natl Acad Sci U S A*, 2005. **102**(3): p. 820-5.
326. Kang, M.S., et al., *Epstein-Barr virus nuclear antigen 1 does not cause lymphoma in C57BL/6J mice*. *J Virol*, 2008. **82**(8): p. 4180-3.
327. Ruf, I.K., et al., *Epstein-barr virus regulates c-MYC, apoptosis, and tumorigenicity in Burkitt lymphoma*. *Mol Cell Biol*, 1999. **19**(3): p. 1651-60.
328. Niedobitek, G. and H. Herbst, *In situ detection of Epstein-Barr virus and phenotype determination of EBV-infected cells*. *Methods Mol Biol*, 2006. **326**: p. 115-37.
329. Hovanessian, A.G., *The double stranded RNA-activated protein kinase induced by interferon: dsRNA-PK*. *J Interferon Res*, 1989. **9**(6): p. 641-7.
330. Ghadge, G.D., et al., *In vitro analysis of virus-associated RNA I (VAI RNA): inhibition of the double-stranded RNA-activated protein kinase PKR by VAI RNA mutants correlates with the in vivo phenotype and the structural integrity of the central domain*. *J Virol*, 1994. **68**(7): p. 4137-51.
331. Bhat, R.A. and B. Thimmappaya, *Two small RNAs encoded by Epstein-Barr virus can functionally substitute for the virus-associated RNAs in the lytic growth of adenovirus 5*. *Proc Natl Acad Sci U S A*, 1983. **80**(15): p. 4789-93.
332. Bhat, R.A. and B. Thimmappaya, *Construction and analysis of additional adenovirus substitution mutants confirm the complementation of VAI RNA function by two small RNAs encoded by Epstein-Barr virus*. *J Virol*, 1985. **56**(3): p. 750-6.
333. Howe, J.G. and J.A. Steitz, *Localization of Epstein-Barr virus-encoded small RNAs by in situ hybridization*. *Proc Natl Acad Sci U S A*, 1986. **83**(23): p. 9006-10.
334. Fok, V., K. Friend, and J.A. Steitz, *Epstein-Barr virus noncoding RNAs are confined to the nucleus, whereas their partner, the human La protein, undergoes nucleocytoplasmic shuttling*. *J Cell Biol*, 2006. **173**(3): p. 319-25.
335. Ruf, I.K., et al., *Protection from interferon-induced apoptosis by Epstein-Barr virus small RNAs is not mediated by inhibition of PKR*. *J Virol*, 2005. **79**(23): p. 14562-9.
336. Swaminathan, S., et al., *Epstein-Barr virus-encoded small RNAs (EBERs) do not modulate interferon effects in infected lymphocytes*. *J Virol*, 1992. **66**(8): p. 5133-6.
337. Wang, Y., et al., *Virus-associated RNA I-deleted adenovirus, a potential oncolytic agent targeting EBV-associated tumors*. *Cancer Res*, 2005. **65**(4): p. 1523-31.
338. Nanbo, A., et al., *Epstein-Barr virus RNA confers resistance to interferon-alpha-induced apoptosis in Burkitt's lymphoma*. *EMBO J*, 2002. **21**(5): p. 954-65.
339. Komano, J., et al., *Oncogenic role of Epstein-Barr virus-encoded RNAs in Burkitt's lymphoma cell line Akata*. *J Virol*, 1999. **73**(12): p. 9827-31.
340. Ruf, I.K., et al., *Epstein-Barr virus small RNAs potentiate tumorigenicity of Burkitt lymphoma cells independently of an effect on apoptosis*. *J Virol*, 2000. **74**(21): p. 10223-8.
341. Kitagawa, N., et al., *Epstein-Barr virus-encoded poly(A)(-) RNA supports Burkitt's lymphoma growth through interleukin-10 induction*. *EMBO J*, 2000. **19**(24): p. 6742-50.
342. Samanta, M., D. Iwakiri, and K. Takada, *Epstein-Barr virus-encoded small RNA induces IL-10 through RIG-I-mediated IRF-3 signaling*. *Oncogene*, 2008. **27**(30): p. 4150-60.
343. Lerner, M.R., et al., *Two small RNAs encoded by Epstein-Barr virus and complexed with protein are precipitated by antibodies from patients with systemic lupus erythematosus*. *Proc Natl Acad Sci U S A*, 1981. **78**(2): p. 805-9.

344. Toczyski, D.P., et al., *The Epstein-Barr virus (EBV) small RNA EBER1 binds and relocalizes ribosomal protein L22 in EBV-infected human B lymphocytes*. Proc Natl Acad Sci U S A, 1994. **91**(8): p. 3463-7.
345. Clarke, P.A., et al., *Binding of Epstein-Barr virus small RNA EBER-1 to the double-stranded RNA-activated protein kinase DAI*. Nucleic Acids Res, 1991. **19**(2): p. 243-8.
346. Fok, V., et al., *Multiple domains of EBER 1, an Epstein-Barr virus noncoding RNA, recruit human ribosomal protein L22*. RNA, 2006. **12**(5): p. 872-82.
347. Houmani, J.L., C.I. Davis, and I.K. Ruf, *Growth-promoting properties of Epstein-Barr virus EBER-1 RNA correlate with ribosomal protein L22 binding*. J Virol, 2009. **83**(19): p. 9844-53.
348. Gilligan, K., et al., *Novel transcription from the Epstein-Barr virus terminal EcoRI fragment, DJhet, in a nasopharyngeal carcinoma*. J Virol, 1990. **64**(10): p. 4948-56.
349. Hitt, M.M., et al., *EBV gene expression in an NPC-related tumour*. EMBO J, 1989. **8**(9): p. 2639-51.
350. Sadler, R.H. and N. Raab-Traub, *Structural analyses of the Epstein-Barr virus BamHI A transcripts*. J Virol, 1995. **69**(2): p. 1132-41.
351. Smith, P.R., et al., *Complex nature of the major viral polyadenylated transcripts in Epstein-Barr virus-associated tumors*. J Virol, 1993. **67**(6): p. 3217-25.
352. Pfeffer, S., et al., *Identification of virus-encoded microRNAs*. Science, 2004. **304**(5671): p. 734-6.
353. Zhang, J., et al., *Epstein-Barr virus BamHI-a rightward transcript-encoded RPMS protein interacts with the CBF1-associated corepressor CIR to negatively regulate the activity of EBNA2 and Notch1C*. J Virol, 2001. **75**(6): p. 2946-56.
354. Kusano, S. and N. Raab-Traub, *An Epstein-Barr virus protein interacts with Notch*. J Virol, 2001. **75**(1): p. 384-95.
355. Smith, P.R., et al., *Structure and coding content of CST (BART) family RNAs of Epstein-Barr virus*. J Virol, 2000. **74**(7): p. 3082-92.
356. Al-Mozaini, M., et al., *Epstein-Barr virus BART gene expression*. J Gen Virol, 2009. **90**(Pt 2): p. 307-16.
357. van Beek, J., et al., *In vivo transcription of the Epstein-Barr virus (EBV) BamHI-A region without associated in vivo BARF0 protein expression in multiple EBV-associated disorders*. J Gen Virol, 2003. **84**(Pt 10): p. 2647-59.
358. Bartel, D.P., *MicroRNAs: genomics, biogenesis, mechanism, and function*. Cell, 2004. **116**(2): p. 281-97.
359. Ambros, V., *The functions of animal microRNAs*. Nature, 2004. **431**(7006): p. 350-5.
360. Choi, H., et al., *Epstein-Barr virus-encoded microRNA BART15-3p promotes cell apoptosis partially by targeting BRUCE*. J Virol, 2013. **87**(14): p. 8135-44.
361. Jung, Y.J., et al., *MicroRNA miR-BART20-5p Stabilizes Epstein-Barr Virus Latency by Directly Targeting BZLF1 and BRLF1*. J Virol, 2014. **88**(16): p. 9027-37.
362. Qiu, J. and D.A. Thorley-Lawson, *EBV microRNA BART 18-5p targets MAP3K2 to facilitate persistence in vivo by inhibiting viral replication in B cells*. Proc Natl Acad Sci U S A, 2014. **111**(30): p. 11157-62.
363. Lo, A.K., et al., *Modulation of LMP1 protein expression by EBV-encoded microRNAs*. Proc Natl Acad Sci U S A, 2007. **104**(41): p. 16164-9.
364. Ramakrishnan, R., et al., *Epstein-Barr virus BART9 miRNA modulates LMP1 levels and affects growth rate of nasal NK T cell lymphomas*. PLoS One, 2011. **6**(11): p. e27271.
365. Choy, E.Y., et al., *An Epstein-Barr virus-encoded microRNA targets PUMA to promote host cell survival*. J Exp Med, 2008. **205**(11): p. 2551-60.
366. Marquitz, A.R., et al., *The Epstein-Barr Virus BART microRNAs target the pro-apoptotic protein Bim*. Virology. **412**(2): p. 392-400.

367. Barth, S., et al., *Epstein-Barr virus-encoded microRNA miR-BART2 down-regulates the viral DNA polymerase BALF5*. *Nucleic Acids Res*, 2008. **36**(2): p. 666-75.
368. Iizasa, H., et al., *Editing of Epstein-Barr virus-encoded BART6 microRNAs controls their dicer targeting and consequently affects viral latency*. *J Biol Chem*, 2010. **285**(43): p. 33358-70.
369. Lei, T., et al., *Targeting of DICE1 tumor suppressor by Epstein-Barr virus-encoded miR-BART3* microRNA in nasopharyngeal carcinoma*. *Int J Cancer*, 2013. **133**(1): p. 79-87.
370. Lin, T.C., et al., *Epstein-Barr virus-encoded miR-BART20-5p inhibits T-bet translation with secondary suppression of p53 in invasive nasal NK/T-cell lymphoma*. *Am J Pathol*, 2013. **182**(5): p. 1865-75.
371. Riley, K.J., et al., *EBV and human microRNAs co-target oncogenic and apoptotic viral and human genes during latency*. *EMBO J*, 2012. **31**(9): p. 2207-21.
372. Cosmopoulos, K., et al., *Comprehensive profiling of Epstein-Barr virus microRNAs in nasopharyngeal carcinoma*. *J Virol*, 2009. **83**(5): p. 2357-67.
373. Edwards, R.H., A.R. Marquitz, and N. Raab-Traub, *Epstein-Barr virus BART microRNAs are produced from a large intron prior to splicing*. *J Virol*, 2008. **82**(18): p. 9094-106.
374. Dolken, L., et al., *Systematic analysis of viral and cellular microRNA targets in cells latently infected with human gamma-herpesviruses by RISC immunoprecipitation assay*. *Cell Host Microbe*, 2010. **7**(4): p. 324-34.
375. Kuzembayeva, M., Y.F. Chiu, and B. Sugden, *Comparing proteomics and RISC immunoprecipitations to identify targets of Epstein-Barr viral miRNAs*. *PLoS One*, 2012. **7**(10): p. e47409.
376. Kerr, J.F., A.H. Wyllie, and A.R. Currie, *Apoptosis: a basic biological phenomenon with wide-ranging implications in tissue kinetics*. *Br J Cancer*, 1972. **26**(4): p. 239-57.
377. Hanahan, D. and R.A. Weinberg, *Hallmarks of cancer: the next generation*. *Cell*, 2011. **144**(5): p. 646-74.
378. Strasser, A., et al., *Bcl-2 and Fas/APO-1 regulate distinct pathways to lymphocyte apoptosis*. *EMBO J*, 1995. **14**(24): p. 6136-47.
379. Strasser, A., P.J. Jost, and S. Nagata, *The many roles of FAS receptor signaling in the immune system*. *Immunity*, 2009. **30**(2): p. 180-92.
380. Kischkel, F.C., et al., *Cytotoxicity-dependent APO-1 (Fas/CD95)-associated proteins form a death-inducing signaling complex (DISC) with the receptor*. *EMBO J*, 1995. **14**(22): p. 5579-88.
381. McIlwain, D.R., T. Berger, and T.W. Mak, *Caspase functions in cell death and disease*. *Cold Spring Harb Perspect Biol*, 2013. **5**(4): p. a008656.
382. Taylor, R.C., S.P. Cullen, and S.J. Martin, *Apoptosis: controlled demolition at the cellular level*. *Nat Rev Mol Cell Biol*, 2008. **9**(3): p. 231-41.
383. Boatright, K.M., et al., *A unified model for apical caspase activation*. *Mol Cell*, 2003. **11**(2): p. 529-41.
384. Timmer, J.C. and G.S. Salvesen, *Caspase substrates*. *Cell Death Differ*, 2007. **14**(1): p. 66-72.
385. Liu, X., et al., *DFF, a heterodimeric protein that functions downstream of caspase-3 to trigger DNA fragmentation during apoptosis*. *Cell*, 1997. **89**(2): p. 175-84.
386. Kuranaga, E. and M. Miura, *Nonapoptotic functions of caspases: caspases as regulatory molecules for immunity and cell-fate determination*. *Trends Cell Biol*, 2007. **17**(3): p. 135-44.
387. Cerretti, D.P., et al., *Molecular cloning of the interleukin-1 beta converting enzyme*. *Science*, 1992. **256**(5053): p. 97-100.
388. Gurcel, L., et al., *Caspase-1 activation of lipid metabolic pathways in response to bacterial pore-forming toxins promotes cell survival*. *Cell*, 2006. **126**(6): p. 1135-45.

389. Nadiri, A., M.K. Wolinski, and M. Saleh, *The inflammatory caspases: key players in the host response to pathogenic invasion and sepsis*. J Immunol, 2006. **177**(7): p. 4239-45.
390. Thornberry, N.A., et al., *A novel heterodimeric cysteine protease is required for interleukin-1 beta processing in monocytes*. Nature, 1992. **356**(6372): p. 768-74.
391. Wang, X., *The expanding role of mitochondria in apoptosis*. Genes Dev, 2001. **15**(22): p. 2922-33.
392. Kaufmann, S.H. and W.C. Earnshaw, *Induction of apoptosis by cancer chemotherapy*. Exp Cell Res, 2000. **256**(1): p. 42-9.
393. Verhagen, A.M., et al., *HtrA2 promotes cell death through its serine protease activity and its ability to antagonize inhibitor of apoptosis proteins*. J Biol Chem, 2002. **277**(1): p. 445-54.
394. Verhagen, A.M. and D.L. Vaux, *Cell death regulation by the mammalian IAP antagonist Diablo/Smac*. Apoptosis, 2002. **7**(2): p. 163-6.
395. Verhagen, A.M., et al., *Identification of DIABLO, a mammalian protein that promotes apoptosis by binding to and antagonizing IAP proteins*. Cell, 2000. **102**(1): p. 43-53.
396. Li, L.Y., X. Luo, and X. Wang, *Endonuclease G is an apoptotic DNase when released from mitochondria*. Nature, 2001. **412**(6842): p. 95-9.
397. Susin, S.A., et al., *Molecular characterization of mitochondrial apoptosis-inducing factor*. Nature, 1999. **397**(6718): p. 441-6.
398. Kelly, G.L. and A. Strasser, *The essential role of evasion from cell death in cancer*. Adv Cancer Res, 2011. **111**: p. 39-96.
399. Strasser, A., S. Cory, and J.M. Adams, *Deciphering the rules of programmed cell death to improve therapy of cancer and other diseases*. EMBO J, 2011. **30**(18): p. 3667-83.
400. Nagata, S., R. Hanayama, and K. Kawane, *Autoimmunity and the clearance of dead cells*. Cell, 2010. **140**(5): p. 619-30.
401. Egerton, M., R. Scollay, and K. Shortman, *Kinetics of mature T-cell development in the thymus*. Proc Natl Acad Sci U S A, 1990. **87**(7): p. 2579-82.
402. Henson, P.M., *Dampening inflammation*. Nat Immunol, 2005. **6**(12): p. 1179-81.
403. Tsujimoto, Y., et al., *Cloning of the chromosome breakpoint of neoplastic B cells with the t(14;18) chromosome translocation*. Science, 1984. **226**(4678): p. 1097-9.
404. Vaux, D.L., S. Cory, and J.M. Adams, *Bcl-2 gene promotes haemopoietic cell survival and cooperates with c-myc to immortalize pre-B cells*. Nature, 1988. **335**(6189): p. 440-2.
405. Kvensakul, M., et al., *Vaccinia virus anti-apoptotic F1L is a novel Bcl-2-like domain-swapped dimer that binds a highly selective subset of BH3-containing death ligands*. Cell Death Differ, 2008. **15**(10): p. 1564-71.
406. Chou, J.J., et al., *Solution structure of BID, an intracellular amplifier of apoptotic signaling*. Cell, 1999. **96**(5): p. 615-24.
407. McDonnell, J.M., et al., *Solution structure of the proapoptotic molecule BID: a structural basis for apoptotic agonists and antagonists*. Cell, 1999. **96**(5): p. 625-34.
408. Hinds, M.G., et al., *Bim, Bad and Bmf: intrinsically unstructured BH3-only proteins that undergo a localized conformational change upon binding to prosurvival Bcl-2 targets*. Cell Death Differ, 2007. **14**(1): p. 128-36.
409. Salter, R.D., et al., *Domain organization and sequence relationship of killer cell inhibitory receptors*. Immunol Rev, 1997. **155**: p. 175-82.
410. Kvensakul, M. and M.G. Hinds, *Structural biology of the Bcl-2 family and its mimicry by viral proteins*. Cell Death Dis, 2013. **4**: p. e909.
411. Kvensakul, M., et al., *Structural basis for apoptosis inhibition by Epstein-Barr virus BHRF1*. PLoS Pathog, 2010. **6**(12): p. e1001236.
412. Hickish, T., et al., *Ultrastructural localization of BHRF1: an Epstein-Barr virus gene product which has homology with bcl-2*. Cancer Res, 1994. **54**(10): p. 2808-11.

413. Fanidi, A., D.C. Hancock, and T.D. Littlewood, *Suppression of c-Myc-induced apoptosis by the Epstein-Barr virus gene product BHRF1*. J Virol, 1998. **72**(10): p. 8392-5.
414. Foghsgaard, L. and M. Jaattela, *The ability of BHRF1 to inhibit apoptosis is dependent on stimulus and cell type*. J Virol, 1997. **71**(10): p. 7509-17.
415. Kawanishi, M., *Epstein-Barr virus BHRF1 protein protects intestine 407 epithelial cells from apoptosis induced by tumor necrosis factor alpha and anti-Fas antibody*. J Virol, 1997. **71**(4): p. 3319-22.
416. Kawanishi, M., S. Tada-Oikawa, and S. Kawanishi, *Epstein-Barr virus BHRF1 functions downstream of Bid cleavage and upstream of mitochondrial dysfunction to inhibit TRAIL-induced apoptosis in BJAB cells*. Biochem Biophys Res Commun, 2002. **297**(3): p. 682-7.
417. McCarthy, N.J., et al., *The Epstein-Barr virus gene BHRF1, a homologue of the cellular oncogene Bcl-2, inhibits apoptosis induced by gamma radiation and chemotherapeutic drugs*. Adv Exp Med Biol, 1996. **406**: p. 83-97.
418. Watanabe, A., et al., *Epstein-Barr virus-encoded Bcl-2 homologue functions as a survival factor in Wp-restricted Burkitt lymphoma cell line P3HR-1*. J Virol, 2010. **84**(6): p. 2893-901.
419. Yee, J., et al., *Latent Epstein-Barr Virus Can Inhibit Apoptosis in B Cells by Blocking the Induction of NOXA Expression*. PLoS One, 2011. **6**(12): p. e28506.
420. Zhao, E.G., et al., *Resistance to etoposide-induced apoptosis in a Burkitt's lymphoma cell line*. Int J Cancer, 1998. **77**(5): p. 755-62.
421. Marshall, W.L., et al., *Epstein-Barr virus encodes a novel homolog of the bcl-2 oncogene that inhibits apoptosis and associates with Bax and Bak*. J Virol, 1999. **73**(6): p. 5181-5.
422. Bellows, D.S., et al., *Epstein-Barr virus BALF1 is a BCL-2-like antagonist of the herpesvirus antiapoptotic BCL-2 proteins*. J Virol, 2002. **76**(5): p. 2469-79.
423. Chen, L., et al., *Differential targeting of prosurvival Bcl-2 proteins by their BH3-only ligands allows complementary apoptotic function*. Mol Cell, 2005. **17**(3): p. 393-403.
424. Kuwana, T., et al., *BH3 domains of BH3-only proteins differentially regulate Bax-mediated mitochondrial membrane permeabilization both directly and indirectly*. Mol Cell, 2005. **17**(4): p. 525-35.
425. Willis, S.N., et al., *Apoptosis initiated when BH3 ligands engage multiple Bcl-2 homologs, not Bax or Bak*. Science, 2007. **315**(5813): p. 856-9.
426. Chipuk, J.E. and D.R. Green, *How do BCL-2 proteins induce mitochondrial outer membrane permeabilization?* Trends Cell Biol, 2008. **18**(4): p. 157-64.
427. Letai, A., et al., *Distinct BH3 domains either sensitize or activate mitochondrial apoptosis, serving as prototype cancer therapeutics*. Cancer Cell, 2002. **2**(3): p. 183-92.
428. Kim, H., et al., *Stepwise activation of BAX and BAK by tBID, BIM, and PUMA initiates mitochondrial apoptosis*. Mol Cell, 2009. **36**(3): p. 487-99.
429. Merino, D., et al., *The role of BH3-only protein Bim extends beyond inhibiting Bcl-2-like prosurvival proteins*. J Cell Biol, 2009. **186**(3): p. 355-62.
430. Lindsten, T., et al., *The combined functions of proapoptotic Bcl-2 family members bak and bax are essential for normal development of multiple tissues*. Mol Cell, 2000. **6**(6): p. 1389-99.
431. Wei, M.C., et al., *Proapoptotic BAX and BAK: a requisite gateway to mitochondrial dysfunction and death*. Science, 2001. **292**(5517): p. 727-30.
432. Gavathiotis, E., et al., *BH3-triggered structural reorganization drives the activation of proapoptotic BAX*. Mol Cell, 2010. **40**(3): p. 481-92.
433. Willis, S.N., et al., *Proapoptotic Bak is sequestered by Mcl-1 and Bcl-xL, but not Bcl-2, until displaced by BH3-only proteins*. Genes Dev, 2005. **19**(11): p. 1294-305.

434. Adams, J.M. and S. Cory, *The Bcl-2 apoptotic switch in cancer development and therapy*. *Oncogene*, 2007. **26**(9): p. 1324-37.
435. Echeverry, N., et al., *Intracellular localization of the BCL-2 family member BOK and functional implications*. *Cell Death Differ*, 2013. **20**(6): p. 785-99.
436. Shamas-Din, A., et al., *BH3-only proteins: Orchestrators of apoptosis*. *Biochim Biophys Acta*, 2011. **1813**(4): p. 508-20.
437. Dewson, G., et al., *Bak activation for apoptosis involves oligomerization of dimers via their alpha6 helices*. *Mol Cell*, 2009. **36**(4): p. 696-703.
438. Dewson, G., et al., *To trigger apoptosis, Bak exposes its BH3 domain and homodimerizes via BH3:groove interactions*. *Mol Cell*, 2008. **30**(3): p. 369-80.
439. Westphal, D., et al., *Molecular biology of Bax and Bak activation and action*. *Biochim Biophys Acta*, 2011. **1813**(4): p. 521-31.
440. Kuwana, T., et al., *Bid, Bax, and lipids cooperate to form supramolecular openings in the outer mitochondrial membrane*. *Cell*, 2002. **111**(3): p. 331-42.
441. Rehm, M., H. Dussmann, and J.H. Prehn, *Real-time single cell analysis of Smac/DIABLO release during apoptosis*. *J Cell Biol*, 2003. **162**(6): p. 1031-43.
442. Leber, B., J. Lin, and D.W. Andrews, *Embedded together: the life and death consequences of interaction of the Bcl-2 family with membranes*. *Apoptosis*, 2007. **12**(5): p. 897-911.
443. Oda, E., et al., *Noxa, a BH3-only member of the Bcl-2 family and candidate mediator of p53-induced apoptosis*. *Science*, 2000. **288**(5468): p. 1053-8.
444. Nakano, K. and K.H. Vousden, *PUMA, a novel proapoptotic gene, is induced by p53*. *Mol Cell*, 2001. **7**(3): p. 683-94.
445. Akhtar, R.S., et al., *BH3-only proapoptotic Bcl-2 family members Noxa and Puma mediate neural precursor cell death*. *J Neurosci*, 2006. **26**(27): p. 7257-64.
446. Yerlikaya, A., E. Okur, and E. Ulukaya, *The p53-independent induction of apoptosis in breast cancer cells in response to proteasome inhibitor bortezomib*. *Tumour Biol*, 2012. **33**(5): p. 1385-92.
447. Dijkers, P.F., et al., *Expression of the pro-apoptotic Bcl-2 family member Bim is regulated by the forkhead transcription factor FKHR-L1*. *Curr Biol*, 2000. **10**(19): p. 1201-4.
448. Fu, Z. and D.J. Tindall, *FOXOs, cancer and regulation of apoptosis*. *Oncogene*, 2008. **27**(16): p. 2312-9.
449. Espina, B., et al., *Regulation of bim in glucocorticoid-mediated osteoblast apoptosis*. *J Cell Physiol*, 2008. **215**(2): p. 488-96.
450. O'Connor, L., et al., *Bim: a novel member of the Bcl-2 family that promotes apoptosis*. *EMBO J*, 1998. **17**(2): p. 384-95.
451. U, M., et al., *Molecular cloning and characterization of six novel isoforms of human Bim, a member of the proapoptotic Bcl-2 family*. *FEBS Lett*, 2001. **509**(1): p. 135-41.
452. Boise, L.H., et al., *bcl-x, a bcl-2-related gene that functions as a dominant regulator of apoptotic cell death*. *Cell*, 1993. **74**(4): p. 597-608.
453. Kim, J.H., et al., *MCL-1ES, a novel variant of MCL-1, associates with MCL-1L and induces mitochondrial cell death*. *FEBS Lett*, 2009. **583**(17): p. 2758-64.
454. Zha, J., et al., *Serine phosphorylation of death agonist BAD in response to survival factor results in binding to 14-3-3 not BCL-X(L)*. *Cell*, 1996. **87**(4): p. 619-28.
455. Datta, S.R., et al., *14-3-3 proteins and survival kinases cooperate to inactivate BAD by BH3 domain phosphorylation*. *Mol Cell*, 2000. **6**(1): p. 41-51.
456. Nijhawan, D., et al., *Elimination of Mcl-1 is required for the initiation of apoptosis following ultraviolet irradiation*. *Genes Dev*, 2003. **17**(12): p. 1475-86.
457. Stewart, D.P., et al., *Ubiquitin-independent degradation of antiapoptotic MCL-1*. *Mol Cell Biol*, 2010. **30**(12): p. 3099-110.

458. Lei, K. and R.J. Davis, *JNK phosphorylation of Bim-related members of the Bcl2 family induces Bax-dependent apoptosis*. Proc Natl Acad Sci U S A, 2003. **100**(5): p. 2432-7.
459. Luciano, F., et al., *Phosphorylation of Bim-EL by Erk1/2 on serine 69 promotes its degradation via the proteasome pathway and regulates its proapoptotic function*. Oncogene, 2003. **22**(43): p. 6785-93.
460. Wiggins, C.M., et al., *BIM(EL), an intrinsically disordered protein, is degraded by 20S proteasomes in the absence of poly-ubiquitylation*. J Cell Sci, 2011. **124**(Pt 6): p. 969-77.
461. Puthalakath, H., et al., *The proapoptotic activity of the Bcl-2 family member Bim is regulated by interaction with the dynein motor complex*. Mol Cell, 1999. **3**(3): p. 287-96.
462. Xiao, C., et al., *Lymphoproliferative disease and autoimmunity in mice with increased miR-17-92 expression in lymphocytes*. Nat Immunol, 2008. **9**(4): p. 405-14.
463. Chipuk, J.E., et al., *Sphingolipid metabolism cooperates with BAK and BAX to promote the mitochondrial pathway of apoptosis*. Cell, 2012. **148**(5): p. 988-1000.
464. Strasser, A., et al., *Novel primitive lymphoid tumours induced in transgenic mice by cooperation between myc and bcl-2*. Nature, 1990. **348**(6299): p. 331-3.
465. Beverly, L.J. and H.E. Varmus, *MYC-induced myeloid leukemogenesis is accelerated by all six members of the antiapoptotic BCL family*. Oncogene, 2009. **28**(9): p. 1274-9.
466. Swanson, P.J., et al., *Fatal acute lymphoblastic leukemia in mice transgenic for B cell-restricted bcl-xL and c-myc*. J Immunol, 2004. **172**(11): p. 6684-91.
467. Campbell, K.J., et al., *Elevated Mcl-1 perturbs lymphopoiesis, promotes transformation of hematopoietic stem/progenitor cells, and enhances drug resistance*. Blood, 2010. **116**(17): p. 3197-207.
468. Frenzel, A., et al., *Suppression of B-cell lymphomagenesis by the BH3-only proteins Bmf and Bad*. Blood, 2010. **115**(5): p. 995-1005.
469. Erlacher, M., et al., *Puma cooperates with Bim, the rate-limiting BH3-only protein in cell death during lymphocyte development, in apoptosis induction*. J Exp Med, 2006. **203**(13): p. 2939-51.
470. Beroukhi, R., et al., *The landscape of somatic copy-number alteration across human cancers*. Nature, 2010. **463**(7283): p. 899-905.
471. Schwickart, M., et al., *Deubiquitinase USP9X stabilizes MCL1 and promotes tumour cell survival*. Nature, 2010. **463**(7277): p. 103-7.
472. Wertz, I.E., et al., *Sensitivity to antitubulin chemotherapeutics is regulated by MCL1 and FBW7*. Nature, 2011. **471**(7336): p. 110-4.
473. Richter-Larrea, J.A., et al., *Reversion of epigenetically mediated BIM silencing overcomes chemoresistance in Burkitt lymphoma*. Blood, 2010. **116**(14): p. 2531-42.
474. Lessene, G., P.E. Czabotar, and P.M. Colman, *BCL-2 family antagonists for cancer therapy*. Nat Rev Drug Discov, 2008. **7**(12): p. 989-1000.
475. Souers, A.J., et al., *ABT-199, a potent and selective BCL-2 inhibitor, achieves antitumor activity while sparing platelets*. Nat Med, 2013. **19**(2): p. 202-8.
476. Wilson, W.H., et al., *Navitoclax, a targeted high-affinity inhibitor of BCL-2, in lymphoid malignancies: a phase 1 dose-escalation study of safety, pharmacokinetics, pharmacodynamics, and antitumour activity*. Lancet Oncol, 2010. **11**(12): p. 1149-59.
477. Roberts, A.W., et al., *Substantial susceptibility of chronic lymphocytic leukemia to BCL2 inhibition: results of a phase I study of navitoclax in patients with relapsed or refractory disease*. J Clin Oncol, 2012. **30**(5): p. 488-96.
478. Anderson, M.A., D. Huang, and A. Roberts, *Targeting BCL2 for the treatment of lymphoid malignancies*. Semin Hematol, 2014. **51**(3): p. 219-27.
479. Quinn, B.A., et al., *Targeting Mcl-1 for the therapy of cancer*. Expert Opin Investig Drugs, 2011. **20**(10): p. 1397-411.

480. Takada, K., et al., *An Epstein-Barr virus-producer line Akata: establishment of the cell line and analysis of viral DNA*. *Virus Genes*, 1991. **5**(2): p. 147-56.
481. Rensing, M.E., et al., *Epstein-Barr virus gp42 is posttranslationally modified to produce soluble gp42 that mediates HLA class II immune evasion*. *J Virol*, 2005. **79**(2): p. 841-52.
482. Gregory, C.D., M. Rowe, and A.B. Rickinson, *Different Epstein-Barr virus-B cell interactions in phenotypically distinct clones of a Burkitt's lymphoma cell line*. *J Gen Virol*, 1990. **71 (Pt 7)**: p. 1481-95.
483. Herold, M.J., et al., *Inducible and reversible gene silencing by stable integration of an shRNA-encoding lentivirus in transgenic rats*. *Proc Natl Acad Sci U S A*, 2008. **105**(47): p. 18507-12.
484. Soboleski, M.R., J. Oaks, and W.P. Halford, *Green fluorescent protein is a quantitative reporter of gene expression in individual eukaryotic cells*. *FASEB J*, 2005. **19**(3): p. 440-2.
485. Tierney, R.J., et al., *The Epstein-Barr Virus BamHI C Promoter Is Not Essential For B Cell Immortalization In Vitro But Greatly Enhances B Cell Growth Transformation*. *J Virol*, 2014.
486. Delecluse, H.J., et al., *Propagation and recovery of intact, infectious Epstein-Barr virus from prokaryotic to human cells*. *Proc Natl Acad Sci U S A*, 1998. **95**(14): p. 8245-50.
487. Neuhierl, B., et al., *Glycoprotein gp110 of Epstein-Barr virus determines viral tropism and efficiency of infection*. *Proc Natl Acad Sci U S A*, 2002. **99**(23): p. 15036-41.
488. Kanda, T., et al., *Production of high-titer Epstein-Barr virus recombinants derived from Akata cells by using a bacterial artificial chromosome system*. *J Virol*, 2004. **78**(13): p. 7004-15.
489. Martin, D.R., R.L. Marlowe, and J.M. Ahearn, *Determination of the role for CD21 during Epstein-Barr virus infection of B-lymphoblastoid cells*. *J Virol*, 1994. **68**(8): p. 4716-26.
490. Rowe, M., et al., *Distinctions between endemic and sporadic forms of Epstein-Barr virus-positive Burkitt's lymphoma*. *Int J Cancer*, 1985. **35**(4): p. 435-41.
491. Evans, T.J., M.G. Jacquemin, and P.J. Farrell, *Efficient EBV superinfection of group I Burkitt's lymphoma cells distinguishes requirements for expression of the Cp viral promoter and can activate the EBV productive cycle*. *Virology*, 1995. **206**(2): p. 866-77.
492. Trivedi, P., et al., *Differential regulation of Epstein-Barr virus (EBV) latent gene expression in Burkitt lymphoma cells infected with a recombinant EBV strain*. *J Virol*, 2001. **75**(10): p. 4929-35.
493. Hughes, D.J., et al., *Trans-Repression of Protein Expression Dependent on the Epstein-Barr Virus Promoter Wp during Latency*. *J. Virol.*, 2011: p. JVI.05158-11.
494. van Engeland, M., et al., *A novel assay to measure loss of plasma membrane asymmetry during apoptosis of adherent cells in culture*. *Cytometry*, 1996. **24**(2): p. 131-9.
495. Vermes, I., et al., *A novel assay for apoptosis. Flow cytometric detection of phosphatidylserine expression on early apoptotic cells using fluorescein labelled Annexin V*. *J Immunol Methods*, 1995. **184**(1): p. 39-51.
496. Junying, J., et al., *Absence of Epstein-Barr virus DNA in the tumor cells of European hepatocellular carcinoma*. *Virology*, 2003. **306**(2): p. 236-43.
497. Doherty, J.P., et al., *Escherichia coli host strains SURE and SRB fail to preserve a palindrome cloned in lambda phage: improved alternate host strains*. *Gene*, 1993. **124**(1): p. 29-35.
498. Inoue, H., H. Nojima, and H. Okayama, *High efficiency transformation of Escherichia coli with plasmids*. *Gene*, 1990. **96**(1): p. 23-8.
499. Leung, C.S., et al., *Nuclear location of an endogenously expressed antigen, EBNA1, restricts access to macroautophagy and the range of CD4 epitope display*. *Proc Natl Acad Sci U S A*, 2010. **107**(5): p. 2165-70.

500. Lee, E.F., et al., *A novel BH3 ligand that selectively targets Mcl-1 reveals that apoptosis can proceed without Mcl-1 degradation*. J Cell Biol, 2008. **180**(2): p. 341-55.
501. Livak, K.J. and T.D. Schmittgen, *Analysis of relative gene expression data using real-time quantitative PCR and the 2(-Delta Delta C(T)) Method*. Methods, 2001. **25**(4): p. 402-8.
502. Bustin, S.A., *Absolute quantification of mRNA using real-time reverse transcription polymerase chain reaction assays*. J Mol Endocrinol, 2000. **25**(2): p. 169-93.
503. Chen, C., et al., *Real-time quantification of microRNAs by stem-loop RT-PCR*. Nucleic Acids Res, 2005. **33**(20): p. e179.
504. Pearson, G.R., et al., *Identification of an Epstein-Barr virus early gene encoding a second component of the restricted early antigen complex*. Virology, 1987. **160**(1): p. 151-61.
505. Rowe, M., et al., *Differences in B cell growth phenotype reflect novel patterns of Epstein-Barr virus latent gene expression in Burkitt's lymphoma cells*. EMBO J, 1987. **6**(9): p. 2743-51.
506. Rowe, D.T., P.J. Farrell, and G. Miller, *Novel nuclear antigens recognized by human sera in lymphocytes latently infected by Epstein-Barr virus*. Virology, 1987. **156**(1): p. 153-62.
507. Shultz, L.D., et al., *Human lymphoid and myeloid cell development in NOD/LtSz-scid IL2R gamma null mice engrafted with mobilized human hemopoietic stem cells*. J Immunol, 2005. **174**(10): p. 6477-89.
508. Ohbo, K., et al., *Modulation of hematopoiesis in mice with a truncated mutant of the interleukin-2 receptor gamma chain*. Blood, 1996. **87**(3): p. 956-67.
509. Bornkamm, G.W., *Epstein-Barr virus and the pathogenesis of Burkitt's lymphoma: more questions than answers*. Int J Cancer, 2009. **124**(8): p. 1745-55.
510. Bianchi, V., E. Pontis, and P. Reichard, *Changes of deoxyribonucleoside triphosphate pools induced by hydroxyurea and their relation to DNA synthesis*. J Biol Chem, 1986. **261**(34): p. 16037-42.
511. Lundin, C., et al., *Different roles for nonhomologous end joining and homologous recombination following replication arrest in mammalian cells*. Mol Cell Biol, 2002. **22**(16): p. 5869-78.
512. Vereide, D. and B. Sugden, *Proof for EBV's sustaining role in Burkitt's lymphomas*. Semin Cancer Biol, 2009. **19**(6): p. 389-93.
513. Weinstein, I.B., *Cancer. Addiction to oncogenes--the Achilles heel of cancer*. Science, 2002. **297**(5578): p. 63-4.
514. Certo, M., et al., *Mitochondria primed by death signals determine cellular addiction to antiapoptotic BCL-2 family members*. Cancer Cell, 2006. **9**(5): p. 351-65.
515. van Maanen, J.M., et al., *Mechanism of action of antitumor drug etoposide: a review*. J Natl Cancer Inst, 1988. **80**(19): p. 1526-33.
516. Baldwin, E.L. and N. Osheroff, *Etoposide, topoisomerase II and cancer*. Curr Med Chem Anticancer Agents, 2005. **5**(4): p. 363-72.
517. Donjerkovic, D. and D.W. Scott, *Activation-induced cell death in B lymphocytes*. Cell Res, 2000. **10**(3): p. 179-92.
518. Sordet, O., et al., *Apoptosis induced by topoisomerase inhibitors*. Curr Med Chem Anticancer Agents, 2003. **3**(4): p. 271-90.
519. Niino, H. and E.A. Clark, *Regulation of B-cell fate by antigen-receptor signals*. Nat Rev Immunol, 2002. **2**(12): p. 945-56.
520. Aagaard-Tillery, K.M. and D.F. Jelinek, *Differential activation of a calcium-dependent endonuclease in human B lymphocytes. Role in ionomycin-induced apoptosis*. J Immunol, 1995. **155**(7): p. 3297-307.

521. Aldoss, I.T., T. Tashi, and A.K. Ganti, *Selaciclib in malignancies*. Expert Opin Investig Drugs, 2009. **18**(12): p. 1957-65.
522. Garrofe-Ochoa, X., et al., *Transcriptional modulation of apoptosis regulators by roscovitine and related compounds*. Apoptosis, 2011. **16**(7): p. 660-70.
523. Ren, Y., et al., *Shp2E76K mutant confers cytokine-independent survival of TF-1 myeloid cells by up-regulating Bcl-XL*. J Biol Chem, 2007. **282**(50): p. 36463-73.
524. Kang, M.-S., et al., *Roscovitine Inhibits EBNA1 Serine 393 Phosphorylation, Nuclear Localization, Transcription, and Episome Maintenance*. J. Virol.: p. JVI.01628-10.
525. Nakamura-Lopez, Y., et al., *Staurosporine-induced apoptosis in P388D1 macrophages involves both extrinsic and intrinsic pathways*. Cell Biol Int, 2009. **33**(9): p. 1026-31.
526. Dupraz, P., et al., *Lentivirus-mediated Bcl-2 expression in betaTC-tet cells improves resistance to hypoxia and cytokine-induced apoptosis while preserving in vitro and in vivo control of insulin secretion*. Gene Ther, 1999. **6**(6): p. 1160-9.
527. Giuliano, M., et al., *Staurosporine-induced apoptosis in Chang liver cells is associated with down-regulation of Bcl-2 and Bcl-XL*. Int J Mol Med, 2004. **13**(4): p. 565-71.
528. Brown, T.L., *Q-VD-OPh, next generation caspase inhibitor*. Adv Exp Med Biol, 2004. **559**: p. 293-300.
529. Degtarev, A., et al., *Identification of RIP1 kinase as a specific cellular target of necrostatins*. Nat Chem Biol, 2008. **4**(5): p. 313-21.
530. Ofengeim, D. and J. Yuan, *Regulation of RIP1 kinase signalling at the crossroads of inflammation and cell death*. Nat Rev Mol Cell Biol, 2013. **14**(11): p. 727-36.
531. Moubarak, R.S., et al., *Sequential activation of poly(ADP-ribose) polymerase 1, calpains, and Bax is essential in apoptosis-inducing factor-mediated programmed necrosis*. Mol Cell Biol, 2007. **27**(13): p. 4844-62.
532. Golstein, P. and G. Kroemer, *Cell death by necrosis: towards a molecular definition*. Trends Biochem Sci, 2007. **32**(1): p. 37-43.
533. Polito, L., et al., *Saporin induces multiple death pathways in lymphoma cells with different intensity and timing as compared to ricin*. Int J Biochem Cell Biol, 2009. **41**(5): p. 1055-61.
534. Oltersdorf, T., et al., *An inhibitor of Bcl-2 family proteins induces regression of solid tumours*. Nature, 2005. **435**(7042): p. 677-81.
535. van Delft, M.F., et al., *The BH3 mimetic ABT-737 targets selective Bcl-2 proteins and efficiently induces apoptosis via Bak/Bax if Mcl-1 is neutralized*. Cancer Cell, 2006. **10**(5): p. 389-99.
536. Puthalakath, H. and A. Strasser, *Keeping killers on a tight leash: transcriptional and post-translational control of the pro-apoptotic activity of BH3-only proteins*. Cell Death Differ, 2002. **9**(5): p. 505-12.
537. Delecluse, H.J., et al., *Episomal and integrated copies of Epstein-Barr virus coexist in Burkitt lymphoma cell lines*. J Virol, 1993. **67**(3): p. 1292-9.
538. Srinivas, S.K., J.T. Sample, and J.W. Sixbey, *Spontaneous loss of viral episomes accompanying Epstein-Barr virus reactivation in a Burkitt's lymphoma cell line*. J Infect Dis, 1998. **177**(6): p. 1705-9.
539. Zuo, J., et al., *Epstein-Barr virus evades CD4+ T cell responses in lytic cycle through BZLF1-mediated downregulation of CD74 and the cooperation of vBcl-2*. PLoS Pathog, 2011. **7**(12): p. e1002455.
540. De-The, G., *The epidemiology of Burkitt's lymphoma: evidence for a causal association with Epstein-Barr virus*. Epidemiol Rev, 1979. **1**: p. 32-54.
541. Iversen, U., et al., *Cell kinetics of African cases of Burkitt lymphoma. A preliminary report*. Eur J Cancer, 1972. **8**(3): p. 305-8.

542. Ressing, M.E., et al., *Impaired transporter associated with antigen processing-dependent peptide transport during productive EBV infection*. J Immunol, 2005. **174**(11): p. 6829-38.
543. Pfeifer, A., *Lentiviral transgenesis--a versatile tool for basic research and gene therapy*. Curr Gene Ther, 2006. **6**(4): p. 535-42.
544. Middleton, T. and B. Sugden, *A chimera of EBNA1 and the estrogen receptor activates transcription but not replication*. J Virol, 1992. **66**(3): p. 1795-8.
545. Reisman, D. and B. Sugden, *trans activation of an Epstein-Barr viral transcriptional enhancer by the Epstein-Barr viral nuclear antigen 1*. Mol Cell Biol, 1986. **6**(11): p. 3838-46.
546. Nanbo, A. and K. Takada, *The role of Epstein-Barr virus-encoded small RNAs (EBERs) in oncogenesis*. Rev Med Virol, 2002. **12**(5): p. 321-6.
547. Rosa, M.D., et al., *Striking similarities are exhibited by two small Epstein-Barr virus-encoded ribonucleic acids and the adenovirus-associated ribonucleic acids VAI and VAII*. Mol Cell Biol, 1981. **1**(9): p. 785-96.
548. Mazabraud, A., et al., *Structure and transcription termination of a lysine tRNA gene from Xenopus laevis*. J Mol Biol, 1987. **195**(4): p. 835-45.
549. Braglia, P., R. Percudani, and G. Dieci, *Sequence context effects on oligo(dT) termination signal recognition by Saccharomyces cerevisiae RNA polymerase III*. J Biol Chem, 2005. **280**(20): p. 19551-62.
550. Akusjarvi, G., et al., *Structure of genes for virus-associated RNAI and RNAII of adenovirus type 2*. Proc Natl Acad Sci U S A, 1980. **77**(5): p. 2424-8.
551. Gunnery, S., Y. Ma, and M.B. Mathews, *Termination sequence requirements vary among genes transcribed by RNA polymerase III*. J Mol Biol, 1999. **286**(3): p. 745-57.
552. Larsson, S., A. Bellett, and G. Akusjarvi, *VA RNAs from avian and human adenoviruses: dramatic differences in length, sequence, and gene location*. J Virol, 1986. **58**(2): p. 600-9.
553. Ma, Y. and M.B. Mathews, *Comparative analysis of the structure and function of adenovirus virus-associated RNAs*. J Virol, 1993. **67**(11): p. 6605-17.
554. Deutscher, M.P., *Ribonucleases, tRNA nucleotidyltransferase, and the 3' processing of tRNA*. Prog Nucleic Acid Res Mol Biol, 1990. **39**: p. 209-40.
555. Maraia, R.J. and T.N. Lamichhane, *3' processing of eukaryotic precursor tRNAs*. Wiley Interdiscip Rev RNA, 2011. **2**(3): p. 362-75.
556. Ruf, I.K. and J. Sample, *Repression of Epstein-Barr virus EBNA-1 gene transcription by pRb during restricted latency*. J Virol, 1999. **73**(10): p. 7943-51.
557. Shimizu, N., H. Yoshiyama, and K. Takada, *Clonal propagation of Epstein-Barr virus (EBV) recombinants in EBV-negative Akata cells*. J Virol, 1996. **70**(10): p. 7260-3.
558. Laux, G., M. Perricaudet, and P.J. Farrell, *A spliced Epstein-Barr virus gene expressed in immortalized lymphocytes is created by circularization of the linear viral genome*. EMBO J, 1988. **7**(3): p. 769-74.
559. Bornkamm, G.W., et al., *Comparison of Epstein-Barr virus strains of different origin by analysis of the viral DNAs*. J Virol, 1980. **35**(3): p. 603-18.
560. Raab-Traub, N., T. Dambaugh, and E. Kieff, *DNA of Epstein-Barr virus VIII: B95-8, the previous prototype, is an unusual deletion derivative*. Cell, 1980. **22**(1 Pt 1): p. 257-67.
561. Samanta, M., et al., *EB virus-encoded RNAs are recognized by RIG-I and activate signaling to induce type I IFN*. EMBO J, 2006. **25**(18): p. 4207-14.
562. Yamamoto, N., et al., *Malignant transformation of B lymphoma cell line BJAB by Epstein-Barr virus-encoded small RNAs*. FEBS Lett, 2000. **484**(2): p. 153-8.
563. Tischer, B.K., G.A. Smith, and N. Osterrieder, *En passant mutagenesis: a two step markerless red recombination system*. Methods Mol Biol, 2010. **634**: p. 421-30.

564. Tischer, B.K., et al., *Two-step red-mediated recombination for versatile high-efficiency markerless DNA manipulation in Escherichia coli*. *Biotechniques*, 2006. **40**(2): p. 191-7.
565. Wu, T.T., et al., *Construction and characterization of an infectious murine gammaherpesvirus-68 bacterial artificial chromosome*. *J Biomed Biotechnol*, 2011. **2011**: p. 926258.
566. Piccaluga, P.P., et al., *Gene expression analysis uncovers similarity and differences among Burkitt lymphoma subtypes*. *Blood*.
567. Deng, J., et al., *BH3 Profiling Identifies Three Distinct Classes of Apoptotic Blocks to Predict Response to ABT-737 and Conventional Chemotherapeutic Agents*. *Cancer Cell*, 2007. **12**(2): p. 171-185.
568. Chonghaile, T.N., et al., *Maturation Stage of T-cell Acute Lymphoblastic Leukemia Determines BCL-2 versus BCL-XL Dependence and Sensitivity to ABT-199*. *Cancer Discov*, 2014. **4**(9): p. 1074-87.
569. Davids, M.S., A. Letai, and J.R. Brown, *Overcoming stroma-mediated treatment resistance in chronic lymphocytic leukemia through BCL-2 inhibition*. *Leuk Lymphoma*, 2013. **54**(8): p. 1823-5.
570. Vo, T.T., et al., *Relative mitochondrial priming of myeloblasts and normal HSCs determines chemotherapeutic success in AML*. *Cell*, 2012. **151**(2): p. 344-55.
571. Glaser, S.P., et al., *Anti-apoptotic Mcl-1 is essential for the development and sustained growth of acute myeloid leukemia*. *Genes Dev*, 2012. **26**(2): p. 120-5.
572. Liu, P., S. Liu, and S.H. Speck, *Identification of a negative cis element within the ZII domain of the Epstein-Barr virus lytic switch BZLF1 gene promoter*. *J Virol*, 1998. **72**(10): p. 8230-9.
573. Bae, J., et al., *MCL-1S, a splicing variant of the antiapoptotic BCL-2 family member MCL-1, encodes a proapoptotic protein possessing only the BH3 domain*. *J Biol Chem*, 2000. **275**(33): p. 25255-61.
574. Bingle, C.D., et al., *Exon skipping in Mcl-1 results in a bcl-2 homology domain 3 only gene product that promotes cell death*. *J Biol Chem*, 2000. **275**(29): p. 22136-46.
575. Kaufmann, S.H., et al., *Specific proteolytic cleavage of poly(ADP-ribose) polymerase: an early marker of chemotherapy-induced apoptosis*. *Cancer Res*, 1993. **53**(17): p. 3976-85.
576. Tewari, M., et al., *Yama/CPP32 beta, a mammalian homolog of CED-3, is a CrmA-inhibitable protease that cleaves the death substrate poly(ADP-ribose) polymerase*. *Cell*, 1995. **81**(5): p. 801-9.
577. Chaitanya, G.V., A.J. Steven, and P.P. Babu, *PARP-1 cleavage fragments: signatures of cell-death proteases in neurodegeneration*. *Cell Commun Signal*, 2010. **8**: p. 31.
578. Luthi, A.U. and S.J. Martin, *The CASBAH: a searchable database of caspase substrates*. *Cell Death Differ*, 2007. **14**(4): p. 641-50.
579. Callus, B.A. and D.L. Vaux, *Caspase inhibitors: viral, cellular and chemical*. *Cell Death Differ*, 2007. **14**(1): p. 73-8.
580. Deveraux, Q.L. and J.C. Reed, *IAP family proteins--suppressors of apoptosis*. *Genes Dev*, 1999. **13**(3): p. 239-52.
581. Silke, J. and P. Meier, *Inhibitor of apoptosis (IAP) proteins--modulators of cell death and inflammation*. *Cold Spring Harb Perspect Biol*, 2013. **5**(2).
582. Thome, M., et al., *Viral FLICE-inhibitory proteins (FLIPs) prevent apoptosis induced by death receptors*. *Nature*, 1997. **386**(6624): p. 517-21.
583. Shisler, J.L., *Viral and Cellular FLICE-Inhibitory Proteins: a Comparison of Their Roles in Regulating Intrinsic Immune Responses*. *J Virol*, 2014. **88**(12): p. 6539-6541.
584. Safa, A.R., *c-FLIP, a master anti-apoptotic regulator*. *Exp Oncol*, 2012. **34**(3): p. 176-84.
585. Roth, W., et al., *Identification and characterization of DEDD2, a death effector domain-containing protein*. *J Biol Chem*, 2002. **277**(9): p. 7501-8.

586. Zhan, Y., et al., *Death effector domain-containing proteins DEDD and FLAME-3 form nuclear complexes with the TFIIIC102 subunit of human transcription factor IIIC*. Cell Death Differ, 2002. **9**(4): p. 439-47.
587. Alcivar, A., et al., *DEDD and DEDD2 associate with caspase-8/10 and signal cell death*. Oncogene, 2003. **22**(2): p. 291-7.
588. Caserta, T.M., et al., *Q-VD-OPh, a broad spectrum caspase inhibitor with potent antiapoptotic properties*. Apoptosis, 2003. **8**(4): p. 345-52.
589. Chauvier, D., et al., *Broad-spectrum caspase inhibitors: from myth to reality?* Cell Death Differ, 2007. **14**(2): p. 387-91.
590. Kuzelova, K., D. Grebenova, and B. Brodska, *Dose-dependent effects of the caspase inhibitor Q-VD-OPh on different apoptosis-related processes*. J Cell Biochem, 2011. **112**(11): p. 3334-42.
591. Imai, Y., et al., *The CED-4-homologous protein FLASH is involved in Fas-mediated activation of caspase-8 during apoptosis*. Nature, 1999. **398**(6730): p. 777-85.
592. Chen, S., H.G. Evans, and D.R. Evans, *FLASH knockdown sensitizes cells to Fas-mediated apoptosis via down-regulation of the anti-apoptotic proteins, MCL-1 and Cflip short*. PLoS One, 2012. **7**(3): p. e32971.
593. Vucic, D. and W.J. Fairbrother, *The inhibitor of apoptosis proteins as therapeutic targets in cancer*. Clin Cancer Res, 2007. **13**(20): p. 5995-6000.
594. Bernasconi, M., et al., *Early gene expression changes by Epstein-Barr virus infection of B-cells indicate CDKs and survivin as therapeutic targets for post-transplant lymphoproliferative diseases*. Int J Cancer, 2013. **133**(10): p. 2341-50.
595. Espinoza, J.L., et al., *Resveratrol prevents EBV transformation and inhibits the outgrowth of EBV-immortalized human B cells*. PLoS One, 2012. **7**(12): p. e51306.
596. Clybouw, C., et al., *TGFbeta-mediated apoptosis of Burkitt's lymphoma BL41 cells is associated with the relocation of mitochondrial BimEL*. Oncogene, 2008. **27**(24): p. 3446-56.
597. Baou, M., et al., *Role of NOXA and its ubiquitination in proteasome inhibitor-induced apoptosis in chronic lymphocytic leukemia cells*. Haematologica, 2010. **95**(9): p. 1510-8.
598. Craxton, A., et al., *NOXA, a sensor of proteasome integrity, is degraded by 26S proteasomes by an ubiquitin-independent pathway that is blocked by MCL-1*. Cell Death Differ, 2012. **19**(9): p. 1424-34.
599. Roset, R., L. Ortet, and G. Gil-Gomez, *Role of Bcl-2 family members on apoptosis: what we have learned from knock-out mice*. Front Biosci, 2007. **12**: p. 4722-30.
600. Komano, J. and K. Takada, *Role of bcl-2 in Epstein-Barr virus-induced malignant conversion of Burkitt's lymphoma cell line Akata*. J Virol, 2001. **75**(3): p. 1561-4.
601. Catz, S.D. and J.L. Johnson, *Transcriptional regulation of bcl-2 by nuclear factor kappa B and its significance in prostate cancer*. Oncogene, 2001. **20**(50): p. 7342-51.
602. Heckman, C.A., J.W. Mehew, and L.M. Boxer, *NF-kappaB activates Bcl-2 expression in t(14;18) lymphoma cells*. Oncogene, 2002. **21**(24): p. 3898-908.
603. Karin, M. and A. Lin, *NF-kappaB at the crossroads of life and death*. Nat Immunol, 2002. **3**(3): p. 221-7.
604. Viatour, P., et al., *NF- kappa B2/p100 induces Bcl-2 expression*. Leukemia, 2003. **17**(7): p. 1349-56.
605. Parrish, A.B., C.D. Freel, and S. Kornbluth, *Cellular mechanisms controlling caspase activation and function*. Cold Spring Harb Perspect Biol, 2013. **5**(6).
606. Porter, A.G. and R.U. Janicke, *Emerging roles of caspase-3 in apoptosis*. Cell Death Differ, 1999. **6**(2): p. 99-104.
607. White, R.E., et al., *Extensive co-operation between the Epstein-Barr virus EBNA3 proteins in the manipulation of host gene expression and epigenetic chromatin modification*. PLoS One, 2010. **5**(11): p. e13979.

608. Petti, L., et al., *A fifth Epstein-Barr virus nuclear protein (EBNA3C) is expressed in latently infected growth-transformed lymphocytes.* J Virol, 1988. **62**(4): p. 1330-8.
609. Skalska, L., et al., *Epigenetic repression of p16(INK4A) by latent Epstein-Barr virus requires the interaction of EBNA3A and EBNA3C with CtBP.* PLoS Pathog, 2010. **6**(6): p. e1000951.
610. Obexer, P., et al., *p16INK4A sensitizes human leukemia cells to FAS- and glucocorticoid-induced apoptosis via induction of BBC3/Puma and repression of MCL1 and BCL2.* J Biol Chem, 2009. **284**(45): p. 30933-40.
611. Pratt, Z.L., J. Zhang, and B. Sugden, *The latent membrane protein 1 (LMP1) oncogene of Epstein-Barr virus can simultaneously induce and inhibit apoptosis in B cells.* J Virol, 2012. **86**(8): p. 4380-93.
612. D'Souza, B., M. Rowe, and D. Walls, *The bfl-1 gene is transcriptionally upregulated by the Epstein-Barr virus LMP1, and its expression promotes the survival of a Burkitt's lymphoma cell line.* J Virol, 2000. **74**(14): p. 6652-8.
613. Henderson, S., et al., *Induction of bcl-2 expression by Epstein-Barr virus latent membrane protein 1 protects infected B cells from programmed cell death.* Cell, 1991. **65**(7): p. 1107-15.
614. Wang, S., M. Rowe, and E. Lundgren, *Expression of the Epstein Barr virus transforming protein LMP1 causes a rapid and transient stimulation of the Bcl-2 homologue Mcl-1 levels in B-cell lines.* Cancer Res, 1996. **56**(20): p. 4610-3.
615. Champion, E.M., et al., *Repression of the proapoptotic cellular BIK/NBK gene by Epstein-Barr virus antagonizes transforming growth factor beta1-induced B-cell apoptosis.* J Virol, 2014. **88**(9): p. 5001-13.
616. Swanton, C., *Intratumor heterogeneity: evolution through space and time.* Cancer Res, 2012. **72**(19): p. 4875-82.
617. Yap, T.A., et al., *Intratumor heterogeneity: seeing the wood for the trees.* Sci Transl Med, 2012. **4**(127): p. 127ps10.
618. Duronio, V., *The life of a cell: apoptosis regulation by the PI3K/PKB pathway.* Biochem J, 2008. **415**(3): p. 333-44.
619. del Peso, L., et al., *Interleukin-3-induced phosphorylation of BAD through the protein kinase Akt.* Science, 1997. **278**(5338): p. 687-9.
620. Datta, S.R., et al., *Akt phosphorylation of BAD couples survival signals to the cell-intrinsic death machinery.* Cell, 1997. **91**(2): p. 231-41.
621. Scheid, M.P. and V. Duronio, *Dissociation of cytokine-induced phosphorylation of Bad and activation of PKB/akt: involvement of MEK upstream of Bad phosphorylation.* Proc Natl Acad Sci U S A, 1998. **95**(13): p. 7439-44.
622. Gardai, S.J., et al., *Phosphorylation of Bax Ser184 by Akt regulates its activity and apoptosis in neutrophils.* J Biol Chem, 2004. **279**(20): p. 21085-95.
623. Bauer, A., et al., *The NF-kappaB regulator Bcl-3 and the BH3-only proteins Bim and Puma control the death of activated T cells.* Proc Natl Acad Sci U S A, 2006. **103**(29): p. 10979-84.
624. Chijioko, O., et al., *Human natural killer cells prevent infectious mononucleosis features by targeting lytic Epstein-Barr virus infection.* Cell Rep, 2013. **5**(6): p. 1489-98.
625. Heckl, D., et al., *Generation of mouse models of myeloid malignancy with combinatorial genetic lesions using CRISPR-Cas9 genome editing.* Nat Biotechnol, 2014. **32**(9): p. 941-6.
626. Marchbank, K.J., et al., *Expression of human complement receptor 2 (CR2, CD21) in Cr2-/- mice restores humoral immune function.* J Immunol, 2000. **165**(5): p. 2354-61.
627. Cragg, M.S., et al., *Unleashing the power of inhibitors of oncogenic kinases through BH3 mimetics.* Nat Rev Cancer, 2009. **9**(5): p. 321-6.

